

Brunel University

**THE APPLICATION OF PHASE
CHANGE MATERIALS TO COOL
BUILDINGS**

Gideon Susman

A thesis submitted in partial fulfilment of the
requirements for the degree of Engineering
Doctorate in Environmental Technology.

School of Engineering and Design, Jan. 2012.

Declaration of Authorship

I, Gideon Susman, declare that this thesis titled *The Application of Phase Change Materials to Cool Buildings* and the work presented in it are my own. I confirm that:

- This work was done wholly or mainly while in candidature for a research degree at this University.
- Where any part of this thesis has previously been submitted for a degree or any other qualification at this University or any other institution, this has been clearly stated.
- When I have consulted the published work of others, this is always clearly attributed.
- Where I have quoted from the work of others, the source is always given.
- With the exception of such quotations, this thesis is entirely my own work.
- I have acknowledged all main sources of help.
- Where the thesis is based on work done by myself jointly with others, I have made clear exactly what was done by others and what I have contributed myself.

Signed:

Date:

ABSTRACT

THE APPLICATION OF PHASE CHANGE MATERIALS TO COOL BUILDINGS

By Gideon Susman

Five projects improve understanding of how to use PCM to reduce building cooling energy. Firstly, a post-installation energy-audit of an active cooling system with PCM tank revealed an energy cost of 10.6% of total cooling energy, as compared to an identical tankless system, because PCM under-cooling prevented heat rejection at night. Secondly, development of a new taxonomy for PCM cooling systems allowed reclassification of all systems and identified under-exploited types. Novel concept designs were generated that employ movable PCM units and insulation. Thirdly, aspects of the generated designs were tested in a passive PCM sail design, installed in an occupied office. Radiant heat transfer, external heat discharge and narrow phase transition zone all improved performance. Fourthly, passive PCM product tests were conducted in a 4.2 m³ thermal test cell in which two types of ceiling tile, with 50 and 70% microencapsulated PCM content, and paraffin/copolymer composite wallboards yielded peak temperature reductions of 3.8, 4.4 and 5.2 °C, respectively, and peak temperature reductions per unit PCM mass of 0.28, 0.34 and 0.14 °C/kg, respectively. Heat discharge of RACUS tiles was more effective due to their non-integration into the building fabric. Conclusions of preceding chapters informed the design of a new system composed of an array of finned aluminium tubes, containing paraffin (melt temperature 19.79 °C, latent heat 159.75 kJ/kg) located below the ceiling. Passive cooling and heat discharge is prioritised but a chilled water loop ensures temperature control on hotter days (water circulated at 13 °C) and heat discharge on hotter nights (water circulated at 10 °C). Test cell results showed similar passive performance to the ceiling tiles and wallboards, effective active temperature control (constant 24.6 °C air temperature) and successful passive and active heat discharge. A dynamic heat balance model with an IES-generated UK office's annual cooling load and PCM temperature-enthalpy functions predicted annual energy savings of 34%.

Acknowledgements

Firstly, thank you to Dr Andrew Cripps and Professor Maria Kolokotroni for giving me the chance to undertake this research in the first place. I would like to say a big thank you to the all the Brunel University students with whom I collaborated over the last few years. It was a really rewarding experience to work with such enthusiastic young talent. In particular, thank you to William Couch whose energy and keen practical mind were much appreciated during the most critical phase of this project. We made great team.

I am grateful to Paul Tuddenham and all at China Shipping House for generously opening their doors and giving time to this work.

I am extremely lucky to have friends, family and colleagues that have the patience and understanding to deal with the highs and lows of my research. I would like to write a piece to all of you but such a work would constitute a dissertation in itself. However, I would like to thank my friend Mr Ross Downes for his assistance in the test cell structural design and, of course, for its construction. Also, a huge thank you to Mrs Hero Tardrew for her brilliantly efficient proof reading and support towards the end. True to my word, I would also like to thank Mr David Raznick for so willingly talking through all those maths and logic problems.

Most importantly, thank you to my supervisors. Since beginning supervision almost two years into the project Dr Zahir Dehouche has given commitment and guidance far beyond what I could have ever expected. Thanks again, Zahir. We covered a lot of ground!

And lastly, thank you Dr Salmaan Craig for picking up the baton at such a crucial time (and not letting go.) I value your opinions and guidance extremely highly but I am most lucky to have had your continued support. You're a true friend.

This research would not have been possible without funding from the EPSRC and Buro Happold Ltd. Additional funding and laboratory space was provided by Brunel University, in the latter half of the project, for which I am very grateful.

Contents

<i>Declaration of Authorship</i>	1
<i>Abstract</i>	2
<i>Acknowledgements</i>	3
<i>List of Figures</i>	8
<i>List of Tables</i>	12
<i>Glossary</i>	14
<i>Nomenclature</i>	19
<i>A note to the reader</i>	24
<i>Executive Summary</i>	26
<i>Chapter 1 INTRODUCTION</i>	58
1.1 Climate change legislation and building energy use	58
1.2 Thermal Comfort.....	59
1.3 Temperature Control.....	62
1.4 Comfort Cooling and Global Warming	63
1.5 Phase change materials	66
1.6 How this work contributes to knowledge	68
References	71
<i>Chapter 2 LITERATURE REVIEW</i>	75
2.1 Phase Change Materials	79
2.1.1 Candidate Materials	82
2.1.2 Testing Thermophysical Properties	85
2.1.3 Containment and Heat Transfer Enhancement	92
2.2 Systems in Buildings	97
2.2.1 Classification	97
2.2.2 Active Systems.....	101
2.2.3 Passive Systems.....	104
2.2.4 Free cooling systems	109
2.2.5 Thermally Activated Systems.....	111
2.3 Modelling.....	112

2.3.2	Modelling PCM cooling systems	114
2.4	Conclusions	116
	References	117
<i>Chapter 3</i>	ACTIVE PCM COOLING SYSTEM	131
3.1	System Description	133
3.1.1	Generation and Water-side Distribution	133
3.1.2	Air-side Distribution	134
3.1.3	PCM Tanks	135
3.1.4	Energy Savings	136
3.2	Method	137
3.2.1	Tank Thermal Capacity	137
3.2.2	Energy and Carbon Savings	138
3.3	Results and Discussion	141
3.3.1	Thermophysical Properties of S-13 and Tank Thermal Capacity	142
3.3.2	Energy and Carbon Savings	143
3.4	Conclusions	147
	References	149
<i>Chapter 4</i>	DESIGN SPACE MAPPING	150
4.1	Problem statement	151
4.2	Problem framing	152
4.3	Mapping the Design Space	157
4.4	System Classification	164
4.4.1	System Type 1	164
4.4.2	System Type 2	166
4.4.3	System Type 3	167
4.4.4	System Type 4	169
4.4.5	System Type 5	171
4.4.6	System Type 6	171
4.4.7	System Type 7	172
4.4.8	System Type 8	173
4.4.9	System Type 9	174

4.4.10	System Type 10.....	175
4.4.11	System Type 11	176
4.5	System Comparison and Selection.....	177
4.6	Conclusions	180
	References	183
	<i>Chapter 5</i> PASSIVE PCM SAILS	185
5.1	Method	187
5.2	Results	196
5.2.1	Validation	196
5.2.2	Average Liquid Fraction and Surface Heat Transfer Rate Profiles	203
5.3	Conclusions	207
	References	208
	<i>Chapter 6</i> PRODUCT TESTING	210
6.1	Test Cell	211
6.1.1	Construction and Dimensions	213
6.1.2	Features	215
6.2	Method	218
6.2.1	RACUS ceiling tiles.....	219
6.2.2	Energain Panels.....	222
6.3	Results and discussion	226
6.4	Conclusions	233
	References	233
	<i>Chapter 7</i> NEWMASS SYSTEM DESIGN	235
7.1	Concept Design.....	235
7.2	System Element Selection.....	239
7.2.1	Unit Envelope Geometry.....	240
7.2.2	Unit envelope material.....	242
7.2.3	Unit envelope finish	243
7.2.4	Finned tube manufacture.....	244
7.2.5	Phase Change Material.....	245

7.2.6	Conductive matrix	249
7.3	Detailed Prototype Design	254
7.3.1	Envelope dimensions	254
7.3.2	Filling units	265
7.3.3	Chilled water circuit	268
	References	271
 <i>Chapter 8</i> NEWMASS SYSTEM TESTING		275
8.1	Calculations and modelling	280
8.1.1	Temperature-enthalpy curves	280
8.1.2	Heat transfer coefficient.....	284
8.1.4	Annual energy savings model	286
8.2	System assembly and installation	289
8.2.1	Unit assembly	289
8.2.2	Unit installation	294
8.2.3	Chilled water system	296
8.3	Main test method	296
8.3.1	Controls and monitoring	296
8.3.2	Test Procedure.....	300
8.4	Results	303
8.4.1	Passive charging	303
8.4.2	Supplemented passive charging.....	314
8.4.3	Passive discharge.....	323
8.4.4	Active discharge	327
8.4.5	Energy savings.....	332
8.3	Conclusions	335
	References	337
 <i>Chapter 9</i> CONCLUSION		339
9.1	Publications	343
9.2	Further work	343
	References	346
	Appendix.....	347

List of Figures

Figure ES.1	The cooling system at China Shipping House	28
Figure ES.2	Active PCM storage	29
Figure ES.3	Active PCM cooling performance data.....	30
Figure ES.4	Design space matrix	32
Figure ES.5	All system types with pictorial representations	33
Figure ES.6	Novel PCM cooling system designs.....	35
Figure ES.7	Module dimensions and thermocouple locations	37
Figure ES.8	Internal and external rigs.....	38
Figure ES.9	Pure paraffin and composite DSC curves	39
Figure ES.10	Temperature contours.....	40
Figure ES.11	Average liquid fraction profiles of the four modules.....	40
Figure ES.12	Surface heat flux profiles of the four modules	41
Figure ES.13	The thermal test cell	42
Figure ES.14	Test cell images.....	43
Figure ES.15	RACUS tiles.....	44
Figure ES.16	Energain panels applied to the internal surfaces of the test cell	46
Figure ES.17	Combined charge period results.....	46
Figure ES.18	Combined discharge period results.....	48
Figure ES.19	NewMass concept	49
Figure ES.20	Images of the NewMass units	50
Figure ES.21	Temperature vs cumulative heat flow	51
Figure ES.22	NewMass system components	52
Figure ES.23	Medium level air temperature profiles of all four installations and the control test.....	53
Figure ES.24	Medium level air temperature profiles of all four installations and the control test with NewMass in supplementary cooling mode.	54
Figure ES.25	Temperature of all NewMass units during active discharge mode. ..	54
Figure 1.1	The Greenhouse effect.....	64
Figure 1.2	Proportion of end use building energy consumption for various countries	65
Figure 2.1	The ice trade	80

Figure 2.2 Categories of thermal storage media and sub-sets of PCM.....	83
Figure 2.3 Typical DSC curves for commercially available paraffin wax	86
Figure 2.4 DSC curves for PCMs tested as part of Brunel's material appraisal programme	89
Figure 2.5 Macroencapsulated PCM	92
Figure 2.6 Microencapsulated PCM	93
Figure 3.1 PCM tank	132
Figure 3.2 The central cooling system at China Shipping House	133
Figure 3.3 Inside PCM tank.....	135
Figure 3.4 Delivered cooling power variation with electrical input at ambient temperatures	137
Figure 3.5 Active cooling system temperatures.	141
Figure 3.6 The DSC curve for one of the S-13 salt samples	142
Figure 3.7 Tank heat exchange and chiller input power profiles.....	144
Figure 3.8 Tank inlet and outlet temperatures.....	146
Figure 4.1 The cyclical thermal charge and discharge process undergone by all diurnal PCM cooling systems.....	153
Figure 4.2 Three illustrations of building insulation	156
Figure 4.3 The thermal storage tank at China Shipping House	157
Figure 4.4 Diagram of all fundamental elements of a PCM cooling system	158
Figure 4.5 Example configurations	159
Figure 4.6 Simple pictorial representations of each configuration	160
Figure 4.7 A matrix of potential LHTES cooling system designs	161
Figure 4.8 All system types with pictorial representations	163
Figure 4.9 The NewMass system as developed in this EngD.....	165
Figure 4.10 Thermally activated system with insulated curtain	167
Figure 4.11 A trombe wall with insulating curtain to retain heat	168
Figure 4.12 System with PCM integrated into the fabric.....	168
Figure 4.13 System with PCM integrated into the fabric.....	170
Figure 4.14 The experimental set up for the Passive PCM Sail experiment.....	170
Figure 4.15 A PCM tank with removable insulation to discharge accumulated heat directly to the night sky.....	173

Figure 4.16 PCM integrated into the building fabric with internal insulation to prevent over-cooling at night.	175
Figure 4.17 Externally located PCM unit with cool water circuit	176
Figure 4.18 New designs with removable insulation and HTF circuits	178
Figure 4.19 New designs with removable insulation	179
Figure 4.20 New design with HTF	180
Figure 5.1 Module dimensions and thermocouple locations	188
Figure 5.2 The internal set up	189
Figure 5.3 The external set up	190
Figure 5.4 DSC curves of pure A26 paraffin and A26-LDPE composite	192
Figure 5.5 DSC curves of pure A22 paraffin and A22-LDPE composite	192
Figure 5.6 FLUENT mesh.....	195
Figure 5.7 Contours of temperature	196
Figure 5.8 Model validation for A26,Al,EC.....	198
Figure 5.9 Model validation for A22,Al,EC	199
Figure 5.10 Model validation for A22,Bl,EC	201
Figure 5.11 Model validation for A22,Bl,IC.....	202
Figure 5.12 Internal air and globe temperatures.	203
Figure 5.13 Average liquid fraction profiles of the four modules.	204
Figure 5.14 Surface heat flux profiles of the four modules	206
Figure 6.1 Conceptual schematic of the thermal test cell	212
Figure 6.2 Images of the thermal test cell.....	213
Figure 6.3 The test cell.....	214
Figure 6.4 Test cell element locations and dimensions in mm.	214
Figure 6.5 Variation in heating capacity of the heater.....	216
Figure 6.6 Test cell features	217
Figure 6.7 Tiles with RACUS 73 and 74	219
Figure 6.8 DSC Curves for micronal	221
Figure 6.9 The RACUS test cell installation.....	222
Figure 6.10 Energain panels applied to the internal surfaces of the test cell.....	223
Figure 6.11 Paraffin extraction	224
Figure 6.12 DSC curves for Energain panel and pure constituent paraffin.	225
Figure 6.13 Charge periods.....	227

Figure 6.14 Combined charge results.....	228
Figure 6.15 Discharge periods.....	231
Figure 6.16 Combined discharge results.....	232
Figure 7.1 NewMass concept.....	237
Figure 7.2 NewMass sub-system hierarchy.....	239
Figure 7.3 Three flat plate design variations.....	241
Figure 7.4 Finned prism options.....	241
Figure 7.5 Anodised aluminium colour swatches.....	243
Figure 7.6 Combined pure A22 and A22/LDPE composite DSC curves.....	247
Figure 7.7 Annular space with and without fins.....	250
Figure 7.8 Raschig rings.....	253
Figure 7.9 Profile applied for load-levelling.....	255
Figure 7.10 Finned tube with circular fin geometry.....	256
Figure 7.11 Final tube design concept.....	262
Figure 7.12 Finned tube engineering drawings.....	263
Figure 7.13 Cap engineering drawings.....	264
Figure 7.14 Finned tube and cap images.....	265
Figure 7.15 Tube with Raschig rings and sealed units.....	268
Figure 7.16 Finned tube array.....	269
Figure 7.17 Chilled water circuit connections.....	270
Figure 8.1 Specific heat flow vs. temperature.....	281
Figure 8.2 Cumulative heat flowing into and being stored by NewMass unit.....	282
Figure 8.3 Polynomial curve fittings.....	283
Figure 8.4 IES UK office model geometry.....	286
Figure 8.5 Stages in the NewMass unit sealing process.....	290
Figure 8.6 The internal thermocouples and guide holes in unit 6.....	292
Figure 8.7 End cap with thermocouple design.....	293
Figure 8.8 NewMass system schematic.....	295
Figure 8.9 Thermocouple locations.....	299
Figure 8.10 NewMass and control comparison for passive charge period.....	304
Figure 8.11 Temperatures at different heights.....	306
Figure 8.12 CFD model results.....	308

Figure 8.13 Temperature profiles for locations within and on the surface of the units.	309
Figure 8.14 The heat transfer coefficient profile for the period	310
Figure 8.15 The heat flux through the cell ceiling for two locations	312
Figure 8.16 Medium level air temperature profiles of all four installations	313
Figure 8.17 NewMass and control comparison for supplemented passive charge period.....	315
Figure 8.18 Temperatures at different heights for a supplemented cooling charge period.....	317
Figure 8.19 Temperature profiles for locations within and on the surface of the units during a supplemented cooling period.	319
Figure 8.20 Heat transfer coefficient profile for passive charge period	320
Figure 8.21 The heat flux through the cell ceiling for two locations	321
Figure 8.22 Inlet and outlet temperatures for water flowing through unit 6.	322
Figure 8.23 Medium level air temperature profiles.....	323
Figure 8.24 Temperatures at different heights during passive discharge period.	324
Figure 8.25 Temperature profiles for locations within and on the surface of the units.	325
Figure 8.26 The heat transfer coefficient profile for the period.....	327
Figure 8.27 Temperatures at different heights during active discharge period....	328
Figure 8.28 Temperature profiles for locations within and on the surface of the units during an active discharge period.....	330
Figure 8.29 Inlet and outlet temperatures for water flowing through unit 6 in active discharge.	331
Figure 8.30 Ambient temperature profile and IES cooling load.....	332
Figure 8.31 Internal air and NewMass unit temperature profiles.....	333
Figure 8.32 Cooling load and ambient temperature.	334

List of Tables

Table ES.1 China Shipping House cooling energy	30
Table ES.2 Passive PCM Sail variations.	36

Table ES.3	Thermophysical properties of the PCM composites.....	39
Table ES.4	Thermophysical properties of micronal and RACUS formulations	45
Table ES.5	Further Micronal and RACUS properties	45
Table ES.6	Thermophysical properties of Energain panel	45
Table ES.7	Results for the product tests with comparisons.....	47
Table ES.8	Masses of all NewMass units and their main constituents	51
Table ES.9	Values for heat transfer coefficient.	53
Table 1.1	Office operative temperature ranges	61
Table 2.1	Thermophysical properties of commercially available PCMs	91
Table 3.1	Thermophysical properties of S-13 salt.....	143
Table 3.2	Energy consumption and savings from the cooling system at China Shipping House	143
Table 3.3	Heat exchanged by the PCM tanks	145
Table 5.1	Thermophysical properties of the tested PCM/LDPE composites.	191
Table 6.1	Thermophysical properties of micronal and RACUS formulations	220
Table 6.2	Further properties of Micronal and RACUS.....	220
Table 6.3	Thermophysical properties of Energain panel	224
Table 6.4	Results for the product tests	229
Table 7.1	Comparative properties of metals	242
Table 7.2	Commerically available PCMs.....	246
Table 7.3	Properties of composite.....	256
Table 7.4	Selected fin tube dimensions.	260
Table 7.5	Thermal expansion results for A22 paraffin.	266
Table 8.1	Summary table of the NewMass system experiment and modelling.	276
Table 8.2	Fabric element specification.....	286
Table 8.3	Heat gains	287
Table 8.4	Masses of all NewMass units and their main constituents	291
Table 8.5	Thermocouple locations.....	298
Table 8.6	Results from flow meter calibration.....	300
Table 8.7	Values for heat transfer coefficient.....	311
Table 8.8	Annual energy use of a conventional cooling system and NewMass.....	334

Glossary

<i>A22</i>	A commercially available paraffin PCM
<i>Active</i>	For charging and discharging processes this refers to the requirement for a secondary heat transfer fluid. For whole systems this refers to those in which the PCM is contained in an isolated tank
<i>AHU</i>	Air handling unit
<i>BMS</i>	Building Management System: Software that allows the management and automatic control of buildings services; often accessed through a desktop terminal
<i>Brunel PCM Research Group</i>	Those students and research staff at Brunel University who collaborated on PCM research projects that provided results that informed this EngD project
<i>BRE</i>	Building Research Establishment
<i>BREEAM</i>	BRE Environmental Assessment Method
<i>Charging</i>	Thermal charging, i.e. the addition of heat to a substance. This happens to a body of PCM when it cools a space
<i>CIBSE</i>	Chartered Institute of Building Services Engineers
<i>Cooling</i>	Unless otherwise explicitly stated the term ‘cooling’ always refers to cooling of air in an occupied space
<i>Cooling capacity</i>	The rate at which a system can provide cooling. Building service terminology often refers to this simply as ‘capacity’, in the case of chillers for instance, but here it is distinguished from ‘thermal capacity’ for clarity.

<i>Coolth</i>	The thermal property possessed by a substance when it has a lower temperature than its surroundings
<i>CFD</i>	Computational Fluid Dynamics
<i>COP</i>	Coefficient of performance. The ratio of cooling power supplied to input power
<i>Design space</i>	The group of all possible solutions to a design problem. See the note to the reader for an extended explanation of this concept
<i>Design space mapping</i>	The development of a set of rules or a taxonomy that allows the various design solutions that inhabit the design space to be classified in a clear and consistent way. See the note to the reader for an extended explanation of this concept
<i>Discharging</i>	Thermal discharging, i.e. the rejection of heat from a substance. This happens to a body of PCM when it loses its accumulated heat at night
<i>DSM</i>	Demand side management
<i>DSC</i>	Differential Scanning Calorimetry
<i>EPRI</i>	Electric Power Research Institute. The US utilities' research institution.
<i>FCU</i>	Fan coil unit
<i>Free cooling</i>	For PCM cooling systems this refers to those that are isolated from the occupied space and external air, requiring fans to transfer heat. Discharge is to cool night air alone.
<i>FLUENT</i>	CFD software programme
<i>HDPE</i>	High density polyethylene
<i>HTF</i>	Heat transfer fluid

<i>HVAC</i>	Heating, ventilation and air conditioning
<i>IES</i>	Integrated Environmental Solutions. A software package for thermal modelling of buildings
<i>Latent heat</i>	The heat exchanged with a substance, per unit mass, when it changes phase
<i>LDPE</i>	Low Density Polyethylene
<i>LEED</i>	Leadership in Energy and Environmental Design
<i>Mean radiant temperature</i>	“The uniform surface temperature of a radiantly black enclosure in which an occupant would exchange the same amount of radiant heat as in the actual non-uniform space” (Humphreys and Nicol, 2007)
<i>NewMass</i>	A PCM cooling system, developed as part of this thesis, consisting of finned tubes containing paraffin which can passively absorb heat and actively discharge it to a chilled water circuit
<i>Operative temperature</i>	A parameter that combines the air temperature and the mean radiant temperature into a single value to take better account of the temperature that an occupant may experience. For air speeds below 0.1 m/s this is equal to the sum of the mean radiant and air temperatures, divided by two
<i>Passive</i>	For charging and discharging processes this refers to direct contact with heat source or sink so no secondary heat transfer fluid required. For whole systems this refers to those in which the PCM is located within the occupied space
<i>PCM</i>	Phase Change Material
<i>PCM cooling system</i>	Any system that employs phase change materials to reduce excessive temperature rise in buildings.

<i>Phase transition zone</i>	The temperature range over which a PCM changes phase
<i>Problem framing</i>	The statement of the set of conditions that are necessarily entailed by the design problem. See the note to the reader for an extended explanation of this concept
<i>Raschig rings</i>	Small cylinders with an equal diameter and length that form a random packing structure with a large surface area for industrial mass transfer processes. In this work they are employed for their conductivity to increase the flow of heat through the paraffin contained in the NewMass units.
<i>Random packings</i>	Rigid shapes that fill a volume, support each other and create a network of interconnected voids
<i>NCM</i>	National Calculation Methodology
<i>RIBA</i>	Royal Institute of British Architects
<i>Sail</i>	A heating or cooling element, normally a flat panel, which is located below the ceiling in an occupied space.
<i>Sensible heat transfer</i>	Exchange of heat with a substance that only causes a rise or fall in temperature not a change of phase
<i>SBEM</i>	Simplified Building Energy Model
<i>Supercooling</i>	See Undercooling
<i>TES</i>	Thermal Energy Storage
<i>Thermal capacity</i>	The heat that can be absorbed by a body over a defined temperature range. Specifically defined in this thesis as distinct from cooling capacity, see above.
<i>Thermal mass</i>	Material in a building that passively absorbs and releases heat thereby dampening temperature

fluctuations and reducing or levelling cooling demand

Thermally activated

For PCM cooling systems this refers to PCM elements that passively absorb heat during the day and discharge it to circulated chilled water, in embedded pipes, at night.

Undercooling

The cooling of a liquid to below its freezing point without freezing

Unit enthalpy

The internal energy held in 1 NewMass unit at a given temperature, relative to a reference unit enthalpy

USGBC

U.S. Green Building Council

Nomenclature

A	Area, m
A_s	Heat transfer surface area, m ²
A_{Tot}	Total surface area of finned tube, m ²
C_p	Specific heat at constant pressure, kJ/kgK (kWh/kgK in chapter 3)
$COP_{cooling}$	Coefficient of performance for cooling through refrigeration (-)
D	Fin diameter, m
d	Base tube diameter, m
e	Distance to opposing boundary in PCM body, m
ED	Energy density, kJ/m ³
g	Acceleration due to gravity, m/s ²
G_{sky}	Radiation emitted by the Earth's atmosphere, kW
F_p	Chiller power factor (-)
$F_{w,p}$	View factor of finned tube (-)
H	Enthalpy of element, kJ/kg
h	Sensible enthalpy content of element, kJ/kg
h	Heat transfer coefficient, kW/m ² K
h_c	Convective heat transfer coefficient, kW/m ² K
$h_{c,eff}$	Effective convective heat transfer coefficient kW/m ² /K
h_{eff}	Effective heat transfer coefficient, kW/m ² K
$h_{r,eff}$	Effective radiant heat transfer coefficient, kW/m ² K
h_{ref}	Reference enthalpy, kJ/kg
I	Current, kA
k	Thermal conductivity, kW/mK
k_{eff}	Effective thermal conductivity of hybrid material kW/mK
L	Length, m
L_c	Characteristic length, m
L_{fus}	Latent heat of fusion, kJ/kg (kWh/kg in chapter 3)
m	Mass of system, kg
$\dot{m}_{1\text{ and }k}$	Mass flow rate of water through both PCM tanks, kg/s
N_{NM}	Number of NewMass units (-)
N_{units}	Number of PCM units (-)
NM_T	Thermal energy contained in one NewMass unit, kJ

Nu	Nusselt number
Nu _s	Nusselt number specific to fin spacing
p	Time in a 10 minute sub-period, (0.167) h (hours)
Pr	Prandtl number
q	Time in a 15 minute sub-period, (0.25) h (hours)
Q	The internal (thermal) energy of a substance, kJ
Q _{saved}	Energy saved by presence of PCM tanks over a specified period, kWh
Q _{conv}	Energy that would have been used by a conventional tankless system, identical in every other way, kWh
Q _{PCM}	Energy that was used by the installed system, kWh
Q _{pump}	Pump energy consumed at night, kWh
Q _{chill,day}	Daytime chiller and pump input energy, kWh
Q _{tank,elec day}	Chiller input energy displaced by presence of PCM tanks, kWh
Q _{chill,night}	The night time chiller and pump input energy, kWh
\dot{Q}	Heat flow rate or power, kW
\dot{Q}_{rad}	Radiative heat transfer rate, kW
Q _{cold}	Heat input at evaporator, kJ
Q _{fus}	Heat lost when substance freezes, kJ
Q _{hot}	Heat output at condenser, kJ
Q _{sens}	Heat required to raise a substance's temperature, kJ
Ra	Rayleigh number (-)
Ra _s	Rayleigh number specific to fin spacing (-)
S	Heat generation in element, kW/m ³
S	Ratio of free volume to total volume in a volume occupied by Raschig rings
S	Fin spacing, m
T	Temperature, K
T _{ref}	Reference temperature, K
T _{cold}	Evaporator temperature, K
T _{hot}	Condenser temperature, K
T _{liquidus}	Melting temperature, K
T _{ref}	Reference temperature, K
T _s	Temperature of surface, K

T_{sky}	Sky temperature, K
T_{solidus}	Solidification or freezing temperature, K
T_{surr}	Temperature of the surroundings, K
T_{∞}	Temperature of the fluid at a sufficient distance, K
T_{in}	Inlet water temperature (of tank in chapter 5 and of NewMass unit in chapter 8) (K)
T_{out}	Outlet water temperature (of tank in chapter 5 and of NewMass unit in chapter 8) (K)
T_{p}	Average radiant temperature of the surroundings (K)
T_{w}	Temperature of base tube, K
TC	Thermal capacity, kJ/kg
t	Time, s (h (hours) in chapter 3)
U_{tanks}	Total thermal storage capacity of the PCM tanks, kWh
U_{max}	Maximum heat required to be stored by NewMass units, kJ
V	Volume, m ³
V	Chiller Voltage, V
V_{unit}	Volume of an individual PCM unit, m ³
ρ	Density, kg/m ³
\vec{v}	Fluid velocity, m/s
W	Work input at the compressor, kJ
x	Distance, m
α	Thermal diffusivity, m ² /s
α_{v}	Volumetric thermal expansion coefficient
β	Liquid fraction (-) as defined by Voller (1996)
β	Coefficient of expansion, 1/K
ε	Emissivity of the surface (-)
η_{fin}	Fin efficiency (-)
ν	Kinematic Viscosity, m ² /s
ρ	Density, kg/m ³
ρ_{relative}	Relative density (-)
σ	Stefan-Boltzmann constant, kW/m ² K ⁴

Subscripts

A(LPCM)	Air in a tube with liquid PCM
A(SPCM)	Air in a tube with solid PCM
A+R(LPCM)	Air and Raschig rings in a NewMass unit with liquid A22.
AV	Annular volume
Al	Aluminium
A22	A22 (PCM)
air	Air
b	Base tube in a finned tube
CB	Chilled beam loop pump
hs	Heat sources in a space
HS	Hydrated Salt
hyb	Hybrid of A22 and Raschig rings
i	Time step number
LPCM	Liquid PCM
m	Total number of 10 minute sub-periods over monitored period
min	Minimum value recorded during the monitored period
max	Maximum value recorded during the monitored period
n	Total number of 15 minute sub-periods over monitored period
NA	Night air flowing into building
NM	NewMass unit
NM _s	NewMass unit surface
PCM	Phase change material
P	Under constant pressure
Pipe	Chilled water pipe in NewMass unit
PP	Primary loop pump
q	Fifteen minute sub-period
r	Phase of electrical power supply
R	Raschig rings. (When referring to volumes this refers to the solid mass of aluminium in the rings not the volume taken up by the rings and any surrounding solid or fluid)
s	Ten minute sub-period

S13	S13 hydrated salt
S	Space; that found in and between the Raschig rings in the NewMass units which can be occupied by PCM or air
sample	Sample of a substance
SPCM	Solid PCM
T	Temperature
t	Ambient temperature at any particular sub-period
w	Water

A note to the reader

It is felt necessary to pre-empt any confusion that may arise from the use of certain terms and the research collaborations that have taken place as part of this EngD project.

In the writing of this thesis every attempt has been made to use plain language but a few terms employed have particular definitions that may confuse the reader if not clearly explained.

Firstly, the term '*PCM cooling systems*' refers to any system that employs phase change materials to reduce excessive temperature rise in buildings. These include passive applications, such as PCM wallboards, that may not normally be thought of as systems. *PCM cooling systems* may be seen as synonymous with, or part of the group known as, '*latent heat thermal energy storage (LHTES) systems*'. However, no reference will be made to LHTES systems as the term introduces another acronym unnecessarily, is less descriptive and is not as specific as *PCM cooling system*, since it can refer to heating applications as well.

All PCM cooling systems are seen to go through two fundamental processes: Absorbing excess heat from a space and rejecting it at some other time (normally at night). The process of absorption is referred to here as '*charging*'. The process of heat rejection is referred to as '*discharging*'.

Two types of '*capacity*' are distinguished in the thesis: '*Cooling capacity*' and '*thermal capacity*'. *Cooling capacity* refers to the rate at which a PCM cooling system may absorb heat from a space. In this way it is synonymous with the term *capacity* as it is applied to chillers; it is a term denoting power. *Thermal capacity* refers to the amount of heat that a PCM cooling system may absorb before saturation. In this way it is very similar to the term *capacity* as it is applied to a battery's storage of charge; it is a term denoting energy.

In chapter 4, three particular terms are used: '*Design space*', '*problem framing*' and '*design space mapping*'. *Design space* refers to the group of all possible solutions to a design problem. The various design solutions that inhabit this design space are the PCM cooling systems that currently exist and those that are yet to be conceived.

The *problem framing* is the statement of the set of conditions that are necessarily entailed by the design problem. These conditions dictate what solutions may inhabit the design space. In this thesis the problem framing consists of defining how any PCM cooling system must function and identifying the essential elements it must possess.

Design space mapping is the development of a set of rules or a taxonomy that allows the various design solutions that inhabit the design space to be classified in a clear and consistent way.

In chapter 5 the term '*sail*' is used. This is a heating or cooling element, normally a flat panel, which is located below the ceiling in an occupied space.

The reader is encouraged to consult the glossary if other terms need clarification.

As part of this EngD a number of collaborations were undertaken with Brunel Masters and level 3 mechanical engineering students to investigate the thermophysical properties of various commercially available PCMs and to perform controlled tests on PCM cooling systems. Those who collaborated in this work are collectively referred to as the '*Brunel PCM Research Group*'. The group was essentially led by Dr Zahir Dehouche and me, and is not intended to refer to a formally recognised research group at Brunel University. Rather, it refers to people who conducted PCM research that provided results used in this thesis. Whenever work of this nature is described, the work conducted by the students is made clear.

Executive Summary

1. Background

Part of a building's function is to provide thermal comfort to its occupants. Depending on building type and climate this may mean the cooling of a space. At present the cooling of buildings accounts for a large proportion of the world's electricity use and carbon dioxide emissions. For example, cooling accounts for around 20 and 57% of total end use consumption of energy in buildings in the U.S. and India, respectively (UNEP/GRID-Arendal, 2008). In 2000, 5% of non-domestic UK building energy was consumed by cooling and ventilation equipment (Hutt *et al.*, 2004) and this is widely acknowledged to be rising. It is now widely acknowledged that the emission of carbon dioxide is causing the earth's climate change, with potentially disastrous consequences for mankind. By reducing the energy required to cool buildings we can limit the damaging effects of climate change. Phase change materials (PCMs) can form part of this solution.

PCMs are materials with a high latent heat capacity and a melt/solidification temperature range that is appropriate to thermal storage and temperature control applications. For cooling buildings they are normally found in one of four types of system:

- ***Passive systems:*** Those that are in direct thermal contact with the space and discharge their accumulated heat to cold night air.
- ***Active systems:*** Those in which the PCM is contained in insulated tanks and a fluid, normally water, is required to transfer heat.
- ***Free-cooling system:*** Those in which PCM units are isolated from the space. Forced internal air flow is used to transfer heat from the space during the daytime and to discharge heat to outside air at night.
- ***Thermally activated systems:*** Those that are in direct thermal contact with the space during the daytime and discharge heat at night to a chilled water loop.

Each has its attendant advantages and disadvantages in terms of practical application, cooling performance and energy savings. It is contended that the systems currently in use can be improved upon to yield greater energy savings and better guarantee cooling performance.

2. Objectives and approach

The main aim of this thesis is to develop new PCM systems to reduce the energy required to cool buildings. A series of inter-related projects are presented that advance our understanding of how PCMs can be employed to reduce cooling energy. This culminates in the design and testing of a novel system called *NewMass*.

Each project may be seen as self-contained and contributing to knowledge, yet each yields conclusions that feed into the *NewMass* design development.

The contributions to knowledge are listed below under the chapters in which they found:

- **Chapter 3 – Study of an active PCM cooling system:** Post-installation energy audit of a central cooling system to establish the energy savings incurred by the presence of two PCM tanks.
- **Chapter 4 – Design space mapping:** The development of a new taxonomy for PCM cooling systems that clearly and consistently defines all possible systems, allowing gaps in the design space to be identified and researched further.
- **Chapter 5 – Passive PCM Sails:** The design and testing of PCM units that demonstrate the advantage of cross-envelope transfer in discharging accumulated heat at night.
- **Chapter 6 – Product testing:** Controlled testing and comparison of two passive PCM products, RACUS tiles and Energain panels.
- **Chapters 7 and 8 – Design, construction and testing of the *NewMass* system:** The design, fabrication, testing and modelling of a prototype PCM cooling system that minimises cooling energy and guarantees next-day performance.

Due to the differences in aims and methodologies of each project, they are each presented in their entirety in these separate chapters.

3. Study of an active PCM cooling system

Savings from active cool storage systems may be possible due to the increased COPs that result from night time operation of chillers. However, studies of active cool storage systems often reveal an energy penalty from a systems installation. To understand better why such systems succeed or fail an installed cooling system incorporating PCM tanks was monitored to establish energy use. The data was used to calculate the energy use of an identical system without the presence of the PCM tanks. It was found that the studied system incurred an energy penalty, chiefly due to the selection of a PCM whose solidification temperature was below that required.

The building is a 3250 m² UK office in which cooling is provided by two no. 241.3 kW chillers serving fan coil units, air handling units and chilled ceilings.

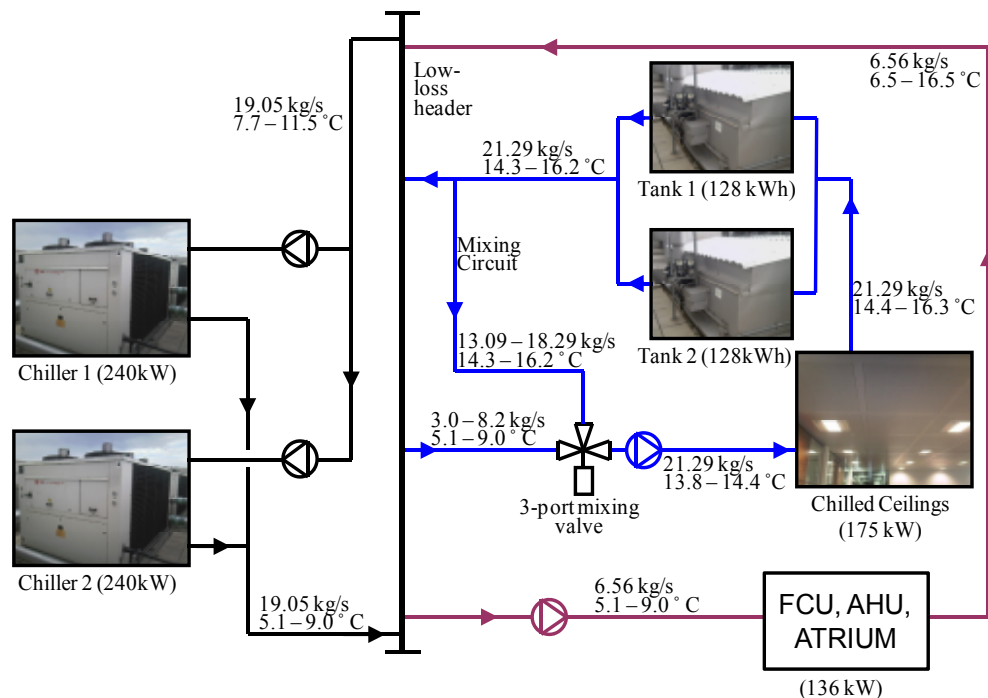


Figure ES.1 The cooling system at China Shipping House.

Two PCM tanks, containing stacks of commercially available hydrated salt, S-13 (peak freezing and melting temperatures 5.09 and 15.2 °C, respectively (Hasan, 2009), encased in high density polyethylene containers, are located on the return of the chilled beam circuit. The tanks are intended to save energy by pre-cooling chiller return water. Discharge of accumulated latent heat is effected at night, when chiller COPs are high.



Figure ES.2 Active PCM storage. One of the roof-mounted PCM tanks (left) and a stack of PCM containers (right).

Chiller power and system temperatures were monitored for 6 days. The additional daytime power input required for a tankless system was calculated using tank inlet and outlet temperatures and chiller performance curves for varying ambient temperatures. Differential scanning calorimetry results were used to calculate tank capacity and determine melt/solidification temperatures.

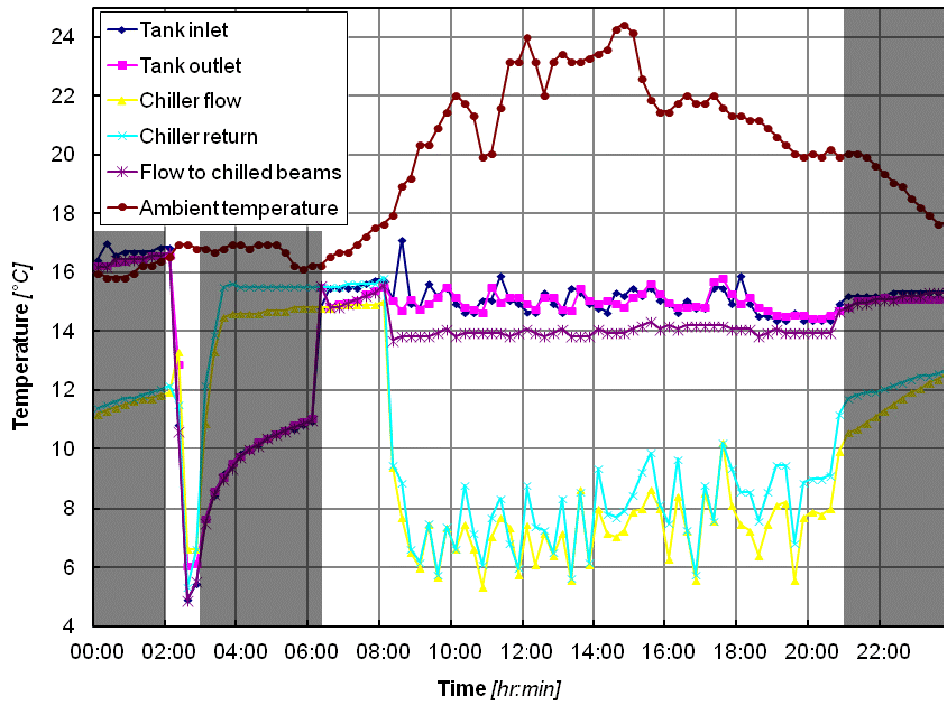


Figure ES.3 Active PCM cooling performance data. Temperature profiles for all relevant points in the system on Tuesday 8th September.

The system incurred an additional 687 kWh energy cost (10.6% of total cooling energy), as compared to an identical tankless system. This is because night chiller and pump electricity usage outweighed daytime savings. Only 28% of the tank capacity is utilised because the solidification temperature of the PCM is too low for sufficient heat rejection to the chilled water.

Table ES.1 China Shipping House cooling energy. Energy consumption and savings from the cooling system at China Shipping House over a 6 day late summer period.

	Energy (kWh)	CO ₂ (kg)	Percentage of cooling electricity consumption	Percentage of total building electricity consumption
Chiller power at night	615.3	318.1	9.5	3.5
Q _{chill,night}	717.3	370.8	11.1	4.1
Chiller power daytime	4910.1	2538.5	75.9	27.8
Q _{chill,day}	5748.6	2972.0	88.9	32.5
Q _{pcm}	6465.9	3342.9	100.0	36.6
Q _{tank,elec,day}	30.3	15.6	0.5	0.2
Q _{conv}	5778.9	2987.7	89.4	32.7
Q _{saved}	-687.0	-355.2	-10.6	-3.9

This work demonstrates that an integrated system design with appropriate PCM selection is essential to reduce energy costs. Under-cooling in the PCM will have a detrimental impact on energy savings if not adequately considered. However, even with an appropriately selected PCM the energy savings from this type of system can only be expected to be marginal since the savings are gained through chiller COP increase at lower night time ambient temperatures. This is normally insufficient to significantly offset the additional energy required for coolth generation.

Research into the systems that can provide energy savings should focus on systems that give options for free cooling and passive operation.

4. Design Space Mapping

One of the conclusions in the literature review was that there is some ambiguity and overlap in the generally accepted taxonomy used to classify PCM cooling systems, as well as a lack of any attempt to map out the design space and thus highlight under-researched system types. In this chapter all potential types of design for PCM cooling systems are mapped out. This was enabled by establishing a new method of classification for PCM cooling systems. There were four stages to this process:

1. The design problem was stated.
2. The problem was precisely framed in terms of all PCM cooling systems' fundamental elements and functions: Internal space, body of PCM, external heat sink/s, insulation between the other elements.
3. These elements were arranged in all possible physical configurations for the two fundamental processes of charging and discharging. This resulted in 11 system variants that constitute the new taxonomy; see Figure ES.4 and Figure ES.5.
4. All existing systems were then classified according to the new taxonomy. This revealed a number of new system types or system types that have been under-researched; see Figure ES.6.






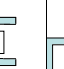


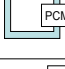
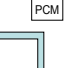

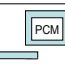
		Discharging					
							
Charging		1.	2.	3.	4.	5.	
			6.		7.		
				8.	9.	10.	
					11.		
							
							

Figure ES.4 Design space matrix. All potential PCM cooling system designs marked in yellow cells. Numbers are for reference to the list in Figure ES.5.

1. PCM located internally for charging and discharging. HTF required for discharge to external heat sinks and/or a chiller.
2. PCM located internally for charging but becomes insulated for discharge. HTF required for discharge to external heat sinks and/or a chiller.
3. PCM is located internally for charging but straddles the building envelope for discharge.
4. PCM is located inside for charging and outside for discharge.
5. PCM is located internally for charging. Internal and external spaces are united for discharge.
6. PCM fully insulated for charge and discharge. HTF fluid required for both heat transfer operations.
7. PCM fully insulated for charge and located externally for discharge. HTF required for charging process.
8. PCM straddles the building envelope for charge and discharge.
9. PCM straddles the building envelope for charging and is located outside for discharging.
10. PCM straddles the building envelope for charging. Internal and external spaces are united for discharging.
11. PCM located externally for charging and discharging. HTF required for charging period.

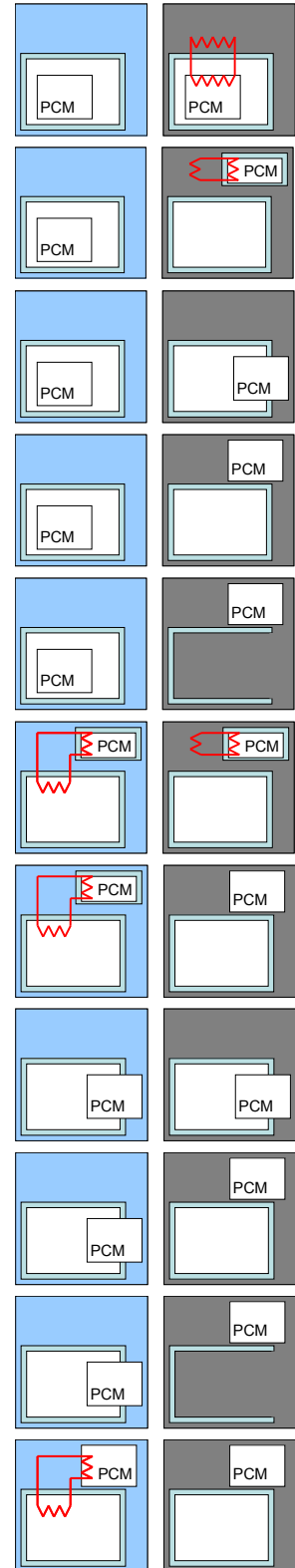
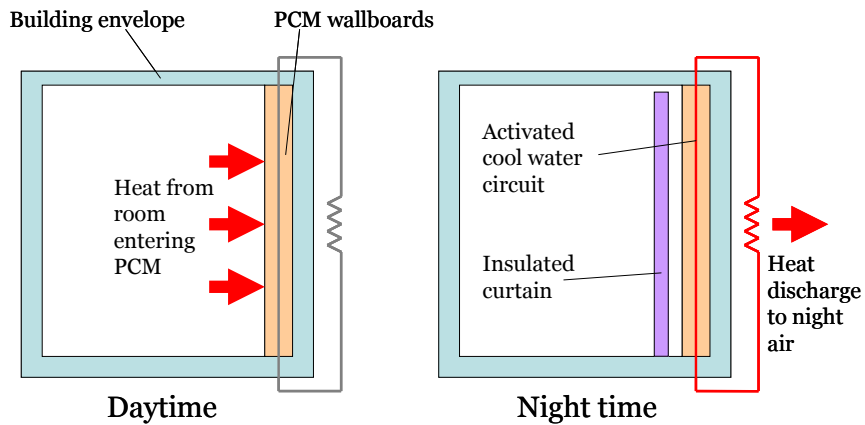
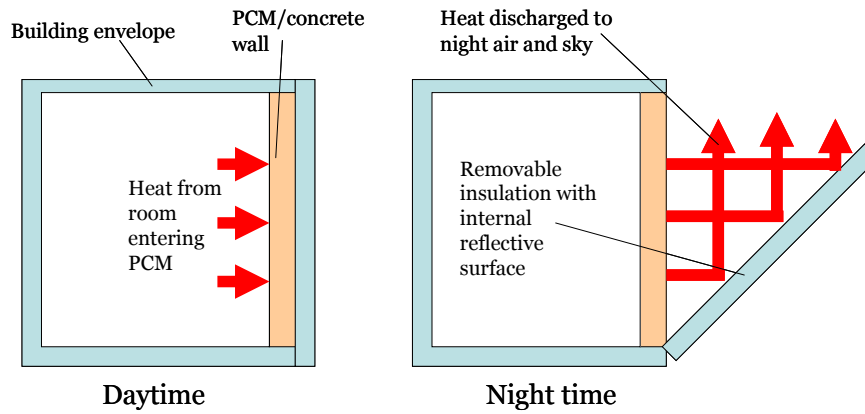


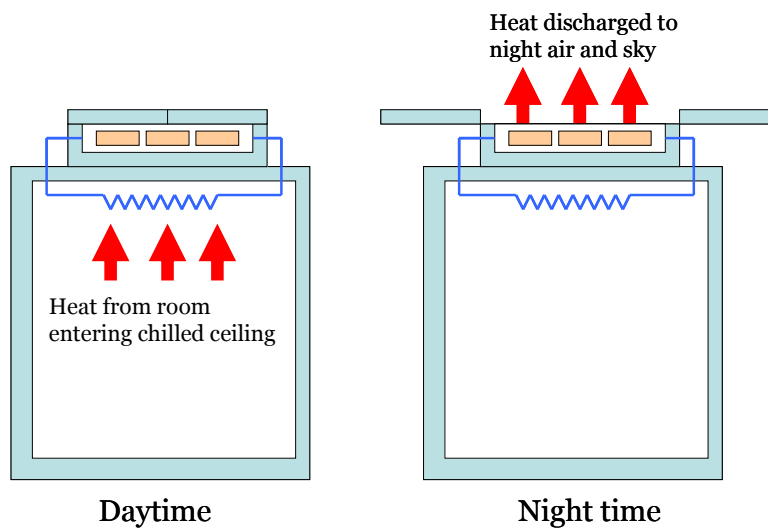
Figure ES.5 All system types with pictorial representations. Red lines indicate the requirement for a heat transfer fluid.



(i)



(ii)



(iii)

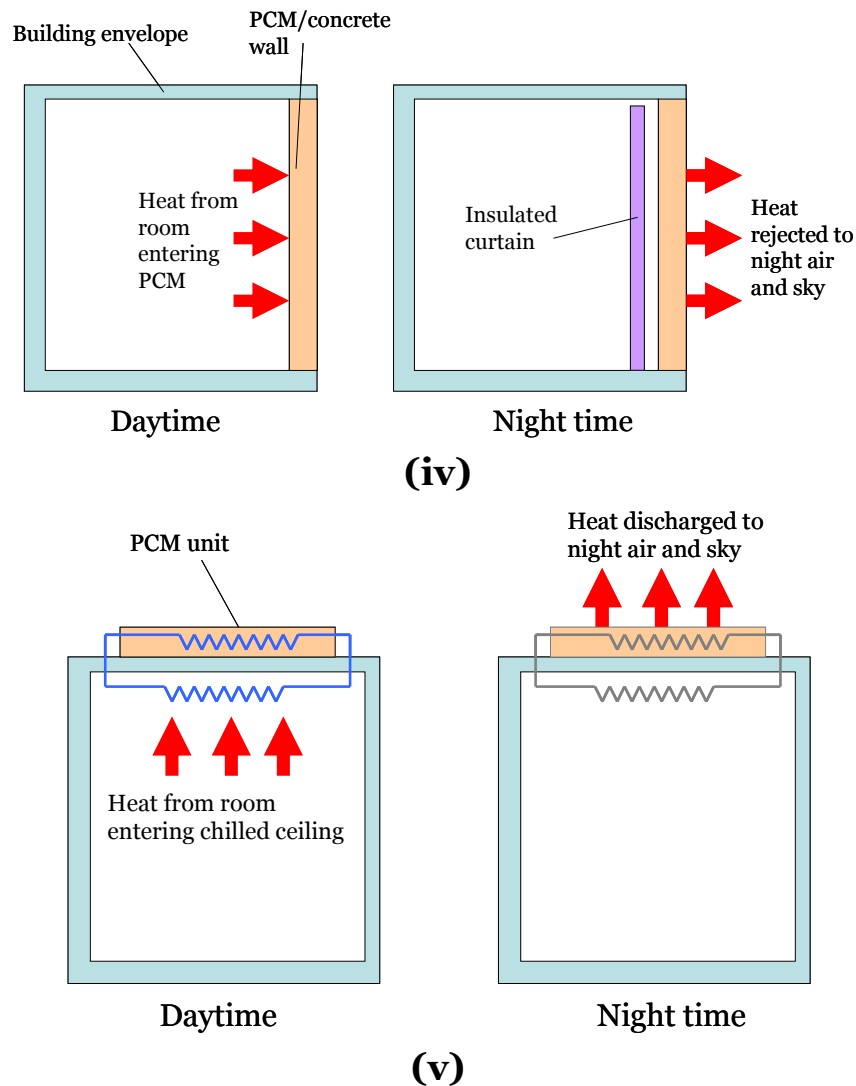


Figure ES.6 Novel PCM cooling system designs. (i) Thermally activated system with insulated curtain to limit heat gains at night. (ii) System with PCM integrated into the fabric and removable insulation to allow heat to escape at night. (iii) A PCM tank with removable insulation to discharge accumulated heat directly to the night sky. (iv) PCM integrated into the building fabric with internal insulation to prevent over-cooling at night. (v) Externally located PCM unit with cool water circuit connection to interior.

System types that have not been exploited commercially or in academic research mostly involve removable insulation or PCM movement. Some of these also involve a heat transfer fluid for charge or discharge. This process of classification and system design generation may be used in the future to develop new PCM systems.

The design of the Passive PCM Sails (chapter 5) and the NewMass system (chapters 7 and 8) resulted from this work.

5. Development of Passive PCM Sails

In this chapter the testing of a concept known as Passive PCM Sails is presented. This concept is intended to satisfy the opportunity for increased *thermal* and *cooling capacity* in passive systems, raised by the literature review, and to go some way to realising the system types 4, 7 and 9, proposed in chapter 4. To these ends, two design innovations were applied:

1. The units were deliberately not integrated into the building fabric. This increases the potential surface area and volume of PCM that may be utilised which consequently increases cooling and thermal capacity, respectively.
2. Three of the units were transferred outside at night to discharge their accumulated heat. This gives an indication of cross-envelope transfer effectiveness and what effect removable insulation could have.

Prototype modules of the Passive PCM Sails were constructed from commercially available paraffin/low-density-polyethylene (LDPE) composite material and positioned below the ceiling of an occupied office space to absorb excess room heat during the daytime. Variations in surface and melt temperature were also applied. Four modules in total were tested and are shown in Table ES.2.

Table ES.2 *Passive PCM Sail variations.*

Module reference	Discharge location	Surface	Manufacturer's melt temperature (PCM Products, 2011)
A22,Al,EC	External	Aluminium foil	22 °C
A26,Al,EC	External	Aluminium foil	26 °C
A22,Bl,EC	External	Aluminium foil and matt black paint	22 °C
A22,Bl,IC	Internal	Aluminium foil and matt black paint	22 °C

All modules were constructed from four 150 mm², 6.75 mm thick, composite tiles. Type-k thermocouples were placed at seven locations throughout the body of each module. The modules' temperatures were monitored along with air flow rate, air

temperature and globe temperature. Their small size meant any effect on room temperature was negligible.

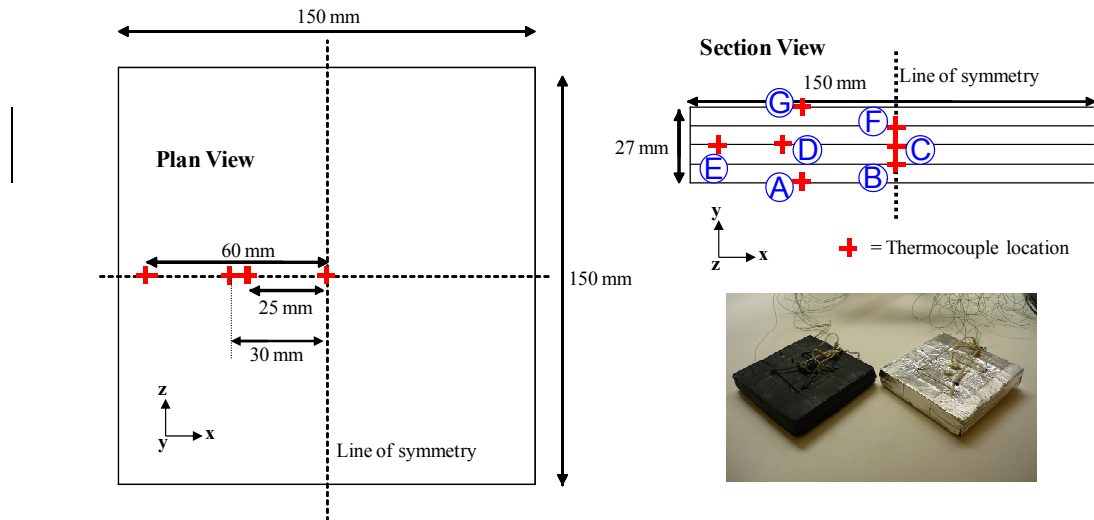


Figure ES.7 Module dimensions and thermocouple locations.

During daytime the modules hung from an internal rig 2.5 m above the ground; see Figure ES.8. At around 8:00pm the A22,B1,IC module remained in its position to discharge, while the rest were hung from a roof-top rig; see Figure ES.8. At around 7:00am the outside cooling modules were transferred from the external rig to the internal rig.

As one of the Brunel PCM Research Group projects, Tanawat Cheechern (Masters student) applied DSC to the composite PCMs and their constituent pure paraffins; see Table ES.3 and Figure ES.9. The in-situ measurements were used in conjunction with these DSC results to produce semi-empirical CFD models of the modules with the solidification/melting solver in FLUENT. This used an enthalpy porosity formulation to model phase change. The models were validated through comparison of predicted temperatures to measured internal module temperatures; see Figure ES.10.

Good validation was obtained for all modules with a notable divergence noted when maximum liquid fraction was reached. The validated model was then used to generate mean liquid fraction and surface heat transfer rate profiles for performance comparisons.

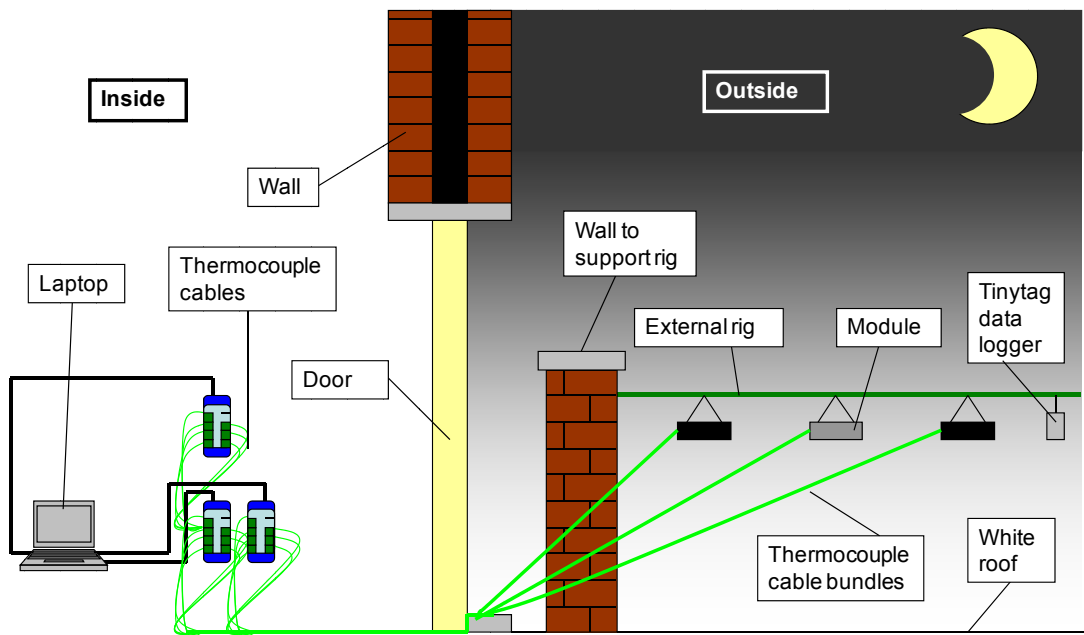
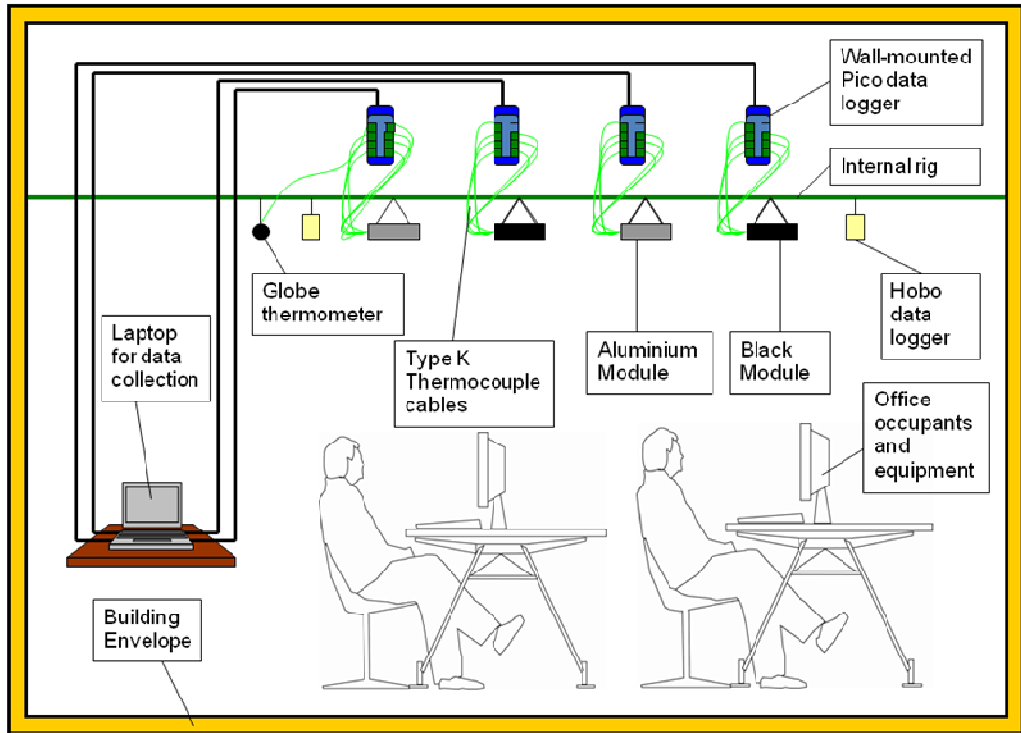


Figure ES.8 Internal and external rigs. The internal daytime set up (top) and external night time set up (bottom).

Table ES.3 Thermophysical properties of the PCM composites (Cheechern, 2009).

PCM Type	Density (kg/m ³)	Conductivity (W/m/K)	Specific Heat (J/kg/K)	Latent Heat (J/kg)	Melt onset temp (°C)	Freeze onset temp (°C)	Melt end temp (°C)	Freeze end temp (°C)
A22 Panel	852.7	0.2000	2304	74020	11.29	21.76	22.44	5.27
A26 Panel	834.4	0.2300	2387	75210	17.21	24.19	29.97	12.19

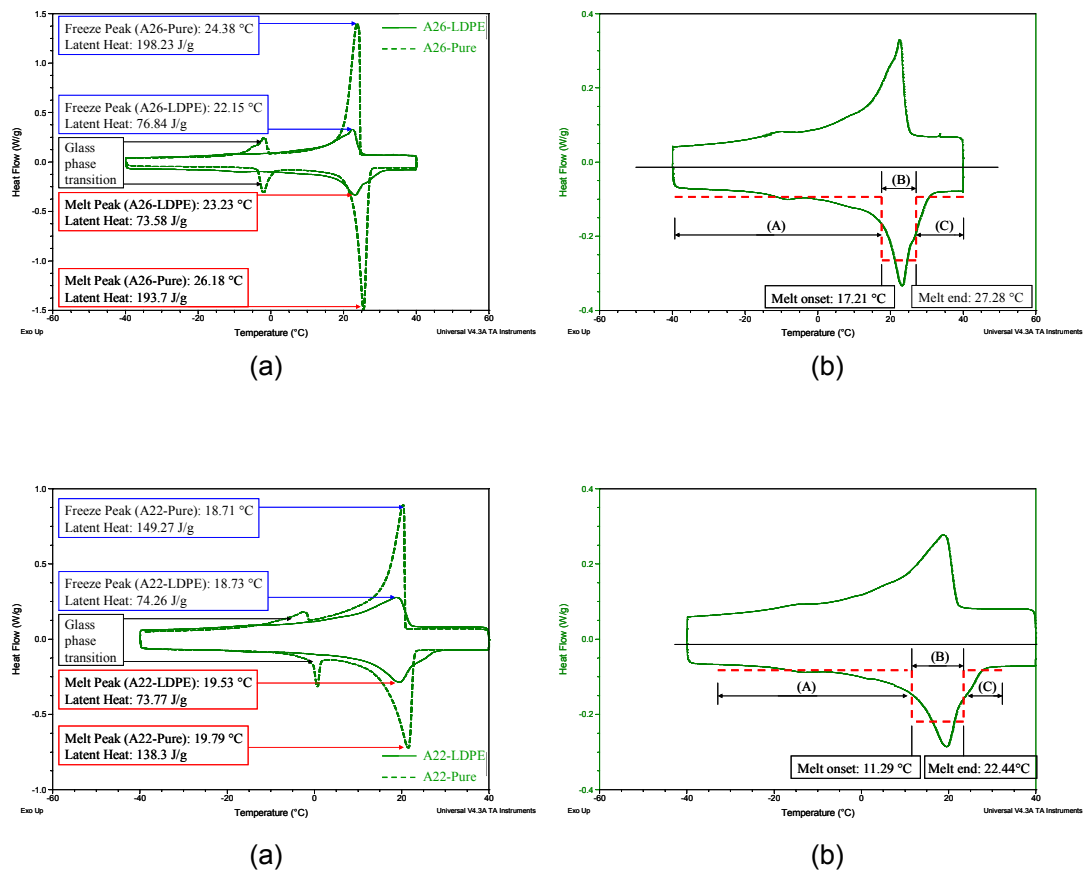


Figure ES.9 Pure paraffin and composite DSC curves (Cheechern, 2009). Top: (a) DSC curves of pure A26 paraffin and A26-LDPE composite. (b) The DSC curve of the composite is displayed here with the dashed red line representing the variation in heat flow rate per unit mass with temperature change, as defined by the FLUENT model. Bottom: (a) DSC curves of pure A22 paraffin and A22-LDPE composite. (b) The DSC curve of the A22-LDPE composite.

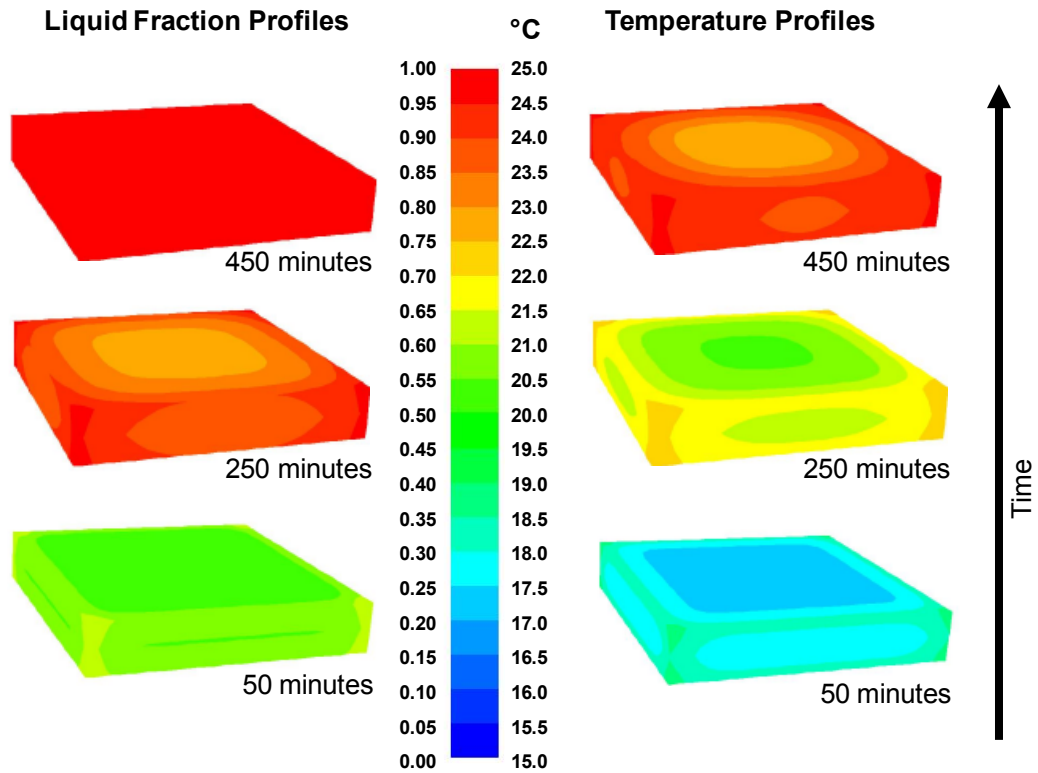


Figure ES.10 Temperature contours. The A22, AI, EC module at three stages of heating.

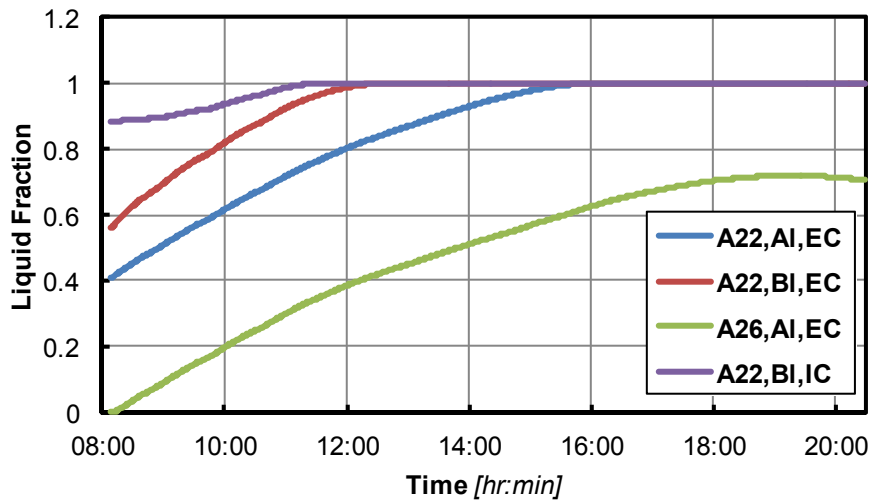


Figure ES.11 Average liquid fraction profiles of the four modules.

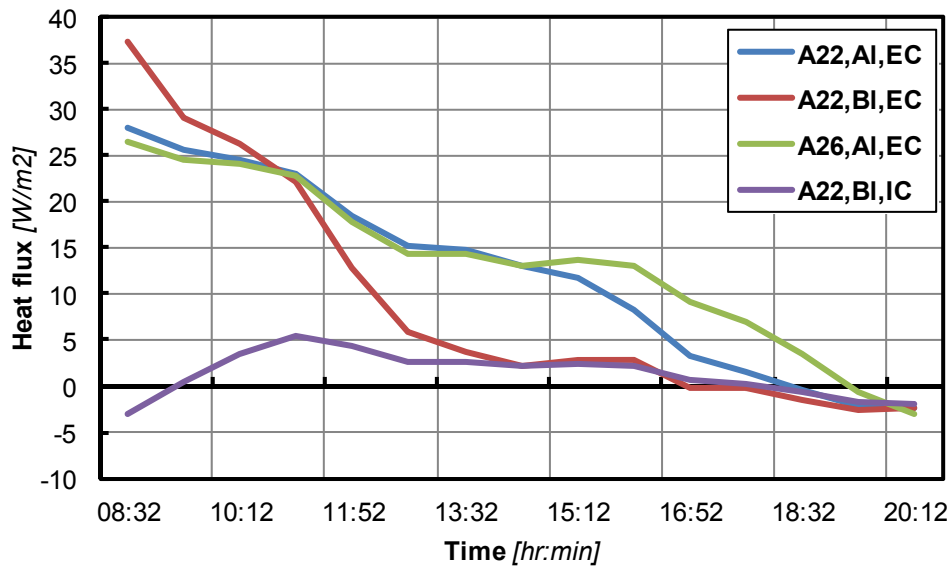


Figure ES.12 Surface heat flux profiles of the four modules. Positive values indicate heat flow into the module.

The DSC results showed that the composite materials had a lower latent heat and a broader melt peak when compared to their pure paraffin constituents; see Figure ES.9. Consequently, valuable thermal capacity was not utilised within the appropriate temperature range for cooling

The black paint raised heat transfer rate showing radiant heat transfer to have a significant effect. The module that discharged its heat inside became fully melted the following day much earlier than its externally cooled counterparts, highlighting an opportunity to greatly increase heat rejection, through the transport of PCM modules outside at night.

6. Testing of two passive PCM products

A thermal test cell was designed and built to assess the performance of PCM cooling products and ultimately to test the NewMass system that was designed as part of this EngD. The two products tested were the RACUS ceiling tile (Datum Phase Change, 2011) and the Energain panel (DuPont, 2007a).

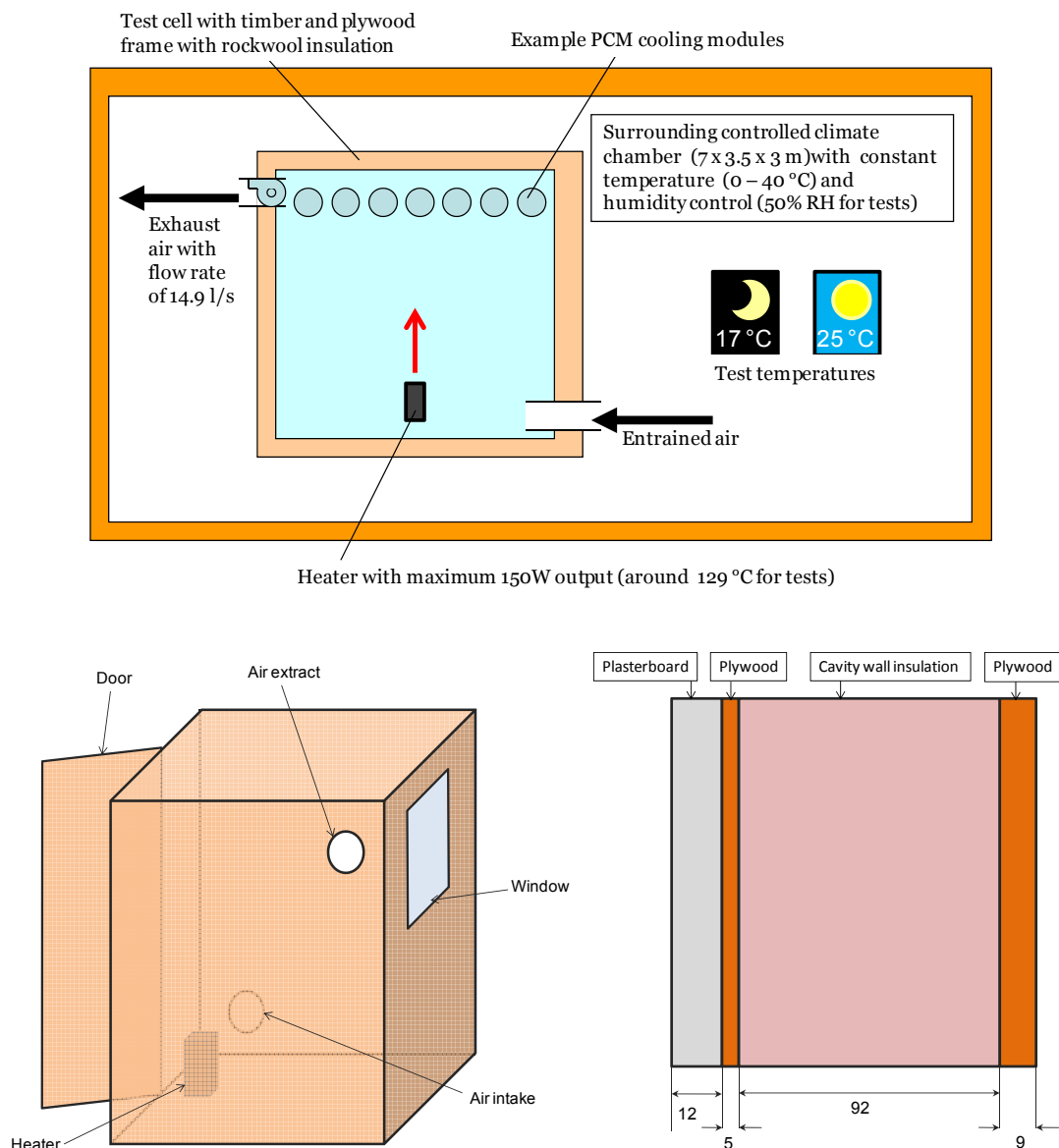


Figure ES.13 The thermal test cell. The test cell concept with test conditions (top). Axonometric representation with heater, ventilation intake and extract, window and door (bottom left). The wall build up; all dimensions in mm (right).

The test cell concept is as follows: One space to represent a building (test cell), containing a heating or cooling system, itself contained within a larger space which represents an external environment (climate chamber). The following conditions were established for both product tests and a control test with the cell empty.

Daytime conditions:

- Climate chamber at 25 °C.
- Test cell 150W rated heater on full power (~129W delivered power).
- No ventilation.

Night time conditions:

- Climate chamber at 17 °C.
- Test cell heater off.
- Fan extracting at 14.9 l/s.

The air temperature in the cell was monitored with thermocouples located 60 cm below the ceiling in the test cell and embedded within the PCM units.



Figure ES.14 Test cell images. Heater and thermocouple connections being checked (top left). Test cell with door open and laptop for data logging (right). Example thermocouple (Pico technology, 2011) (bottom left). Heater, Omega CS060 150W (bottom centre). Extract fan, XIL 100T Xpelair (bottom right).

RACUS tiles are 600 x 600 x 15 mm steel ceiling tiles filled with BASF micronal and a patented binder. They are designed to be installed in a false ceiling grid, primarily for offices. Two formulations were tested, one with 50% micronal content per unit weight, RACUS 73, and one with 70% micronal content by weight, RACUS 74.

The tiles tested were custom made to fit the test cell and arranged as shown in Figure ES.1.15.

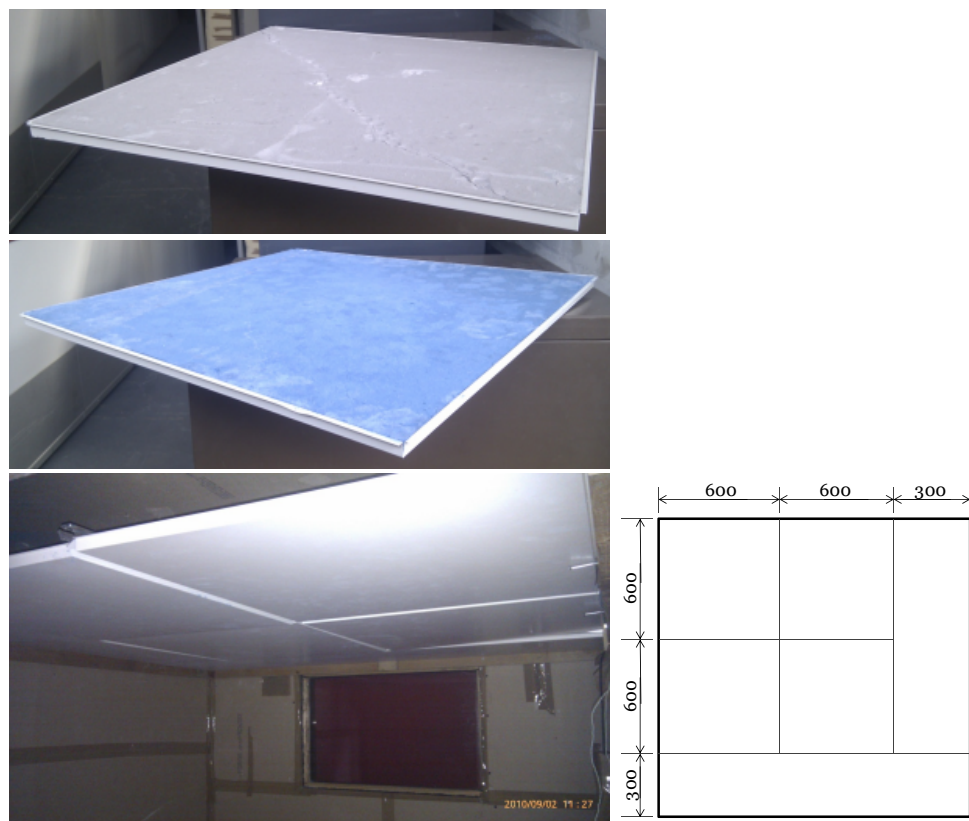


Figure ES.1.15 RACUS tiles. RACUS 73 (top left), RACUS 74 (middle left), ceiling grid installation (bottom left) (Oyeleke, 2010). The ceiling grid layout (bottom right).

As part of the Brunel PCM Research group, James Oyeleke (Masters student) performed DSC analysis on samples of both compounds to determine the thermophysical properties; see Table ES.4.

Table ES.4 Thermophysical properties of micronal and RACUS formulations (Oyeleke, 2010).

PCM formulation	Freeze onset temp (°C)	Melt onset temp (°C)	Melt peak temp (°C)	Freeze peak (°C)	Specific heat capacity (kJ/kgK)
Micronal	21.85	23.23	24.67	20.44	1.85
RACUS 73	21.97	23.24	24.42	21.16	2.04
RACUS 74	21.86	23.23	24.89	20.81	1.72

The latent heats, micronal concentrations, densities and resultant latent heats per unit volume are displayed in Table ES.5.

Table ES.5 Further Micronal and RACUS properties. Latent heats (Oyeleke, 2010), concentrations by weight (Underwood, 2011), densities (Underwood, 2011) (BASF, 2011), and calculated latent heat per unit volume.

PCM formulation	Latent heat (kJ/kg)	Concentration Micronal by weight (%)	Density (kg/m ³)	Latent heat per unit volume (m ³)
Micronal	122.5	100	300	36750
RACUS 73	60.13	50	802	48220
RACUS 74	85.57	70	569	48690

Energain panels are supplied in 1 x 1.2 m, 5.26mm thick units. Formed of a shape-stabilised paraffin/copolymer composite (60% paraffin, 40% copolymer, by weight) and covered with thin aluminium sheeting they are designed to be cut to size in order to fit any wall or ceiling (DuPont, 2007b). Panels were to cover all internal walls and the entire ceiling in the test cell. Again, as part of the Brunel PCM Research Group work, Adrien Capitani (mechanical engineering exchange student) conducted DSC tests on the panel material and its constituent paraffin; see Table ES.6

Table ES.6 Thermophysical properties of Energain panel and pure constituent paraffin (Capitani, 2011).

PCM	Latent heat (kJ/kg)	Melting onset temp (°C)	Melting peak temp (°C)	Freezing onset temp (°C)	Freezing peak temp (°C)
Energain panel	73	8.64	19.98	22.44	15.55
Energain pure	151.6	16.51	22.45	22.05	21.8



Figure ES.16 Energain panels applied to the internal surfaces of the test cell.

I designed the test procedure but the day to day running of the tests was carried out by Oyeleke and Capitani. The results showed that all units have a clear moderating effect on temperature rise within the cell; see Figure ES.17. Energain panels performed best in this respect but when the peak temperature reduction was normalised with respect to the PCM content, the RACUS 73 formulation was shown to be most effective; see Table ES.7 Results for the product tests with comparisons on the basis of peak temperatures and energy savings and the same parameters normalised with respect to mass of PCM and floor area. CO₂ emissions are calculated assuming a 0.517 kgCO₂/kWh carbon factor.

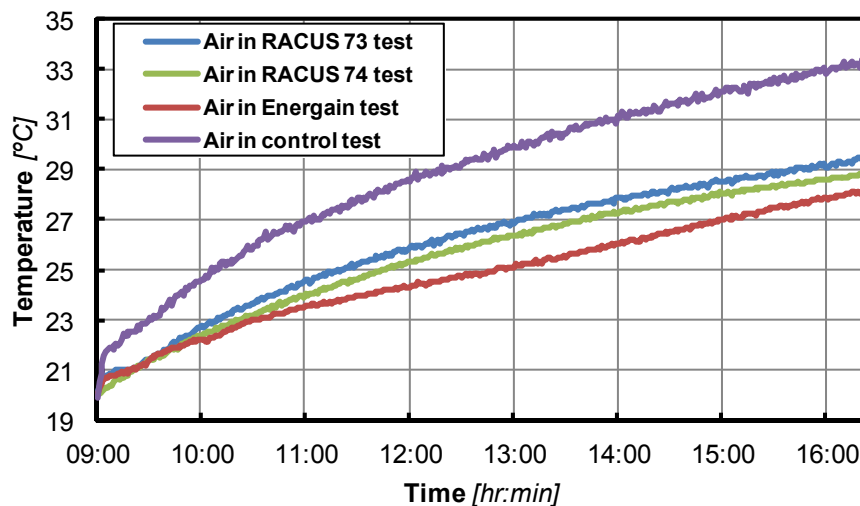


Figure ES.17 Combined charge period results.

Table ES.7 Results for the product tests with comparisons on the basis of peak temperatures and energy savings and the same parameters normalised with respect to mass of PCM and floor area. CO₂ emissions are calculated assuming a 0.517 kgCO₂/kWh carbon factor.

	RACUS 73	RACUS 74	Energain	Control
Mass of PCM (kg)	13.33	13.24	36.28	0
Floor area (m)	2.45	2.45	2.45	2.45
Peak air temperature (°C)	29.5	28.8	28.1	33.3
Peak air temperature reduction (°C)	3.76	4.44	5.16	0
Peak air temperature reduction per unit mass (°C/kg)	0.28	0.34	0.14	0
Peak air temperature reduction per unit floor area (°C/m²)	1.53	1.81	2.11	0
Projected cooling energy required (Wh)	649	596	456	808
Projected cooling energy saved (Wh)	159	213	353	0
Percentage cooling energy saved (%)	19.7	26.3	43.6	0
Projected cooling energy saved per unit mass (Wh/kg)	11.9	16.1	9.7	0
Projected cooling energy saved per unit floor area (Wh/m²)	64.9	86.9	143.9	0
Projected carbon dioxide emissions (g)	95.9	88.0	67.3	119.4
Projected carbon dioxide savings (g)	23.5	31.4	52.1	0.0

The RACUS tiles were also able to discharge their heat more effectively than the Energain panels since they are better exposed to the passing cool air; see Figure ES.18 Combined discharge period results.. Furthermore they are easier to install and remove, requiring only the ceiling grid to be put in place.

The advantages of the RACUS design arise from the fact that the tiles are not integrated into the building fabric and are encased in a relatively conductive metal shell to promote heat transfer.

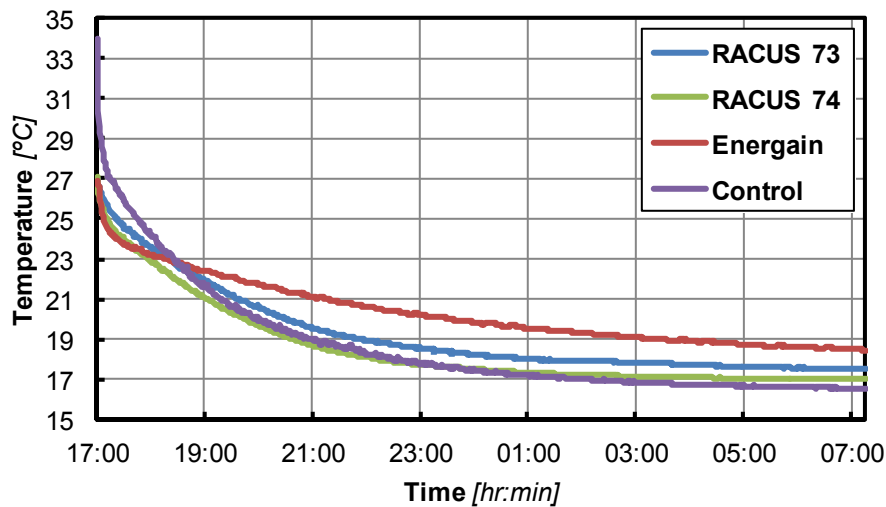


Figure ES.18 Combined discharge period results.

7. NewMass system design

The findings of the previously described projects fed into the design of a novel PCM cooling system known as NewMass. It consists of an array of black anodised finned tubes, for enhanced convective and radiant heat absorption, located below the ceiling of an occupied space. The tubes contain a hybrid material formed of pure A22 paraffin (peak melting temperature of 19.8 °C) and a lattice of small aluminium cylinders, or Raschig rings, for enhanced conduction. An aluminium pipe runs along the axis of each finned tube and allows accumulated heat to be discharged to a chilled water loop. These features in concert constitute an entirely new design.

The system is designed to passively absorb heat from the space during the day. Heat is then discharged at night to circulated night air. This passive discharge is prioritised but should the system be unable to sufficiently reject its heat to the air, the chilled water loop can be engaged to reject any remaining heat and thus guarantee performance the following day. During daytime operation if internal temperatures rise beyond a specified set point then the chilled water loop may be engaged again to maintain thermal comfort. Through passive and active operation the system is able to minimise electricity consumption and guarantee cooling performance, respectively.

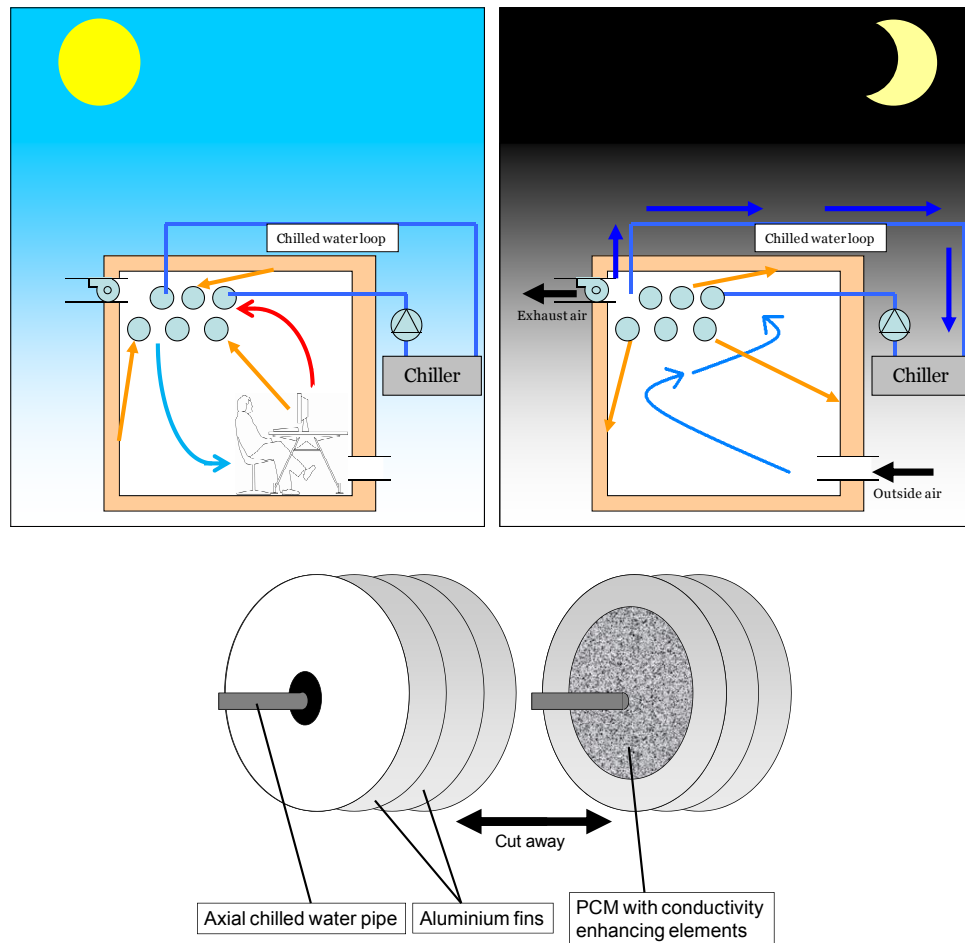


Figure ES.19 NewMass concept. System in charging mode during the day (top left), system in discharge mode (top right) and example of single unit (bottom).

The fin arrangement chosen was a compromise between the optimum arrangement that would give maximum heat transfer under natural convection and the arrangement that allowed reliable tube fabrication on a CNC machine.



Figure ES.20 Images of the NewMass units. Completed unit (top), uncapped unit exposing Raschig rings and the chilled water pipe (left), cap with O-ring (upper right) and all finned tubes prior to assembly (bottom right).

8. NewMass system testing

The aim of the NewMass system tests was to assess the performance of the system, in terms of its ability to control internal temperature, and to establish what energy savings could be made from its installation and use.

As part of this process the relationship between the temperature of each unit and the thermal energy was sought. This allowed tracking of the NewMass unit enthalpy and heat absorption rate. It also allowed for the construction of the annual energy savings model.

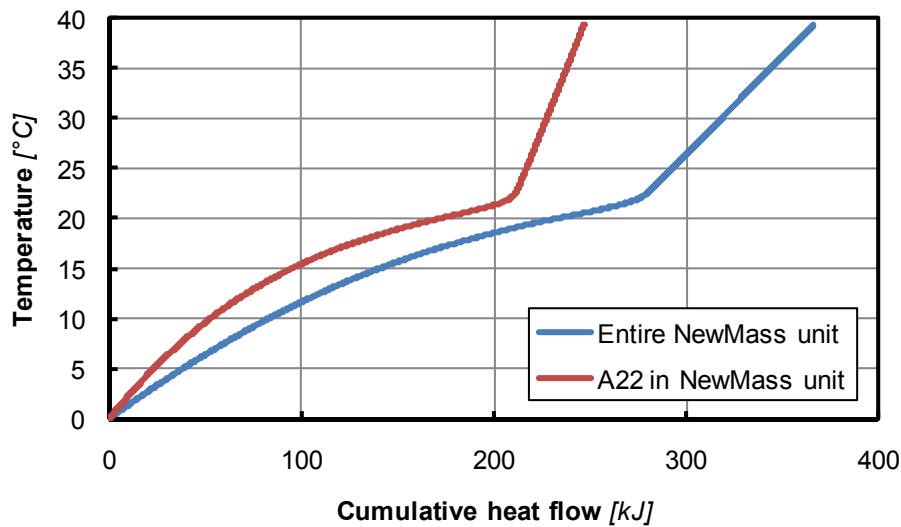


Figure ES.21 Temperature vs cumulative heat flow.

The blue curve in Figure ES.21 Temperature vs cumulative heat flow can be seen to be formed of 3 sections which can be accurately described as polynomials, allowing any temperature of the NewMass unit to be calculated from its enthalpy value and vice versa. This allowed the construction of an annual energy savings model.

Table ES.8 Masses of all NewMass units and their main constituents. All figures in kg.

Tube	Total	Empty tube	Raschig	
			rings	A22
1	4.585	2.485	0.869	1.230
2	4.540	2.467	0.877	1.196
3	4.565	2.480	0.888	1.197
4	4.575	2.490	0.871	1.214
5	4.575	2.495	0.889	1.191
6	4.740	2.495	0.960	1.256
Total	27.580	14.912	5.354	7.285

The system was installed in the thermal test cell and connected to a chilled water circuit comprising a chilled water bath, pump needle valve and flow meter.

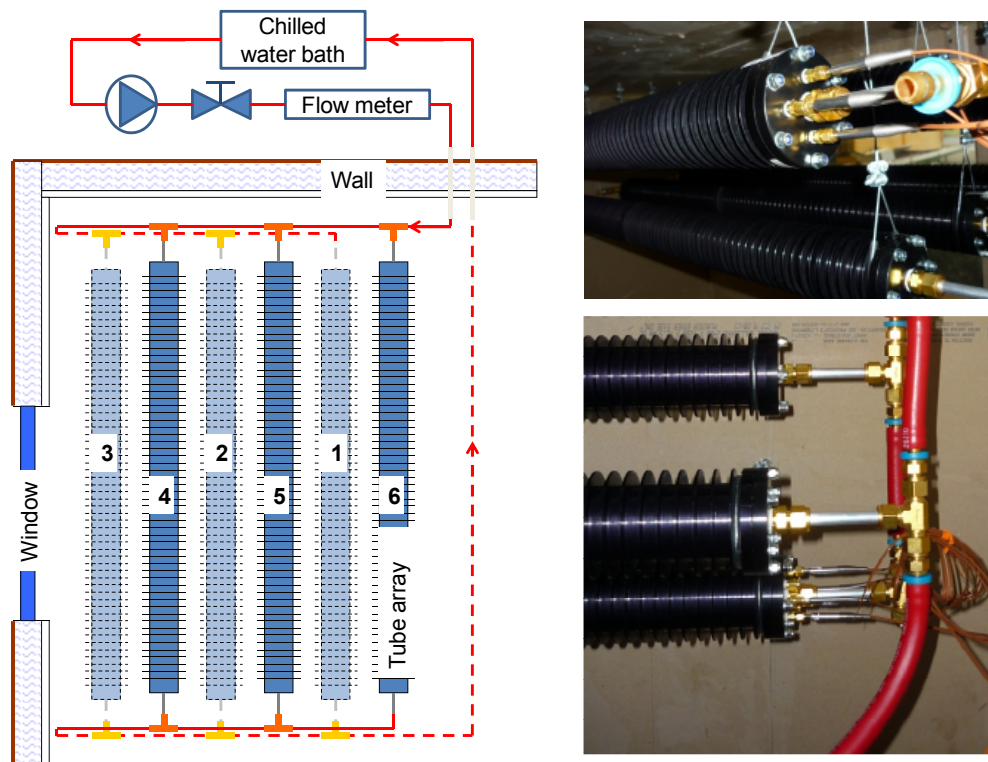


Figure ES.22 *NewMass system components. Schematic of array and chilled water circuit (left), images of the installed tubes (right).*

A series of charge and discharge tests were conducted to establish system performance. The system was clearly seen to suppress the room air temperature rise during passive charge, performing similarly to the RACUS tile sand Energain panels; see Figure ES.23 Medium level air temperature profiles of all four installations and the control test..

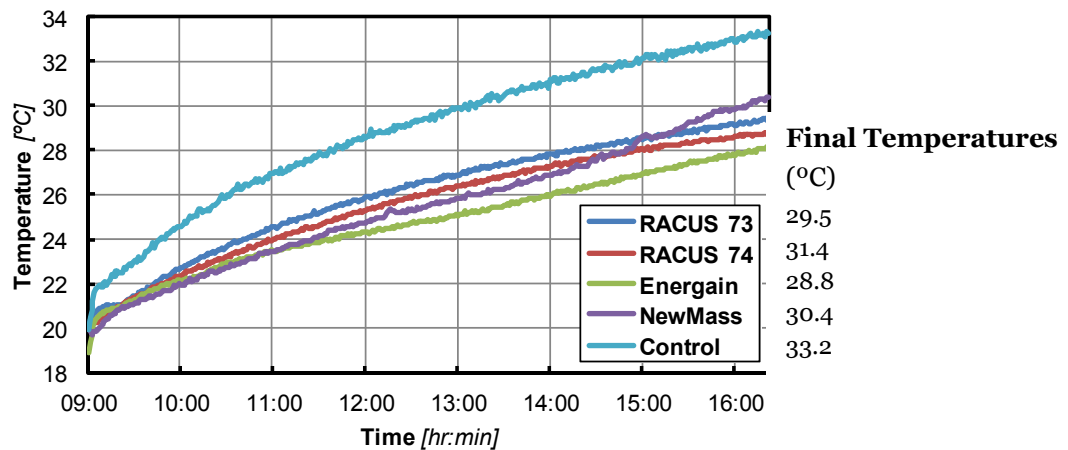


Figure ES.23 Medium level air temperature profiles of all four installations and the control test.

During this test the heat transfer coefficient at the finned tube surface was found by applying the derived temperature-enthalpy polynomials to the internal NewMass unit temperatures recorded see Table ES.9.

Table ES.9 Values for heat transfer coefficient from empirically derived equation, CFD modelling and experiment.

Source of value	Heat transfer coefficient W/m ² /K
Prediction from empirically derived equation	2.31
Prediction from CFD model	3
Mean experimentally determined value	3.28

A supplemented cooling test was conducted in which the chilled water loop was engaged, at 13 °C and 2 l/min, when the temperature in the test cell rose above 25 °C. This led to near perfect temperature control of around 24.5 °C.

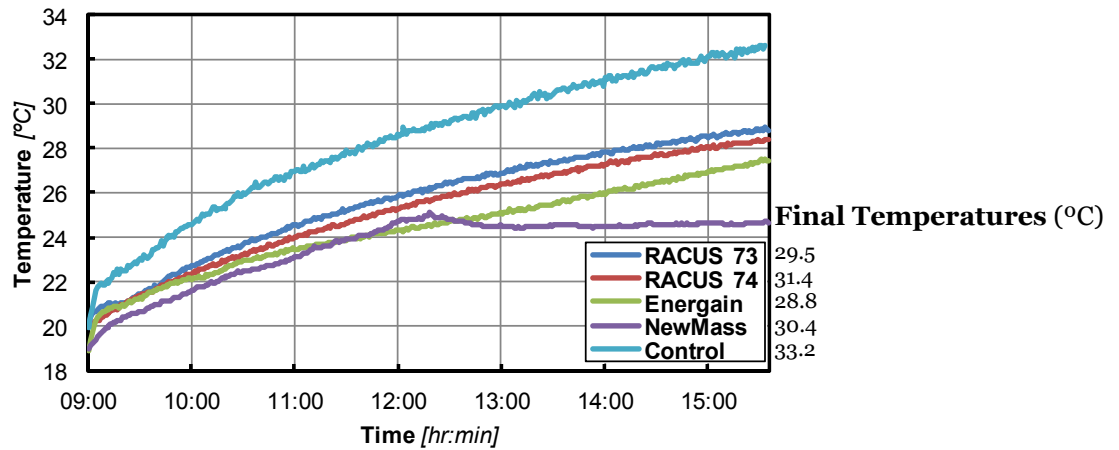


Figure ES.24 Medium level air temperature profiles of all four installations and the control test with NewMass in supplementary cooling mode.

In passive discharge mode there was a low rate of discharge from units due to a low heat transfer coefficient of $1.0 \text{ W/m}^2/\text{K}$ and a low temperature difference between the NewMass units and the surrounding air. The low heat transfer coefficient is most likely due to flow of air across rather than between fins. In contrast the chilled water system was extremely good at discharging heat.

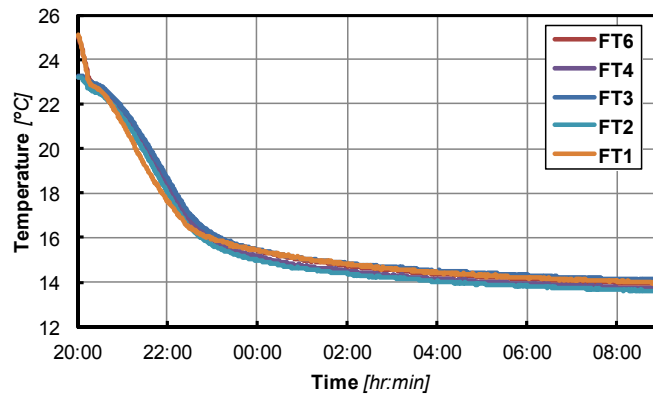


Figure ES.25 Temperature of all NewMass units during active discharge mode.

A thermal conductivity for the paraffin/Raschig ring composite of 3.4 W/mK was calculated by monitoring water NewMass temperatures in steady state conditions.

The system has potential to dramatically reduce the energy consumed in cooling buildings. The annual energy savings model predicted the NewMass system to save 34% of energy consumption as compared to a conventional fan coil cooling system in a UK office building.

9. Publications

As a result of this research two conference papers and one journal paper have been published:

- ‘Tests of PCM ‘Sails’ for Low Energy Office Cooling.’ Presented at *The 11th UK National Heat Transfer Conference*, 6th – 8th September 2009, London
- ‘Development of passive and active PCM ‘sails’ for low energy cooling.’ Presented at the *Passive and Low Energy Cooling Conference (PALENC) 2010*, 29th September – 1st October 2010, Rhodes
- ‘Tests of Prototype PCM Sails for Office Cooling.’ Published in *Applied Thermal Engineering* (Volume 31, Issue 5, April 2011)

At the time of writing a further article was in peer-review for publication in *ICE Energy*: ‘Energy Performance of an Office Cooling System with PCM Tank’, based on the work described in chapter 3.

Also, at the time of writing a third journal paper concerning the development, testing and modelling of the NewMass system was being prepared for submission to the journal, *Building and Environment*.

References

Artica (2009) *Artica Technologies: Classic*. Available:

<http://www.articatechnologies.com/solutions.php> [03/01/2012].

BASF (2011) *Micronal PCM*. Available:

http://www.micronal.de/portal/load/fid443847/BASF_Micronal_PCM_Brochure%202009_English.pdf [01/03/2012].

- Cabeza, L.F., Roca, J., Nogues, M., Zalba, B. and Marin, J.M. (2002)
 "Transportation and conservation of temperature sensitive materials with phase change materials: state of the art", *ECES IA Annex 17, Advanced Thermal Energy Storage Techniques - Feasibility Studies and Demonstration Projects, 2nd Workshop*, IEA.
- Capitani, A. (2011) *Energy savings in buildings: Phase change materials*, Brunel University, Uxbridge.
- Cheechern, T. (2009) *The Application of the Shrinking Core Model to Phase Change Materials (Masters Dissertation)*, Brunel University, Uxbridge.
- Datum phase change (2011) *Suspended ceiling tiles*. Available:
<http://www.datumphasechange.com/index.php?racus-honeycomb-ceiling-tile>
 [02/01/2012].
- DuPont (2007a) *DuPont Energain - Energy saving thermal mass systems: Installation Guidelines*, DuPont, Luxembourg.
- DuPont (2007b) *DuPont Energain*. Available:
http://www2.dupont.com/Energain/en_GB/ [29/04/2007].
- Hasan, R. (2009) *Monitoring and modelling of an air-conditioning system utilising phase change material (PCM) to establish energy savings (Masters dissertation)*, Brunel University, Uxbridge.
- Humphreys, M. and Nicol, F. (2007) "Environmental Criteria for Design" in *Environmental Design - CIBSE Guide A*, ed. D. Braham, 7 - Issue 2 edn, CIBSE, London, pp. 1-1-1-37.
- Ilkazell (2010) *Ilkatherm Ceiling*. Available:
http://www.ilkazell.de/en_baudecke.php [21/02/2010].
- Oyeleke, A.J. (2010) *Controlled tests and monitoring of a semi-active PCM cooling system (Masters dissertation)*, Brunel University, Uxbridge.

PCM Products (2011) *PlusICE PCM (Organic) (A) range*. Available:
http://www.pcmproducts.net/files/a_range.pdf [21/01/2012].

Pico Technology (2011a) *Thermocouples*. Available:
<http://www.picotech.com/thermocouples.html> [22/01/2012].

Rekacewicz, P. *Greenhouse Effect*. Available:
<http://maps.grida.no/go/graphic/greenhouse-effect> [03/10/2011].

Underwood, S. (2011) *Density of RACUS ceiling tile*, Datum Phase Change, London.

Voller, V.R. (1996) "An Overview of Numerical Methods for Solving Phase Change Problems" in *Advances in Numerical Heat Transfer (Volume 1)*, eds. W.J. Minkowycz and E.M. Sparrow, 1st edn, Taylor & Francis, Abingdon, pp. 341-375.

INTRODUCTION

1.1 Climate change legislation and building energy use

The burning of fossil fuels to generate power is causing the earth's climate to heat up. The resulting threat to life is considerable. By reducing the energy we use, the damaging effects of climate change can be limited. The international community has attempted to develop strategies to achieve this by establishing agreements through the United Nations. The Kyoto Protocol to the United Nations Framework Convention on Climate Change committed 37 industrialised nations to binding targets for greenhouse gas emission reduction (UNFCCC, 2008). These targets were then made legally binding through interpretation at the supranational and/or national level. The UK's Kyoto protocol target is a reduction in carbon emissions of 12.5% as compared to 1990 levels between 2008 and 2012 (DECC, 2011).

In step with the domestic and international desire to tackle the causes of climate change the UK government passed The Climate Change Act 2008 (DECC, 2010a). This introduces a legally binding framework for medium and long-term carbon emission reductions based on 5 yearly carbon budgets up to the year 2050 (DECC, 2010a). The Climate Change Committee, the body appointed to advise on carbon emission reductions (DECC, 2010b), recommended that the UK reduce emissions by 80%, as compared to 1990 levels, by 2050 and that 'carbon budgets' be introduced for the period 2008 to 2022 (Turner et al., 2008).

Any work to reduce global energy use must have a major focus on the built environment. The Intergovernmental Panel on Climate Change state that in 2004 buildings were responsible for the emission of 8.6 GtCO₂ or almost 25% of global emissions. Furthermore, they predict buildings to be responsible for approximately

30% of global CO₂ emissions (11.4 to 15.6 Gt) in the years leading up to 2030 (Metz et al., 2007).

In the UK buildings account for 41.5% of total CO₂ emissions (Turner et al., 2011). Emission reductions are driven by Part L of the building regulations which require minimum standards in construction for efficient buildings and a reduction in predicted emissions from new buildings as compared to a nominal standard case (HM Government, 2010).

The regulations were introduced in 2005 as a national response to the EU's Energy Performance in Buildings Directive which requires an enhancement of national building regulations and energy certification for all new buildings (Directorate-General for Energy and Transport, 2008).

Two of the main reasons why buildings use so much energy are their heating and cooling, required to maintain thermal comfort.

1.2 Thermal Comfort

Buildings have many functions but the provision of shelter is commonly said to be essential. A better way to understand this function is to see the building as creating an environment in which humans can comfortably exist. As well as the more obvious protection from wind, rain and sun, the internal environment should have good air quality and be at an appropriate temperature. The sense of whether the room is at the right temperature may be termed 'thermal comfort'. This is defined as:

“Satisfaction with the thermal environment.” (ASHRAE, 2004)

Thermal comfort is about more than just feeling comfortable. The metabolic activity of the human body results in the generation of heat that must be dissipated. At the same time the body must maintain a well-defined temperature profile in order to avoid falling into ill health. The core must remain between 36.5 and 37.5 °C, the skin must be around 30 °C at the extremities and the body stem and the head must be 34 – 35 °C (Shapiro & Epstein, 1984).

Body temperature is controlled by the hypothalamus which is located in the brain and bathed in arterial blood allowing it to monitor the body's temperature. The hypothalamus also receives information from temperature sensors in the skin and other parts of the body (ASHRAE, 2009). Deviations from the body's optimum temperature profile will result in thermal discomfort and the hypothalamus will act to realign the body's temperature. This is done through several physiological processes, the most important of which is the regulation of blood flow to the skin. Vasodilation increases the size of blood vessels and therefore blood flow to the skin. This allows the body to lose heat at a higher rate. Vasoconstriction does the opposite, slowing blood flow to the skin and reducing heat loss from it. The second main process of temperature regulation is sweating. Sweating allows the body to cool itself through the evaporation of water (ASHRAE, 2009).

A healthy body will be able to keep its temperature within a certain range but control of the local environment is often required to remain comfortable and healthy. The thermal comfort of human beings will vary with several factors:

- Activity level.
- Air temperature.
- Relative humidity.
- Radiant temperature.
- External climate conditions.
- Clothing.
- Metabolic condition of the subject.

When the local environmental conditions, the dry bulb, wet bulb and radiant temperatures exceed certain thresholds, the human body will fail to be able to control its temperature. In extreme cases the body will go into hyperthermia (overheating) or hypothermia (overcooling) (ASHRAE, 2009). Cases of hyperthermia appear to be on the rise. For example deaths and health issues increased due to heat waves in California and New York in 2006 and the summer of 2007 saw temperatures in Athens reach dangerously high levels leading to a large rise in the number of heat related health issues (Pantavou et al., 2011). However it was in 2003 that Europe experienced its most extreme heat wave with 52,000 deaths (Larsen, 2006).

It is not just the extreme cases that we should be mindful of. The chartered institute of building services engineers (CIBSE) point out that the world health organisation's constitution defines health in terms of general well-being, not just the lack of illness. They conclude that the maintaining of thermal comfort is properly seen as the promotion of good health (Humphreys et al., 2007). Logically this applies equally in less than extreme cases. In general, therefore, we can conclude that the temperature control in buildings is always important for our health and well-being.

The temperature range for thermal comfort is known as the thermal comfort zone and may be thought of as the target for a well performing cooling or heating system. Clearly, there is a variation in what is comfortable according to the factors listed above, hence the zone shifts. CIBSE provide guidance on the operative temperature range for different building types depending on season, activity level and clothing. An example is given in Table 1.1.

Table 1.1 Office operative temperature ranges. Variables: Season, clothing and activity level (Humphreys et al., 2007)

Season	Activity level	Activity (met)	Clothing	Clothing (clo)	Operative temperature range (°C)
Winter	Filing, seated	1.2	Underwear, shirt, trousers, socks, shoes, thin over-garment	0.85	21 – 23
Summer	Filing, seated	1.2	Underwear, shirt, trousers, socks, shoes	0.7	22 – 24

Further variation is found with cooling strategy. Unconditioned offices may tolerate temperatures of 25 °C for most of the year and 28 °C for less than 1% of the year (Humphreys et al., 2007).

Despite this variation it is clear that the zone of thermal comfort does not stray far outside the 21 to 25 °C (28 °C maximum) range for relatively sedentary activities and regular indoor clothing.

1.3 Temperature Control

Temperature control requires a little more sophistication than just erecting a simple barrier against the weather's more inclement elements. Pre-historic man was able to use wood fires for warmth (Derry & Williams, 1960) and even in the early stone age an indoor fire was essential (James & Thorpe, 1995). The practice of indoor heating with a wood fire has persisted to the present day, with the only major innovation being the widespread addition of a chimney to 12th century European dwellings to channel the smoke produced (James & Thorpe, 1995). Other notable heating innovations over the last few thousand years include the central heating of buildings by the Romans, where hot air created by a furnace was channelled through passageways beneath buildings to heat the spaces within, and the piping of natural gas to dwellings for heat and light by the Chinese before 350 AD (James & Thorpe, 1995).

The provision of heat is a simpler problem to solve than its removal. The ancient Persians were particularly ingenious when it came to cooling, employing several techniques such as channelling wind through damp passageways where the air would be cooled evaporatively and then released into the building (Bahadori, 1976). A technique employed by the Tang Emperors of China in the 8th century A.D. was a water-powered fan to keep air moving (James and Thorpe, 1995). A simpler and more widely used method is to employ thermal mass, building material with a high specific heat capacity that can absorb excess heat during the daytime and release it at night to the cool night air or sky. The most common forms of thermal mass in modern buildings are concrete and brick. Other examples of thermally massive materials include stone, mud-brick (Ogoli, 2003) and rammed earth.

In the developed world wood fire heating has largely been replaced by gas boilers and radiators. Cool stone walls and evaporative cooling, on the other hand, have given way to refrigeration through the compression cycle and distribution systems such as a fan coil units and variable air volume HVAC systems.

Design responsibility for the thermal comfort of the occupants of a building falls chiefly to the building services engineer who will attempt to satisfy the requirement for temperature control and humidification as dictated by the use of the space. These heating and cooling systems will regulate a room's temperature by

supplying or removing heat when a threshold temperature, or set point, is passed. These set points will correspond to the boundaries of the thermal comfort zone as discussed in the previous section. The operation of these systems can make up a large proportion of building's energy use.

1.4 Comfort Cooling and Global Warming

It is normal for weather to change over the short term. It is also normal for the climate to change over much longer periods. Climate change is measured by averages of temperature, sunlight, precipitation and other variables. Recent studies have shown that climate change is caused by mankind and by natural means (Gevorkian, 2010). The cause of this change is the heating up of the earth's atmosphere.

The temperature of the atmosphere is affected by the amount of carbon dioxide in it. This is because incoming solar radiation is absorbed by the earth, re-released as infrared radiation and then trapped by the carbon dioxide. This trapping of heat is known as the greenhouse effect and is essential to prevent the atmosphere overcooling.

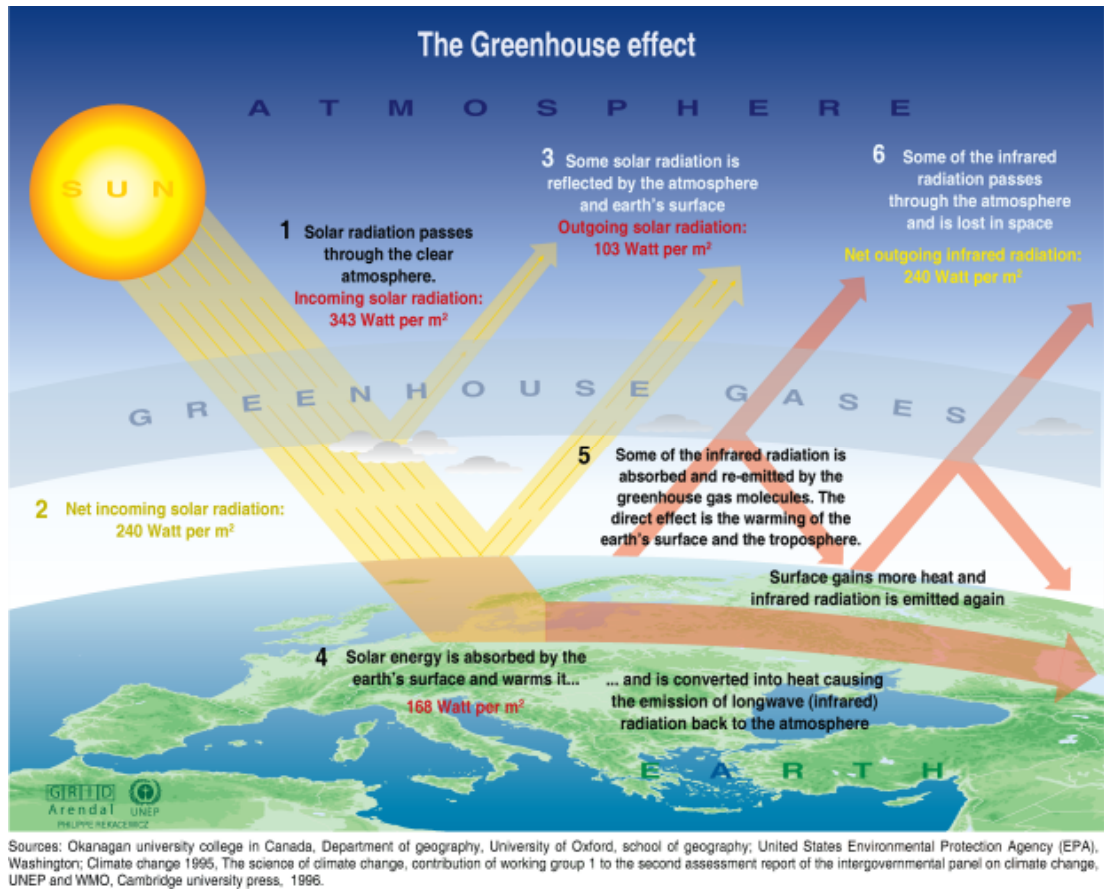


Figure 1.1 The Greenhouse effect. A global energy balance (Rekacewicz, 2011).

However, if the amount of carbon dioxide in the atmosphere rises more infra red radiation is trapped and this causes a global temperature rise. This is currently happening. One of the main sources of carbon dioxide is the burning of fossil fuels to generate electricity. Reducing our requirement for electricity, in any of its applications, will ultimately reduce the damaging effects of climate change.

En masse cooling devices consume a large amount of electricity and are therefore responsible for the entailed carbon dioxide emissions. The International Institute of Refrigeration states that approximately 15% of the world's electricity is used for refrigeration and air conditioning (Coulomb, 2011). The proportion of energy that is devoted to cooling a building will vary greatly depending on its location. Figure 1.2 gives several examples of this.

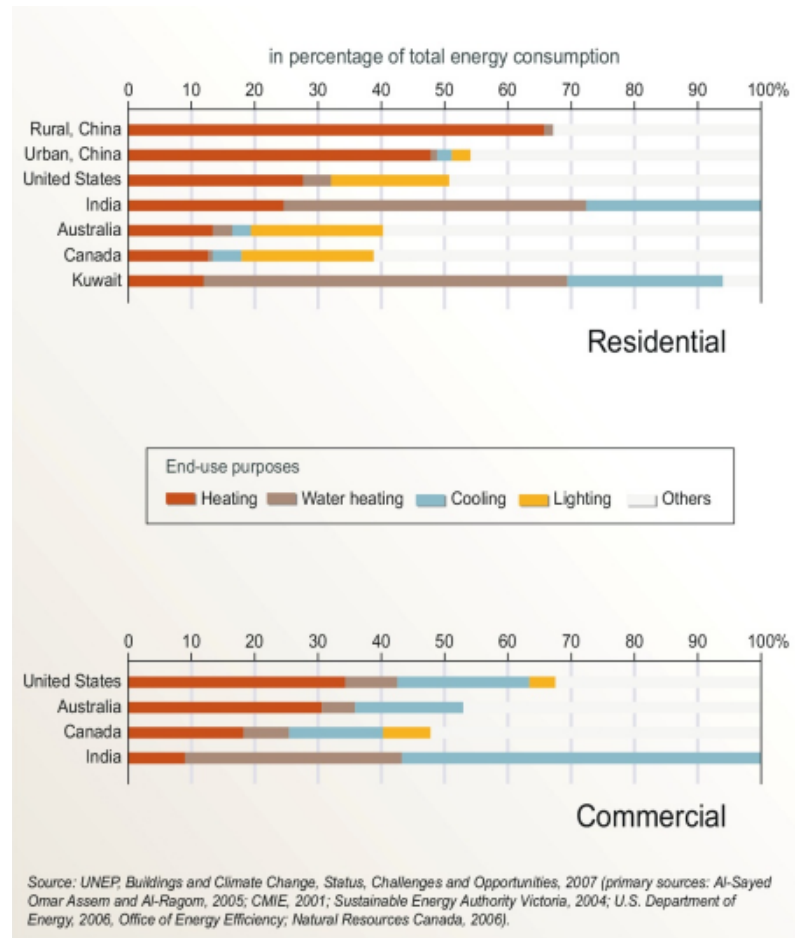


Figure 1.2 Proportion of end use building energy consumption for various countries (UNEP/GRID-Arendal, 2008).

In 2000, 5% of non-domestic UK building energy was consumed by cooling and ventilation equipment (Hutt et al., 2004) and this is widely acknowledged to be rising. In the Organisation for Economic Co-operation and Development (OECD) almost 46% of houses have air conditioning. This is rising at 7% per year (Santamouris, 2007). Santamouris attributes the intensive use of air conditioning to:

- Adoption of an international building style that is not sensitive to local climate conditions.
- The urban heat island effect which increases urban ambient temperatures.
- Increasing standards in thermal comfort of occupants.
- Increasing affluence and improvement in living standards.
- Higher internal loads (Santamouris, 2007).

As global temperatures rise, so will the use of air-conditioning. The problem is exacerbated by the fact that many developing countries are situated in hot climates. As living standards improve, air-conditioning systems will increase in number and capacity. This trend was witnessed in Europe where sales of air conditioning equipment rose sharply in the 80s and 90s with industry turnover standing at 1.7 billion euros in 1996. In Greece the annual sales of packaged air conditioners jumped from 2000 to 100,000 between 1986 and 1988 (Santamouris and Asimakopoulous, 1996).

It clearly makes sense for buildings to be cooled for the sake of the health and happiness of its occupants but it is also clear that this has become an extremely energy intensive process which contributes to the damaging effects of climate change. Part of the solution to this problem may be found in the use of phase change materials (PCMs) which have the potential to reduce the energy consumed to cool buildings.

1.5 Phase change materials

PCMs are materials with a high latent heat of fusion that melt and solidify in a temperature range which is useful for a particular application. In the case of cooling buildings, phase change temperatures are in the region of 0 °C to around 26 °C. This allows them to remove heat from a space release it at night when ambient temperatures and/or electricity prices are lower.

A good example of a low temperature PCM is ice which is produced and stored in insulated tanks. Heat may be transferred to ice at a high rate due to its low melt temperature and because it has a high latent heat of fusion (333 kJ/kg) (Halliday et al., 1992) it can store 13 times the amount of coolth (assuming a 6 °C temperature range) than the equivalent mass of water (specific heat 4.2 kJ/kg/°C) (Halliday et al., 1992). This means that a much smaller mass and volume is required. Another example of a PCM applied in buildings is paraffin wax which is increasingly used to replace thermally massive materials in buildings such as concrete. In hot conditions exposed concrete can passively absorb heat in a building and release it at

night when the ambient temperature falls. This can reduce cooling energy. In buildings that are lightweight in construction the thermal mass is much lower but this can be replaced by panels containing paraffin. Because of its high latent heat of fusion 10 mm of a commercially available paraffin based wall board can be said to be equivalent to 80 mm of concrete in terms of heat usefully exchanged (DuPont, 2011).

PCM applications need recognition in the building regulations or other building certification schemes to gain widespread specification in building services design. However they are not yet accounted for explicitly in the same way as, for example, low U value thermal elements or renewable energy sources.

In the UK, under approved document Part L (Conservation of Fuel and Power) of the Building Regulations, the National Calculation Methodology is used to calculate the energy savings of a building. The beneficial impact of the use of PCMs cannot currently be explicitly accounted for (HM Government, 2010).

Opportunities may be found at a local government level. Planning policy statements 1 and 22 respectively advise on sustainable development, including prudent use of natural resources and therefore energy (ODPM, 2005), and a minimum percentage of energy required from renewable resources (ODPM, 2004). Interpretation of the statement is determined by the local authority. The London Plan states that boroughs should adopt a presumption that developments will reduce their carbon emissions by 20% through renewable technology (Mayor of London, 2008) but neither passive nor active PCM cooling systems are included in this. However, the London Borough of Camden has a 20% renewables obligation and where this is not feasible other carbon reduction measures may be sought. A PCM cooling system could be included as one of these 'other' measures (London Borough of Camden, 2008). Camden also requires developments that are greater than 1000 m², or 5 or more dwellings, obtain at least 60% of the energy credits available from BREEAM or EcoHomes (now the Code for Sustainable Homes) (London Borough of Camden, 2007).

Environmental certification schemes are a voluntary means of proving a building's environmental credentials in the absence of mandatory regulation. The most prominent is LEED and BREEAM.

LEED is an internationally recognised environmental performance certification system for buildings produced by the US Green Building Council (USGBC). It allows innovative energy saving measures to be factored into the assessment process. The PCM can be included to improve the overall building energy performance credits by way of an exceptional calculation method, as well as the possibility of earning a separate innovation credit (USGBC, 2005). If a building incorporates an innovative PCM cooling system, it is likely that this would improve the LEED performance.

BREEAM is an environmental performance certification system by the BRE. Innovation points may also be similarly gained with this system (BRE, 2009).

1.6 How this work contributes to knowledge

This thesis explores ways in which PCMs can be applied for cooling in buildings and proposes a novel solution that minimises energy consumption and maximises system resilience. Five inter-related projects are presented, each of which contributes to knowledge. These contributions to knowledge are listed below under the chapters in which they found:

Chapter 3 – Active PCM cooling system: The post-installation energy audit of a central cooling system to establish the energy savings incurred by the presence of two PCM tanks.

Chapter 4 – Design space mapping: The development of a new taxonomy for PCM cooling systems that clearly and consistently defines all possible systems, allowing gaps in the design space to be identified and researched further.

Chapter 5 – Passive PCM Sails: The design and testing of PCM units that demonstrate the advantage of cross-envelope transfer in discharging accumulated heat at night.

Chapter 6 – Product testing: Controlled testing and comparison of two passive PCM products: Energain panels and RACUS ceiling tiles.

Chapters 7 and 8 – NewMass: The design, fabrication and testing of a prototype PCM cooling system that minimises cooling energy and guarantees

next-day performance by prioritising passive operation whilst retaining a back-up refrigeration element.

In addition to these deliverables a noteworthy contribution to knowledge was made by the Brunel PCM Research Group in the appraisal of several commercially available PCMs. DSC analysis was applied by Brunel students to obtain values of latent heat, specific heat capacity, melting and freezing temperatures and thermal conductivity. The research was inspired by this EngD project and directed by Dr Zahir Dehouche and I. Many of the results are presented in this thesis.

The over-arching structure of the work is best seen as a design development process that leads to the detailed design and testing of the novel system named NewMass in chapters 7 and 8. Chapters 3 to 6 are self-contained projects and at the same time yield conclusions which contribute to the over-arching design process.

The literature review identifies the gaps in knowledge exploited by each of the following chapters. Although all aspects of research into the use of PCMs to cool buildings are covered here (e.g. materials range, modelling techniques etc), the most important part focuses on the various types of PCM cooling system that have been studied and developed thus far. It is there that the opportunities for original research are found.

One general conclusion made in the literature review is that there is not currently enough evidence concerning the potential energy savings resulting from using an active PCM cooling system in conjunction with conventional chillers. Chapter 3 answers the question of whether active systems save energy for the specific case of a system installed in a UK office building. This work demonstrates the need to hybridise, employ free-cooling principles or select a PCM with relatively high transition temperature range if savings are to be made with active systems incorporating chillers.

Another general conclusion made in the literature review is that the *design space* for PCM cooling systems has not been effectively mapped due to the general acceptance of a number of overlapping and sometimes ill-defined system type definitions. Chapter 4 establishes a new method of classification which can be consistently applied to all current and future PCM cooling systems.

The Passive PCM Sails design, covered in chapter 5, was a result of identifying areas in the design space not occupied by existing PCM cooling systems; in particular the use of cross-envelope transfer for heat discharge. Several conclusions are reached informed the design of the NewMass system.

- That cross-envelope transfer is beneficial for heat transfer but is problematic to achieve in many circumstances.
- That radiant effects are significant for the thermal charging of passive systems.
- That an appropriate and narrowly defined transition temperature range should be sought in the PCM selected for passive cooling.

The literature review reveals a general lack of systems tested and compared under exactly the same test conditions. This fact coupled with the need to reliably compare the performance of the NewMass system with other PCM cooling systems motivated the work, which is described in chapter 6, to test Energain panels and RACUS ceiling tiles in a purpose built thermal test cell. The results reveal that although the Energain panels achieve a greater peak air temperature reduction, as compared to a control test, the RACUS tiles achieve more for a lower PCM content and are able to discharge their accumulated heat faster.

Chapter 7 describes the design of the NewMass system, building as described on the results of the previous studies as well as the wider literature. The design consists of an array of finned aluminium tubes containing paraffin and a conductive lattice of aluminium rings (Raschig rings). The tubes can passively absorb heat from a space and passively discharge it to cool night air or actively discharge it to a chilled water circuit for guaranteed performance the following day. The system can also actively absorb heat through the chilled water circuit during the daytime if the PCM's thermal capacity is exhausted.

Chapter 8 describes the installation and testing of the system in the thermal test cell, demonstrating the advantages that result. The system performs well in passive operation, as compared to the Energain panels and RACUS ceiling tiles, and stabilises the test cell's air to a constant temperature around 24.5 °C. Active discharge of heat is also shown to be effective. Modelling of the system predicts 34% energy savings in a typical UK office building.

At the time of writing Buro Happold were in talks with several manufacturers concerning collaboration to develop the NewMass system into a commercial product.

References

ASHRAE (2009) *ASHRAE Handbook: Fundamentals*. Atlanta: ASHRAE.

ASHRAE (2004) *ASHRAE Standard 55: Thermal Environmental Conditions for Human Occupancy*. ASHRAE, Atlanta.

Bahadori, M.N. (1976) 'Passive Cooling Systems in Iranian Architecture', *Scientific American*, February 1976.

Coulomb, D. (2006) *Statement given by Didier Coulomb, Director of the International Institute of Refrigeration*. Available:
http://www.un.org/webcast/unfccc/2006/statements/061117iir_e.pdf
[03/10/2011].

DECC (2011) *Carbon Emissions Reduction Target (CERT)*. Available:
http://www.decc.gov.uk/en/content/cms/funding/funding_ops/cert/cert.aspx
[16/12/2011].

DECC (2010a) *Climate Change Act 2008*. Available:
http://www.decc.gov.uk/en/content/cms/legislation/cc_act_08/cc_act_08.aspx
[06/05/2010].

DECC (2010b) *Committee on Climate Change*. Available:
http://www.decc.gov.uk/en/content/cms/what_we_do/change_energy/tackling_clima/committee/committee.aspx [06/05/2010].

Derry, T.K. and Williams, T.I. (1960) *A Short History of Technology from the Earliest Times to A.D. 1900*. 1st edn. London: OUP.

Directorate-General for Energy and Transport (2008) *Concerted Action: Energy Performance of Buildings Directive*. Available: <http://www.epbd-ca.org/> [26/03/2009].

DuPont (2011) *Equivalence DuPont Energain to Concrete*. Available: http://energain.co.uk/Energain/en_GB/assets/downloads/documentation/download/energain_Concrete_Relation.pdf [18/12/2011].

Gevorkian, P. (2010) *Alternative Energy Systems in Building Design*. 1st edn. New York: McGraw-Hill.

Halliday, D., Resnick, R. and Krane, K.S. (1992) *Physics*. 4th edn. Chichester: John Wiley & Sons, Inc.

HM Government (2010) *The Building Regulations 2000: Conservation of fuel and power*. 2010 Edition. London: RIBA.

Humphreys, M. and Nicol, F. (2007) 'Environmental Criteria for Design' in: Braham, D. (ed) *Environmental Design - CIBSE Guide A*. 2nd edn. London: CIBSE, pp. 1-1 - 1-37.

Hutt, B., Field, J., Hobbs, D., Johnson, T., Palmer, J. and Watson, A. (2004) *Energy Efficiency in Buildings - CIBSE Guide F*. 2nd edn. London: CIBSE.

James, P. and Thorpe, N. (1995) *Ancient Inventions*. 1st edn. London: Michael O'Mara Books.

Larsen, J. (2006) *Setting the Record Straight: More than 52,000 Europeans Died from Heat in Summer 2003*. Available: http://www.earth-policy.org/plan_b_updates/2006/update56 [09/12/2011].

London Borough of Camden (2008) *Shaping Camden: Camden's Local Development Framework*. London: London Borough of Camden.

London Borough of Camden (2007) *Camden Planning Guidance 2006*. London: Camden Design and Print.

- Mayor of London (2008) *The London Plan: Spatial Development Strategy for Greater London (Consolidated with Alterations since 2004)*. London: GLA.
- Metz, B., Davidson, O.R., Bosch, P.R., Dave, R. and Meyer, L.A. (2007) *Climate Change 2007: Mitigation of Climate Change*. 4. Cambridge: CUP.
- ODPM (2005) *Planning Policy Statement 1: Delivering Sustainable Development*. Norwich: HMSO.
- ODPM (2004) *Planning Policy Statement 22: Renewable Energy*. Norwich: HMSO.
- Ogoli, D.M. (2003) 'Predicting indoor temperatures in closed buildings with high thermal mass', *Energy and Buildings*, 35(9) pp. 851-862.
- Pantavou, K., Theoharatos, G., Mavrakis, A. and Santamouris, M. (2011) 'Evaluating thermal comfort conditions and health responses during an extremely hot summer in Athens', *Building and Environment*, 46, pp. 339-344.
- Rekacewicz, P. (1996) *Greenhouse Effect*. Available:
<http://maps.grida.no/go/graphic/greenhouse-effect> [03/10/2011].
- Santamouris, M. (ed) (2007) *Advances in Passive Cooling*. 1st edn. London: Earthscan.
- Santamouris, M. and Asimakopoulous, D. (1996) *Passive Cooling of Buildings*. 1st edn. London: James & James.
- Shapiro, Y. and Epstein, Y. (1984) 'Environmental Physiology and Indoor Climate - Thermoregulation and Thermal Comfort' *Energy and Buildings*, 7, pp. 29-34.
- Turner, J.A., Kennedy, D., Fankhauser, S., Grubb, M., Hoskins, B., King, J., May, R.M. and Skea, J. (2008) *Building a low carbon economy - the UK's contribution to tackling climate change*. Norwich: TSO.
- Turner, J.A., Kennedy, D., Fankhauser, S., Hoskins, B., King, J., Krebs, J., May, R.M. and Skea, J. (2011) *Meeting carbon budgets - 3rd progress report to parliament*. 3rd edn. London: CCC.

USGBC (2005) *LEED-NC for New Construction*. 2.2 edn. Washington DC: U.S. Green Building Council.

UNEP/GRID-ARENDAL (2008) *Energy consumption by usage in a building*.

Available: <http://maps.grida.no/go/graphic/energy-consumption-by-usage-in-a-building1> [18/12/2011].

UNFCCC (2008) *Kyoto Protocol*. Available:

http://unfccc.int/kyoto_protocol/items/2830.php [26/03/2009].

Chapter 2

LITERATURE REVIEW

This literature review is divided into three sections; one on the materials that we call PCMs, one on the systems in which they are employed and one on the techniques for modelling the process of phase change and the systems in which PCMs are employed.

The section on materials is an introduction to and appraisal of the range of materials available, their thermophysical properties, the methods by which we can establish these properties and the ways in which we can contain the materials and enhance their heat transfer characteristics. This was essential for the development of the Passive PCM Sails and NewMass system designs.

The section on the various potential PCM cooling systems is the most important element in this literature review as it identifies the gaps in current knowledge which are filled by the contributions to knowledge delivered in chapters 3 to 8. A great number of PCM systems have been proposed, tested and in some cases commercialised, over the past few decades. The section on PCM systems reviews such systems and draws the general conclusion that there is an opportunity to overcome existing system disadvantages through the development of new systems.

The section on modelling, like that of materials, is a necessary introduction to the various techniques employed so that the modelling undertaken in this EngD can be understood in context.

With regards to the systems, this review (and the wider work of the thesis) will look in detail solely at those applications which cool buildings, i.e. those that remove excess heat from a space. This obviously excludes any heating technology but it also excludes the use of PCM to limit the rate of heat flow as in cases of insulation. It is worth noting that this review only covers systems intended to diurnally store heat or

coolth. This should be distinguished from systems which seek to seasonally store heat or coolth, such as those studied by Ozturk (Öztürk, 2006). Seasonal storage with PCM is considered outside the scope of this EngD.

PCM may provide cooling to a space in many ways and combinations. For example, through incorporation into the building fabric, inclusion in a chilled water distribution network or integration into an air handling system. This has led to a review of the various methods of classification applied to PCM cooling systems which is located at the start of the section on systems. One of the upshots of the review of approaches to classification is the establishment of the categories used to define all PCM systems in the literature review. They are:

- **Passive systems:** Those which are in direct thermal contact with the cooled space and discharge their accumulated heat to circulated night air.
- **Active systems:** Those which consist of PCM contained in insulated tanks that transfer coolth to the conditioned space via a heat transfer fluid (normally water) and discharge their heat to a chilled water circuit.
- **Free-cooling system:** Those which consist of PCM units that are isolated from the conditioned space and cool it through heat exchange with a forced air flow. Accumulated heat is rejected to circulated night air.
- **Thermally activated systems:** Those which are in direct thermal contact with the space being cooled during the daytime but reject their accumulated heat at night to chilled water circulated through embedded pipe networks.

These categories will be used throughout the thesis however it will be argued that the current methods of classification are not clearly defined and that this obscures the design space and fails to illuminate the potential PCM cooling system designs that could exist.

This difficulty with the classifying of certain systems gave rise to the design space mapping work described in chapter 4. This work seeks to better define systems to avoid ambiguity and reveal any potential system designs that have not been thus far exploited. This, in combination with the conclusions about shortcomings of existing systems led to the development of the new PCM cooling system designs featured in chapters 5, 7 and 8.

Several conclusions will be drawn from the section on PCM cooling systems. Active PCM systems will be reviewed first. These may be seen as a sub-set of active cool thermal energy storage (TES) systems which also include chilled water. Here we will see that:

- Due to depressed dry bulb temperatures at night, chiller COPs increase and energy savings may be made if coolth generation is shifted to the night time.
- However, in most, but crucially not all, studies of installed active TES systems the reverse is found to be true and an energy cost is incurred due to a range of factors.
- The question of whether active PCM systems save energy has not been definitively answered. Many of the problems encountered by the installed systems studied appear to be avoidable.
- There is therefore an opportunity to gather further system performance data to improve our understanding of the factors that cause a system to succeed or fail to save energy.

This conclusion led to the monitoring and energy savings calculation of the active system in a UK office, described in chapter 3. The results of that study revealed some of the factors that can lead to energy costs but also supported the need for a relatively high phase change temperature in the PCM employed. These considerations fed through to the final NewMass design.

Passive systems will be reviewed second. We will see that:

- The systems have the advantages of being easily installed, reduce peak temperatures and can save energy.
- The systems may often prove less effective than intended because the exposed surface area is necessarily limited by the available wall and ceiling area for them to be installed. This area can often be covered by false ceilings, service ducts, light fittings, wall displays and furniture etc.
- The systems suffer from an inability to discharge heat on warm nights due to insufficient heat transfer rates. This leads to a loss of function the following day so a separate full scale cooling system is required.

- There is an opportunity to develop new systems that do not have limited heat transfer rates, and thermal storage capacity, and can reject heat more reliably at night and guarantee next day performance.

These considerations fed into the development of the Passive PCM Sails, described in chapter 5, and the NewMass system described in chapters 7 and 8. The Passive PCM Sail design aims to solve the problems of limited heat transfer rate during the day and night. The NewMass system does the same and guarantees next day performance.

Free cooling systems will be reviewed third. Here it will be concluded that:

- These systems have the advantage of targeted air flow to discharge heat more efficiently than purely passive systems.
- Because these systems require forced air flow for charge and discharge operation their energy use can only be reduced to the power of the fan, which may be high.
- Without an option for refrigeration to guarantee overnight freezing of the PCM modules the system may be useless the following day and so may require a full scale back up cooling system.
- There is an opportunity to develop new systems that rely on passive operation, and so do not require power for mechanical air movement, and can guarantee next day performance.

As with the conclusions based on the passive systems, these conclusions fed through to the development of the Passive PCM Sails and the NewMass systems.

Thermally activated systems will be reviewed last. The conclusions here will be that:

- The systems has the advantage of operating passively during the daytime.
- It also has the ability to discharge heat to a chilled water circuit to guarantee next day performance.
- As with passive systems, the surface area available for heat transfer and therefore cooling is limited.

The final NewMass design, presented in chapter 7, is an extension of the thermally activated systems discussed with the potential for increased thermal and cooling capacity.

2.1 Phase Change Materials

The earliest recorded use of a material for its latent heat capacity is the storage of ice by the Persians. By 400 BC the Persians were using ice houses, known as Yakhchals (Earth Architecture, 2009) containing ice manually transported from ponds that radiated heat to the night sky to induce phase change (Bahadori, 1985). The ice would not have been used to cool buildings but would have chiefly been used to preserve food and cool drinks (Earth Architecture, 2009). The process of night sky cooling allows one to radiatively transfer heat to the upper atmosphere on clear nights. The Persians were able to effectively access this heat sink whilst minimising convective heat gains from the surrounding ambient air. This was achieved through the erection of walls along the edges of the long shallow ponds, shielding the contained water from air flow (Bahadori, 1976).

By establishing an energy balance between the water and the heat transfer modes of radiation, evaporation and convection, Bahadori was able to demonstrate that ice could be formed below ambient temperatures of 12 °C and 20% relative humidity (Bahadori, 1984). All objects emit thermal radiation and night sky cooling occurs because a body emits more radiation to the sky than it receives. The rate for radiant heat transfer from a surface exposed to the night sky is given in Eq. 2.1.

$$\dot{Q}_{rad} = \epsilon \sigma A_s (T_s^4 - T_{sky}^4) \quad (2.1)$$

The sky temperature given here is a fictitious value that is found by considering the atmosphere as a black-body emitting radiation. It is defined by Eq. 2.2 (Cengel, 2003).

$$G_{sky} = \sigma T_{sky}^4 \quad (2.2)$$

It should be noted that the practice of night sky cooling may be applied to any material from which heat rejection is desired. Sensible cooling of thermal mass through radiation to the night sky was alluded to as a form of temperature control in the introduction. The night sky features as a heat sink for PCM in chapters 4 and 5.

From the 17th to 20th centuries ice storage became popular in British stately homes (Martin, 2009) and was a largely upper class affair. However, in the 19th century an ice trade was established between Norway and the UK. Norwegian glaciers contain very pure ice which was cut and shipped to central London. This allowed large numbers of common people to preserve food for the first time (London Canal Museum, 2011).



Figure 2.1 *The ice trade. Ice is cut from a glacier (left), transported by dedicated railway to the dock (middle) and shipped to the UK (right) (London Canal Museum, 2011).*

It is partly the capacity of ice to absorb large amounts of latent heat that led to its use as a PCM. As it changes phase it absorbs heat from the surrounding environment and so can regulate the temperature.

Under the right conditions, all substances may absorb or reject heat in a sensible or latent way. The sensible heating of a substance simply involves raising its temperature. On a molecular level this corresponds to an increase in the kinetic and potential energies of the constituent molecules or atoms (Halliday et al., 1992). In a closed system of fixed mass, the amount of heat, Q_{sens} , required to raise the temperature is that given in Eq. 2.3.

$$Q_{\text{sens}} = m \int_{T_{\text{ref}}}^T C_p dT \quad (2.3)$$

(Cengel, 2003)

By adding the sensible internal energy already contained in the system and then dividing by the mass, we have the sensible enthalpy of the system, h , as shown in Eq. 2.4.

$$h = h_{\text{ref}} + \int_{T_{\text{ref}}}^T C_p dT \quad (2.4)$$

(Voller, 1996)

Here the reference enthalpy is defined as a fixed value that is said to be the enthalpy of the substance when it is at the reference temperature. This may essentially be arbitrarily chosen but allows the enthalpies at all other temperatures to be evaluated with respect to that value. For example a value of 0 °C may be selected for the reference temperature and a value of 0 kJ/kg may be selected as the corresponding reference enthalpy at that temperature.

PCMs will always transfer heat sensibly when they change temperature but during phase change a much larger amount of heat will be transferred over a relatively small temperature change. This is because bonds are broken or created between the PCM's molecules/atoms. (Halliday et al., 1992) The amount of heat absorbed/rejected upon total change of phase is that given in Eq. 2.5 (Halliday et al., 1992).

$$Q_{\text{fus}} = mL_{\text{fus}} \quad (2.5)$$

The other reason ice was used in this way was that it melts and freezes at an application–appropriate temperature. This means it will exchange heat only so far as to maintain the temperature of the object being cooled.

The use of materials as latent heat stores diversified into inorganic PCMs at the turn of the 20th century. Around this time the first use in a space heating application was made by British Rail who employed containers of salt-hydrate to provide some heating to its coaches over the winter months (Lane, 1983). Various product designs were pursued over the following decades including hot bottles for direct warming of the body and designs for warming babies' milk bottles and coffee pots etc (Lane, 1983).

Today PCMs are used in a wide variety of applications for temperature control. Examples include medical and food transport, where drugs, blood and food must be kept within a certain temperature range to avoid degradation which would lead to serious health consequences. Another example is cooling clothing where people in environments of extreme heat, such as deserts or burning buildings can remain within an otherwise unattainable temperature range (Cabeza *et al.*, 2002).

PCMs may be applied in a great variety of ways to control the temperature in a building. Heating applications include Trombe walls, investigated by Stritih and Novak (2002), solar rooms, analytically investigated by Xiao *et al.* (2009), and solar collector applications, as studied by Koca *et al.* (2008).

Further uses of PCM include the transparent insulation looked at by Buddhi and Sharma (1999) in their investigation into light transmittance through stearic acid at different temperatures. A product which makes use of this aspect of the material is GLASSX (2011). Another insulation application was investigated by Ismail and Henriques (2001) who conducted a study using the liquid properties of the PCM to create a moveable insulating curtain for a window.

In this work we are interested in diurnal cooling applications only.

2.1.1 Candidate Materials

PCMs may be seen as a sub-set of a wider group of thermal storage media that includes sensible heat, chemical energy and other types of phase transition. They may also be broken down into further sub-sets of materials with organic and inorganic being the chief groups. The structure of this hierarchy is shown in Figure 2.2.

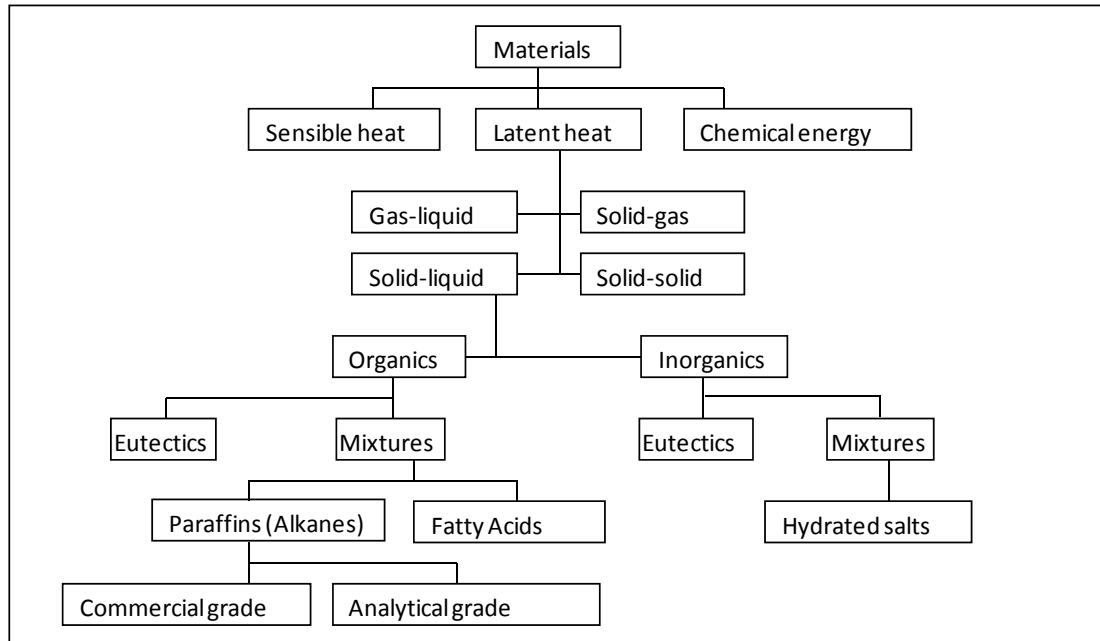


Figure 2.2 Categories of thermal storage media and sub-sets of PCM. (Zalba et al., 2003)

In order for PCMs to function well in building applications they must possess certain thermophysical, kinetic and chemical properties. Tyagi and Buddhi (2007) list these:

Thermophysical properties:

- Appropriate melt temperature.
- High latent heat per unit volume.
- High specific heat if possible.
- High thermal conductivity in solid and liquid phases.
- To limit containment issues, a small volume change on freezing/melting and low vapour pressure.
- Congruent phase change of the PCM leading to a consistent storage capacity.

Kinetic Properties:

- High nucleation rate for the avoidance of under-cooling.
- High crystal growth rate so that heat may be recovered.

Chemical Properties:

- Reversible phase change cycle, without degradation for a large number of cycles.

- No corrosiveness to the construction materials.
- Non-toxic, non-flammable, non-corrosive, non-explosive.

In actual fact no PCM is a perfect manifestation of these qualities. Tyagi and Buddhi (2007) describe the main material categories of PCM as follows, with additional information from Zalba et al. (2003):

- **Organic:** Carbon-based materials that are further divided into paraffins and non-paraffins (fatty acids), and have the properties of congruent melting, self-nucleation and (usually) non-corrosiveness to the container.
- **Inorganic:** Non-carbon-based materials that are further divided into salt hydrates and metallics, they have a high latent heat per unit mass/volume, are low in cost and are non-flammable, but suffer from decomposition and under-cooling. [They may also corrode their containers, attested to by several authors. (Zalba *et al.*, 2003)]
- **Eutectic materials:** Compositions of minimum melting temperature, comprising two or more congruently melting/freezing components.

Paraffins are mixtures of mostly straight chain alkanes, strings of carbon atoms bonded on all sides by hydrogen atoms. The general chemical formula of an alkane is C_nH_{2n+2} . The longer the alkane molecules in the mixture, the higher the transition zone of the paraffin (Lane, 1983). This means that different paraffins will be solid, liquid or in transition at room temperature.

Salt hydrates are a solution of salt and water. The definition of a salt is an ionic compound which is created by the reaction of an acid and a base. A typical salt hydrate PCM is a calcium chloride solution; $CaCl_2 \cdot 6H_2O$. All salt hydrates have a chemical formula of the form:

Salt chemical formula $\cdot nH_2O$

where n is the number of water molecules.

Several authors, Zalba et al., (2003), Agyenim et al. (2010) and Kenisarin & Mahkamov (2007), for example, have collated lists of PCMs used in building applications. Appendix A contains reproductions of selected tables that indicate the range of materials that have been subject to research and application as PCMs and a list of companies that supply them.

2.1.2 Testing Thermophysical Properties

Differential scanning calorimetry (DSC) has been the most widely used mode of thermophysical analysis for PCMs. The technique involves subjecting a small sample of the PCM and a reference material to a steady increase or decrease in temperature and simultaneously monitoring the heat flowing to or from them. For a PCM this technique will generate a characteristic curve which describes the heat flow required for melting and freezing and the temperatures at which this happens. An example for a commercially available paraffin, A26, and a composite of A26 and LDPE (low density polyethylene – see ‘shape stabilisation’ in the following section) is shown in Figure 2.3. The substances were tested separately but are displayed together for useful comparison.

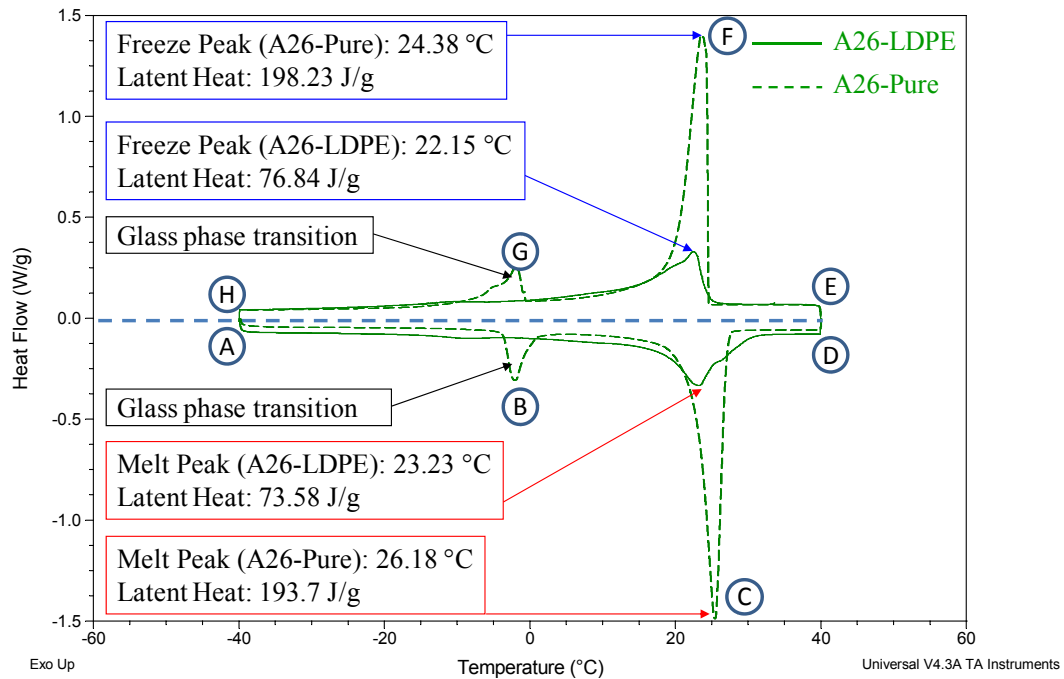


Figure 2.3 Typical DSC curves for commercially available paraffin wax. A26 and a composite of A26 and LDPE (Cheechern, 2009).

The tests start at point A; this is where each substance is cooled down to -40 °C. Each sample is then heated at a constant rate causing a temperature increase. This can be seen by the near horizontal lines leading right from point A. The heat being absorbed by the substance in this period is largely sensible which is why the line is horizontal; the rate of heat transfer is near constant. In the region leading to point B the amount of heat flowing into the pure A26 begins to increase with every unit temperature increase. This is because a solid-solid phase transition occurs, corresponding to a realignment of the alkane chains that constitute the paraffin. This effect is not seen in hydrated salts. The composite material also experiences a solid-solid phase transition because of its paraffin content but it is too small to see in the graph.

Between points B and C there is a period of largely sensible heating which is increasingly dominated by a latent absorption of heat indicated by the steepening gradient and peak at point C. This corresponds to the melting of each substance over a range of temperature. This is evident for both substances but the greater height (depth) of the pure substance's peak indicates that it absorbs more latent heat per unit mass than the composite. We can also see that the ratio of height to breadth of

the base of the pure substance's peak is larger than that of the composite. This is referred to as the narrowness of the transition zone in later chapters of the thesis. A narrower transition zone means a greater amount of latent heat is exchanged over a smaller temperature range. This can allow the exchange of heat to be better targeted to a temperature range suitable for the application.

Between points C and D the peak ends corresponding to the end of the phase change; the substances are now fully liquid and heat exchanged from thereon is purely sensible. When the liquid reaches 40 °C each sample is held at that temperature and then the reverse process occurs. Between points E and F there is a period of largely sensible cooling which is interrupted by the sudden rise of a peak corresponding to latent heat loss and the re-solidification of the material. This process occurs at a slightly lower temperature than the melting of the substance due to what is referred to as undercooling or supercooling. This happens because substances require nucleation, the beginning of crystal growth, to occur for freezing to begin. This tends to happen below the melting point.

Between F and G the substance refreezes and is cooled sensibly until it reaches the solid-solid phase transition. After this it is sensibly cooled until it reaches – 40 °C at point H.

With a differential scanning calorimeter, the following properties can be determined:

- Specific heat capacity
- Latent heat of fusion
- Melt transition zone
- Solidification transition zone
- Thermal conductivity (obtained through a lesser known process explained by Dehouche et al. (2005))

An alternative method is the T-history method proposed by Zhang and Jiang ((Zhang & Jiang, (1999) cited in (Peck *et al.*, 2006)). It involves filling two test tubes with a reference sample (normally water) and a PCM. The tubes are placed in a water bath and heated to above the melt temperature of the PCM.

They are then removed and allowed to cool whilst their temperatures are monitored. The thermophysical properties of the PCM may then be derived from the temperature profiles that result (Hong et al., 2004).

Improvements have been suggested by amongst others, Peck et al. who increased accuracy by orientating the test tubes horizontally to prevent internal convection (Peck *et al.*, 2006).

DSC has come under some criticism in recent years because if the sample size is too large and the rate of temperature increase is too high the transition temperature range can shift and the specific heat capacity can vary (Mehling et al., 2006).

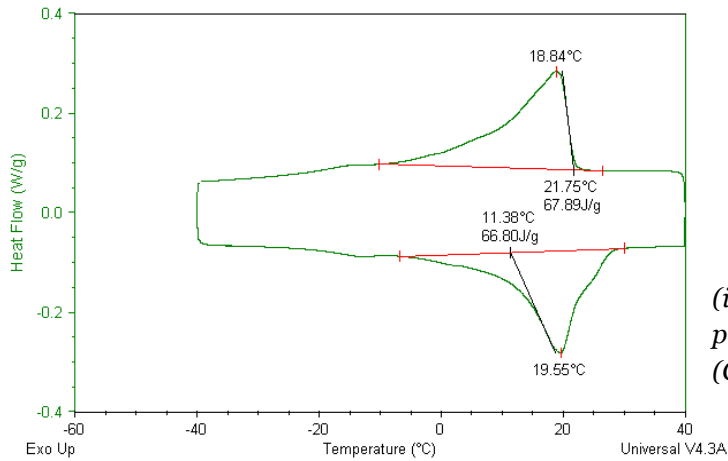
However, DSC may still be used to effectively determine thermophysical properties. Mehling et al. (2006) explain the issues well. If sample size is too large and temperature change rate is too high (rates of 10 K to 20 K/min are mentioned as standard for sensibly heated materials) then due to its latent heat capacity the sample will not reach equilibrium which effectively causes a shift in transition zone. If the sample size is very small and the material sampled is not particularly homogeneous, erroneous readings may also result.

If care is taken over sampling of material and the rate of temperature increase or decrease then successful DSC measurements can be taken. Examples of successful research using DSC include Feldman & Banu (1996) and Shilei et al. (2007) who effectively predicted the heat absorbed by PCM wallboards through prior DSC analysis. Quanying et al (2008) used DSC measurements to analyse the suitability for use in internal walls of paraffins mixed in various proportions.

At Brunel a significant programme of work to determine and document the thermophysical properties of several commercially available PCMs has been undertaken by a research team working in collaboration with this EngD. Due to the need to understand the properties of materials used in the experiments documented in this dissertation, Brunel students were set the task of sampling and testing PCMs that I obtained. The results of these tests are summarised here. Figure 2.4 displays the characteristic DSC curves for the main substances tested and Table 2.1 displays the thermophysical parameters obtained.

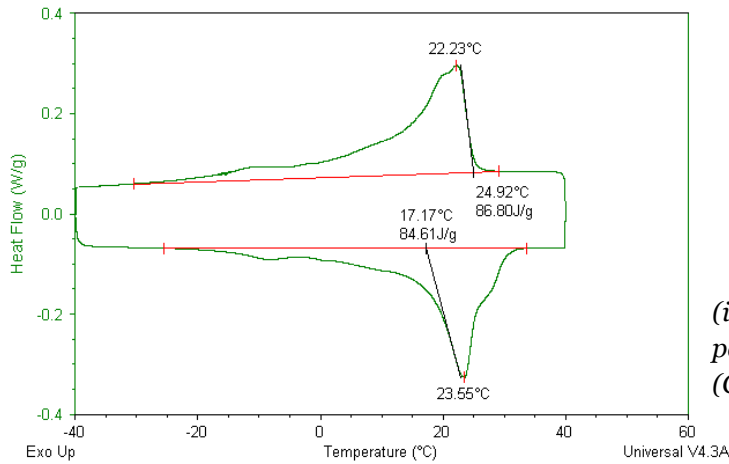
Figure 2.4 DSC curves for PCMs tested as part of Brunel's material appraisal programme

(i)



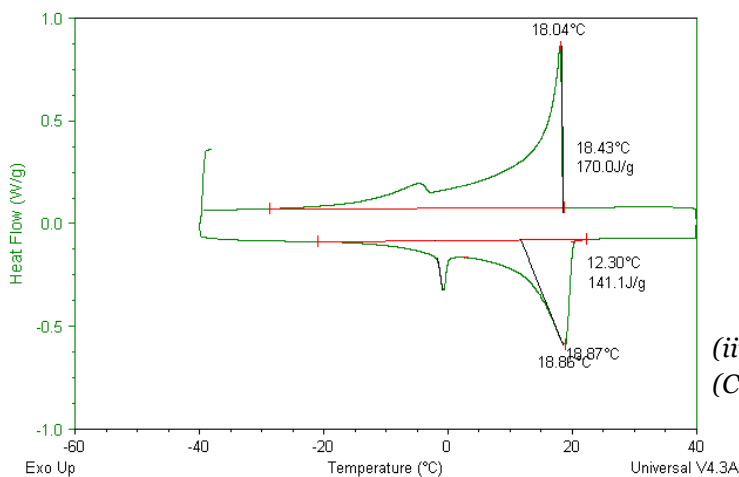
(i) A22 panel material – paraffin/LDPE composite (Cheechn, 2009)

(ii)



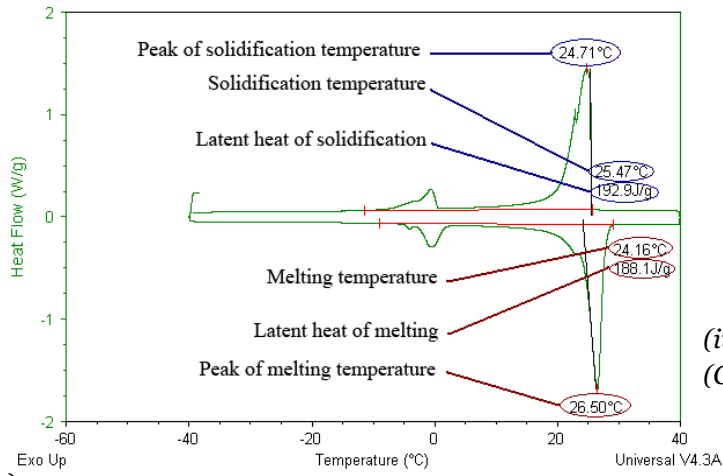
(ii) A26 panel material – paraffin/LDPE composite (Cheechn, 2009)

(iii)



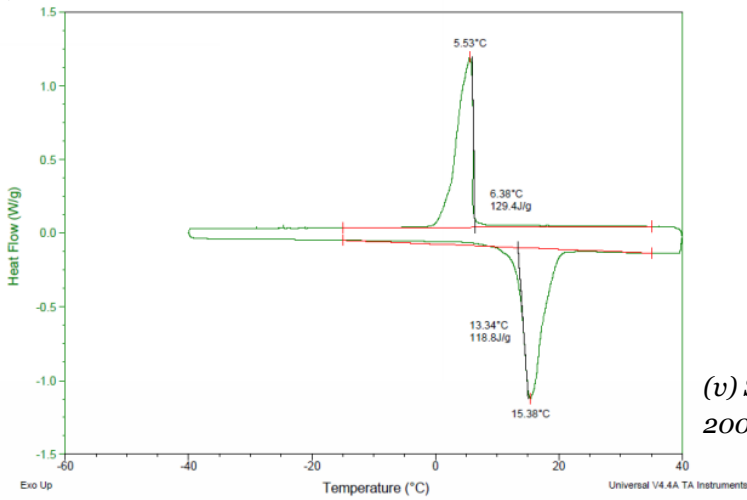
(iii) A22 – pure paraffin (Cheechn, 2009)

(iv)



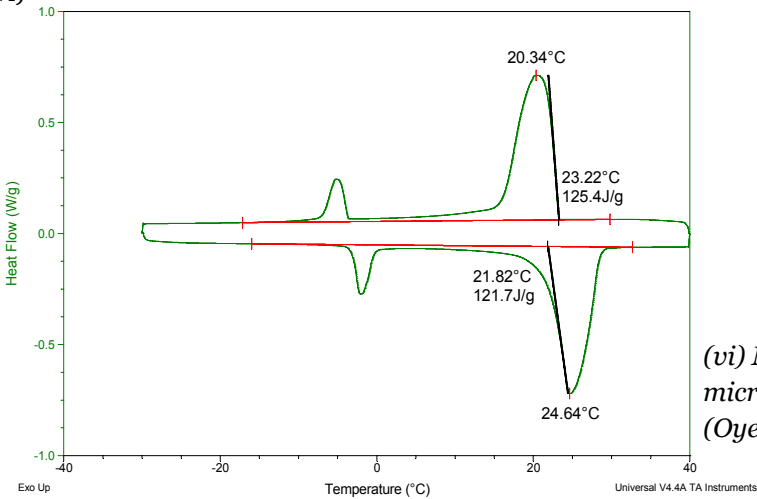
(iv) A26 – pure paraffin (Cheechem, 2009)

(v)



(v) S13 – hydrated salt (Hasan, 2009)

(vi)



(vi) Micronal – microencapsulated paraffin (Oyeleke, 2010).

Table 2.1 Thermophysical properties of commercially available PCMs as obtained by the Brunel PCM Research Group.

PCM Type	Specific Heat (kJ/kg/K)	Latent heat of melting (kJ/kg)	Latent heat of freezing (kJ/kg)	Melting onset temperature (°C)	Melting peak temperature (°C)	Freezing onset temperature (°C)	Freezing peak temperature (°C)	Thermal Conductivity (W/m/K)
A22 (Cheechn, 2009)	2.12	142.17	169.33	13.46	19.79	19.09	18.71	0.18
A26 (Cheechn, 2009)	2.01	185.30	195.40	23.70	26.18	25.13	24.38	0.21
A22 panel (Cheechn, 2009)	2.30	72.38	73.41	11.27	19.31	21.56	18.512	0.26
A26 panel (Cheechn, 2009)	2.31	87.19	90.68	17.15	23.33	24.51	22.25	0.27
A22 ball (Cheechn, 2009)	2.59	53.92	52.91	9.79	19.88	23.59	17.65	0.26
S-13 (Hasan, 2009)	1.54	118.15	111.75	13.46	15.20	6.47	5.09	-
Energain (Capitani, 2011)	-	71	75	8.64	19.98	22.44	15.55	-
Energain pure (Capitani, 2011)	-	155.2	147.9	16.51	22.45	22.05	21.8	-
Micronal (Oyeleke, 2010)	1.85	120.57	124.43	21.85	24.67	23.23	20.44	-
RACUS 73 (Oyeleke, 2010)	2.047	58.27	61.99	21.97	24.42	23.24	21.16	-
RACUS 74 (Oyeleke, 2010)	1.72	83.85	87.29	21.86	24.89	23.23	20.81	-

2.1.3 Containment and Heat Transfer Enhancement

Due to the fact that PCMs become liquid they must be somehow contained to prevent loss of material. This broadly can be done in three ways:

1. Macro-encapsulation
2. Micro-encapsulation
3. Shape stabilisation

Macro-encapsulation is arguably the simplest form of containment. Here bulk quantities of PCM are held in a container, often a ball or panel shape – see Figure 2.5.



Figure 2.5 Macroencapsulated PCM. A PlusICE unit containing salt hydrate.

The units may be used in many ways but are often the main sub-components in insulated tanks. Water to or air acts as a heat transfer fluid passing into the tank, flowing over the modules to exchange heat via forced convection, and then exiting to either discharge accumulated heat or cool an occupied space. This type of system is discussed further in the section on PCM cooling systems later in this chapter.

Micro-encapsulation involves covering microscopic quantities of PCM (normally paraffin) in a hard polymer casing – see Figure 2.6.



Figure 2.6 Microencapsulated PCM. BASF micronal powder (Oyeleke, 2010).

This forms a powder or an emulsion if required, which can be incorporated into many different material types, such as concrete or plasterboard without reacting chemically or leaking upon phase change.

Shape stabilisation is commonly achieved through the blending of paraffin with polyethylene, as in the work of Krupa et al. (2007) and Sari (2004). Here the polyethylene forms a matrix or scaffold which traps the paraffin in small voids. When the paraffin melts it becomes liquid but because it is completely surrounded by the polyethylene it cannot flow. The polyethylene maintains a solid form over the paraffin's phase transition zone, thus allowing the composite to maintain its shape. This technique has formed the basis of commercially available products, the most widely known being the DuPont Energain panel (DuPont, 2007a).

Another way of viewing shape stabilisation is to see the PCM as an additional element in already existing material. In the case of polymeric stabilisation using a substance such as polyethylene, as discussed above, the polyethylene is present purely to stabilise the PCM. In the case of concrete, as explored by Bentz and Turpin (2007) and Hadjeva et al. (2000), the PCM's shape is indeed stabilised but through absorption into a lightweight aggregate which is the primary material. The addition of PCM can increase the thermal capacity of concrete, a topic discussed further in the forthcoming section on passive applications.

As noted earlier the conductivity of PCMs tends to be low but in a space cooling application conductivity is ideally high. Zhang et al. (2006) conducted a study looking for the ideal thermophysical properties of building materials. The general

conclusion was that for passive space cooling high values of specific heat capacity, density and conductivity were preferable for internal surfaces. By generalising to heat capacity that includes latent heat PCMs with enhanced conductivity may be said to have all these properties.

Conductivity enhancement in active systems such as for the storage of solar heat for domestic hot water increases charge or discharge rates of the storage elements (Velraj *et al.*, 1999).

As a result of these considerations a significant amount of research has been aimed at enhancing heat the transfer of heat through the body of the PCM.

The enhancement of conductivity in PCM always involves its combination with a more conductive material. The result may be seen as a hybrid material, i.e. a material formed from more than one material such that it possesses a set of characteristics not all found in the pure substances (Ashby, 2005). Hybrids may be structurally defined as multiple materials combined in a particular configuration and on a particular scale (Ashby, 2005). In all cases the materials used are the PCM (whether it be pure or itself a hybrid through shape stabilisation or the addition of nucleating agents etc) and a more thermally conductive material. There is always a trade off between the thermal capacity of the hybrid and its thermal conductivity. The thermal capacity is the sum of the latent and specific heats of the constituent materials. Here the resultant thermal capacity will be proportionally higher with more PCM content. The effective thermal conductivity of the hybrid is much more complex to determine and the approach will vary with configuration, scale and material.

It is the configuration and scale that are the main differences between cases of hybridising PCM and a more thermally conductive material. Ashby (2005) makes a distinction between configurations of hybrids which is interpreted here.

- **Composite:** Hybrids whose constituent materials are combined on a sufficiently small scale (measured in μm) such that its macroscopic characteristics are uniform.
- **Lattice:** Hybrids composed of a solid network of one material surrounded by a fluid which is in continuous contact with itself. These tend to lie between

composites and segmented systems in terms of scale (measured in mm). Metal foams are a good example of a lattice.

- **Segmented:** Hybrids in which one material forms separate segments which the other material occupies. These tend to be the largest in scale of structure (measured in cm).

Composite configurations have been explored by researchers through the addition of graphite or carbon to paraffin. Sari and Karaipekli (2007) added various quantities of expanded graphite to paraffin. At 10% concentration by weight the graphite increased the conductivity of the composite to 0.82 W/m/K, as compared to 0.22 W/m/K for the pure paraffin (Sari & Karaipekli, 2007). At this concentration the composite was shape-stabilised.

Marin et al. (2005) incorporated a graphite matrix into PCM units in a ventilation system to reduce fan power and charge/discharge time. Hamada et al. compared the addition of carbon chips and carbon fibre.

Lattice structures are porous media and in chemical process industries, from which they originate, are referred to as packed beds. Of interest here are metal foams, single-piece lattice structures formed of porous metal, and random packings, rigid metallic shapes that fill a volume, support each other and create a network of interconnected voids.

In both cases the lattice is formed of the conductive material and the voids are occupied by the PCM. Much research has been undertaken to establish effective thermal conductivities in porous media and packed beds but these often involve the flow of a fluid through the bed and are based on empirical correlations of numerical models, as in the work of Elsari and Hughes (2002), Wang and Pan (2008) and Edouard et al. (2010). Some recent research of this kind, specific to integration with PCM, has been conducted on metal foams. Zhao et al. (2010) derived a thermal conductivity using a method specifically describing foams. They found that the presence of the foam greatly decreased melting and solidification time.

Treles and Dufly (2003) modelled containers of PCM and aluminium foams, of various porosities. It was suggested that an appropriate porosity could be chosen that would increase the effective conductivity sufficiently without displacing too much paraffin.

Velraj et al. (1999) studied the heat discharge rate from an aluminium cylinder containing paraffin and Lessing rings. The effective thermal conductivity was then found by varying its value in their numerical model until real and simulated temperature profiles matched. A value of 2 W/m/K was obtained, 10 times that of the paraffin alone for the loss of just 20% of the volume to the rings.

Hybrids employing segmentation are often realised through the use of fins; a well-established method of heat transfer in fluids. In the paper by Velraj et al. (1999) just mentioned the effect of longitudinal fins was also studied for comparison. In the finned case the reduction of thermal capacity was 7%, but the discharge time was also reduced to a fourth of what it was with pure paraffin; in the case of the Lessing rings it was a ninth.

Agyenim et al. (2009) compared a control cylinder of a PCM known as Erythritol with equivalent cylinders containing internal longitudinal and circular fins. It was found that longitudinal fins had the quickest discharge time.

Another form of segmentation has recently been employed Datum Phase Change (2011) in a new ceiling tile containing a conductive honeycomb structure that divides the contained PCM into discrete units. No data on its performance is available yet. Segmentation can also be commercially found in the multi-purpose panel available from Rubitherm (2011). The idea here is to not only segment but to create completely independent units to maximise surface area and heat transfer rate. This approach has been explored in the academic literature too. For instance the addition of graphite to units in a ventilation system, as studied by Marin et al. (2005), clearly incorporated such segmented units. That experiment may therefore be seen as an example of two heat transfer enhancement techniques employed in the same system.

Agyenim et al. (2010) performed a review of several different heat transfer enhancement studies concluding that the heat transfer characteristics can be improved by a range of techniques. The best results, in terms of effective conductivity, were found in the addition of Lessing rings in the study by Velraj et al. (1999).

The various techniques for enhancing conductivity were reviewed specifically with the design of the NewMass system in mind. In chapter 7 which covers the

system design, these techniques are critically appraised in order to select the most appropriate option for the application.

2.2 Systems in Buildings

The first example of published research on using PCMs for temperature control in buildings came in the form of Telkes and Raymond's seminal paper concerning the use of a solution of Na_2SO_4 to store solar energy for space heating (Telkes & Raymond, 1949). As well as it being the first, this work is notable for several reasons. Telkes and Raymond filled purposely designed voids between rooms with barrels of hydrated salt amounting to 21 tons (19.1 tonnes). This was then heated with air supplied through ducting from simple glazed collectors. The thermal capacity was sufficient to heat the house for 12 days.

In their closing remarks it is mentioned that some optimists may see this system as the "doom of the home furnace"(Telkes & Raymond, 1949). In fact, improvements in heating have focussed on more efficient combustion and improved insulation, with water being the pre-eminent medium for any storage.

Space cooling applications, however, have increasingly been seen as opportunities for the use of PCMs. The past three decades have seen much research in the field and several commercialised products are now available.

2.2.1 Classification

There are several ways in which PCMs have been designed and employed to cool buildings. These systems have been subject to a certain amount of loose classification which has allowed the research community and those with a wider interest in PCMs to conduct a meaningful dialogue. This tacitly agreed upon terminology has for the most part served its purpose; however, some confusion has occurred due to overlapping and/or ill-defined concepts. Furthermore, it is contended that because there is some ambiguity in the concepts of various system

types, potential systems that might exist have not been highlighted due their lack of position in the current taxonomy.

This section reviews the various categories that have been applied to PCM cooling systems with a view to highlighting the conflicts found between these concepts. The general conclusion is that the current arrangement of concepts produces overlaps and gaps, i.e. that certain system types may fall into two categories whilst others may fall into none. This motivated the work presented in chapter 4 on 'design space mapping' which seeks to classify all PCM cooling systems according to a consistent set of rules that leaves no gaps or overlaps in the design space.

Before this new taxonomy is derived the current definitions will be elucidated and applied to the systems reviewed in this chapter. The following subsections will all take their titles from these currently accepted classifications.

We start with the definitions of passive and active TES systems, as expounded by Tyagi and Buddhi (Tyagi & Buddhi, 2007):

- Passive TES systems automatically store heat or coolth when the temperature of the environment rises or falls beyond the temperature of the TES medium.
- Active TES systems are thermally isolated from the environment to be controlled. These systems require a secondary heat transfer fluid to exchange heat with the heat source and sink.

These general definitions of TES systems can (and have been) applied to PCM cooling systems. Some systems, such as a wall boards, fall comfortably into the passive category. Other systems, such as isolated tanks containing PCM modules with flowing water to transfer coolth to the building, fall comfortably into the active category. Some systems do not conform so easily, however, having aspects which are both passive and active. Systems exist that passively cool a room, as they are in direct contact with the space but can actively discharge the accumulated heat to a heat transfer fluid that travels through an embedded pipe network. In this thesis these systems are termed 'thermally activated'. These thermally activated systems

are related to the more commonly known thermally activated building systems (TABS).

TABS are cooling (or heating) systems consisting of pipe networks embedded in the fabric of the building. During the daytime heat may be absorbed by the thermally massive fabric and at night, and/or during the day as necessary, the heat is discharged through circulation of cool water through the pipe network (Lehmann et al., 2007). In partial response to the existence of TABS some systems have been developed which have an active discharge element but are not integrated into the building fabric, such as false ceiling tiles (Koschenz & Lehmann, 2004) and sails. In this work these systems are called ‘thermally activated systems’ to distinguish them from TABS.

The remaining system that has been significantly researched and developed is that which integrates PCM into an air-handling system. Zalba et al. (2004) presented a paper on such a system. The system was said to be a ‘free-cooling’ system and free-cooling was defined as:

“a means to store outside coolness during the night, to supply indoor cooling during the day.” (Zalba *et al.*, 2004)

This definition excludes a refrigerating element to cool the storage medium (in our case PCM) and is very inclusive. In fact it would seem to admit wholly passive systems as well but Butala and Stritih state that free-cooling

“combines increased thermal mass and night ventilation.” (Butala & Stritih, 2009)

Butala and Stritih appear to be referring to a specific instance in which additional thermal mass is added to a ceiling plenum and mechanical ventilation is used to transfer the heat; as attested to by the images in the same paper. However, it is conceded that the definition does not indicate that the PCM must be isolated.

The essential elements can be said to be forced air flow which allows heat to be transferred to PCM elements during the daytime for cooling and from PCM elements during the night time for discharge of that heat.

This appears to be close to the definition of ‘indirect night cooling’ given by Barnard’s (Barnard, 2006), amongst others.

There is clearly inconsistency here. Other researchers, such as Yanbing et al. (2003), for instance, talk of ‘night ventilation’ with packed bed storage.

Barnard, Butala and Stritih, Yanbing et al. and potentially Zalba et al. appear to all talking about the same type of system: One that is isolated from the conditioned space but transfers coolth to it via forced convection and discharges accumulated heat by the mechanical ventilation of night air. We therefore have three terms that refer to the same concept; a significant overlap.

For clarity, all systems that conform to this definition and are reviewed in this chapter will be grouped under the heading ‘Free-cooling’. This does conflict with important sources, such as CIBSE (Barnard & Jaunzens, 2005), who apply a looser definition that does not explicitly require isolation of the PCM units and may also apply during the daytime. In this thesis the term only applies to the more specific case just described only.

The direct night cooling system that Barnard refers to is considered synonymous with the passive system defined earlier and all systems of this type will be grouped under the heading ‘Passive.’

It is worth noting that Santamouris and Asimakopoulous make the distinction between ‘Passive cooling’, which can be used to prevent and modulate heat gains, and ‘Natural cooling’, which refers to the use of natural heat sinks to dissipate heat through ventilation, evaporative cooling, ground cooling and radiative cooling (Santamouris & Asimakopoulous, 1996). The problem here is that the modulation of heat gains under passive cooling involves the cooling of a building’s thermal mass at night. This sinking of heat is also a natural cooling technique. This constitutes another overlap of concepts.

These overlapping concepts are believed to be the result of an evolving consensus between members of the research community, born of a practical need to label

systems for meaningful discussions. However, this approach fails to effectively map the design space. There is no underlying logic that effectively delineates the various potential system types and sets out their relation to one another. Instead this form of classification just maps out the existing systems studied. As well as this approach allowing overlaps to occur, it does not highlight potential new types of system. It does not represent all potential systems and thereby highlight potentially new and fruitful areas of research.

Chapter 4 will address this issue by establishing a new way to categorise all systems according to fundamental principles of heat flow between media.

2.2.2 Active Systems

By the definition given above active cool storage systems are defined by the isolation of the PCM (normally in an insulated tank) and the consequential need for a secondary heat transfer fluid. In addition, the vast majority of active systems incorporate, or rather, are based on refrigeration – i.e. a conventional chiller.

After the energy shocks of the 1970s, there was a growing awareness in the USA of environmental issues, economic pressure and fuel security which led to particular interest in demand side management (DSM), a term coined by the electric power research institute (EPRI) (Gellings, 1996). DSM is the management of power at the point of use rather than at the point of generation. The now familiar concept had not been previously exploited by power companies so the only way to deal with high power demand was to build additional capacity. By encouraging the consumer to shift his/her energy use from daytime to night time, generators were better able to cope with demand. The motive for building operators to make the shift was financial; a tariff structure which priced night time electricity at lower rates would yield savings if it was possible to utilise. The means of utilisation was thermal storage. By generating coolth at night for use in the day, building operators would save money. With this in mind the EPRI funded a comprehensive research programme on DSM which generated substantial interest in the cool thermal storage (Gellings, 1996). By 1994 cool TES installations numbered between 1500 and 2000 in the US (Potter *et al.*, 1995).

By shifting chiller operation from day to night time the coefficient of performance (COP) is increased, in the case of air-cooled chillers, due to depressed night time temperatures. It has been suggested that this can lead to overall energy savings but evidence for this is very limited. For instance, Sebzali and Rubini (2007) conducted a study of the predicted performance of chilled water storage facilities in Kuwait. Here they found that with full storage an energy saving of 4% could be made, as compared to a conventional system.

There are three main media for active cool storage: Chilled water, ice and PCM. Storage temperature is normally maintained somewhere between 0 and 9 °C. The potential for savings is explained as follows:

Conventional chillers operate on a vapour compression cycle which consists of four stages through which the refrigerant passes:

- Compression (Pressure increased, volume reduced.)
- Condensation (Gas becomes liquid – heat lost.)
- Expansion (Pressure reduced.)
- Evaporation (Liquid becomes gas – heat gained.) (Tassou, 2005)

Eq. 2.6 shows the variation of the coefficient of performance (COP) with temperature, assuming Carnot efficiency.

$$COP_{cooling} = \frac{Q_{cold}}{W} = \frac{Q_{cold}}{Q_{hot} - Q_{cold}} = \frac{T_{cold}}{T_{hot} - T_{cold}} \quad (2.6)$$

(Tassou, 2005)

The COP of a vapour compression chiller will vary with the temperature at the condenser. A lower condenser temperature yields a higher COP. For air-cooled chillers, the condenser temperature will reduce with the ambient dry bulb temperature. This is true for actual chillers, as well as idealised ones. By operating chillers at times of lower air temperature, i.e. the night time, the overall energy use of the system may be reduced. For this to happen, thermal storage is required. As

mentioned above, this may come in the form of ice storage, chilled water storage or PCM storage. Systems incorporating ice storage are inherently inefficient because the chiller has to operate at a lower evaporator temperature. From Eq. 2.4 we can see that this results in a lower COP than would be the case for system with no storage. The system incorporating chilled water storage may well be more efficient but due to the small difference in flow and return temperature the thermal capacity of the water per unit volume is small and a relatively large tank is required to store the generated coolth.

Both of these problems can be overcome by using a PCM with a relatively high melt temperature. The COP will remain at a maximum and the tank size may be reduced to an acceptable level.

Studies of installed active latent heat thermal energy storage systems, and their associated energy use, are not common. Hasnain (1998) compared working cool thermal storage systems but only one eutectic salt system was covered and energy savings were not calculated. Bedecarrats et al. (1996) monitored and modelled the charge and discharge of a tank containing spheres of pure water which underwent phase change but did not calculate energy savings. Chan et al. (2006) modelled several versions of a district cooling system in Hong Kong using ice storage and sea water for cooling. The control case with no ice storage used least energy because the chillers could operate at a higher COP. The focus of this work however was financial rather than energetic. Potter et al. (1995) conducted a major review of TES installations in the US but these did not include energy savings. Liu et al. (1994) studied four TES installations, including one eutectic salt installation, but did not calculate energy savings. Studies with calculated energy savings or system COP often reveal design or operational drawbacks leading to energy costs rather than savings. Merten et al. (1989) studied several TES installations and found that the eutectic salt system, like the chilled water and ice systems studied, used more energy than a conventional system. This was attributed to marginal COP gains at night and large pumping energy costs. System control was blamed for the poor performance of a University ice storage system in a study by Aziz et al. (2010). Piette (1990) monitored an ice storage system in a San Franciscan office building where the system's overall COP was initially at a higher value than the equivalent storeless

system, due to depressed night time temperatures, but this reduced rapidly because of operational issues. Akbari and Sezgen (1995) built on this work by studying the same system plus one more. They calculated heavy energy costs for one and energy use comparable to a conventional system for the other. The energy costs were attributed to low ice-making COPs and poor heat exchangers.

It is worth noting examples of unreviewed work. Some case studies by CIBSE are: A Brewery in Dundalk, Ireland, where a sub-zero eutectic salts installation is reported to save electricity by improving system efficiency through operating compressors under steady state conditions and raising low temperature and high temperature circuits by 5 °C; a bank in London where a eutectic salt store has yielded a 300 kW reduction in electrical requirement but overall savings are not given; and a Cambridge building in which a unitary heat pump and eutectic salt store system resulted in CO₂ savings of 48 kg/m² (CIBSE & ARUP Research Committee, 1998). Miller et al. (2005) refer to a large eutectic tank system with unitary heat pumps for heating and cooling in Bristol, UK. The system reduces the cooling load but energy savings are not given. A new council house building in Melbourne employs 30,000 stainless steel balls with 920 kWh of storage. Energy savings have not been calculated (Melbourne City Council, 2006).

Due to the lack of definitive evidence on the energy savings that may be incurred by active PCM systems there is an opportunity to gain more post-installation data to understand the issues that may be affecting modern functioning active LHTES systems. This conclusion led to the post-installation energy audit of an office cooling system with PCM tank which will be presented in chapter 3. The apparent marginal savings also, however, confirmed the need to research other types of PCM cooling application for significant energy savings.

2.2.3 Passive Systems

As well as the definition just given passive PCM systems may be said to refer to PCM systems which seek to replace thermal mass. This aim to mimic thermal mass is

clearly seen by the integration into the building fabric of most passive systems, wallboards and ceiling tiles being the most common.

One early full-scale laboratory wallboard test was carried out by Scalat et al. (1996) who impregnated ordinary gypsum wall boards with fatty esters. The impregnated wallboards and plain control wallboards were installed in identical test cells of dimensions: 2.29 x 2.27 x 2.45m. The time taken to reach peak air temperatures from 18 to 22 °C was found to be 24.1 and 45.6 hours for the control and PCM cells respectively.

Castell et al. (2010) constructed cubicles from brick and lined the non-control cubicles with macro-encapsulated PCM panels produced by Rubitherm, as mentioned in the heat transfer enhancement section. This resulted in peak temperature reductions of up to 1 °C, for free-floating temperature tests, and energy reductions of 15% and 17% for the PCMs RT27 and SP25, respectively, in air conditioned tests with a set point of 24 °C.

Ahmad et al. (2006) constructed externally located test cells with and without PCM panels (5 in total, each containing 20 kg of polyethylene glycol in a PVC alveolar panel) backed with vacuum insulation panels (VIPs). Here it was found that the cell containing PCM panels reached a maximum of 40 °C, whereas the one without exceed 60 °C.

Impregnation and macro-encapsulation are both said to entail practical issues which prevented commercialisation of wall board products. Schossig et al. (2005) refer to the tendency to leak PCM in impregnated materials and the protection against casing damage required of macro-encapsulated units. Their research proposed micro-encapsulation as the way to avoid these issues. Successful full-scale tests revealed a 4 °C reduction in peak temperature as compared to the test room.

Due to the peak cooling load reductions achieved coupled with improvements to their practical implementation, wallboard products have emerged. The most well-known of these are the Knauf Smartboard, plasterboard with integrated micro-encapsulated paraffin and DuPont Energain, paraffin combined with a polyethylene shape stabiliser for installation behind plasterboard.

Kuznik et al. (2008) studied the Energain panel and determined its optimum thickness (~10cm) using the software CODYMUR. The panel has achieved

considerable commercial success due to its 'off-the-shelf' usability and can be installed by labourers able to install typical plasterboard.

Kuznik and Virgone (2009) went on to make a full scale test cell study of Energain panels. The decrement factor (the ratio between the amplitude of the room temperature variation with PCM and the room temperature variation without PCM) was found to be 0.79 in the high cooling case.

Research into the use of wall boards or panels extends beyond the obvious application. Variations on the typically internally applied units include work conducted by Huang et al. (2006) who predicted the impact of integrating PCM panels into the cavity of a cavity wall construction with positive benefits for the control of internal temperatures.

All of this research reveals the benefits in using PCM wall boards and panels. The main benefit is the control of internal temperature, as attested to by commonly displayed graphs of dampened temperature oscillation. We can readily conclude therefore that PCM wallboards and panels can reduce the cooling energy required in buildings. What the research does not always do is quantify this energy saving. Exceptions to this may be found in examples such as Castell et al.'s work (see above) and that of Shileih et al. (2007) who compared PCM wallboards to normal wallboards by successively testing them in a controlled test cell and monitoring the electrical input required to heat the cell to 24 °C. This resulted in proportional savings of 41%. However it is questionable whether this figure would actually represent savings since it is the energy required to limit further temperature rise that should be avoided, not the energy required to reach a comfortable temperature of 24 °C in the first place.

Another approach to passive application is rather than replacing thermal mass, increase the thermal capacity of the mass to increase the daily cooling load it can bear. Hawes et al. (1993) discussed the integration of various types of PCM into wallboards and concrete through direct integration or immersion and macro-encapsulation. In the case of macro-encapsulation it was noted that further research was needed.

Cabeza et al. (2007) constructed concrete cubicles from concrete panels, three of which contained 5% by weight of Micronal PCM. Results showed a dampening of cubicle temperature fluctuations, 1 °C lower and 2 °C higher than the maximum and minimum temperatures seen in a control cubicle of pure concrete. A further interesting feature was a significant reduction in heat flux through the cubicle wall when phase transition was reached. Although the cooling requirement would not be reduced a great deal by this work, largely because the concrete has high thermal mass in the first place, some benefit is seen.

A related approach is to integrate PCM in a concrete construction by locating a panel between two concrete slabs, rather than infusing concrete at the micro level. This is done by Pasupathy and Velraj (2008) who found excellent internal temperature moderation enhancement by locating a layer of PCM between slabs of brick and mortar and concrete.

More recently, significant new products in the form of ceiling tiles, known as RACUS have emerged. This product was noted in the heat transfer enhancement section and has not been subject to controlled academic testing. The opportunity was therefore taken to test the product and compare its performance to that of the more established Energain panel. This work is presented in chapter 6.

The research discussed thus far does not question the approach of fabric incorporation, preferring to exist within the paradigm of thermal mass as a constituent building component. At the opening of Cabeza et al.'s article it is pointed out that such approaches are logical since the large exposed floor and ceiling areas are exploited for heat transfer. However in many buildings this concrete or general thermal mass exposure is not found. Complex ceiling geometries, services conduits, furniture, wall hangings and many other objects will often limit heat exchange to much of these surfaces. In relation to this, Barnard (2006) discusses the issues associated with exposure of the soffit, which include acoustics, high level service integration and aesthetics. Furthermore the surface area to volume ratio found in a typical room will be much larger than the cubicles constructed. This reduces the cooling potential yet further.

Work that questions fabric integration, and in a more general sense the limitations of passive applications, is less voluminous than the work which examines their positive aspects. DuPont claim that building operators using DuPont Energain panels which may be applied to all walls and ceiling in the right circumstances are told that they can expect to up to 35% of their air conditioning energy (DuPont, 2010). The reason there is a limit to the potential savings is the limited surface area for cooling and the limited amount of PCM that can be put in the space, since the panels are only 5 mm thick. There is therefore an opportunity to save more cooling energy if the surface area and volume of the PCM units is increased.

Another disadvantage is the potential inability of the PCM units to reject heat at night due to elevated night time temperatures that do not allow the PCM to refreeze. The work conducted by Schossig et al. (2005) revealed an inability to sufficiently reject heat at night. Higher air flow rates were desired. However, the fan power required for this can become prohibitive. CIBSE advise that for large systems, with pressure drops of over 1000 Pa any energy savings may be outweighed (Barnard & Jaunzens, 2005).

In conclusion, it is clear that existing research shows that passive applications can have a significant positive impact on the peak temperatures, decrement factors and cooling energy usage of cooled spaces. However, they can suffer from the disadvantages of a lack of thermal and cooling capacity, an inability to reject heat on warm nights and the possibility of prohibitively high fan energy. There is an opportunity to develop new systems that do not have heat transfer capacities that are limited by the exposed surface area of thermal mass in a space and can guarantee the rejection of accumulated heat at night.

The majority of research has been on active and passive systems but thermally activated and free cooling systems have also both been subject to significant research in recent years. A description is found in the following two sections.

2.2.4 Free cooling systems

Free cooling systems have generated a large amount of research interest because they may offer a way to control the cooling delivered to a space, to improve the prospects for accumulated heat discharge and to save energy. A significant advantage over purely passive systems is the targeted flow of air to reject heat effectively at night and deliver cooling when required during the day.

Zalba et al. (2004) produced a study of a prototype free cooling system using PCM panels in a ducted air circuit. This indicated savings could be made over a conventional system if fan power was minimised. This work was then extended by Marin et al. (2005) who used the same testing apparatus but incorporated a graphite matrix into the PCM units to reduce fan power and charge/discharge time.

A similar study by Lazaro et al. also used PCM panels containing paraffin, obtained from Rubitherm. The panels were located in a prototype ventilation system which was able to deliver 1 kW of cooling over 3 hours (Lazaro *et al.*, 2009). Both of these systems would be suited to a centralised air handling system.

Butala and Stritih (2009) tested a ventilation system incorporating a PCM unit with external fins to promote convective heat transfer and internal fins to promote conductive heat transfer. Here it was noted that for this application PCMs with a phase transition zone in the range 19 to 24 °C should be used for free cooling since this allows for an adequate temperature difference for heat transfer between passing air and the PCM in both charge and discharge. RT20 was the chosen PCM. This work corroborates the work done by Arkar and Medved in which a ventilation system was filled with spheres of RT20 after it was numerically found that PCMs that melt in the range 20 to 22 °C are most suitable for free cooling applications. Clear heating and cooling of the air was produced but the work focussed on the modelling techniques employed rather than the system operation (Arkar & Medved, 2007).

Similar work was done by Yanbing et al. (2003) in which a ducted system clearly provided cooling when compared to control rooms but not enough detail about fan power was given. Consequently system COPs appeared unrealistically high.

A product which has emerged along these lines is the Artica system (Artica, 2011). This product is charged and discharged with ventilation air and claims to save up to 90% of cooling energy as compared to conventional air conditioning systems. What is not clear is how this figure is arrived at and whether additional fan power due to additional pressure drop has been factored in. It is highly probable that the high savings are only achieved in climates with sufficiently low night time temperatures and fairly low cooling loads, as thermal capacity would be limited.

Other products that have emerged from this field do not conform so closely to a conventional ducting design, being low level modular units, such as a product from EMCO (2008). All of these are self contained units that are integrated into the facade. They mechanically draw in external or internal air which passes over cooled PCM units and then into the occupied space. At night accumulated heat is discharged by mechanically circulating cool night air. The advantage of these systems is that they are modular units and maybe be easier to install than integration into existing mechanical ventilation systems. They also have a small path for the air to travel through so pressure drops may be expected to be low. The disadvantages are that their thermal storage capacity is quite limited and they cannot guarantee cooling if the night air temperature is not low enough.

Further iterations on the free cooling theme have emerged. One example of this is the work conducted by Turnpenny et al. (2000) who designed and tested a system using heat pipes to transfer heat to PCM stores at ceiling level. Barnard (2006) presented a hybrid night cooling system that entrained circulated night air into gaps between a concrete soffit and a cassette containing packs of PCM. This cooled the soffit and the PCM, allowing the system fan to operate during the day to supply cool air to the room. With a high control temperature of 27 °C the system used only 25% of the conventional cooling system power and allowed DX units to be downsized.

Free cooling systems may start to acquire commercial success in the next few years due to their ability to be installed in new-builds and retrofits with beneficial results in terms of energy performance. Their application is not suited to climates with high night time temperatures as they will not be able to reject accumulated heat. Thermal

storage capacity will be limited and fan power may become prohibitively high depending on the system design.

There is an opportunity to develop systems which reject heat more reliably, have greater thermal capacity and do not rely on fan energy for the transfer of heat.

2.2.5 Thermally Activated Systems

Thermally activated systems are the least researched and applied of the systems reviewed here. This may be due to their relative complexity. Passive systems are extremely simple in the sense that no attendant mechanical devices are required. Active and free cooling systems are both incorporated into systems which have to exist anyway. Thermally activated systems require a more radical redesign of the space and its cooling provision as systems may need to be incorporated into the fabric along with the attendant pipework for heat discharge.

Commercially BASF Micronal has proven to be an effective product for integration into various system designs. This is partly publicised on their website by a study by Fisch and Kuhl (2011). Here two rooms in a Berlin office building were compared, one with walls coated in a micronal-plaster compound, the other with conventional plaster. Both contained capillary mats to create TABS. Modest results were seen with a maximum temperature difference of 2 °C seen between the rooms.

Koschenz and Lehmann (2004) made the point that it is not always possible to expose mass because of acoustic and service location issues. Their solution was to design and test a prototype system consisting of internally finned ceiling panels containing a gypsum and micronal composite and capillary tube network. The results indicated that an average load of 39 W/m² could be absorbed over a 7.5 hour period by the melting paraffin. The capillary tubes would then be able to discharge the accumulated heat at night. The system's limited thermal capacity was noted but the lack of perceivable energy savings without passive discharge was not.

A product that (potentially) emerged from this limited research was the Ilkatherm panel from Ilkazell (2010). This comes in modular board-type units consisting of Knauf plasterboard backed with insulation. A capillary tube network runs through the intersection of these components. It can be installed as a ceiling board, wall board or sail. The main disadvantage is its limited heat capacity due to a

limit to the Micronal material that can be incorporated into the plasterboard and the number that can be usefully incorporated into the space.

Another interesting system was installed the WILO building in Westzaan, Holland. This employed a corrugated ceiling filled with a concrete-micronal composite. Copper pipes run through the composite to discharge accumulated heat (Bouwman, 2011). No performance data has been obtained.

The advantage of these systems is that they are passive in their thermal charging operation and discharge of heat can be guaranteed through the circulation of chilled water. The drawback is the same as the passive applications: limited thermal and cooling capacity. The concept was developed and became the NewMass system design, which seeks to increase the system's capacity, described in chapters 7 and 8.

2.3 Modelling

This section is divided into two parts. The first looks at the problem of modelling phase change itself. The second looks at the modelling of systems that employ phase change elements.

2.3.1 Modelling a change of phase

A wide variety of approaches to modelling phase change have been applied in recent decades. Moving boundary, or Stefan, problems may only be solved analytically in one dimension and only in a limited number of scenarios. Examples of relatively recent analytical solutions that have been derived are Bansal and Buddhi (1992), for a cylindrical thermal store in a solar heating system, and Lamberg and Siren (2003), for PCM melting due to a thin heated fin.

Other approaches have been taken. Neeper (2000) presented a one-dimensional model of an idealised PCM wall board that assumed a sinusoidal variation in room temperature. From this he derived rules for specification of PCMs in wall board applications but the model was not validated. Huang et al. (2006), in their examination of applying PCM to internal wall cavities, used a previously

validated numerical two dimensional model based on temperature to predict temperature profile evolution over time under different boundary conditions.

Numerical methods are now routinely used to evaluate phase change in two and three dimensional geometries with a shift towards methods that do not explicitly track the phase change boundary. There are many examples of variations on the commonly employed enthalpy method: Voller and Cross (1981) presented an accurate method applicable in one and two dimensions and applied it to a welding problem. Costa et al. (1998) used a one and two dimensional modelling of a space heating system. Zivkovic and Fujii (2001) modelled a simple cuboid PCM container. Frusteri et al. (2006), modelled a one dimensional heat transfer diffusion scenario of a PCM cylinder containing carbon fibres. The enthalpy-porosity approach is often used in the modelling of finned heat sinks, as in the examples of Shatikian et al. (2005) and Wang et al. (2008). Tan et al. (2009) used the enthalpy porosity formulation to model spherical capsules of commercially available paraffin.

In the enthalpy porosity formulation the liquid front is not tracked explicitly. Instead an enthalpy balance,

$$\frac{\partial}{\partial t}(\rho H) + \nabla \cdot (\rho \vec{v} H) = \nabla \cdot (k \nabla T) \pm S, \quad (2.7)$$

in which

$$H = h_{\text{ref}} + \int_{T_{\text{ref}}}^T C_p dT + \beta L_{\text{fus}} \quad (2.8)$$

is used to compute the liquid fraction, β , where,

¹ ∇ (del) is the mathematical operator that may be seen as a contraction of a first order differential in three dimensions, i.e. $\nabla \phi = i \frac{\partial \phi}{\partial x} + j \frac{\partial \phi}{\partial y} + k \frac{\partial \phi}{\partial z}$, where i, j and k are unit vectors of value 1. In other words, when del applies it finds the gradient of whatever function it is applied to, in the three spatial dimensions.

$$\beta = 0 \text{ if } T < T_{\text{solidus}}$$

$$\beta = 1 \text{ if } T > T_{\text{liquidus}}$$

$$\beta = \frac{T - T_{\text{solidus}}}{T_{\text{liquidus}} - T_{\text{solidus}}} \text{ if } T_{\text{solidus}} < T < T_{\text{liquidus}}, \quad (2.9)$$

at each time step of a finite difference model. This method has been well explained by Voller (1996). This may be done using CFD software such as FLUENT.

FLUENT performs iterations between equations 2.7 and 2.8 in order to find the temperature in each element of a finite matrix of cells (Voller, 1996). If the substance is shape stabilised all particles will have permanent zero velocity. In addition, no heat generation occurs and so the associated terms go to zero and drop out of Eq. 2.7

$$\frac{\partial(\rho H)}{\partial t} = \nabla(k\nabla T) \quad (2.10)$$

Substituting for H (Eq. 2.8), Eq. (2.11) results:

$$\left[\rho C_p + \frac{\rho L}{(T_{\text{liquidus}} - T_{\text{solidus}})} \right] \frac{\partial T}{\partial t} = \nabla(k\nabla T) \quad (2.11)$$

This modelling method was applied in the Passive PCM Sails tests presented in chapter 5.

2.3.2 Modelling PCM cooling systems

Various approaches have been taken to the problem of accounting for the influence of a PCM cooling system on the temperature of a building. Due to the variety of ways they interact with a space (directly through passive systems, indirectly through

ducted air flow or fan coils in active systems for instance) the techniques employed may be extremely different.

Passive systems are probably most suitably modelled by existing thermal modelling software such as IES (2011) or TAS (EDSL, 2011b). Unfortunately the industry is slow to respond to this need. Many building physicists will model passive systems as equivalent thermal mass but because this does not properly account for the great variation in enthalpy rise inherent in PCMs the results can be rather inaccurate.

TAS has recently produced a plug-in with DuPont that models Energain panels as small separate zones with well validated results (EDSL, 2011a). DuPont have until recently had exclusive access to their in-house software, CoDyBa (DuPont, 2007c), preferring to do the modelling themselves. However as the market for PCM products has expanded this ability is being given to engineering consultancies.

Kuznik et al. (2008) used CODYBA software to determine the optimal thickness of DuPont Energain wallboards. This models walls containing PCM assuming one-dimensional heat transfer and employing an explicit Eulerian scheme (one that calculates successive parameter values by using the previous time step's parameters as inputs.)

Popular in academic circles, TRNSYS (TESS inc., 2007) has been used by various researchers to model passive systems. For example Ahmad et al. (2006) modelled their PCM wallboard test cell experiment with TRNSYS. The model used a step function and finite difference model to represent the melting of the PCM. This approach was justified based on the same successfully applied method in previous works.

The U.S. Department of Energy's modelling software, EnergyPlus, can also be used to model PCMs in the built environment (U.S. Department of Energy, 2011). This software has the advantages of employing a Google sketch-up interface for building geometry realisation and effectively accepting DSC curve data to describe the thermophysical behaviour of a range of PCMs.

2.4 Conclusions

This literature review covered all subjects relevant to the study of PCM cooling systems.

Methods for obtaining thermophysical characteristics, T-history and DSC, were reviewed, with the conclusion that both methods are valid but care must be taken to test small samples at sufficiently slow rates to ensure accuracy with the DSC method. For inhomogeneous substances testing several samples can ensure reliable macroscopic property values are obtained.

Described approaches to containment were micro-encapsulation, macro-encapsulation and shape-stabilisation. Approaches to heat transfer enhancement were seen as hybridising PCM with a more thermally conductive material and were divided into composite, lattice and segmented categories operating a different scales.

Opportunities for further research were identified in the section on PCM cooling systems.

Active systems were reviewed first. Here it was shown that active systems have the potential to gain marginal energy savings but fail to do so in most, but not all, cases. There is an opportunity to gather more evidence on system to operation and the reasons for success or failure. This prompted the work conducted in chapter 3.

Passive systems were reviewed second. Here it was shown that installed systems (mainly wallboards) reduce peak temperatures and save cooling energy. System drawbacks are a limited thermal and cooling capacity, an inability to reject heat on warm nights and potentially high fan power. These considerations ultimately led to the development of the Passive PCM Sails, described in chapter 4, and the NewMass system described in chapters 7 and 8. The Passive PCM Sail design aims to solve the problems of limited heat transfer rate during the day and night. The NewMass system does the same and guarantees next day performance.

Free cooling systems were reviewed third. These systems have the advantage of targeted air flow to discharge heat more efficiently than purely passive systems. Disadvantages can be an inability to reject heat on warm nights and the fan power required for active operation. As with the conclusions based on the passive systems,

these conclusions led to the development of the Passive PCM Sails and the NewMass systems.

Thermally activated systems were reviewed last. These systems have the advantage of operating passively during the day, have the ability to discharge heat to a chilled water circuit to guarantee next day performance but, as with passive systems, the surface area available for heat transfer and therefore cooling is limited. The final NewMass design, presented in chapter 7, is an extension of the thermally activated systems discussed with the potential for increased thermal and cooling capacity.

References

- Agyenim, F., Eames, P. & Smyth, M. (2009) "A comparison of heat transfer enhancement in a medium temperature thermal energy storage heat exchanger using fins", *Solar Energy*, vol. 83, pp. 1509-1520.
- Agyenim, F., Hewitt, N., Eames, P. & Smyth, M. (2010) "A review of materials, heat transfer and phase change problem formulation for latent heat thermal energy storage systems (LHTESS)", *Renewable and Sustainable Energy Reviews*, vol. 14, pp. 615-628.
- Ahmad, M., Bontemps, A., Sallee, H. & Quenard, D. (2006) "Thermal testing and numerical simulation of a prototype cell using light wallboards coupling vacuum isolation panels and phase change material", *Energy and Buildings*, vol. 38, pp. 673-681.
- Akbari, H. & Sezgen, O. (1995) "Performance evaluation of thermal energy storage systems", *Energy and Buildings*, vol. 22, pp. 15-24.
- Arkar, C. & Medved, S. (2007) "Free cooling of a building using PCM heat storage integrated into the ventilation system", *Solar Energy*, vol. 81, pp. 1078-1087.

- Artica (2009) *Artica Technologies: Classic*. Available: <http://www.articatechnologies.com/solutions.php> [03/01/2012].
- Artica (2011) *Artica Technologies*. Available : <http://www.articatechnologies.com/> [25/09/2011].
- Ashby, M.F. (2005) "Hybrids to fill holes in material property space", *Philosophical magazine*, vol. 85, no. 26, pp. 3235-3257.
- Aziz, M.B.A., Zain, Z.M., Baki, S.R.M.S. & Muslam, M.N. (2010) "Review on performance of thermal energy storage system at S & T complex", *Control and system graduate research colloquium*, IEEE, .
- Bahadori, M.N. (1985) "Natural production, storage and utilization of ice in deep ponds for summer air conditioning", *Solar Energy*, vol. 34, no. 2, pp. 143-149.
- Bahadori, M.N. (1984) "Natural cooling system and an economic feasibility study of long-term storage of coolness", *Energy*, vol. 9, no. 7, pp. 589-604.
- Bahadori, M.N. (1976) "Passive Cooling Systems in Iranian Architecture", *Scientific American*, February 1976.
- Bansal, N.K. & Buddhi, D. (1992) "An Analytical Study of a Latent heat Storage System in a Cylinder", *Energy Conversion Management*, vol. 33, no. 4, pp. 235-242.
- Barnard, N. (2006) *Hybrid Cooling Solutions: Night Cooling and Mechanical Refrigeration*, Advance Proof edn, Institute of Refrigeration, London.
- Barnard, N. & Jaunzens, D. (2005) "Section 2: Ventilation and air conditioning" in *Heating, ventilating, air conditioning and refrigeration: CIBSE guide B*, ed. K. Butcher, CIBSE, London, pp. 2-1-2-142.
- BASF (2011) *Micronal PCM*. Available: http://www.micronal.de/portal/load/fid443847/BASF_Micronal_PCM_Brochure%202009_English.pdf [01/03/2012].

- Bédécarrats, J.P., Strub, F., Falcon, B. & Dumas, J.P. (1996) "Phase-change thermal energy storage using spherical capsules: performance of a test plant", *International Journal of Refrigeration*, vol. 19, no. 3, pp. 187-196.
- Bentz, D.P. & Turpin, R. (2007) "Potential applications of phase change materials in concrete technology", *Cement & Concrete Composites*, vol. 29, pp. 527-532.
- Bouwman, I.M. *PCM in the built environment: Combining comfort and sustainability*. Available:
http://www.deerns.nl/documents/PCM_Deerns_IBouwman_20081113_v2.0_1.pdf [24/09/2011].
- Buddhi, D. & Sharma, S.D. (1999) "Measurements of transmittance of solar radiation through stearic acid: a latent heat storage material", *Energy Conversion and Management*, vol. 40, no. 18, pp. 1979-1984.
- Butala, V. & Stritih, U. (2009) "Experimental investigation of PCM cold storage", *Energy and Buildings*, vol. 41, pp. 354-359.
- BWGA (2011) *Other ice houses in the UK*. Available:
<http://bohemiawga.weebly.com/other-ice-houses.html> [22/09/2011].
- Cabeza, L.F., Roca, J., Nogues, M., Zalba, B. & Marin, J.M. (2002) "Transportation and conservation of temperature sensitive materials with phase change materials: state of the art", *ECES IA Annex 17, Advanced Thermal Energy Storage Techniques - Feasibility Studies and Demonstration Projects, 2nd Workshop*, IEA.
- Cabeza, L.F., Castellón, C., Nogués, M., Medrano, M., Leppers, R. & Zubillaga, O. (2007) "Use of microencapsulated PCM in concrete walls for energy savings", *Energy and Buildings*, vol. 39, no. 2, pp. 113-119.
- Capitani, A. (2011) *Energy savings in buildings: Phase change materials*, Brunel University, Uxbridge.

- Castell, A., Martorell, I., Medrano, M., Pérez, G. & Cabeza, L.F. (2010) "Experimental study of using PCM in brick constructive solutions for passive cooling", *Energy and Buildings*, vol. 42, no. 4, pp. 534-540.
- Cengel, Y.A. (2003) *Heat Transfer: A Practical Approach*, 2nd edn, McGraw-Hill, New York.
- Chan, A.L.S., Chow, T., Fong, S.K.F. & Lin, J.Z. (2006) "Performance evaluation of district cooling plant with ice storage", *Energy*, vol. 31, pp. 2750-2762.
- Cheechern, T. (2009) *The Application of the Shrinking Core Model to Phase Change Materials (Masters Dissertation)*, Brunel University, Uxbridge.
- CIBSE & ARUP Research Committee (1998) *Thermal Storage: Environmental Benefits*, CIBSE, London.
- Costa, M., Buddhi, D. & Oliva, A. (1998) "Numerical Simulation of a Latent heat Thermal Energy Storage System with Enhanced Heat Conduction", *Energy Conversion Management*, vol. 39, no. 3/4, pp. 319-330.
- Cristopia Energy Systems (2011) *Products*. Available:
<http://www.cristopia.com/cristopia/english/products/indproducts.html>
[14/092011].
- Datum phase change (2011) *Suspended ceiling tiles*. Available:
<http://www.datumphasechange.com/index.php?racus-honeycomb-ceiling-tile>
[02/01/2012].
- Dehouche, Z., Grimard, N., Laurencelle, F., Goyette, J. & Bose, T.K. (2005) "Hydride alloy properties investigation for hydrogen sorption compressors", *Journal of Alloys and Compounds*, vol. 399, no. 1-2, pp. 224-236.
- DuPont (2010) *Energy Management*. Available:
http://energain.co.uk/Energain/en_GB/benefits/energy_management.html
[11/01/2011].

DuPont (2007a) *DuPont Energain*. Available:

http://www2.dupont.com/Energain/en_GB/ [29/04/2007].

DuPont (2007b) *DuPont Energain - Energy saving thermal mass systems: Installation Guidelines*, DuPont, Luxembourg.

DuPont (2007c) *Examples of CoDyBa*. Available:

http://www2.dupont.com/Energain/en_GB/products/simulation/simulation2/examples_codyba.html [09/07/2007].

Earth Architecture (2009) *Yakhchal: Ancient Refrigerators*. Available:

<http://www.eartharchitecture.org/index.php?/archives/1045-Yakhchal-Ancient-Refrigerators.html> [27/09/2011].

Edouard, D., Huu, T.T., Huu, C.P., Luck, F. & Schweich, D. (2010) "The effective thermal properties of solid foam beds: Experimental and estimated temperature profiles", *International Journal of Heat and Mass Transfer*, vol. 53, pp. 3807-3816.

EDSL (2011a) *Energain Thermal Mass Builder*. Available:

<http://www.edsl.net/main/software/ThermalMassBuilder.aspx> [15/10/2011].

EDSL (2011b) *TAS Building Designer*. Available:

<http://www.edsl.net/main/software/Designer.aspx> [16/12/2011].

Elsari, M. & Hughes, R. (2002) "Axial effective thermal conductivities of packed beds", *Applied Thermal Engineering*, vol. 22, pp. 1969-1980.

EMCO (2008) *EMCO PCM Module*. Available: <http://www.emco-klima.de/en/d/457/koid/22/start/o/productfinder.8.html> [15/09/2008].

EMCO (2007) *EMCO pcm room tempering*, EMCO-Klima, Lingen.

Everett-Haynes, M. (2008) *Electricity load shifted for cost savings*. Available:

<http://uanews.org/node/20121> [02/01/2012].

- Feldman, D. & Banu, D. (1996) "DSC analysis for the evaluation of an energy storing wallboard", *Thermochimica Acta*, vol. 272, pp. 243-251.
- Fisch, M.N. & Kuhl, L. *Use of Micronencapsulated Phase Change Materials in Office Blocks*. Available: <http://www.micronal.de/portal/streamer?fid=290431> [25/09/2011].
- Frusteri, F., Leonardi, V. & Maggio, G. (2006) "Numerical approach to describe the phase change of an inorganic PCM containing carbon fibres", *Applied Thermal Engineering*, vol. 26, pp. 1883-1892.
- Gellings, C.W. (1996) "Then and now: The perspective of the man who coined the term 'DSM'", *Energy Policy*, vol. 24, no. 4, pp. 285-288.
- GLASSX *GLASSXcrystal - The glass that stores, heats and cools*. Available: <http://glassx.ch/index.php?id=331> [22/09/2011].
- Hadjieva, M., Stoykov, R. & Filipova, T. (2000) "Composite salt-hydrate concrete system for building energy storage", *Renewable Energy*, vol. 19, no. 1-2, pp. 111-115.
- Halliday, D., Resnick, R. & Krane, K.S. (1992) *Physics*, 4th edn, John Wiley & Sons, Inc., Chichester.
- Hamada, Y., Ohtsu, W. & Fukai, J. (2003) "Thermal response in thermal energy storage material around heat transfer tubes: effect of additives on heat transfer rates", *Solar Energy*, vol. 75, pp. 317-328.
- Hasan, R. (2009) *Monitoring and modelling of an air-conditioning system utilising phase change material (PCM) to establish energy savings (Masters dissertation)*, Brunel University, Uxbridge.
- Hasnain, S.M. (1998) "Review on sustainable thermal energy storage technologies, Part II: cool thermal storage", *Energy Conversion and Management*, vol. 39, no. 11, pp. 1139-1153.

- Hawes, D.W., Feldman, D. & Banu, D. (1993) "Latent heat storage in building materials", *Energy and Buildings*, vol. 20, pp. 77-86.
- Hong, H., Kim, S.K. & Kim, Y. (2004) "Accuracy improvement of T-history method for measuring heat of fusion of various materials", *International Journal of Refrigeration*, vol. 27, pp. 360-366.
- Huang, M.J., Eames, P.C. & Hewitt, N.J. (2006) "The application of a validated numerical model to predict the energy conservation potential of using phase change materials in the fabric of a building", *Solar Energy Materials & Solar Cells*, vol. 90, pp. 1951-1960.
- IES (2011) *Integrated Environmental Solutions*. Available: <http://www.iesve.com/> [05/01/2012].
- Ilkazzell (2010) *Ilkatherm Ceiling*. Available: http://www.ilkazzell.de/en_baudecke.php [21/02/2010].
- Ismail, K.A.R. & Henriquez, J.R. (2001) "Thermally effective windows with moving phase change material curtains", *Applied Thermal Engineering*, vol. 21, pp. 1909-1923.
- Kenisarin, M. & Mahkamov, K. (2007) "Solar energy storage using phase change materials", *Renewable and Sustainable Energy Reviews*, vol. 11, no. 9, pp. 1913-1965.
- Koca, A., Oztop, H.F., Koyun, T. & Varol, Y. (2008) "Energy and exergy analysis of a latent heat storage system with phase change material for a solar collector", *Renewable Energy*, vol. 33, pp. 567-574.
- Koschenz, M. & Lehmann, B. (2004) "Development of a thermally activated ceiling panel with PCM for application in lightweight and retrofitted buildings", *Energy and Buildings*, vol. 36, no. 6, pp. 567-578.

- Krupa, I., Mikova, G. & Luyt, A.S. (2007) "Phase change materials based on low-density polyethylene/paraffin wax blends", *European Polymer Journal*, vol. 43, pp. 4695-4705.
- Kuznik, F. & Virgone, J. (2009) "Experimental assessment of a phase change material for wall building use", *Applied Energy*, vol. 86, no. 10, pp. 2038-2046.
- Kuznik, F., Virgone, J. & Noel, J. (2008) "Optimization of a phase change material wallboard for building use", *Applied Thermal Engineering*, vol. 28, no. 11-12, pp. 1291-1298.
- Lamberg, P. & Siren, K. (2003) "Analytical model for melting in a semi-infinite PCM storage with an internal fin", *Heat and Mass Transfer*, vol. 39, pp. 167-176.
- Lane, G.A. (ed)(1983) *Solar Heat Storage: Latent Heat Materials - Volume 1: Background and Scientific Principles*, 1st edn, CRC Press, Boca Raton.
- Lazaro, A., Dolado, P., Marin, J.M. & Zalba, B. (2009) "PCM-air heat exchangers for free-cooling applications in buildings: Experimental results of two real-scale prototypes", *Energy Conversion and Management*, vol. 50, pp. 439-443.
- Lehmann, B., Dorer, V. & Koschenz, M. (2007) "Application range of thermally activated building systems tabs", *Energy and Buildings*, vol. 39, pp. 593-598.
- Liu, K., Guven, H., Beyene, A. & Lowrey, P. (1994) "A comparison of the field performance of thermal energy storage (TES) and conventional chiller systems", *Energy*, vol. 19, pp. 889-900.
- London Canal Museum (2011) *Ice Import - Norway's Ice to London*. Available: <http://www.canalmuseum.org.uk/ice/iceimport.htm> [22/09/2011].
- Mansel, C. (2009) *Yakhchal: Ancient refrigerators*. Available: <http://mediafromdantetothelostandfound.blogspot.com/2009/09/yakhchal-ancient-refrigerators.html> [22/09/2011].

- Marín, J.M., Zalba, B., Cabeza, L.F. & Mehling, H. (2005) "Improvement of a thermal energy storage using plates with paraffin–graphite composite", *International Journal of Heat and Mass Transfer*, vol. 48, no. 12, pp. 2561-2570.
- Martin, R.G. (2009) *Ice houses and the commercial ice trade in brighton*. Available: <http://www.icehouses.co.uk/brighton.htm> [22/09/2011].
- Mehling, H., Ebert, H.P. & Schossig, P. (2006) "Development of standards for materials testing and quality control of PCM", *7th IIR Conference on Phase Change Materials and Slurries for Refrigeration and Air Conditioning*, IIR.
- Melbourne City Council (2006) *Centralised PCM Systems for Shifting Cooling Load During Peak Demands in Buildings*. Available: <http://www.melbourne.vic.gov.au/rsrc/PDFs/CH2/CH2SupplementaryPaper.pdf> [15/09/2008].
- Merten, G.P., Shum, S.L., Sterrett, R.H. & Racine, W.C. (1989) *Operation and performance of commercial cool storage systems. Vol. 1: 1987 Cooling Season*, EPRI, San Diego.
- Miller, A., Ip, K., Shaw, K. & Lam, M. (2005) *Phase Change Materials: A Review of Innovative Technological Applications in a Sustainable Built Environment*, University of Brighton, Brighton.
- Myslewski, R. (2011) *Boffins triple battery life with metal foam*. Available: http://www.theregister.co.uk/2011/06/29/aluminum_celmet/ [02/01/2012].
- Neeper, D.A. (2000) "Thermal dynamics of wallboard with latent heat storage", *Solar Energy*, vol. 68, no. 5, pp. 393-403.
- Oyeleke, A.J. (2010) *Controlled tests and monitoring of a semi-active PCM cooling system (Masters dissertation)*, Brunel University, Uxbridge.

- Öztürk, H.H. (2006) "Experimental evaluation of energy and exergy efficiency of a seasonal latent heat storage system for greenhouse heating", *Energy Conversion and Management*, vol. 46, no. 9-10, pp. 1523-1542.
- Pasupathy, A. & Velraj, R. (2008) "Effect of double layer phase change material in building roof for year round thermal management", *Energy and Buildings*, vol. 40, no. 3, pp. 193-203.
- Peck, J.H., Kim, J., Kang, C. & Hing, H. (2006) "A study of accurate latent heat measurement for a PCM with a low melting temperature using T-history method", *International Journal of Refrigeration*, vol. 29, pp. 1225-1232.
- Piette, M.A. (1990) "Analysis of a commercial ice-storage system: Design principles and measured performance", *Energy and Buildings*, vol. 14, pp. 337-350.
- Potter, R.A., Boettner, D.D., King, D.J. & Weitzel, D.P. (1995) "ASHRAE RP - Study of operational experience with thermal storage systems", *ASHRAE transactions*, vol. 101, pp. 549-557.
- Quanying, Y., Chen, L. & Lin, Z. (2008) "Experimental study on the thermal storage performance and preparation of paraffin mixtures used in the phase change wall", *Solar Energy Materials and Solar Cells*, vol. 92, no. 11, pp. 1526-1532.
- Rubitherm (2011) *CSM module*. Available:
<http://www.rubitherm.de/english/index.htm> [02/01/2012].
- Rubitherm (a) *Comfort and Medical Therapy Products*. Available:
http://www.rubitherm.com/english/pages/03c_medical_therapy_products.htm [22/09/2011].
- Rubitherm (b) *Latent heat food transport elements*. Available:
http://www.rubitherm.com/english/pages/03b_latent_heat_food_transport_elements.htm [22/09/2011].
- Santamouris, M. & Asimakopoulous, D. (1996) *Passive Cooling of Buildings*, 1st edn, James & James, London.

- Sari, A. (2004) "Form-stable paraffin/high density polyethylene composites as solid-liquid phase change material for thermal energy storage: preparation and thermal properties", *Energy Conversion and Management*, vol. 45, pp. 2033-2042.
- Sari, A. & Karaipekli, A. (2007) "Thermal conductivity and latent heat thermal energy storage characteristics of paraffin/expanded graphite composite as phase change material", *Applied Thermal Engineering*, vol. 27, pp. 1271-1277.
- Scalat, S., Banu, D., Hawes, D., Paris, J., Haghigata, F. & Feldman, D. (1996) "Full scale thermal testing of latent heat storage in wallboard", *solar Energy Materials and Solar Cells*, vol. 44, pp. 49-61.
- Schossig, P., Henning, H.-., Gschwander, S. & Haussmann, T. (2005) "Micro-encapsulated phase-change materials integrated into construction materials", *Solar Energy Materials and Solar Cells*, vol. 89, no. 2-3, pp. 297-306.
- Sciencephoto *PLM of calcium chloride crystals*. Available:
http://www.sciencephoto.com/image/8908/530wm/A6300313-PLM_of_calcium_chloride_crystals-SPL.jpg [03/10/2011].
- Sebzali, M.J. & Rubini, P.A. (2007) "The impact of using chilled water storage systems on the performance of air cooled chillers in Kuwait", *Energy and Buildings*, vol. 39, no. 8, pp. 975-984.
- Shatikian, V., Ziskan, G. & Letan, R. (2005) "Numerical investigation of a PCM-based heat sink with internal fins", *International Journal of Heat and Mass Transfer*, vol. 48, pp. 3689-3706.
- Shilei, L., Guohoi, F., Neng, Z. & Li, D. (2007) "Experimental study and evaluation of latent heat storage in phase change materials wallboards", *Energy and Buildings*, vol. 39, pp. 1088-1091.
- Sohn, C.W., Fuchs, J. & Gruber, M. (1998) *Chilled Water Storage System at Fort Jackson, SC*. Available:

http://owww.cecer.army.mil/techreports/soh_stor/Soh_Stor-04.htm

[03/06/2008].

Stritih, U. & Novak, P. (2002) "Thermal Storage of Solar Energy in the Wall for Building Ventilation", *ECES IA Annex 17, Advanced thermal energy storage techniques - Feasibility studies and demonstration projects 2nd Workshop*, IEA.

Tan, F.L., Hossienizadeh, S.F., Khodadadi, J.M. & Fan, L. (2009) "Experimental and computational study of constrained melting of phase change materials (PCM) inside a spherical capsule", *International Journal of Heat and Mass Transfer*, vol. 52, pp. 3464-3472.

Tassou, S.A. (2005) *Energy conversion technologies: Part 1*, Brunel University, Uxbridge.

Telkes, M. & Raymond, E. (1949) "Storing Solar Heat in Chemicals - A Report on the Dover House", *Heating and Ventilating*, vol. 46, no. 11, pp. 80-86.

TESS inc. (2007) *TRNSYS - The Transient Energy System Simulation Tool*.

Available: <http://www.trnsys.com/about.htm> [29/12/2008].

The Molecular Universe *Building Up Molecules: Rings and Chains*. Available:

<http://ru.wikipedia.org/wiki/%D0%A4%D0%B0%D0%B9%D0%BB:Hexadecane3D.png> [03/10/2011].

Trelles, J.P. & Dufly, J.J. (2003) "Numerical simulation of porous latent heat thermal energy storage for thermoelectric cooling", *Applied Thermal Engineering*, vol. 23, pp. 1647-1664.

Turnpenny, J.R., Etheridge, D.W. & Reay, D.A. (2000) "Novel ventilation cooling system for reducing air conditioning in buildings.: Part I: testing and theoretical modelling", *Applied Thermal Engineering*, vol. 20, no. 11, pp. 1019-1037.

Tyagi, V.V. & Buddhi, D. (2007) "PCM thermal storage in buildings: A state of art", *Renewable and Sustainable Energy Reviews*, vol. 11, no. 6, pp. 1146-1166.

- U.S. Department of Energy (2011) *EnergyPlus Energy Simulation Software*.
Available: <http://apps1.eere.energy.gov/buildings/energyplus/> [01/02/2012].
- Velraj, R., Seeniraj, R.V., Hafer, B. & Faber, C.S., K. (1999) "Heat Transfer Enhancement in a Latent Heat Storage System", *Solar Energy*, vol. 65, no. 3, pp. 171-180.
- Voller, V.R. (1996) "An Overview of Numerical Methods for Solving Phase Change Problems" in *Advances in Numerical Heat Transfer (Volume 1)*, eds. W.J. Minkowycz & E.M. Sparrow, 1st edn, Taylor & Francis, Abingdon, pp. 341-375.
- Voller, V. & Cross, M. (1981) "Accurate Solutions of Moving Boundary Problems Using The Enthalpy Method", *International Journal of Heat and Mass Transfer*, vol. 24, pp. 545-556.
- Wang, M. & Pan, N. (2008) "Modeling and prediction of the effective thermal conductivity of random open-cell porous foam", *International Journal of Heat and Mass Transfer*, vol. 51, pp. 1325-1331.
- Wang, X., Yap, C. & Mujumdar, S.A. (2008) "A parametric study of phase change material (PCM)-based heat sinks", *International Journal of Thermal Sciences*, vol. 47, pp. 1055-1068.
- Xiao, W., Wang, X. & Zhang, Y. (2009) "Analytical optimisation of interior PCM for energy storage in a lightweight passive solar room", *Applied Energy*, vol. 86, pp. 2013-2018.
- Yanbing, K., Yi, J. & Yinping, Z. (2003) "Modeling and experimental study on an innovative passive cooling system—NVP system", *Energy and Buildings*, vol. 35, no. 4, pp. 417-425.
- Zalba, B., Marín, J.M., Cabeza, L.F. & Mehling, H. (2004) "Free-cooling of buildings with phase change materials", *International Journal of Refrigeration*, vol. 27, no. 8, pp. 839-849.

- Zalba, B., Marín, J.M., Cabeza, L.F. & Mehling, H. (2003) "Review on thermal energy storage with phase change: materials, heat transfer analysis and applications", *Applied Thermal Engineering*, vol. 23, no. 3, pp. 251-283.
- Zhang, Y. & Jiang, Y. (1999) "A simple method, the T-history method, of determining the heat", *Measurement and science technology*, vol. 10, pp. 201-205.
- Zhang, Y., Lin, K., Zhang, Q. & Di, H. (2006/10) "Ideal thermophysical properties for free-cooling (or heating) buildings with constant thermal physical property material", *Energy and Buildings*, vol. 38, no. 10, pp. 1164-1170.
- Zhao, C.Y., Lu, W. & Tian, Y. (2010) "Heat transfer enhancement for thermal energy storage using metal foams embedded within phase change materials (PCMs)", *Solar Energy*, vol. 84, pp. 1402-1412.
- Zivkovic, B. & Fujii, I. (2001) "An analysis of isothermal phase change of phase change material within rectangular and cylindrical containers", *Solar Energy*, vol. 70, no. 1, pp. 51-61.

Chapter 3

ACTIVE PCM COOLING SYSTEM

In this chapter a post-installation energy audit of an active PCM cooling system is presented. In case of confusion it is important to point out that this system was designed by a third party and this is only a study to examine its performance.

In the literature review it was shown that savings from active cool storage systems may be possible due to the increased COPs that result from night time operation of chillers. However, studies of the energy use of active cool storage systems often reveal an energy penalty from a systems installation. With ice this is an inherent problem that results, at least partly, from the requirement to reach 0 °C, which reduces the chiller COP. With water, savings have been predicted since the raising of the COP due to depressed night time temperatures is not off-set by a reduction due to lower evaporator temperatures.

In the case of hydrated salts it would appear to be possible, in principle, to save energy since melt/solidification temperatures may be chosen that allow chillers to operate at higher temperatures than those required for ice production. In order to explore this potential further an installed cooling system which incorporates PCM tanks was monitored to establish energy use and make a comparison to the energy use of an identical system without the presence of the PCM tanks. It was found that this system did incur an energy penalty, chiefly due to the selection of a PCM whose solidification temperature was below that required.

China Shipping House is a 3250 m² office building in the port of Felixstowe, Suffolk, UK. Cooling is provided by two 241.3 kW Trane CGAN900 chillers serving fan coil units, air handling units and chilled ceilings. The system is controlled by a Trend Building Management System (BMS). Two PCM tanks containing stacks of commercially available hydrated salt (see Figure 3.1), S-13 (peak freezing and

melting temperatures 5.09 and 15.2 °C, respectively), encased in high density polyethylene containers, are located on the return of the chilled beam circuit.



Figure 3.1 PCM tank. Roof-mounted PCM tank (left) and stacks of FlatICE containers as they would be found inside (right).

The tanks are intended to save energy by pre-cooling chiller return water. Discharge of accumulated latent heat is effected at night, when chiller COPs are high. Chiller power and system temperatures were monitored for 6 days. The additional daytime power input required for a tankless system was calculated using tank inlet and outlet temperatures and chiller performance curves for varying ambient temperatures. DSC was performed on the PCM to obtain thermophysical characteristics. The system incurred an additional 687 kWh energy cost (10.6% of total cooling energy), as compared to an identical tankless system. This is because night chiller and pump electricity usage outweighed daytime savings. Only 28% of the tank capacity is utilised because the freeze temperature of the PCM is too low for sufficient heat transfer to the chilled water.

From the 3rd to the 9th of September water temperatures at key points in the chilled water system and the electrical input to the chillers were recorded. This data was combined with plant specification figures and manufacturers data in order to calculate the energy savings/costs that resulted from the PCM tanks' presence.

3.1 System Description

3.1.1 Generation and Water-side Distribution

A simplified schematic of the cooling system is shown in Figure 3.2.

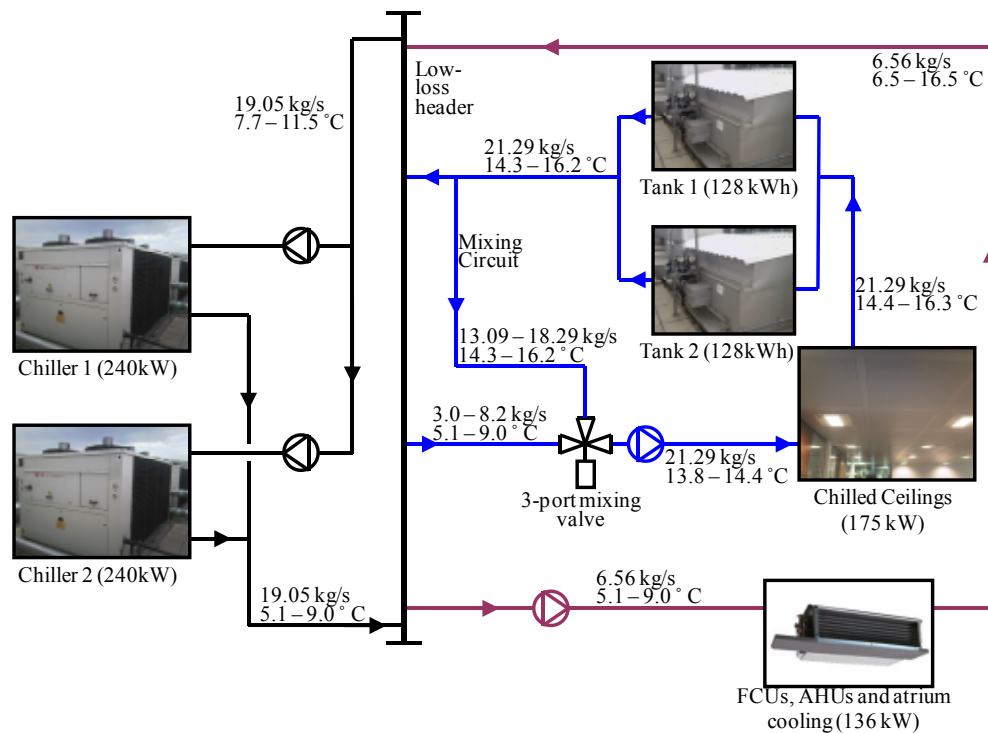


Figure 3.2 The central cooling system at China Shipping House. This simplified schematic shows the primary chilled water circuit in black and the secondary chilled water circuits in blue and pink for chilled ceilings and FCU/AHUs, respectively. Parallel pump sets have been replaced by single pumps and valve arrangements have been entirely omitted apart from the 3-port control valve that regulates the mixing of water to the chilled ceilings. Individual cooling units have been amalgamated into single representations on each secondary circuit. Temperature and flow rate ranges, referring to typical daytime operation, have been included on all major sections of the system.

Chilled water is generated by 2 Trane CGAN900 241.3 kW chillers which are located on the roof of the building. Whilst serving a full load, with an ambient temperature of 25 °C, these machines have a COP of 3.64. They are connected in parallel with a main low loss header through which water is circulated by 2 Grundfos LMD

100/200 pumps producing a combined volume flow rate of 19.05 kg/s. Chilled water is distributed to the building via two secondary circuits: A lower temperature circuit serving air handling units (AHUs), fan coil units (FCUs) and an atrium cooling coil, and a higher temperature circuit serving chilled ceilings. Single Grundfoss LMD 80/160-173 and LPD 125/125-121 pumps circulate the water at rates of 6.56 kg/s, in the lower temperature circuit, and 21.29 kg/s, in the higher temperature circuit, respectively. Water returned from the chilled ceilings passes through the two parallel PCM tanks and is then split into two streams: One, a mixing circuit for flow back to the chilled ceilings and the other, a return to the main header. The ratio of flow rates in the two streams is determined by a three-port control valve situated between header and pumps on the chilled beam circuit. This mixes flow water from the header and return water from the PCM tanks to give a near constant flow temperature of 14 °C to the chilled ceilings. This operation takes place between 8:00am and 9:00pm throughout the cooling period.

Between 2:00am and 3:00am the chillers, the primary circuit pumps and the chilled beam circuit pump all operate to discharge the accumulated heat from the PCM tanks. At this time the three-port control valve opens fully to allow 6 °C water from the header to flow to the tanks. The chilled beam pump also operates between 6:15am and 8:00am.

A low outside air temperature hold-off facility disables the chillers and chilled water system when ambient temperatures depress sufficiently.

3.1.2 Air-side Distribution

Three AHUs account for 73% of the capacity of the mechanical air-side cooling. The majority of this is done by two roof-mounted AHUs: an Envirotec ENV100/200 with 66.87 kW cooling capacity and an Envirotec ENV100SQ with 31.95 kW cooling capacity. A third AHU serves the ground floor kitchen, a 6 kW Envirotec Enviropac80/80SQ, and the 8 kW atrium cooling coil. Smaller offices and meeting rooms are served by 7 Biddle Air Systems K95-8 FCUs with cooling capacities ranging from 2.5 – 5.25 kW. Chilled ceilings, a combination of beams and panels, serve all open plan office spaces with a combined capacity of 175 kW.

3.1.3 PCM Tanks

The PCM tanks have the following dimensions: 5000mm x 5000mm x 1800mm with 75mm of insulation. Flow and return connections are 100mm in diameter. They are located on the roof, adjacent to the chillers and plant room. A cross section is shown in Figure 3.3.

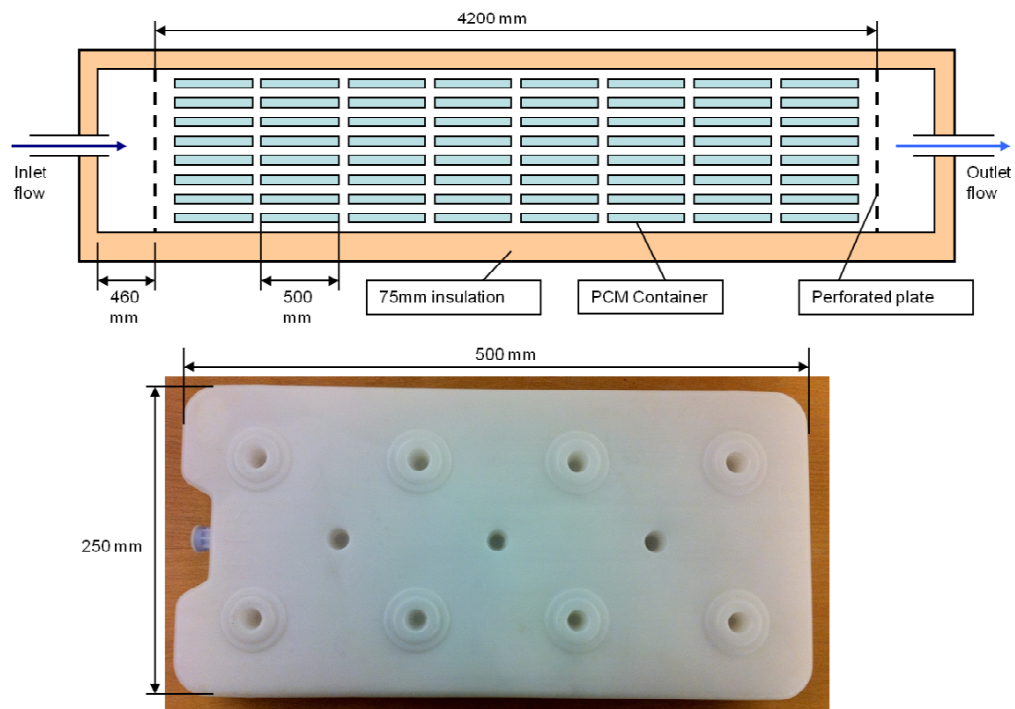


Figure 3.3 Inside PCM tank. Cross section of one PCM tank (top). FlatICE container (below).

The tanks each contain 704 FlatICE units, themselves containing a commercially available hydrated salt - S13, stacked in 8 x 8 columns of 11 units. The units, also displayed in Figure 3.3, are made out of 2mm thick high density polyethylene which is shaped to interlock with units above and below, leaving a 6mm gap for water to pass through. When the PCM in the units is in a liquid state it can freeze by transferring heat via forced convection, to any passing water below the PCM freezing temperature. Water flows through a plastic pipe into the tank and then through a perforated plate to ensure equal flow rate across all FlatICE units. Water flows

between the modules in a generally horizontal direction before exiting through another perforated plate and outlet pipe. The units are broad with minimal height. This promotes heat transfer, due to the large surface area, and is intended to prevent stratification over successive melt/freeze cycles.

3.1.4 Energy Savings

The system is intended to make energy savings by reducing the temperature of the water returned to the chillers and the mixing circuit that feeds back to the chilled beams. Lower temperature return water reduces the load on the chillers. Lower temperature water for mixing also reduces the load on the chillers as less chilled water is taken from the header. These savings are off-set by the energy required to discharge the heat accumulated in the tanks overnight. Due to depressed dry bulb temperatures at night, the chillers should operate at a higher COP and thus use less energy to generate the coolth than they would have done in the daytime. The operation of a CGAN 900 chiller at part loads and differing ambient temperatures is displayed in Figure 3.4.

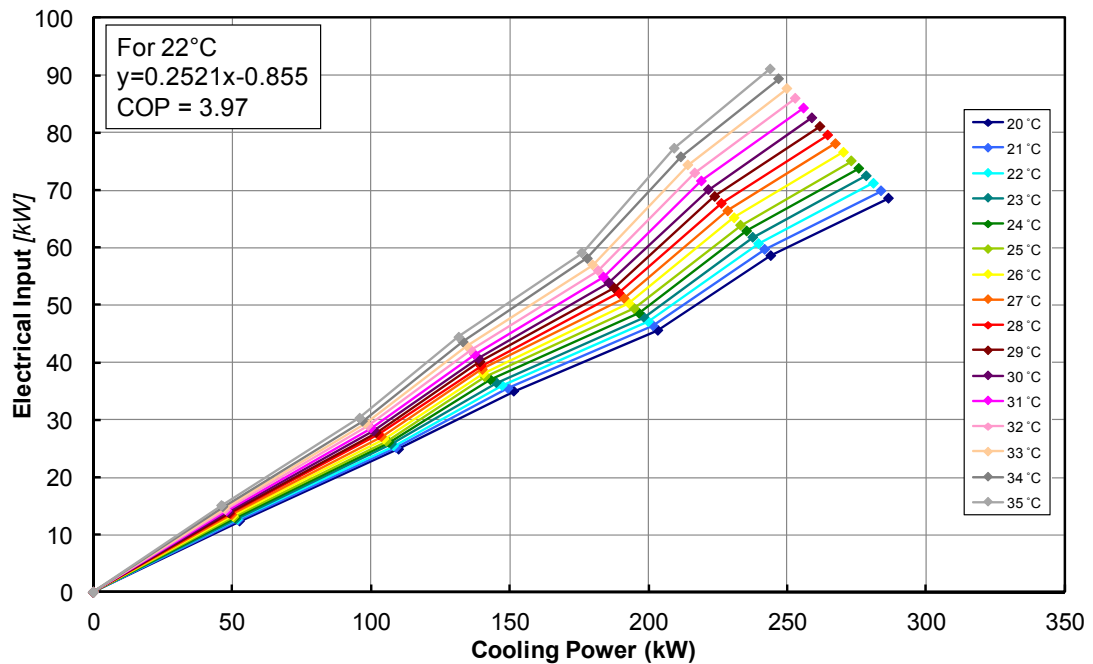


Figure 3.4 Delivered cooling power variation with electrical input at ambient temperatures. Trane CGAN900 chiller. Approximate linear relationship and COP shown for the example temperature of 22 °C.

For temperatures between 20 °C and 35 °C, lower temperatures will always provide more cooling for less electrical input. This relationship is most pronounced at higher loads but can still be seen at loads around 50 kW. We can also see that for each ambient temperature there is an almost linear relationship between the electrical input and chiller power. This is due to the chillers containing multiple screw compressors which can be engaged individually to accommodate a varying load.

3.2 Method

3.2.1 Tank Thermal Capacity

A sample of the S-13 hydrated salt was obtained for DSC analysis by the Brunel PCM research group (not by me personally) as described in the literature review. S-13 is generally not a homogenous solution in a solid or partially molten state so 4 samples were tested to ensure an excess of salt crystal/s or aqueous solution did not give a

false impression of the macroscopic properties of the material. The thermal capacity of the tank was then calculated with Eq. 3.1.

$$U_{\text{tanks}} = N_{\text{units}} V_{\text{unit}} \rho_{S13} (L_{\text{fus},S13} + C_{p,S13} (T_{\text{in,max}} - T_{\text{in,min}})) \quad (3.1)$$

3.2.2 Energy and Carbon Savings

The energy savings that result from the presence and use of PCM tanks is calculated by subtracting the energy that the installed system used from the energy that would have been used by a conventional system – i.e. one without a PCM tank. This is represented algebraically in the following equations.

$$Q_{\text{saved}} = Q_{\text{conv}} - Q_{\text{PCM}}, \quad (3.2)$$

$$Q_{\text{conv}} = Q_{\text{chill,day}} + Q_{\text{tank,elec day}} \quad (3.3)$$

and

$$Q_{\text{PCM}} = Q_{\text{chill,day}} + Q_{\text{chill,night}} \quad (3.4)$$

Eq. 3.3 states that the energy used by a conventional system is equal to the sum of the daytime energy used by the existing system and the daytime energy that the chillers would have used, were the PCM tanks not present. Eq. 3.4 simply states that the energy used by the existing system (with PCM tanks) is equal to the sum of the actual daytime and night time chiller energies. By definition Eq. 3.5 results:

$$Q_{\text{saved}} = Q_{\text{tank,elec day}} - Q_{\text{chill,night}} \quad (3.5)$$

The electrical energy used at night was found using Eq. 3.6:

$$Q_{\text{chill,night}} = pVF_p \sum_{s=1}^m \left(\sum_{r=1}^3 I_r \right)_s + Q_{\text{pump}} \quad (3.6)$$

where

$$Q_{pump} = \dot{Q}_{PP}t_{PP} + \dot{Q}_{CB}t_{CB} \quad (3.7)$$

The chillers have a 3-phase supply. Measurements of current from one phase input on each chiller were taken every 10 minutes with Pico TAO11 current clamps connected to a Pico ELO40 current monitor and a Pico ELO05 data logger. Phase ratios were established prior to this by monitoring all three phases of each chiller. These ratios were then used to calculate the unmonitored phases for each ten minute interval. Two phases were monitored on chiller 2 to verify the lack of phase ratio variation throughout monitoring. The voltage applied was the rated voltage of the chillers, 400V, as was the power factor, 0.85.

The pumps have a constant flow rate and the electricity they use at night is taken to be equal to their rated powers, 6 (2 x 3) kW on the primary circuit and 4 kW on the secondary circuit, multiplied by their operation time, 1 hour per night.

For context and comparison the electrical energy used during the daytime was found by applying the equivalents of Eq.s 3.6 and 3.7 to daytime chiller and pump operations with addition of the AHU and FCU circuit pump which uses 0.75 kW of power.

The chiller input energy that was displaced by the tank during the day was found by applying Eq. 3.8.

$$Q_{\tan k,elecday} = \dot{m}_{\tan k} q C_{p,w} \sum_q^n \left(\frac{(T_{in} - T_{out})_t}{COP_t} \right) \quad (3.8)$$

Here the mass flow rate was found from the stated balanced flow in the equipment schedules, 21.29 kg/s. The C_p of water was taken to be 4.18 kJ/kg/K. The two tanks were taken to function as one unit with an outlet temperature equal to the mean of the two readings obtained from the BMS. The outlet temperatures are extremely close and have a maximum difference of 0.48 °C over the whole period. The COP for

each time stamp was found by obtaining linear relationships between chiller input powers and cooling capacity for ambient temperatures above 20 °C. The approximate linearity of these relationships is evidenced in Figure 3.4. Below an ambient temperature of 20 °C the COP was assumed to be equal to that of 20 °C, the lower limit of its designed ambient temperature operating range. This is because the CGAN900 chillers are designed to maintain a minimum heat transfer rate at the condenser and thus the fan power reduces accordingly. Although this reduction in fan power does result in a reduction in overall COP, the electrical power input is dominated by the compressor which operates at a constant rate below 20 °C ambient temperature.

Energy savings were calculated for a monitoring period of 6 days: 8:00am, Thursday 3rd – 8:00am, Wednesday 9th September 2009. To calculate carbon savings the carbon factor for electricity, 0.517 kgCO₂/kWh as quoted in the National Calculation Methodology modelling guide (Department for Communities and Local Government, 2010), was multiplied by the energy savings.

3.3 Results and Discussion

Figure 3.5 displays temperature profiles of all relevant parts of the system, along with the ambient temperature.

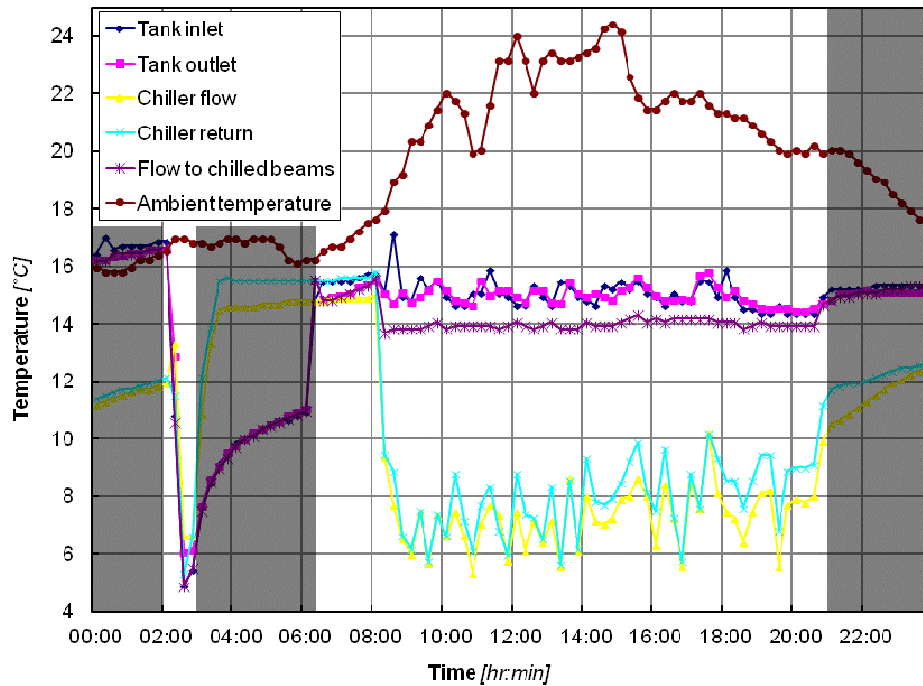


Figure 3.5 Active cooling system temperatures. Profiles for all relevant points in the system on Tuesday 8th September. Ambient temperature is also included. For the cooling system, temperatures recorded during idle hours, 2:00am to 6:15am and 9:00pm to 2:00am, have been greyed out.

Between 2:00am and 3:00am, all system temperatures fall to below 6 °C as the chillers operate to discharge the accumulated heat from the PCM tanks. During daytime operation chiller flow and return oscillate between 11 °C and 5 °C as the chillers modulate their power to maintain low temperature water flowing through the header. At the same time the chilled beam flow temperature is maintained at a very constant flow temperature between 14.4 °C and 15.7 °C due to effective mixing of water from the PCM tank outlet and water flowing from the header. After picking up heat from the chilled ceilings, water flows into the PCM tanks at a maximum temperature of 18.1 °C. Between the hours of 6:15am and 12:00am a cooling effect from the PCM tanks can be seen; outlet temperatures are clearly lower than inlet

temperatures. Over the rest of the day this cooling effect becomes less apparent and a small amount of heating occurs.

Throughout this time the external air temperature rises from a minimum of 17.1 °C, at 12:30am, to a maximum of 24.4 °C, at 13:15 pm. The internal temperature is suitably maintained between minima and maxima of 21.5 °C and 24.6 °C, respectively.

3.3.1 Thermophysical Properties of S-13 and Tank Thermal Capacity

Figure 3.6 shows the melt/freezing curve for one of the S-13 samples, as obtained by DSC.

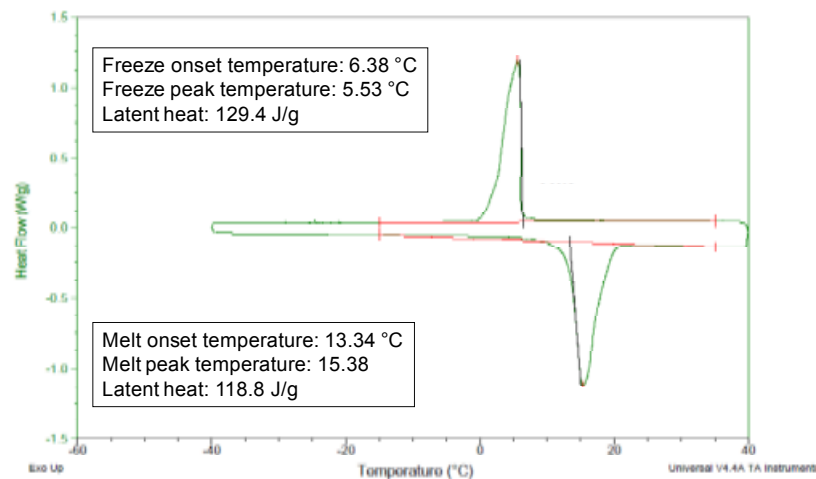


Figure 3.6 The DSC curve for one of the S-13 salt samples (Hasan, 2009). The values given for temperatures and latent heats differ from those found in **Table 3.1** as that contains mean values from all samples tested.

The melting and freezing peaks are very well defined. Only sensible heating occurs until the onset of melting at 13.34 °C and the melting peak is just over 2 °C higher than this. The freezing peak is slightly better defined, with the peak occurring less than 1 °C after the onset, at 5.53 °C and 6.38 °C, respectively. A considerable degree of under-cooling is apparent with around 10 °C difference between melting and freezing peaks. **Table 3.1** shows the mean thermophysical property results obtained from the four samples.

Table 3.1 Thermophysical properties of S-13 salt. Found using DSC testing (Hasan, 2009). These values differ to those seen in Figure 3.6 as they are mean values of four tested samples.

Specific Heat (kJ/kg/K)	Latent heat of melting (kJ/kg)	Latent heat of freezing (kJ/kg)	Melting onset temperature (°C)	Melting peak temperature (°C)	Freezing onset temperature (°C)	Freezing peak temperature (°C)
1.54	118.15	111.75	13.46	15.2	6.47	5.09

The minimum and maximum tank inlet temperatures were 4.91 °C and 18.08 °C, respectively. As per Eq. 3.1 this yielded a total thermal capacity of 256 kWh for both tanks combined.

3.3.2 Energy and Carbon Savings

Table 3.2 displays energy consumption and saving results.

Table 3.2 Energy consumption and savings from the cooling system at China Shipping House, 3rd to 9th September.

	Energy (kWh)	CO2 (kg)	Percentage of cooling electricity consumption	Percentage of total building electricity consumption
Chiller power at night	615.3	318.1	9.5	3.5
$Q_{chill,night}$	717.3	370.8	11.1	4.1
Chiller power daytime	4910.1	2538.5	75.9	27.8
$Q_{chill,day}$	5748.6	2972.0	88.9	32.5
Q_{pcm}	6465.9	3342.9	100.0	36.6
$Q_{tank,elec,day}$	30.3	15.6	0.5	0.2
Q_{conv}	5778.9	2987.7	89.4	32.7
Q_{saved}	-687.0	-355.2	-10.6	-3.9

Analysis shows that the tanks are producing negative energy savings of 687 kWh for the period 8:00am Friday 4th to 8:00am Wednesday 9th September. This is equivalent to 355 kg of CO₂. The reason for this is that the additional energy input at night, 717 kWh, is not sufficiently offset by the savings made, due to reduced chiller power, during the day, 30 kWh. The total energy lost by the system is equivalent to 10.6 % of the total electricity consumed by the cooling system, 6466 kWh, and 3.9%

of the total electricity consumption of the building, 17676 kWh, over the same period.

Figure 3.7 shows the flow of energy in and out of the tanks with the concurrent power input to the chillers.

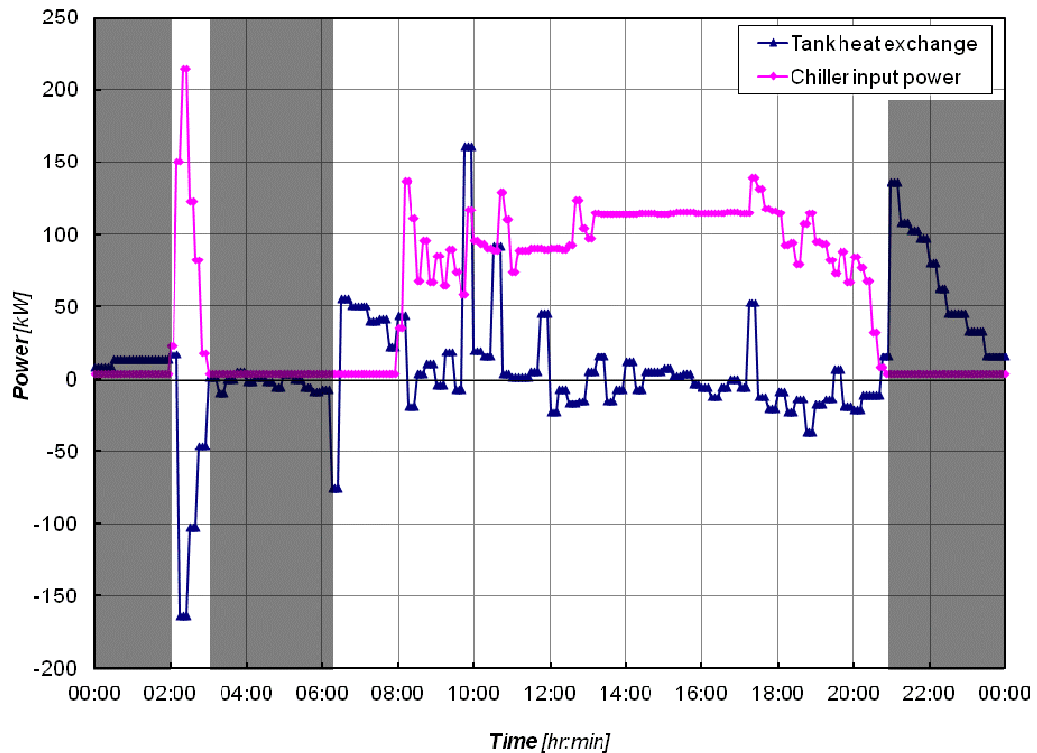


Figure 3.7 Tank heat exchange and chiller input power profiles. Tuesday 8th September. Negative tank heat exchange values indicate a flow of heat out of the tank. Periods in which the system is idle, 2:00am to 6:15am and 9:00pm to 2:00am, have been greyed out.

A direct correspondence between chiller input power and tank heat discharge is evident between 2:00am and 3:00am, indicating the operation of chillers to solely remove accumulated latent heat from the tanks. During daytime operation the influence of tank heat exchange on chiller operation is not discernable as it is so small, just 0.5 % of the total cooling electricity consumption. At the start of daytime operation, the tanks successfully absorb heat, indicated by a positive heat flow. Unfortunately, this heat flow reverses and the PCM units start heating the water flowing through the tanks around mid-morning. In effect, the tanks are transposing some of the cooling, which would have been done during early morning hours, to

later in the day. For the system to work efficiently, all cooling should be transposed to night time operation.

Table 3.3 displays figures for the heat exchanged by the PCM tanks and the percentage of the total tank capacity that these exchanges equal. This partly explains why the system is making negative energy savings; only 28% of the PCM tanks' capacity (256 kWh) is discharged.

Table 3.3 Heat exchanged by the PCM tanks.

	Heat exchanged (kWh)	Percentage of total tank capacity
Daytime heat exchanged by tanks over whole period	363.8	-
Mean daily heat exchanged by tanks	60.64	23.65
Night time heat exchanged by tanks over whole period	-435.9	-
Mean nightly heat exchanged by tanks	-72.64	-28.33

The cause of this may be the heat transfer characteristics of the material. The DSC results for S-13 show that the material starts melting at 6.47 °C, peaking at 5.09 °C. In fact it only finishes freezing at around 0 °C. The temperature of the water flowing in and out of the PCM tanks is shown in Figure 3.8.

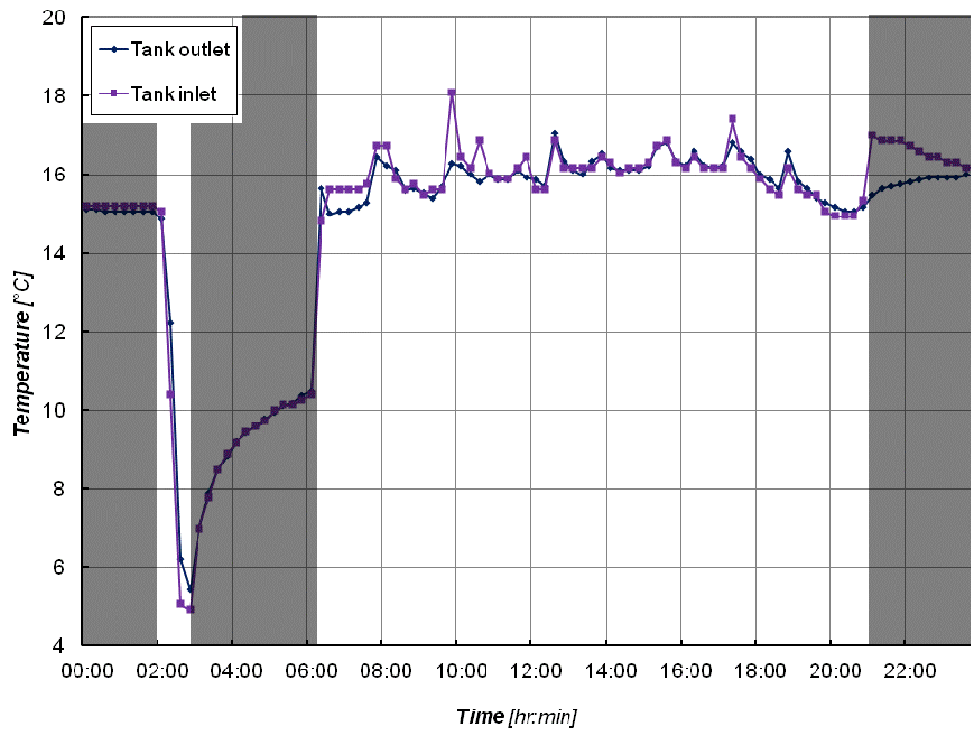


Figure 3.8 Tank inlet and outlet temperatures. As with Figs. 3.5 and 3.7 periods in which the system is idle, 2:00am to 8:00am and 8:30pm to 2:00am, have been greyed out.

The very small difference in inlet and outlet temperature shows that the rate of heat transfer within the tank is extremely small. A minimum outlet and inlet of 5.4 and 4.9 °C, respectively, is achieved. The inlet temperature is only just low enough to initiate nucleation but not low enough to effect full freezing of the PCM. The temperature difference between the flow water and the FlatICE units is not high enough; only a maximum of 1.6 °C difference between the lowest water temperature and the freeze onset temperature is achieved. Heat transfer is therefore probably mostly limited to the sensible heating and cooling of the units. A PCM with less under-cooling would greatly improve the system performance. The ASHRAE Design Guide for Cool Thermal Storage states that a tank containing PCM with a freeze temperature of 8.3 °C is normally charged with 4 - 6 °C chilled water (Dorgan & Elleson, 1993). This gives a mean temperature difference of 3.3 °C, far more than is achieved here.

These results only pertain to the system operation during the monitored period. Proportionate savings will vary with daytime cooling load and night time ambient temperature. Cooling load may be expected to rise with increased ambient temperature and solar gains. This would exhaust any coolth stored in the PCM tanks quicker. Assuming similar ambient night time temperatures, it would also mean that the energy cost of the system, as a proportion of the total cooling load over the day, would be lower. A small proportion of this would be driven by the increased difference in day and night time COPs resulting from higher ambient daytime temperatures. The reverse would be true for reduced cooling loads found at the beginning and end of the cooling season.

A rise in ambient temperature at night would reduce the COP of the chillers and increase the proportionate energy cost of the PCM tanks, assuming similar daytime loads. A fall in night time ambient temperature would not make much difference since the chiller COPs were close to or at their minimum during the monitored period.

3.4 Conclusions

During the period of monitoring the cooling system performed well by maintaining suitable thermal conditions in the office. A clear cooling effect from the PCM tanks was observed in the early part of the days monitored but this diminished significantly around noon. Overall the presence of the PCM tanks appears to increase the energy used by the system. This is due to the fact the tanks' capacity is not fully utilised because the freeze-phase transition zone of the salt hydrate is too low for the chillers to adequately transfer heat to the FlatICE units. As a consequence the energy expended by chillers and pumps at night is not off-set by chiller load reductions during the daytime.

The energy cost of the PCM tanks will vary across the cooling period depending on daytime cooling load and ambient temperature but savings will never be achieved.

By using an alternative PCM that freezes at a higher temperature, perhaps 8.3 °C as recommended by ASHRAE, tank discharge would be ensured every night and chiller load-reductions could yield overall energy savings.

This work has presented another case to add to those found in the literature that reveals an energy cost resulting from the presence of PCM tanks and the resulting system operation. This type of active PCM cooling system appears to have the potential to save energy but in reality rarely does. These systems are suited for financial savings, made through exploitation of a varied day/night electricity tariff structure, not energy savings.

One aspect of system design that has been highlighted here is that of PCM selection. Butala and Stritih (2009) discussed the need to appropriately select the PCM for free cooling and in this work their assertion may be said to more broadly apply to active PCM cooling systems. The appropriate selection of PCM, in terms of phase transition zone, is an aspect of design that is touched on in the Passive PCM Sails experiments in chapter 5 and informs the design of the NewMass system, covered in chapter 7.

Even with an appropriately selected PCM the energy savings from this type of system can only be expected to marginal since the savings are gained through chiller COP increase at lower night time ambient temperatures. This is normally insufficient to significantly offset the additional energy required for coolth generation.

Research into the systems that can provide energy savings should focus on systems that give options for free cooling and passive operation. To better understand what potential systems could be developed the following chapter on design space mapping focuses on establishing a consistent taxonomy for PCM systems and using this to redefine new and existing system designs.

References

Butala, V. & Stritih, U. (2009) 'Experimental investigation of PCM cold storage', *Energy and Buildings*, 41, pp. 354-359.

Department for Communities and Local Government (2010) *National Calculation Methodology (NCM) modelling guide*, London: Department for Communities and Local Government.

Dorgan, E.C. & Elleson, J.S. (1993) *Design Guide for Cool Thermal Storage*, 1st edn, Atlanta, Georgia: ASHRAE.

Hasan, R. (2009) *Monitoring and modelling of an air-conditioning system utilising phase change material (PCM) to establish energy savings (Masters dissertation)*, Uxbridge: Brunel University.

DESIGN SPACE MAPPING

The previous chapter added evidence to the conclusion that active systems generally incur marginal or negative energy savings. This would seem to suggest that passive, free cooling or thermally activated systems should therefore be the focus of any attempts to develop PCM cooling systems that can reliably save energy. However, one of the conclusions in the literature review was that there is considerable ambiguity and overlap in the generally accepted taxonomy used to classify PCM cooling systems, as well as a lack of any attempt to map out the design space. Therefore, prior to any design development, it was deemed necessary to develop a coherent taxonomy that logically mapped the design space for PCM cooling systems. This allowed all existing systems to be classified and thus revealed areas of under research and new system designs.

Before proceeding, a brief recap of the definitions of *design space*, *problem framing* and *design space mapping* may be useful. The *design space* is the group of all possible solutions to a design problem. *Problem framing* is the statement of the set of conditions that are necessarily entailed by the design problem. *Design space mapping* is the development of a set of rules or a taxonomy that allows the various design solutions that inhabit the design space to be classified in a clear and consistent way.

There were four stages to the process:

1. The design problem was stated.
2. The problem was precisely framed in terms of all PCM cooling systems' fundamental elements and functions: Internal space, body of PCM, external heat sink/s, insulation between the other elements.

3. These elements were arranged in all possible physical configurations for the two fundamental processes of charging and discharging. This resulted in 11 system variants that constitute the new taxonomy – the design space map.
4. All existing systems were then classified according to the new taxonomy. This revealed a number of new system types or system types that have been under-researched.

In general, the work presented in this chapter is like the task of tessellation. When shapes are arranged they are said to tessellate if they fill a space with no gaps and no overlaps. When seeking to map the design space all potential system types must be classifiable such that they do not overlap and do not leave any gaps. Unlike the generally accepted categories of classification, the taxonomy developed here avoids these flaws. It should be highlighted however that the aim was not to supplant the current terms of reference; rather it was to more logically define all PCM cooling systems. What was found was that not only does the new taxonomy usefully highlight potentially fruitful avenues of research and development but also that the pre-existing taxonomy still proves more useful when grouping and referring to system types in general discourse.

4.1 Problem statement

The essential question that this thesis asks is:

How can PCMs be applied to save cooling energy in buildings?

With the problem stated it can be framed in terms of system function and constituent elements. (It should be pointed out that this question assumes the PCM engages in diurnal heat/coolth storage, as opposed to seasonal storage.)

4.2 Problem framing

We begin with two examples; those of passive and active systems, as described in the literature review. The passive system directly cools a space by absorbing heat from the air, through convective heat transfer, and from the objects and occupants of the room through radiative heat transfer. As it absorbs this heat it melts. When the day ends it loses the accumulated heat via convection to circulated night air and resolidifies.

The PCM in an active system indirectly cools the space by absorbing heat via forced convection from water flowing past it. The water is simultaneously cooled and pumped to the space. Here it exchanges heat with the space, typically through the natural or forced convection of a chilled beam or fan coil unit. At night the heat accumulated in the melted PCM is rejected via forced convection to cooler water that flows past it. This water may in turn reject heat to a chiller or directly to the cool night air if ambient temperatures are low enough.

Despite their differences, in both these cases the same basic processes are taking place:

- Solid PCM absorbs excess room heat during the daytime and melts.
- Liquid PCM rejects accumulated heat to a heat sink at night and freezes.

This description can be applied equally to free cooling systems (those employing mechanical ventilation to transfer heat to PCM units isolated from the internal space) and thermally activated systems (those that passively absorb heat from the space and reject it later to a chilled water loop). In fact any diurnal PCM cooling system will have the basic cyclical operation just described and represented in Figure 4.1.

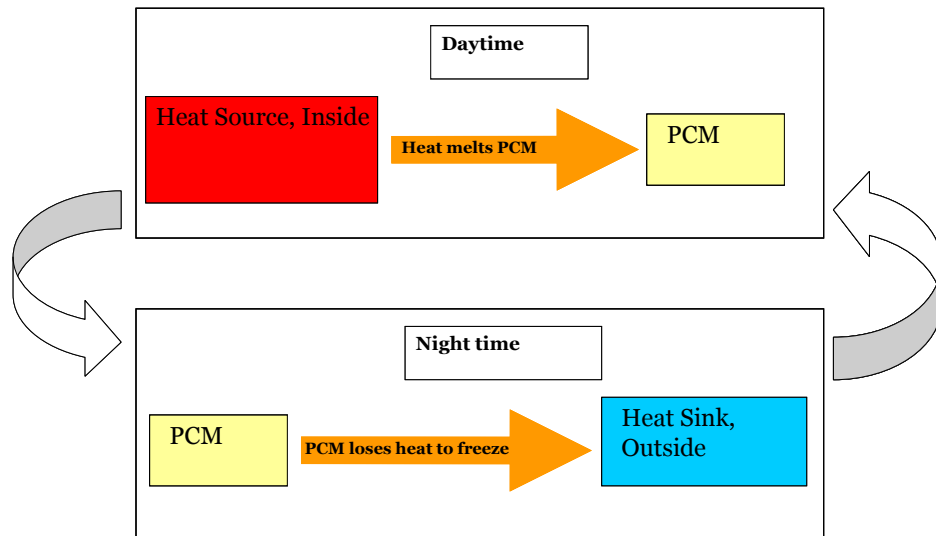


Figure 4.1 The cyclical thermal charge and discharge process undergone by all diurnal PCM cooling systems.

We can now make use of the terms passive and active already encountered. Here, instead of defining an entire system as ‘passive’ or ‘active’ we define the system’s charging or discharging operation as passive or active. This means considering whether the PCM is in direct thermal contact or thermally isolated from the heat source or sink it is intended to exchange heat with. A charge or discharge is passive if no HTF is required and active if it is.

With this method of classification the systems previously defined as active are now defined as active in their charging and active in their discharging; no real difference between the taxonomies is seen there.

The situation is slightly more complicated for the systems previously defined as passive. This type of system is always termed passive in its charging operation but in discharge it may be defined as passive or active. It is active in the case where mechanical ventilation is engaged to blow night air into the building to cool the PCM fabric elements. This is because the night air is now seen as the HTF transferring heat from the internally situated PCM to the external heat sink of the night air.

The systems previously defined as passive are now defined as passive in discharge when natural ventilation is engaged to allow cool night air to freely circulate through open windows. The distinction made here is that by opening windows the internal and external spaces are united thus bringing the internally located PCM into direct

contact with the external night air heat sink. In the case of mechanical ventilation the cool night air is taken from outside, ducted into the space where it absorbs heat from the PCM and is then ducted out of the space. This happens in much the same way as the PCM in a tank rejects its accumulated heat to water which is pumped from a chiller into the tank and then pumped back round to the chiller.

This description also allows us to classify the free cooling and thermally activated systems in terms of passive and active operation. The free cooling systems are now seen as active in the charging operation due to the need to drive air (the HTF) over the modules to cool it before it enters the space. They are also active in discharge for the same reason; cool night air must be forced over the PCM modules to discharge their heat.

The thermally activated systems are now seen as passive in their charging operation, since the PCM elements are in direct contact with the space, and active in their discharging operation due to the necessary presence of water to transfer the accumulated heat from the units to the night air or chiller.

The problem of cooling a space with PCM has now been correctly framed in terms of function and we have a way of broadly defining the operations which all PCM cooling systems must go through on a diurnal basis. We can therefore now turn to the physical arrangement of the essential system components. Any PCM cooling system is composed of four fundamental elements:

- An internal space – location of a heat source (normally during the day)
- A body of PCM to absorb this excess heat
- An external space – location of a heat sink (normally at night)
- One or several forms of insulation that limit the heat flows between the other three constituent elements.

The first two elements are obviously essential. A cooling system must have something to cool and a PCM cooling system must contain some form of PCM.

The PCM can be present in many forms. For instance, as described in the literature review, wallboards, ceiling tiles, tanks filled with modular units and more.

The cooling load of a space results from its heat gains. These consist of internal gains, from people and equipment, and external gains, from conduction through the fabric and direct solar gains through glazing. Cooling loads are normally experienced during the day but in particularly hot climates or in certain building types, such as server rooms or night clubs, cooling loads may be experienced at night. The systems studied as part of this project operate on a diurnal basis which requires the opportunity to reject heat at night when an external heat sink is made available. The analysis presented here proceeds on this basis but it should be noted that the division of charging and discharging operations between day and night, respectively, may not always apply.

The existence of the external heat sink may not always be so simply conceived. A chiller can clearly provide a heat sink for a cooling system. Here the potential presence of a chiller is seen as an additional component to a diurnally operating system. It therefore functions as part of the process of heat rejection from the molten PCM to the external night time heat sink. The chiller boosts the ability of a chilled water circuit to reject the heat accumulated by the body of PCM to the night air. After all, the chiller may be seen as a 'heat pump' in reverse. Without the chiller's presence heat is transferred from the PCM to the flowing water and then to the night air. With the chiller, heat is transferred to the flowing water, then to the chiller's evaporator and then ultimately to the night air again, through the condenser.

In any system like this the design is ultimately aimed at controlling the heat flows between the elements to regulate the temperatures. This is done with some form of insulation which is removed or bypassed as necessary. The detail of building envelope design can vary greatly with examples from the simple design of an external wall in a timber frame house to a more sophisticated curtain wall façade. In both cases insulation, often in the form of mineral wool or fibreglass, will constitute a fundamental element in the build up, limiting heat flow across the building envelope. Insulation will also normally be present in floor and roof build up. Part L2A of the UK building regulations stipulates maximum permissible values U-values for these elements of 0.25, 0.35 and 2.2 W/m²/K for roof and floor, walls and windows, respectively (HM Government, 2010).

In hot climates the insulation in the building fabric will prevent unwanted additional heat flowing into the cooler internal space from outside. This helps maintain internal thermal comfort conditions and saves cooling energy. In a more moderate climate insulation may be present to prevent heat loss from the building in cool weather. This results in thermal comfort maintenance and heating energy savings.

Insulation may begin to have a negative impact as the seasons change the requirement for heating to a requirement for cooling. This is often the case in UK office buildings over the summer when internal gains and fabric insulation combine to cause internal air temperatures to rise above that of the external air. In this case the insulation may be bypassed by opening windows to increase the ventilation rate and lose the unwanted heat.

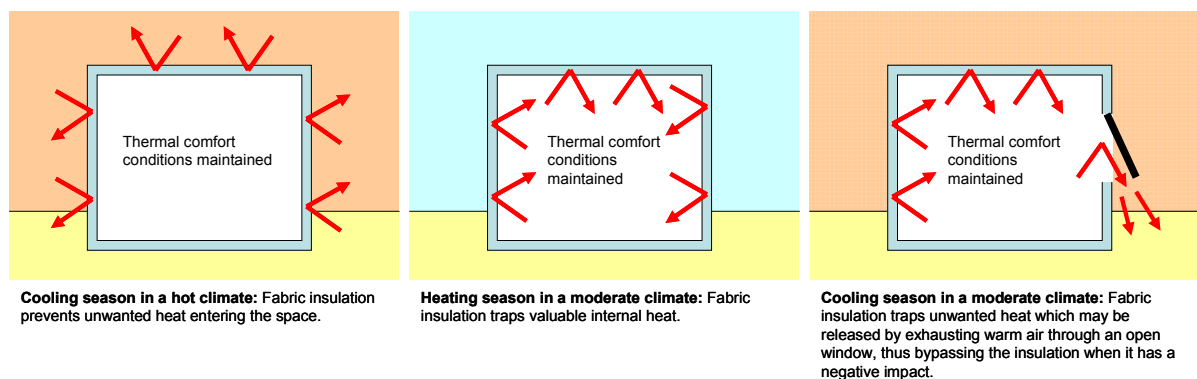


Figure 4.2 Three illustrations of building insulation. The first two represent situations in which the insulation has a positive impact on internal thermal comfort conditions. The third represents a situation in which that insulation is bypassed as it does not have a positive effect at that time.

Another important example is the insulation that surrounds a PCM tank to limit its heat gain and preserve whatever coolth has been accumulated; see Figure 4.3.

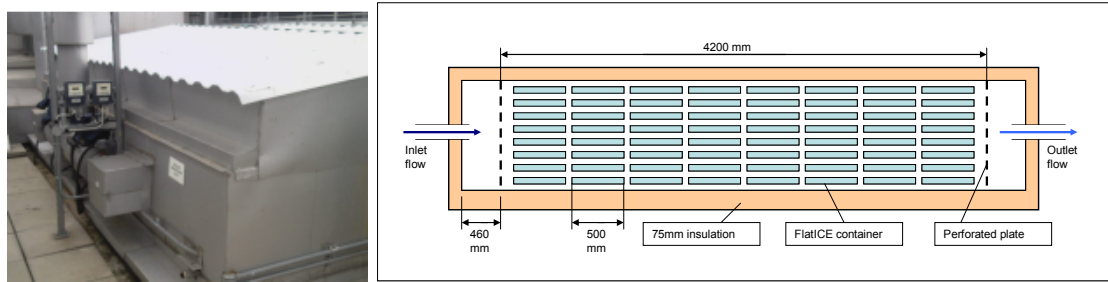


Figure 4.3 The thermal storage tank at China Shipping House, featured in chapter 3, which contains 75mm of rockwool insulation.

Here the insulation may be very similar, mineral wool for instance, and will often be clad in steel or aluminium. In all cases the presence of the insulation is to limit heat flow across a boundary.

With the fundamental functions defined and necessary elements identified the problem has been clearly framed. We can now begin to establish what potential types of system may result.

4.3 Mapping the Design Space

By considering the system as always being composed of these four fundamental elements, we have a very limited number of ways in which the system can be physically arranged. Here we call the particular arrangement of the elements the system's configuration. To determine all possible configurations the system elements may be simply represented by the diagram in Figure 4.4.

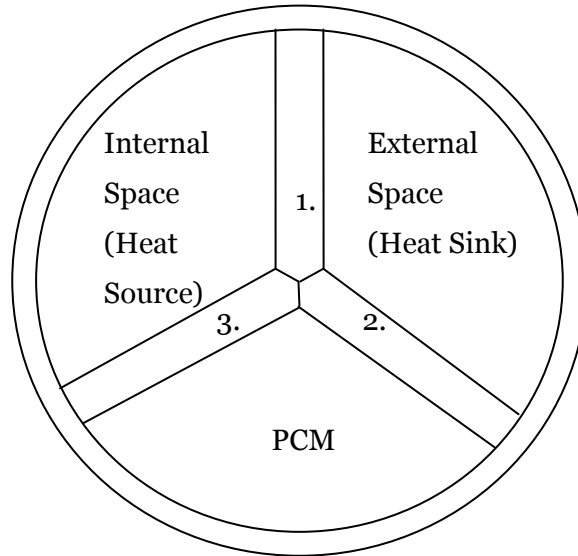


Figure 4.4 Diagram of all fundamental elements of a PCM cooling system. The three spokes represent insulation that may exist between any of the elements.

By removing one or more of the spokes, which represent insulation, the internal space, external space and PCM can be brought into direct contact. For instance, removing the spoke between the PCM and the internal space means that the PCM and internal space are in direct contact; i.e. the PCM is located inside, perhaps in the form of a ceiling tile (see Figure 4.5). There are only eight configurations that can result from this process. Either each spoke is removed individually (three), two spokes are removed at once (three more to make six), no spokes are removed (one more to make seven), or all spokes are removed (one more to make eight).

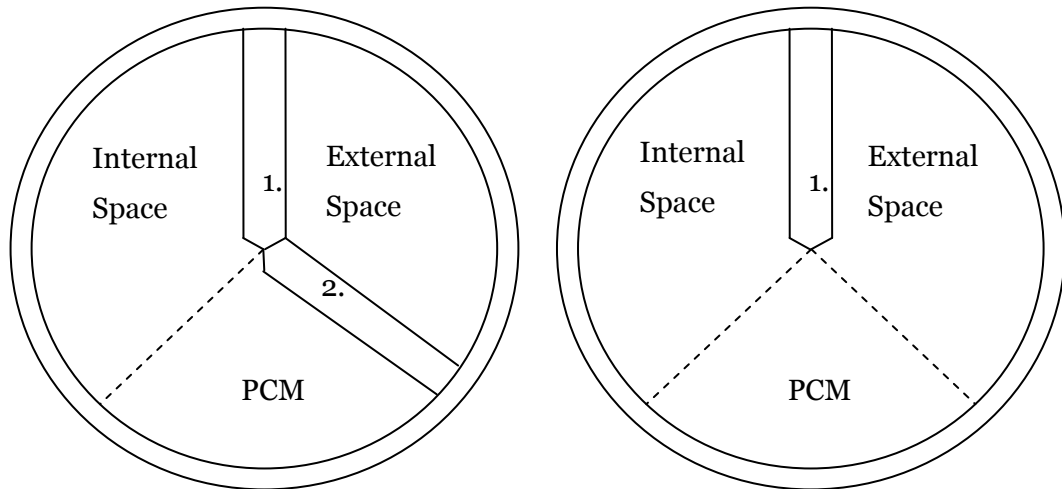


Figure 4.5 Example configurations. Spoke 3 has been removed meaning that the PCM is in direct thermal contact with the internal space, perhaps in the form of a ceiling tile, and both are insulated from the outside by building envelope insulation (left). Spokes 2 and 3 have been removed meaning that the PCM is in direct thermal contact with the internal and external spaces but the spaces are not in thermal contact with each other – i.e. the PCM constitutes at least part of the building envelope, perhaps in the form of micro-capsules incorporated into concrete, but at no point is the envelope open between inside and outside (right).

Two of the possible configurations are not considered meaningfully different to all spokes being removed. These are when both spokes 1 and 2 or 1 and 3 are removed. This is because in all three cases all elements are essentially in thermal contact. The six remaining configurations are represented in Figure 4.6.

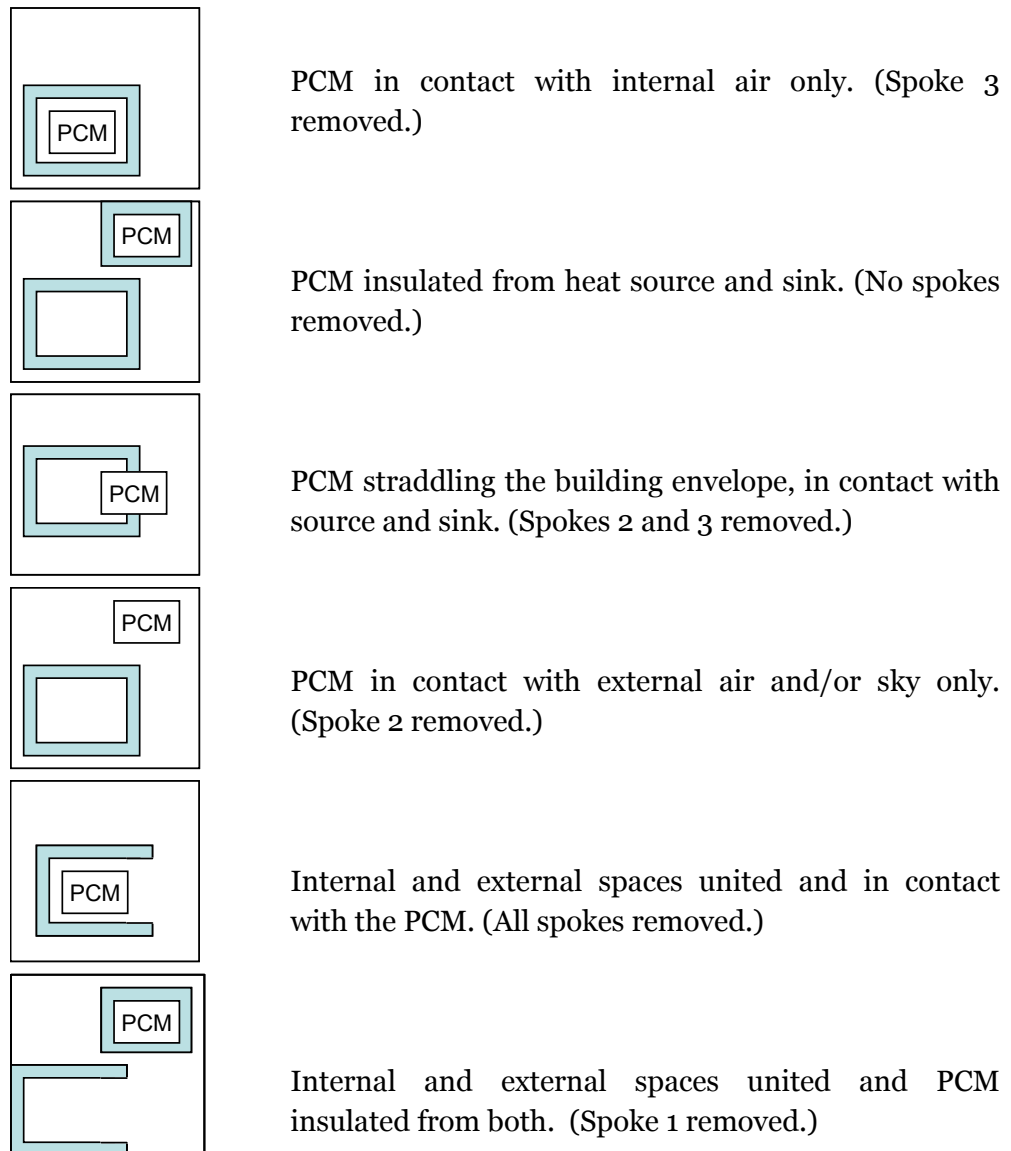


Figure 4.6 Simple pictorial representations of each configuration with attendant descriptions. When the PCM is insulated in its own container its location is not specified and so could be inside or outside.

The configuration of the system may remain the same throughout its day/night cycle or it may change. An example of the configuration changing is the opening of windows for night cooling of PCM wallboards: The window which provided insulation during the charge period is effectively removed to unite the internal and external spaces. Where the insulation does not allow for desired passive heat flow, a

HTF must be employed to bypass the insulation. As noted previously this would commonly be water in a pipe network or air, commonly in a mechanical ventilation system.

In principle each configuration may be implemented for charging and/or discharging so a total of 36 complete system types result from all combinations. These are laid out in the matrix in Figure 4.7.

		Discharging					
Charging		1.	2.	3.	4.	5.	
			6.		7.		
				8.	9.	10.	
					11.		

Figure 4.7 A matrix of potential LHTES cooling system designs. Note that numbers are only for reference to the list below.

Of these 36, 25 are not considered worth exploring further. One reason for this is because that the design is nonsensical since the transition between configurations, when changing from charging to discharging or vice versa, leads to clearly detrimental restrictions or promotions of heat transfer processes. An example of this is a system that contains the PCM in a tank for discharging but then locates it outside for charging. This system would be enabling a negative accumulation of heat

during the charging period and then restricting a positive rejection of heat in the discharging period.

The other reason that designs are disregarded is that the internal and external spaces are united during charging and discharging and yet the PCM is insulated the entire time. This would seem to lead to no beneficial cooling capability. The eleven remaining systems are numbered in the matrix in Figure 4.7 and described Figure 4.9.

1. PCM located internally for charging and discharging. HTF required for discharge to external heat sinks and/or a chiller.
2. PCM located internally for charging but becomes insulated for discharge. HTF required for discharge to external heat sinks and/or a chiller.
3. PCM is located internally for charging but straddles the building envelope for discharge.
4. PCM is located inside for charging and outside for discharge.
5. PCM is located internally for charging. Internal and external spaces are united for discharge.
6. PCM fully insulated for charge and discharge. HTF fluid required for both heat transfer operations.
7. PCM fully insulated for charge and located externally for discharge. HTF required for charging process.
8. PCM straddles the building envelope for charge and discharge.
9. PCM straddles the building envelope for charging and is located outside for discharging.
10. PCM straddles the building envelope for charging. Internal and external spaces are united for discharging.
11. PCM located externally for charging and discharging. HTF required for charging period.

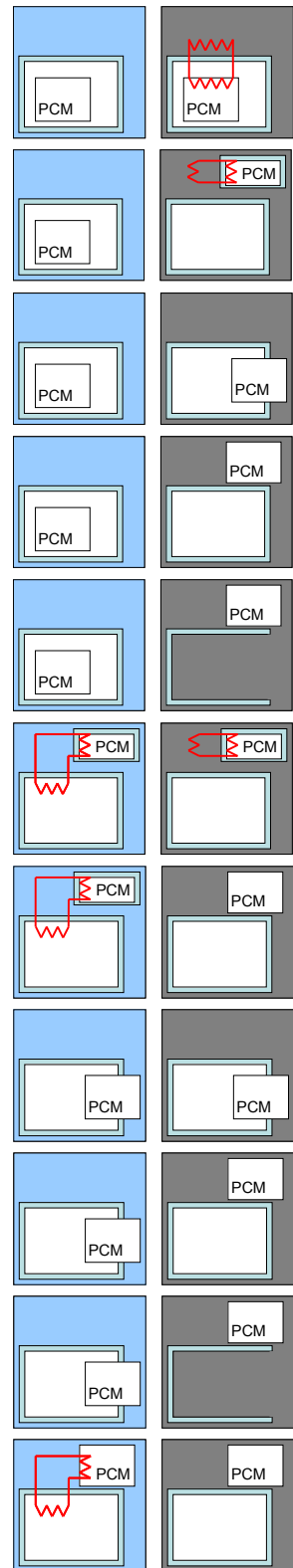


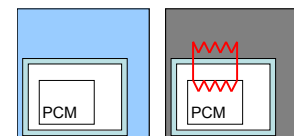
Figure 4.8 All system types with pictorial representations. Red lines indicate the requirement for a heat transfer fluid.

All existing systems and any potential new systems can be categorised as one of the 11 system types.

4.4 System Classification

The following paragraphs set out the system types, notable features, existing or studied designs as well as examples of new designs. In each case many variations could be realised and the proposed designs are not intended to be exhaustive but rather to provide a valid example of what could be achieved to realise the system in question.

Furthermore each system component could be subject to multiple variations and enhancements. For instance the conductivity of the PCM may be enhanced in a number of ways. The literature review referred to an instance where a free cooling system was tested by Zalba et al. (2004) and the component PCM units were then enhanced with a graphite matrix but Marin et al. (2005) for improved heat transfer rates. This kind of enhancement is not discussed as part of the new design concepts that follow but should appear as part of a later more detailed design development process. Indeed this may be seen in chapter 7 where the need to enhance the conductivity of the NewMass units is addressed.



4.4.1 System Type 1

General description:

PCM located internally for charging and discharging. HTF required for discharge to external heat sinks and/or a chiller.

Notable aspects:

This type of system has the clear advantage of zero energy passive operation during the daytime and the ability to sink heat without the PCM having to be mechanically moved.

Its major disadvantage is the power required to induce a flow in the heat transfer fluid.

Research, products and new designs:

The commonly studied and commercialised wall board systems such as Energain (DuPont, 2007a) or the RACUS ceiling tile system from RACUS (Datum Phase Change Limited, 2010) can be grouped under this system type if the discharge operation relies on mechanical ventilation, since air may then be seen as the HTF.

The systems previously defined as thermally activated may now be classified here. This type of system is far less common than the simpler wallboards or ceiling tiles. An obvious research example is the system developed and tested by Koschenz and Lehman (2004). A commercialised product is the Ilkatherm system (Ilkazell, 2010) from Ilkazell.

Thermally activated systems have been subject to less research than the other PCM systems (passive, active and free cooling) covered in the literature review. They have also been shown to demonstrate the potential for effective low energy performance with the guarantee of heat rejection if connected to a chilled water circuit. For these reasons the NewMass system was developed as a thermally activated system as part of this EngD.

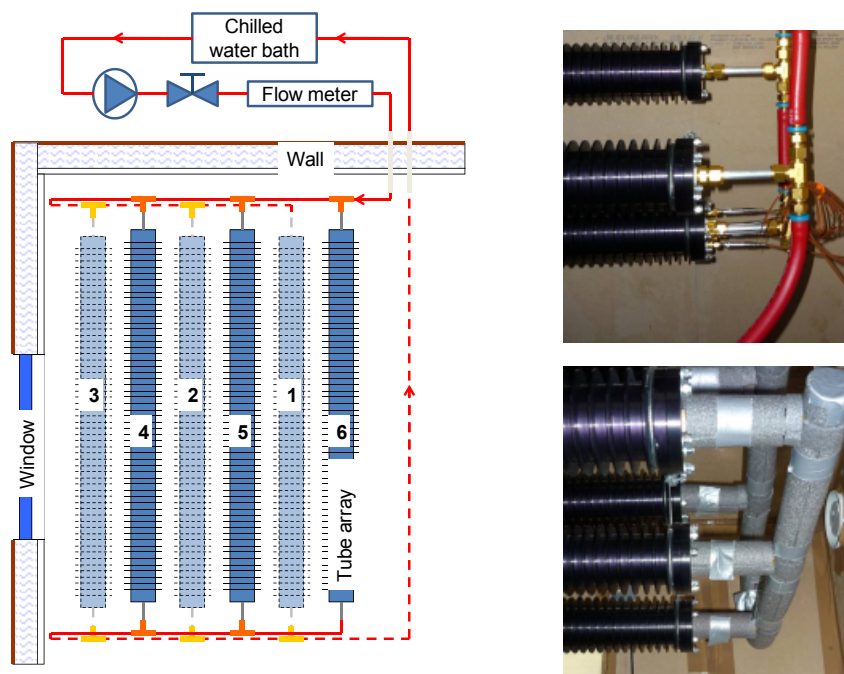
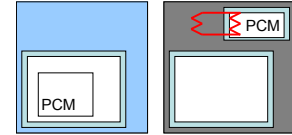


Figure 4.9 The NewMass system as developed in this EngD. Schematic of experimental set up (left) and photos of installed units (right).

The design development that took place with this work is described in chapters 7 and 8 of this dissertation.

4.4.2 System Type 2



General description:

PCM located internally for charging but becomes completely insulated for discharge. HTF required for discharge to external heat sinks and/or a chiller.

Notable aspects:

With this system it is necessary to introduce the concept of removable insulation. If the system has direct thermal contact with the internal space during charging but is totally isolated for discharging then it must make use of dynamic insulation.

This type of system could work well as an extension of the thermally activated systems just mentioned in the above section. Heat would be absorbed passively and discharged actively to a cool water circuit. Between charging and discharging the PCM units would become insulated.

The advantage of a system like this is that when it is discharged it potentially gains less heat from its surroundings than a system that remains uninsulated in the occupied space. Ultimately this will mean higher energy savings.

Research, products and new designs:

No research or products are known about that can be categorised as this type of system. One conceivable way in which it could be realised is for wall boards to be covered by a curtain at night whilst cool water removes accumulated heat. The curtain is drawn back when occupants come into the space.

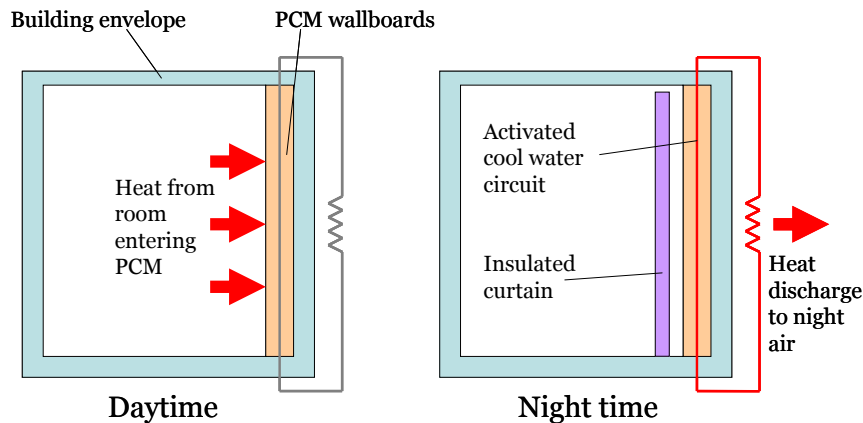
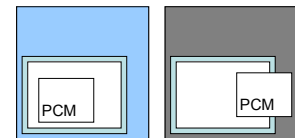


Figure 4.10 Thermally activated system with insulated curtain to limit heat gains at night. The cool water circuit is dormant during the day and activated at night to discharge heat.

Another idea is to utilise the NewMass system but to mechanically wrap the units in insulation when discharge is taking place. This idea is further described in the conclusion under recommendations for further research.

4.4.3 System Type 3



General description:

PCM is located internally for charging but straddles the building envelope for discharge.

Notable aspects:

This system would work like an inverted Trombe wall. A Trombe wall is situated behind a glazed south facing façade and absorbs radiation from the low winter sun, thus accumulating heat. At night the wall may be insulated by a curtain or similar so that it only radiates its heat usefully into the internal space, reducing heating demand.

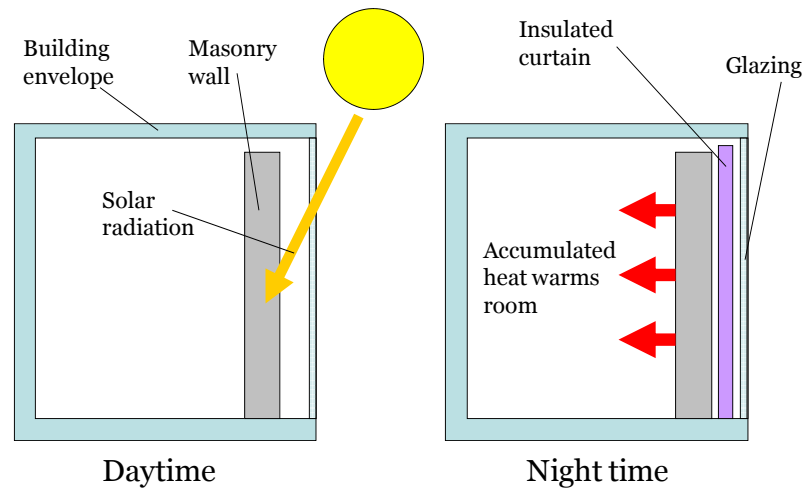


Figure 4.11 A trombe wall with insulating curtain to retain heat.

System type 3 is cooled by thermal contact with the external air and/or sky at night. During the daytime it is protected from solar and/or ambient air convective gains by a layer of removable insulation. This system would be entirely passive and the only energy input required would be to remove and replace the insulation.

Research, products and new designs:

No research or products are known about that can be categorised as this type of system. One idea is to employ removable insulation on a roof or wall which would allow accumulated heat to radiate to the night sky.

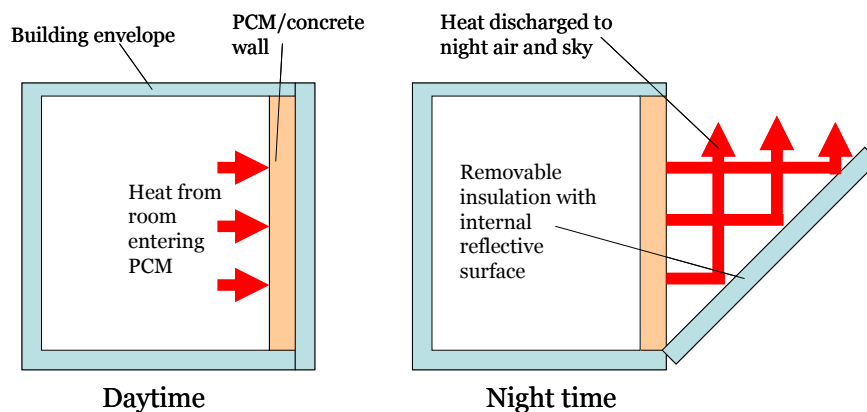
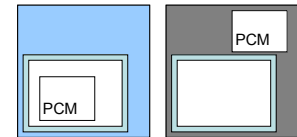


Figure 4.12 System with PCM integrated into the fabric and removable insulation to allow heat to escape at night.

Part of the design challenge here would be for the system to allow the PCM to perform its function thermally but also maintain the integrity of the building envelope in terms of structure and weather protection. The design in Figure 4.12 is fairly simple but a more sophisticated approach could be taken.

The Adaptive Building Initiative (ABI, 2011) is relevant here. A joint venture between Buro Happold and Hoberman Associates, the ABI seeks to design dynamic façade elements that can control the flow of energy and matter across the building envelope. Often this is based around light transmission but the concept may be extended usefully to thermal control. A roof with removable insulation could become part of an integrated envelope element in this context.

4.4.4 System Type 4



General description:

PCM is located inside for charging and outside for discharge.

Notable aspects:

This type of system may be seen as the ideal scenario in terms of desired heat flow control. The PCM is in direct thermal contact with the internal space for charging where it functions entirely passively and is protected from any external heat gains by the building envelope. At night the PCM is in direct thermal contact with the night air and/or sky for discharge. This system would transfer heat most effectively and for the least energy input in both charging and discharging operations. The engineering challenge is to successfully reconfigure the system at dawn and dusk.

Research, products and new designs:

No research or products are known about that can be categorised as this type of system. It is similar to system type 3 in that it may be seen as an inverted trombe wall. In this capacity the PCM would form part of the roof or façade with removable insulation on the inside and outside.

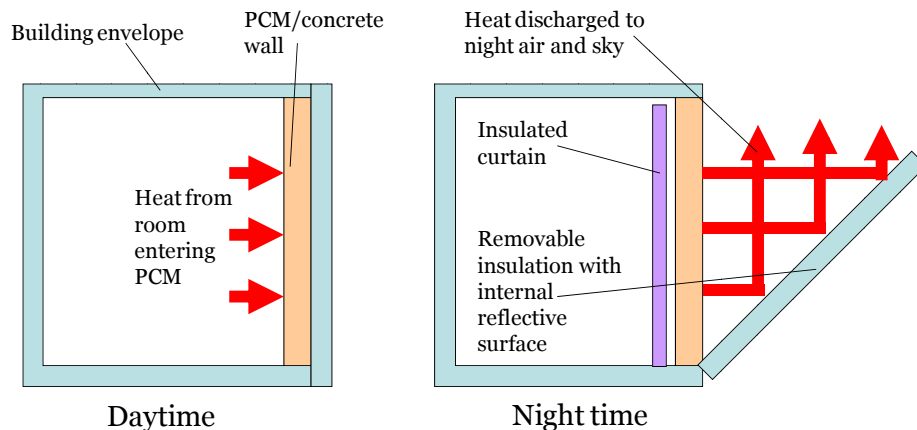


Figure 4.13 System with PCM integrated into the fabric and removable insulation to allow heat to escape at night. At the same time as the external insulation is removed the internal insulation is drawn to prevent internal heat gain.

An alternative would be to mechanically transport the PCM across the building envelope. This idea formed the basis of the Passive PCM Sail design and experiment described in chapter 5.

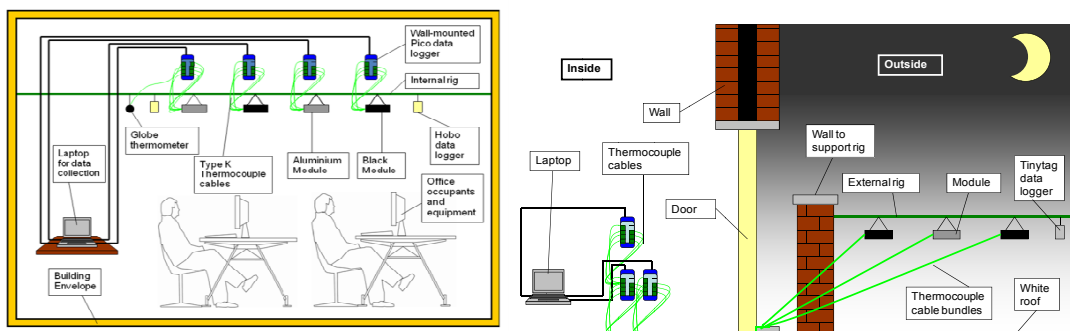
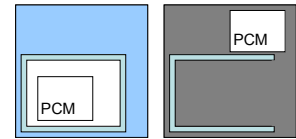


Figure 4.14 The experimental set up for the Passive PCM Sail experiment. Daytime (left) and night time (right).

A full realisation of such a scheme could be conceived of as a rotating roof element in which PCM is located internally during the daytime and externally at night after an insulated roof element rotates 180°. This again draws on the work shown to be possible by the ABI.

4.4.5 System Type 5



General description:

PCM is located internally for charging. Internal and external spaces are united for discharge.

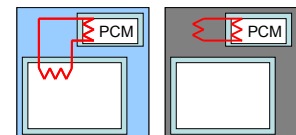
Notable aspects:

This type of system is closely linked to system type 1 because it can employ the same PCM units such as wallboards and ceiling tiles. However, this type of system requires natural night ventilation to reject accumulated heat.

Research and Products:

As with system type 1 the commonly studied and commercialised wall board systems such as Energain (DuPont, 2007a) or the ceiling tile system from RACUS (Datum Phase Change Limited, 2010) can be grouped under this system type if the discharge operation relies on natural ventilation.

4.4.6 System Type 6



General Description:

PCM fully insulated for charge and discharge. HTF fluid required for both heat transfer operations.

Notable Aspects:

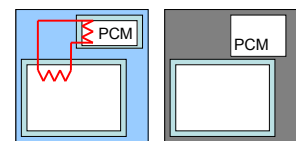
Due to its being fully insulated in both charging and discharging operations this system may make use of the same heat transfer through flowing fluid in both cases. No other reconfiguration of system elements is required. It is unique in these two aspects. This highly controlled system forfeits a great deal of energy efficiency due to its thermal isolation.

Research and Products:

This type of system corresponds to the previously defined active systems and is most commonly found in regular use in the form of ice stores. These systems do not save energy, they actually cost more energy than systems with no storage provision at all. Systems employing hydrated salts with higher melt temperatures do exist and one is studied in chapter 5 to establish energy performance.

This type of system also encompasses the free cooling systems described in the literature review with air being the HTF.

4.4.7 System Type 7



General Description:

PCM fully insulated for charge and located externally for discharge. HTF required for charging process.

Notable Aspects:

This system may be seen to emphasize the heat rejection operation of the cycle. Greater exposure to external heat sinks is gained at the expense of having to employ a HTF to enable cooling during the daytime.

This system is the logical inverse of system type 1; heat is absorbed actively but rejected passively.

Research and Products:

No research or products are known about that can be categorised as this type of system. One design that could realise this type of system could be an insulated tank located on the roof. During the daytime water is circulated to transfer heat from the space to the PCM units in the tank. At night the top layer of insulation is removed from the tank allowing it to radiate heat to the night sky.

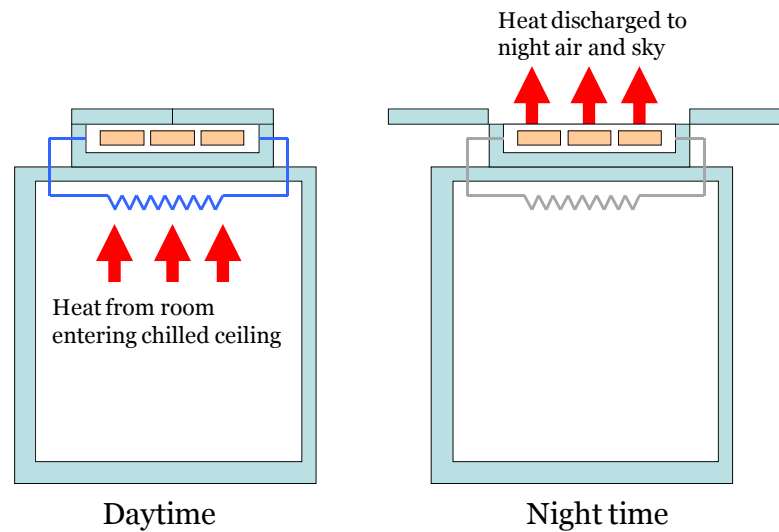
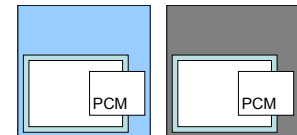


Figure 4.15 A PCM tank with removable insulation to discharge accumulated heat directly to the night sky. The chilled water circuit operates during the daytime to transfer heat to the PCM units but at night it is dormant.

An obvious disadvantage to this system is the external location of the PCM allowing it to pick up undesired heat gains from incident solar radiation and the surrounding air; however these effects would be mitigated by shading and insulation.

4.4.8 System Type 8



General Description:

PCM straddles the building envelope for charge and discharge.

Notable Aspects:

Of all the systems examined this has the potential for the least energy input since no heat transfer fluid is required for charging or discharging and no mechanical movement to reconfigure the system is required between charging or discharging operations.

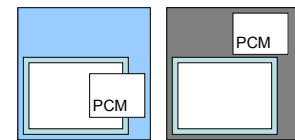
What limits this system is the climate in which it could operate. The climate must allow excess heat to be absorbed by the internal fabric surfaces and then released at night through the external fabric surfaces. At the same time as absorbing internal heat the fabric may also be absorbing external heat from the external air and incident solar radiation. If the fabric cannot lose all the heat it has accumulated

during the daytime it will eventually become saturated and will not perform. In reality a system like this will require supplementary heating or cooling input and is suited to moderate climates.

Research and Products:

In sensible thermal storage terms this type of system conforms to the vernacular architecture of hot countries in which the buildings are thermally massive and thus able to dampen temperature fluctuations, absorbing heat into cool walls during the daytime and rejecting it to the night air and sky later. The research work conducted by Cabeza et al. (2007) and arguably Pasupathy and Velraj (2008) is the latent version of this technique. Crucially the PCM is integrated into the concrete building envelope which is not insulated on either side allowing heat to be freely transferred to internal and external spaces.

4.4.9 System Type 9



General Description:

PCM straddles the building envelope for charging and is located outside for discharging.

Notable Aspects:

This type of system would be potentially well suited to climates with moderate to high temperatures during the day but very low temperatures at night. It is the opposite of system type 3 in this respect and for the same reasons similar to system type 7. The emphasis is on losing heat very effectively at night and not picking up a large amount from external gains during the day.

Research and Products:

No research or products are known about that can be categorised as this type of system. An obvious idea would be to use a wall with integrated PCM which could be internally insulated at night, perhaps with a curtain, to prevent unwanted heat loss.

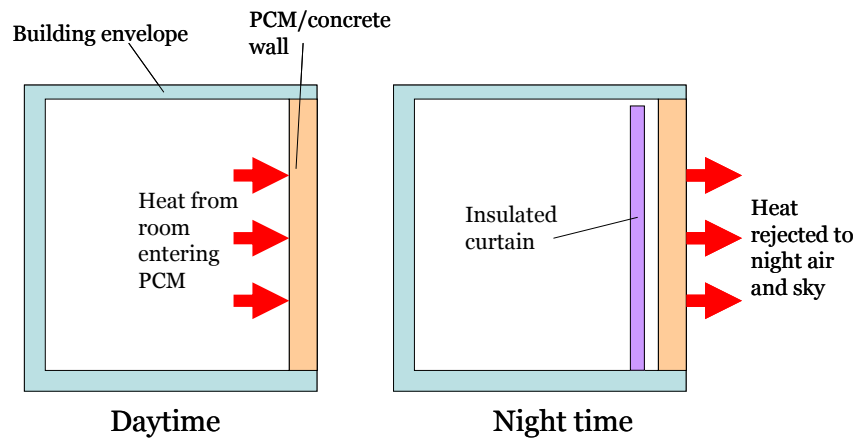
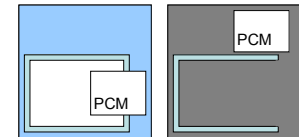


Figure 4.16 PCM integrated into the building fabric with internal insulation to prevent over-cooling at night.

4.4.10 System Type 10



General Description:

PCM straddles the building envelope for charging. Internal and external spaces are united for discharging.

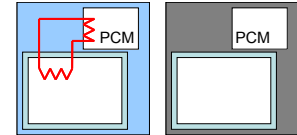
Notable Aspects:

This type of system is potentially well suited to climates with moderate to high temperatures during the day and the moderate to low temperatures at night. The opening of the facade at night would allow internal air flow to increase overall heat transfer rate.

Research and Products:

The system consisting of concrete blocks with integrated PCM could form part of this system if natural ventilation was used to improve heat rejection at night.

4.4.11 System Type 11



General Description:

PCM located externally for charging and discharging. HTF required for charging period.

Notable Aspects:

This type of system is potentially suited to a building with high internal loads and a climate with moderate insolation and daytime temperatures but lower night time temperatures.

Research and Products:

No research or products are known about that can be categorised as this type of system. A roof-mounted PCM unit with connection to the internal space through a cool water circuit would fit the description.

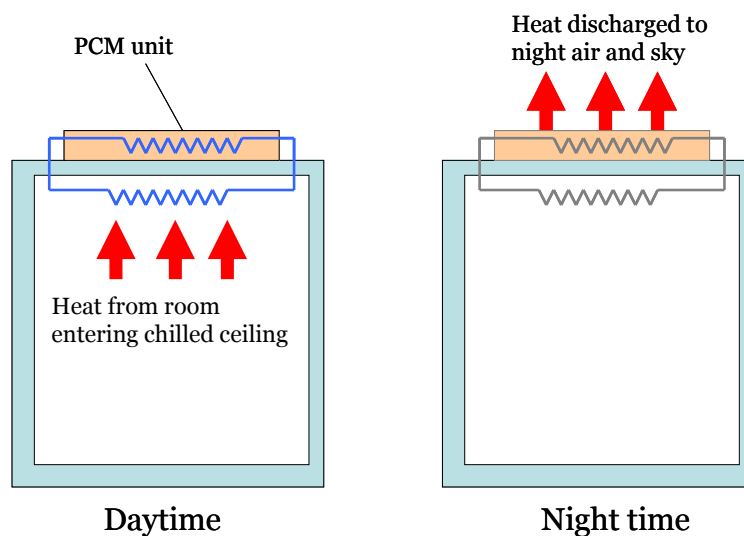


Figure 4.17 Externally located PCM unit with cool water circuit connection to interior. The chilled water circuit operates during the daytime to transfer heat to the PCM units but at night it is dormant.

This system is not considered applicable to most buildings and climates since it would absorb external heat gains and lose its utility. It may however have application in very cold countries which experience a cooling problem in the

summer when building fabric insulation causes internal temperatures to rise to uncomfortable levels even when external temperatures remain below the thermal comfort zone.

4.5 System Comparison and Selection

Several system types are exploited by existing systems, either commercially or in academic research:

- System type 1 is realised by wallboard and ceiling tile systems if coupled with mechanical ventilation. It is also, to a far lesser extent, realised by the thermally activated systems that discharge accumulated heat to chilled water units.
- System type 5 is realised by the same wallboard and ceiling tile PCM elements but relies on natural, rather than mechanical, ventilation to reject the accumulated heat at night.
- System type 6 is realised by the previously defined ‘active systems’ and ‘free cooling systems’. These contain the PCM in an insulated tank with which heat is transferred by water, or in ceiling voids or modular units with which heat is transferred by air.
- System type 8 is realised by the PCM/concrete units that have been academically studied.
- System type 10 is closely related to system 8, the only difference being the use of natural ventilation to aid heat rejection.

System types that have not been exploited commercially or in academic research mostly involve removable insulation. Some of these also involve an active element for charge or discharge:

- System type 2 may be realised by employing internal thermally activated PCM elements that are covered at night to preserve accumulated coolth on discharge. This may be seen as an extension to the NewMass system (design

and testing in chapters 7 and 8) if the design incorporated removable insulation.

- System type 7 may be realised by employing an externally located PCM tank that transfers heat from the space through a water circuit during the day and radiates the accumulated heat at night by the removal of the top layer of insulation.

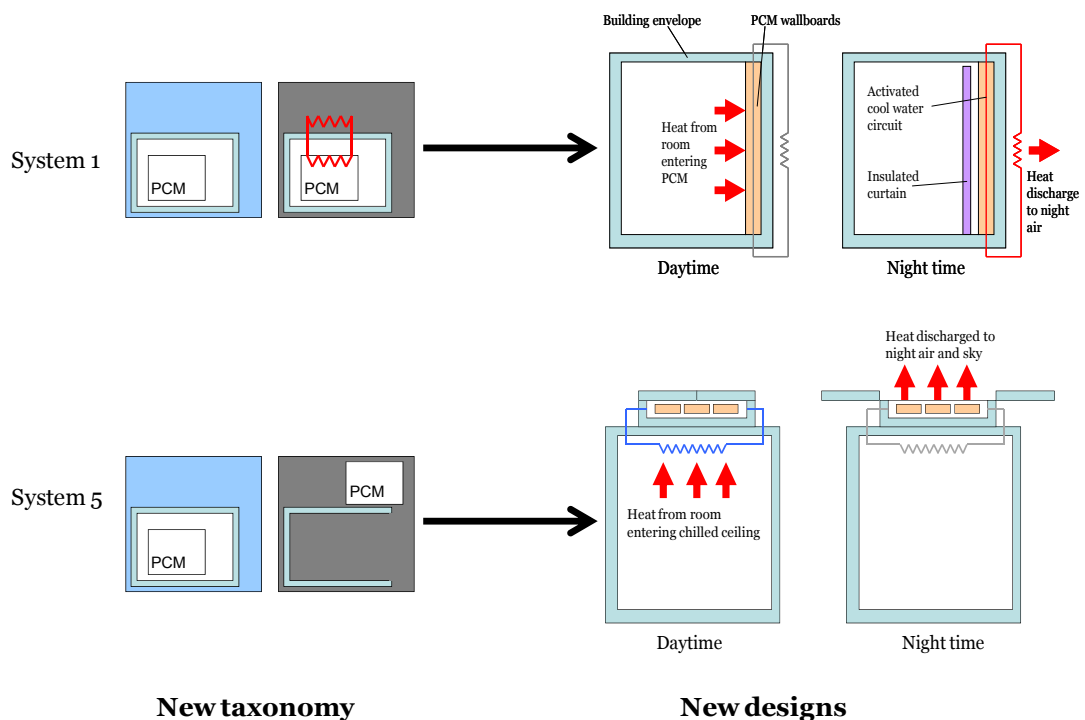


Figure 4.18 New designs with removable insulation and HTF circuits. An alternative to the system 1 design displayed is an extension of the NewMass system design with removable insulation.

Other system types incorporate removable insulation with no active charge or discharge element:

- System type 3 may be realised by removing external insulation for discharge at night.
- System type 4 is similar but internal insulation is simultaneously added to prevent heat gain from the internal space. System type 4 may also be realised

by transporting the PCM across the building envelope, as featured in the new Passive PCM Sails design in chapter 5.

- System type 9 is the opposite of system type 3 and may be realised by removing internal insulation for charge during the day.

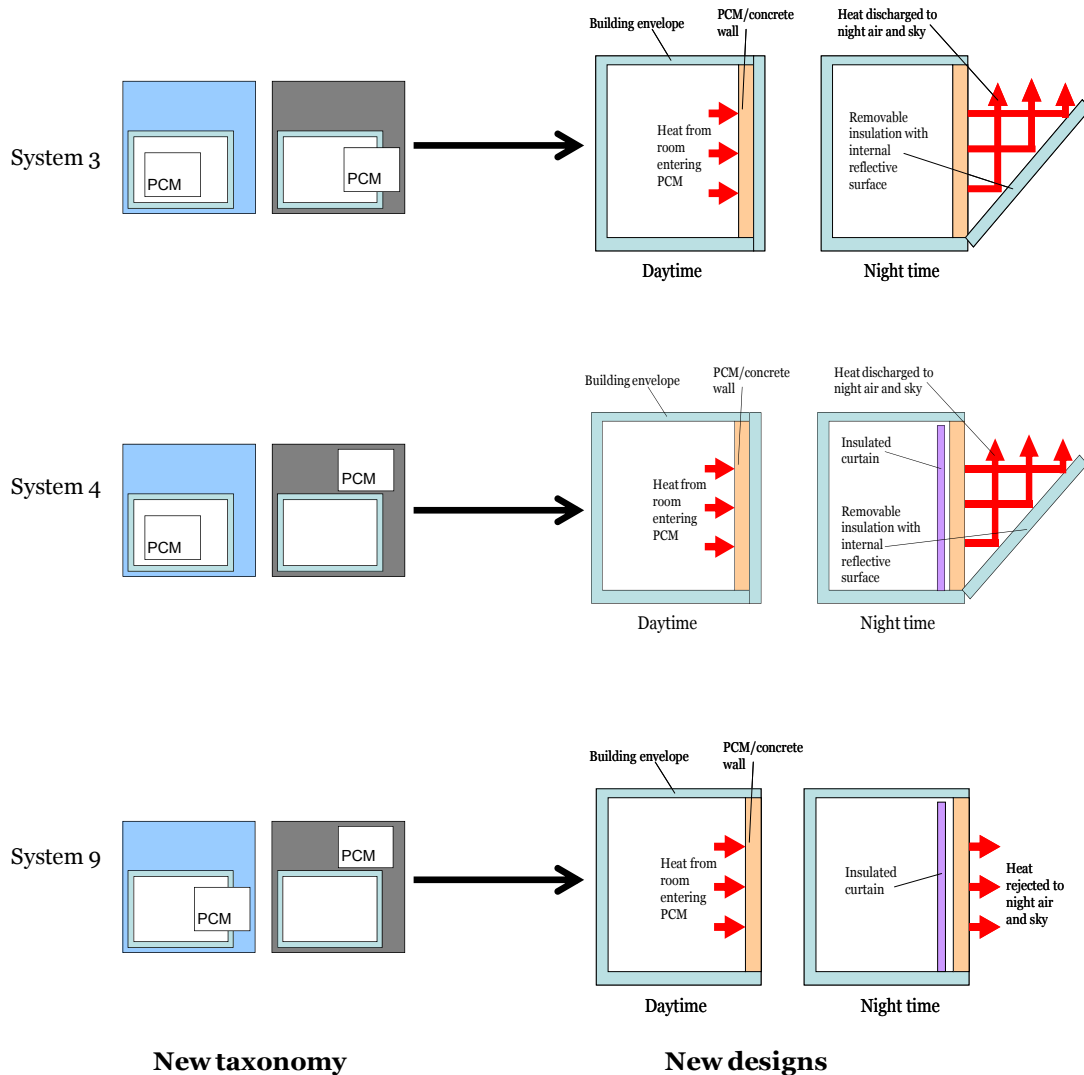


Figure 4.19 New designs with removable insulation. An alternative to the system 4 design displayed is a system with PCM moving across the envelope between charge and discharge. This idea is explored in chapter 4.

The remaining system that has not been compared is system type 11. This may be seen as the opposite of system 1. Here a HTF is required to transfer heat from the space during the daytime. This system is only conceivable in a climate with low or zero external heat gains. This type of system is considered unlikely to be used

because the building would have to have extremely high internal gains and particular difficulty sinking that heat in a climate with low ambient temperatures.

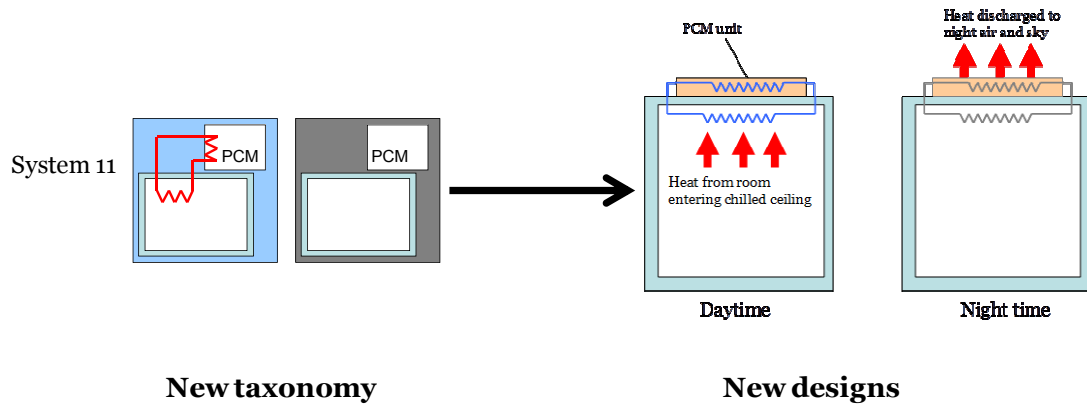


Figure 4.20 *New design with HTF. This design may be seen as the opposite of design 1 or potentially an inverted thermally activated system with the PCM located outside for effective discharge and coolth delivered inside via the HTF.*

A data centre is a good example of a building or room with very high internal gains. If the data centre is situated in a climate where a cooling season does not exist then it should be designed so that it is able to sink the heat directly, i.e. it should not need to make use of energy storage in the first place.

4.6 Conclusions

In this chapter a new taxonomy for the classification of PCM cooling systems was developed based on the system's fundamental elements and the degree to which the PCM may be actively or passively charged or discharged. This taxonomy was used to establish all potential system types, based on the fact that any system's fundamental elements may only be configured in a limited number of ways. This allowed all existing system to be classified and new potential system designs to be conceived. The design options with the potential for valuable new research are a range of systems that may be seen as generally more passive or active. The more passive systems allow the PCM to gain contact with the heat source or sink through

mechanical movement between charge and discharge. The more active systems have less mechanical movement and employ a fluid to transfer heat.

It is clear that the systems employing movable PCM elements and/or insulation are least researched. There are 6 in total: Two which also employ a heat transfer fluid and 4 which do not. There is an opportunity to research this type of system further. In order to cover this aspect as well as several others, system 4 was selected for development. Here, removable insulation was not tested explicitly but an analysis of cross-envelope transport was undertaken in the form of the Passive PCM Sail experiment presented in chapter 4. The attraction of this system is that it locates the PCM units within the heat source or sink with which they should be gaining heat from or losing heat to. This maximises heat transfer rate and reduces pump and fan energy to zero since no movement of a secondary heat transfer fluid is required. The experiment also allowed some understanding of a system with removable insulation to be gained since the modules that discharged their heat externally could be seen to have had external insulation removed from them to discharge. In this sense, for discharge, the Passive PCM Sails correspond to system types 7 and 9, as well as 4.

The Passive PCM Sails were also tested as versions of system type 5; the conventional passive system with natural ventilation for heat discharge. System type 5 is one of the 5 systems identified as having been subject to research or commercialisation already. Of the already existing systems, types 1, 5, 8 and 10, are variations on passive products integrated into the building fabric in the form of wallboards, ceiling tiles or concrete/PCM blocks. The fifth, system type 6, is realised by the active systems incorporating PCM tanks containing hydrated salts or pure ice, as described in the study in chapter 3.

Of the existing systems, the thermally activated system is considered the most worthy of further development. This is for several reasons. Firstly, as compared to passive systems such as wall boards it has not had much academic research or commercialisation. The only known research project on this type of system is the conducted by Koschenz and Lehman (Koschenz and Lehmann, 2004) and few known products are known about. Examples are the Ilkatherm panel (Ilkazell, 2010) on which it relies, and EBB boards (AECB). Secondly, this type of system has the

potential to be extremely low energy since it can be employed as a passive system with natural ventilation for discharge with sufficient air flow and temperatures. This means that it can correspond to system type 5 in terms of its operation. Thirdly, it gives the opportunity to reliably control and guarantee heat discharge through the inclusion of a refrigeration element in the water circuit. Fourthly, it may be developed so as not to require modification of the façade which, although presenting an interesting avenue of architectural and façade design, is not likely to be widely deployed and cannot be retrofitted.

The NewMass system is the system developed as part of this EngD to fulfil the potential of a system to realise a combination of system types 1 and 5, through the combination of natural ventilation and thermally activated PCM units. This and further design innovations are presented in chapter 7.

After discussing many system types and identifying some which can be usefully researched further as part of this EngD, we are left with a considerable number of system types that could yield valuable energy efficient and practically realisable future designs.

Further work that is therefore proposed is twofold: Firstly, a general research project into what type of newly proposed system would perform well in which buildings and which climates could be performed. This could take the form of a number of thermal models that could be run with different internal load patterns and different weather files to represent different building types and different climates, respectively.

Secondly, particular system types could be chosen for development into fully realised systems. This EngD project seeks to cover some of the ground in the development of the Passive PCM Sails and NewMass systems but there are many more system types that could be explored; the ones involving removable insulation being particularly interesting.

References

ABI (2011) *Adaptive Building Initiative*. Available:

<http://www.adaptivebuildings.com/systems.html> [20/10/2011].

AECB (2011) *Clay Building Boards and Function Elements*. Available:

<http://www.ebb.im/> [30/10/2011].

Alumet (2011) *Curtain Walling*. Available:

http://www.alumet.co.uk/curtain_walling.php [30/10/2011].

Artica (2009) *Artica Technologies: Classic*. Available at:

<http://www.articatechnologies.com/solutions.php> [03/01/2012].

Cabeza, L.F., Castellón, C., Nogués, M., Medrano, M., Leppers, R. & Zubillaga, O. (2007) "Use of microencapsulated PCM in concrete walls for energy savings", *Energy and Buildings*, vol. 39, no. 2, pp. 113-119.

Datum Phase Change Limited (2010) *Suspended Ceiling Tiles* Available:

<http://datumphasechange.com/index.php?products> [23/09/2010].

DuPont (2007a) *DuPont Energain*. Available:

http://www2.dupont.com/Energain/en_GB/ [29/04/2007].

DuPont (2007b) *DuPont Energain - Energy saving thermal mass systems: Installation Guidelines*, DuPont, Luxembourg.

HM Government (2010) *The Building Regulations 2000: Conservation of fuel and power*, RIBA, London.

Ilkazell (2010) *Ilkatherm Ceiling*. Available:

http://www.ilkazell.de/en_baudecke.php [21/02/2010].

- Koschenz, M. & Lehmann, B. (2004) "Development of a thermally activated ceiling panel with PCM for application in lightweight and retrofitted buildings", *Energy and Buildings*, vol. 36, no. 6, pp. 567-578.
- Marín, J.M., Zalba, B., Cabeza, L.F. & Mehling, H. (2005) "Improvement of a thermal energy storage using plates with paraffin–graphite composite", *International Journal of Heat and Mass Transfer*, vol. 48, no. 12, pp. 2561-2570.
- Pasupathy, A. & Velraj, R. (2008) "Effect of double layer phase change material in building roof for year round thermal management", *Energy and Buildings*, vol. 40, no. 3, pp. 193-203.
- Zalba, B., Marín, J.M., Cabeza, L.F. & Mehling, H. (2004) "Free-cooling of buildings with phase change materials", *International Journal of Refrigeration*, vol. 27, no. 8, pp. 839-849.

PASSIVE PCM SAILS

In this chapter the testing of a concept known as Passive PCM Sails is presented. This concept is intended to satisfy the opportunity for increased thermal and cooling capacity in passive systems, raised by the literature review, and to go some way to realising the system types 4, 7 and 9, proposed in chapter 4. To these ends, two innovations are made: Firstly, the units are deliberately not integrated into the building fabric. This increases the potential surface area and volume of PCM that may be utilised which consequently increases cooling and thermal capacity, respectively. Secondly, three of the units are transferred outside at night to discharge their accumulated heat. This gives an indication of how effective cross-envelope transfer of the PCM might be and also what effect removable insulation could have. Systems that utilise cross-envelope transfer and/or removable insulation have not been subject to previous research and have the potential to be extremely low energy since the aim is to bring the PCM into direct thermal contact with the source and sink it is exchanging heat with.

In the literature review it was seen that most research into PCM cooling systems examines passive applications, normally in the form of wall boards, ceiling tiles or PCM integrated concrete. These systems have the advantage of passively absorbing heat from a space, thus reducing cooling energy. If heat is rejected through natural ventilation at night then the system will consume no energy. However if mechanical ventilation is required, fan power may become a significant factor. Passive applications are limited by the available wall and ceiling surface area to which they can be applied. Limited surface area entails limited heat transfer rates. The consequence of this is a limited cooling capacity and capacity to effectively reject accumulated heat at night. Limited surface area also means a limited thermal

capacity since only a certain depth of the unit will be accessed through conduction over a 24 hour cycle.

The limit on thermal capacity and cooling capacity limits the proportion of the cooling load that can be covered by the PCM. Customers using DuPont Energain panels which may be applied to all walls and ceiling in the right circumstances are told that they can expect to up to 35% of their air conditioning energy (DuPont, 2010). The reason there is a limit is the limited surface area for cooling and the limited amount of PCM that can be put in the space, since the panels are only 5 mm thick. There is therefore an opportunity to save more cooling energy if the surface area and volume of the PCM units is increased.

This increase in surface area will also aid the rejection of heat at night due to higher heat transfer rates. In this work, to increase the surface area available, PCM units have been designed to sit within the space rather than being integrated into the building fabric. Some passive units that are not integrated into the building fabric have been developed already. The Ilkatherm panel from Ilkazell (Ilkazell, 2010) may be integrated into a wall or ceiling or be located below the soffit as a sail. The TubeICE units available from PCM products (Phase Change Material Products Ltd, 2010) are designed to be installed at ceiling height or behind false ceilings. In the case of Ilkazell only one surface is active as the other side is insulated. In the case of TubeICE the units' casing is plastic which inhibits heat transfer. Both of these designs can be improved upon to maximise surface area and increase thermal conductivity.

In summer, 2008, prototype modules of the Passive PCM Sails were constructed from commercially available paraffin/low-density-polyethylene (LDPE) composites and positioned below the ceiling of an occupied office space. The modules were intended to absorb excess room heat during the daytime, through the melting of the contained paraffin, and then discharge this heat at night, through the freezing of the paraffin. As well as examining the performance of passive PCM units that are not integrated into the fabric and transported outside for discharge, two other design variations were chosen for examination. Four modules were constructed for this purpose.

The first variation was in the location for cooling. Every evening three modules were transported to a roof-top rig to discharge their heat while one remained inside to cool. Transporting PCM modules outside presents a mechanical engineering challenge but has the advantage of greater contact with night time heat sinks.

The second variation was in the surface of the modules: aluminium foil and tape or the same combination coated with matt black paint. The black modules were intended to interact radiantly (as well as convectively) with the surroundings during both charge and discharge; the aluminium modules were only intended to interact convectively.

The third variation was in the choice of PCM itself. Both were paraffins but one had a manufacturer-quoted transition zone of 22°C and the other of 26°C, known as A22 and A26, respectively (PCM Products, 2009). A22 was intended to begin transferring heat faster at lower temperatures, with A26 reacting only at higher temperatures. The anticipated result was that, assuming full freezing occurred the previous night, during days in which the dry bulb air temperature reached a maximum between 22°C and 26°C, only A22 would melt, while A26 would remain fully frozen.

The modules tested were an externally-cooled, aluminium-covered, A22 module (A22,Al,EC), an externally-cooled, aluminium-covered, A26 module (A26,Al,EC), an externally-cooled, black, A22 module (A22,Bl,EC), module and an internally-cooled, black, A22 module (A22,Bl,IC). Each variation was present in at least two modules, which were identical in every other respect. This allowed comparison of each variation between two modules which were otherwise identical.

5.1 Method

All modules were constructed from four 150 mm² paraffin/LDPE composite tiles, covered with aluminium foil and held firmly together with aluminium tape and nylon cord. (The LDPE stabilized the shape of the paraffin upon melting.) Type-k thermocouples were placed at seven locations throughout the body of the module. Five between the layers and two buried in the top and bottom surfaces - see Figure 5.1.

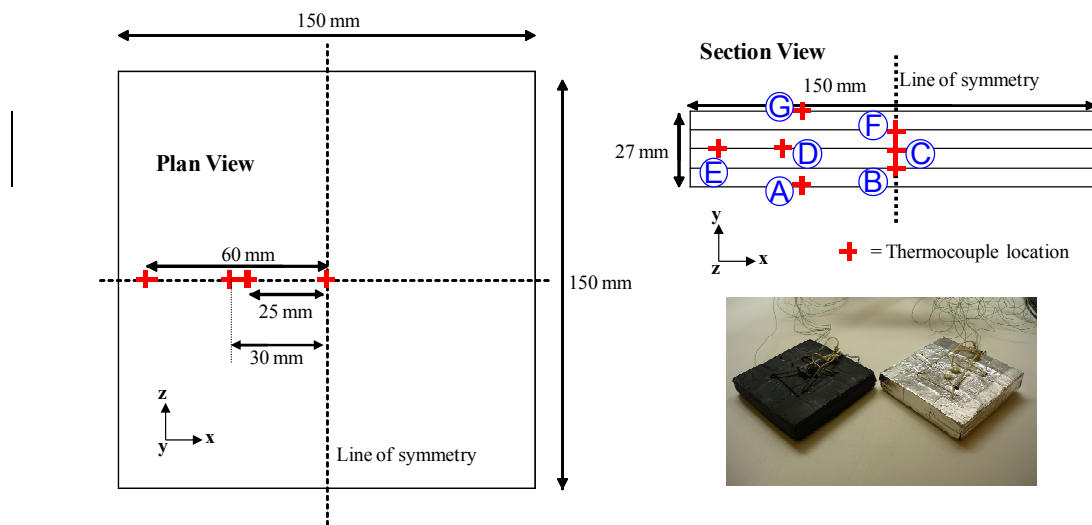


Figure 5.1 Module dimensions and thermocouple locations. The section dimensions apply to all four sides of the panel. The plan dimensions apply to the top and bottom. Thermocouples are labelled A – G to allow identification of validation curves in section 5.2.1. The photo displays an example of the black-painted and aluminium covered modules. Each module was constructed from four panels, with an average thickness of 6.75mm each.

During daytime the modules were hung from a rig 2.5 m above the ground: the height at which full scale systems would be located - see Figure 5.2.

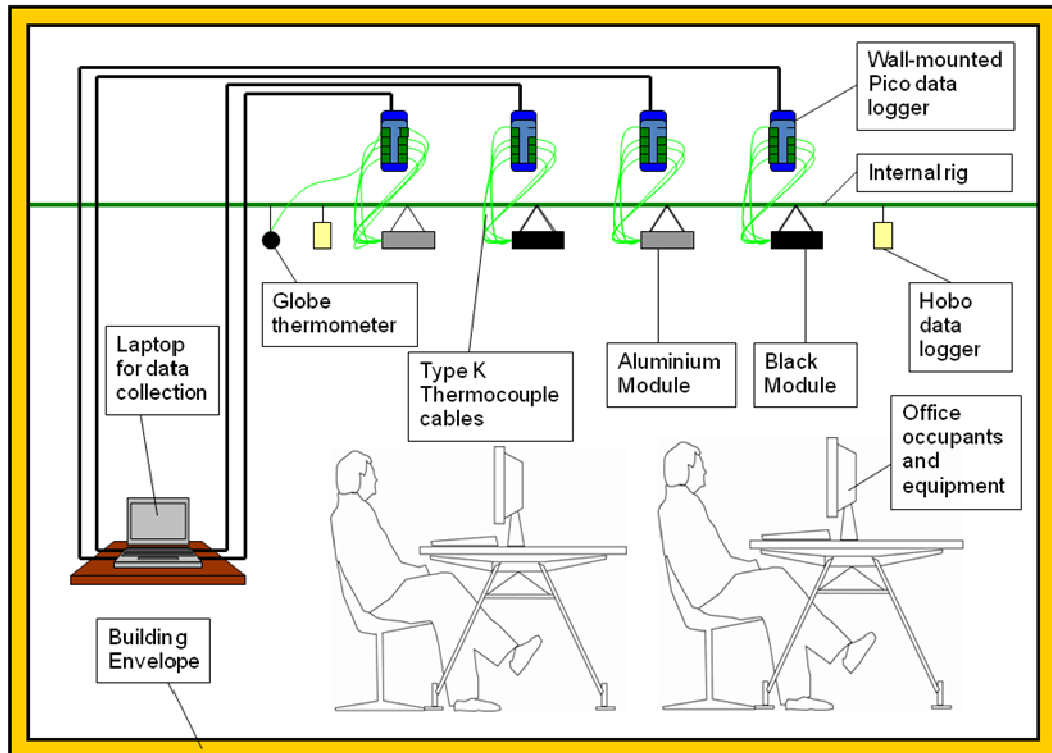


Figure 5.2 The internal set up. Modules were placed between 0.25 and 0.5 m apart. This ensured the same local environmental conditions but negligible mutual interaction.

The thermocouples were connected to wall-mounted data loggers, which in turn were connected to a laptop for recording temperature at single minute intervals. This allowed near constant recording over several days without disturbance to occupants. Due to their small size, it was assumed that no detectable effect on the room temperature would occur.

Two hobo data loggers were hung from either end of the rig to record the dry bulb temperature, taken to be the mean, every three minutes. This also verified that the air temperature around the modules was near uniform. A globe thermometer was also hung from the rig and recorded at minute intervals.

At around 8:00pm the A22,Bl,IC module remained in its position to discharge, while the rest were hung from a roof-top rig - see Figure 5.3.

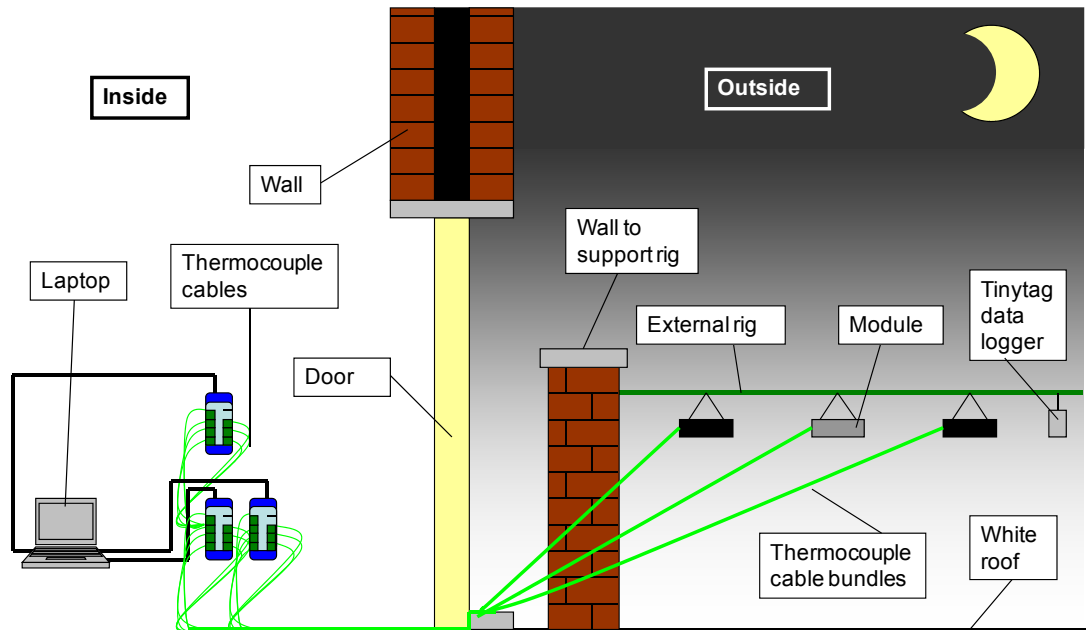


Figure 5.3 The external set up. Modules given an equal view of the night sky and were placed between 0.25 and 0.5m apart. This ensured the same local environmental conditions but negligible mutual interaction.

The thermocouples in the external modules were connected to internally located loggers and a laptop, for monitoring throughout the night. A tinytag logger was hung from the external rig to record the external air temperature at three minute intervals.

At around 7:00 am the outside cooling modules were transferred from the external rig to the internal rig. This procedure took around 30 to 50 minutes, during which time data logging ceased. The reverse procedure took the same time. Maximum and average wind speeds, as well as dry bulb temperature, were recorded at the time of each transfer.

The in-situ measurements were used in conjunction with DSC measurements of thermophysical properties, obtained by Tanawat Cheechern, to produce semi-empirical CFD models of the modules with the solidification/melting solver in FLUENT. This uses the enthalpy porosity formulation described in the literature review. The thermophysical properties of the PCM are shown in Table 5.1.

Table 5.1 Thermophysical properties of the tested PCM/LDPE composites (Cheechern, .

PCM Type	Density (kg/m ³)	Conductivity (W/m/K)	Specific Heat (J/kg/K)	Latent Heat (J/kg)	Melt onset temp (°C)	Freeze onset temp (°C)	Melt end temp (°C)	Freeze end temp (°C)
A22 Panel	852.7	0.2000	2304	74020	11.29	21.76	22.44	5.27
A26 Panel	834.4	0.2300	2387	75210	17.21	24.19	29.97	12.19

Here “Melt onset temp” refers to the temperature at which melting begins, as the temperature of the substance is increased, found through analysis of DSC data. “Melt end temperature” refers to the temperature at which melting ceases. “Freeze onset temp” and “Freeze end temp” equivalently refer to start and finish temperatures for freezing, off-set from the melting temperatures because of under-cooling.

During charge periods T_{solidus} is taken to be equal to “Melt onset temp” and T_{liquidus} is taken to equal “Melt end temp”, for that material. FLUENT models the sensible heating and melting of the material as a step function, illustrated in Figure 5.4 and Figure 5.5.

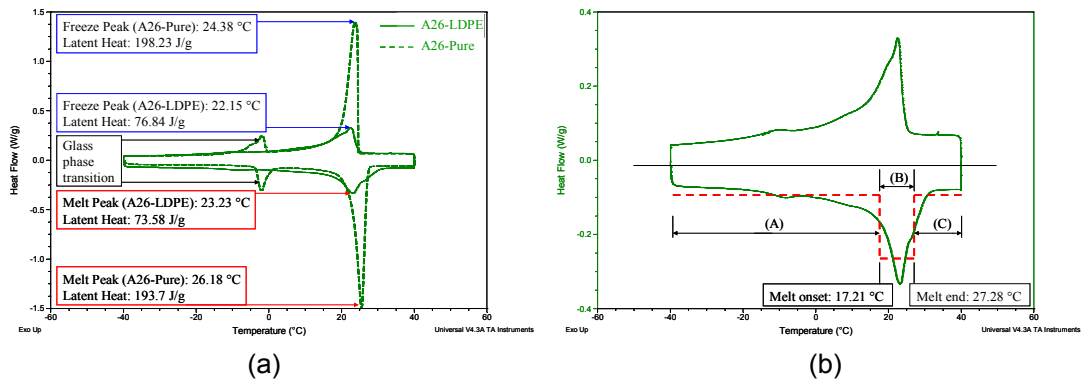


Figure 5.4 (a) DSC curves of pure A26 paraffin and A26-LDPE composite. Peaks of melting and freezing are indicated along with melting and freezing latent heats. It may be observed that the presence of the LDPE scaffold has the effect of reducing the pure A26 peak and widening the phase transition zone. See Table 5.1 for all thermophysical property figures of the A26-LDPE composite. (b) The DSC curve of the composite is displayed here with the dashed red line representing the variation in heat flow rate per unit mass with temperature change, as defined by the FLUENT model. Regions marked A and C are those in which sensible heating occurs. In region B sensible and latent heating occurs.

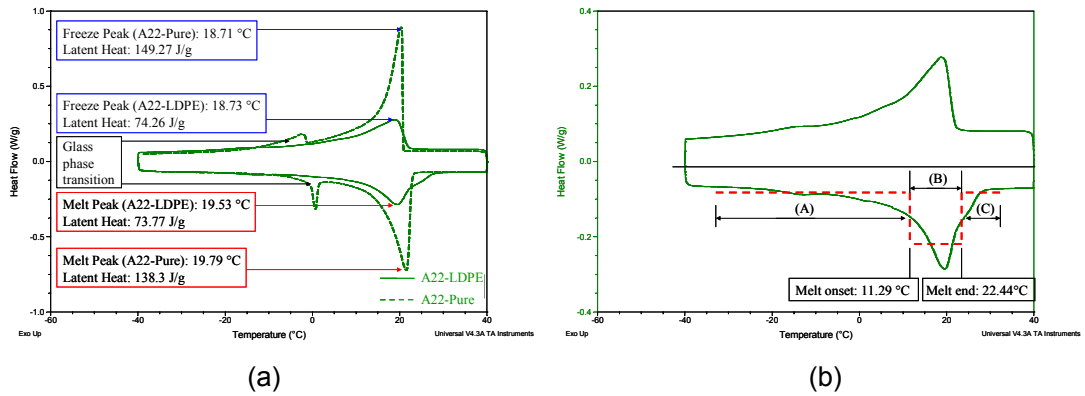


Figure 5.5 DSC curves of pure A22 paraffin and A22-LDPE composite. In all other respects the same as Fig. 5.4 – see Fig 5.4 caption. (b) The DSC curve of the A22-LDPE composite. In all other respects the same as Fig. 5.4 – see Fig. 5.4 caption.

FLUENT read the boundary conditions as shown in Eq.s 5.1, 5.2, 5.3 and 5.4:

For heating the modules:

$$\forall t, x = 0, \quad -k \frac{\partial T}{\partial x} = h(T_{\infty} - T) + \varepsilon \sigma (T_{surr}^4 - T^4) \quad (5.1)$$

$$\forall t, x = e, \quad -k \frac{\partial T}{\partial x} = h(T_{\infty} - T) + \varepsilon \sigma (T_{surr}^4 - T^4) \quad (5.2)$$

For cooling the modules:

$$\forall t, x = 0, \quad k \frac{\partial T}{\partial x} = h(T - T_{\infty}) + \varepsilon \sigma (T^4 - T_{surr}^4) \quad (5.3)$$

$$\forall t, x = e, \quad k \frac{\partial T}{\partial x} = h(T - T_{\infty}) + \varepsilon \sigma (T^4 - T_{surr}^4) \quad (5.4)$$

In Eq.s 5.3 and 5.4 the emissivity, ε , is taken to be equivalent to the absorptance of the surface. These conditions apply equally in the y and z directions, exchanging x for y or z and e for f or g, respectively.

For the black modules, T_{surr} was taken to equal the recorded globe temperature and an emissivity of 0.98 was used (Cengel, 2003). The aluminium modules were assumed to only interact convectively with the environment and so had an emissivity of zero. The convective heat transfer coefficient was calculated for all surfaces individually using Eq. 5.5:

$$Nu = \frac{hL_c}{k} \quad (5.5)$$

Characteristic lengths of 0.15 and 0.035 were used for the top/bottom and side surfaces, respectively. Nusselt numbers were calculated using Eq.s 5.6, 5.7 and 5.8 for the bottom, top and side surfaces, respectively.

$$Nu = 0.54Ra^{1/4} \quad (5.6)$$

$$Nu = 0.27Ra^{1/4} \quad (5.7)$$

$$Nu = \left\{ 0.825 + \frac{0.387Ra^{1/6}}{\left(1 + (0.492/Pr)^{9/16}\right)^{8/27}} \right\}^2 \quad (5.8)$$

A weighted average of 5.00 W/m²/K was found and applied to all surfaces equally; however validation was improved by applying heat transfer coefficients in the range 7 – 9 W/m²/K. These values are broadly consistent with converted surface resistances from ASHRAE: 6.25 W/m²/K and 8.33 W/m²/K for downward facing horizontal and vertical surfaces (Bagheri *et al.*, 2009).

Over the course of each charge simulation the free stream temperature was periodically altered to reflect the fluctuation in dry bulb temperature in the room. For the black modules this also applied to the globe temperature. The average of all thermocouple temperatures at the beginning of each charge period was taken to be the uniform temperature of a given module at the start of any charge simulation. Validation was achieved by comparison of measured thermocouple temperatures and the temperatures found at corresponding locations in the corresponding CFD models – see Figure 5.6.

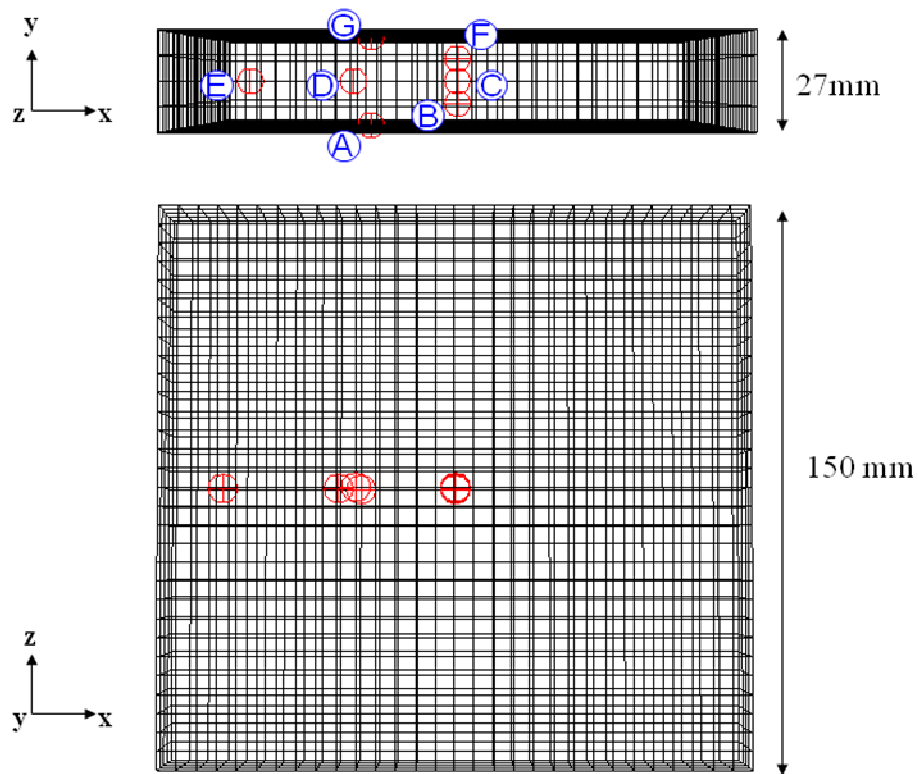


Figure 5.6 FLUENT mesh. A panel with point surfaces labelled and located so as to correspond with thermocouples in the actual modules.

It was important to validate the models to ensure that the generated profiles of average liquid fraction and total surface heat transfer rate could be taken to be true. The profiles were then used for performance comparisons.

The heat transfer rate profiles had a misleading number of sharp peaks resulting from the periodic changes in air and globe temperatures. The curve was smoothed out by taking the centrally occurring heat transfer values for each sub-period and disregarding the rest of the data.

5.2 Results

5.2.1 Validation

Fig. 5.7 shows the temperature and liquid fraction contours for the A22,Al,EC module at three stages in the charging process. The rise in both parameters can be seen to start from the corners and edges of the module. At 450 minutes the module has just achieved a liquid fraction of 1, when no region is below 22.44°C.

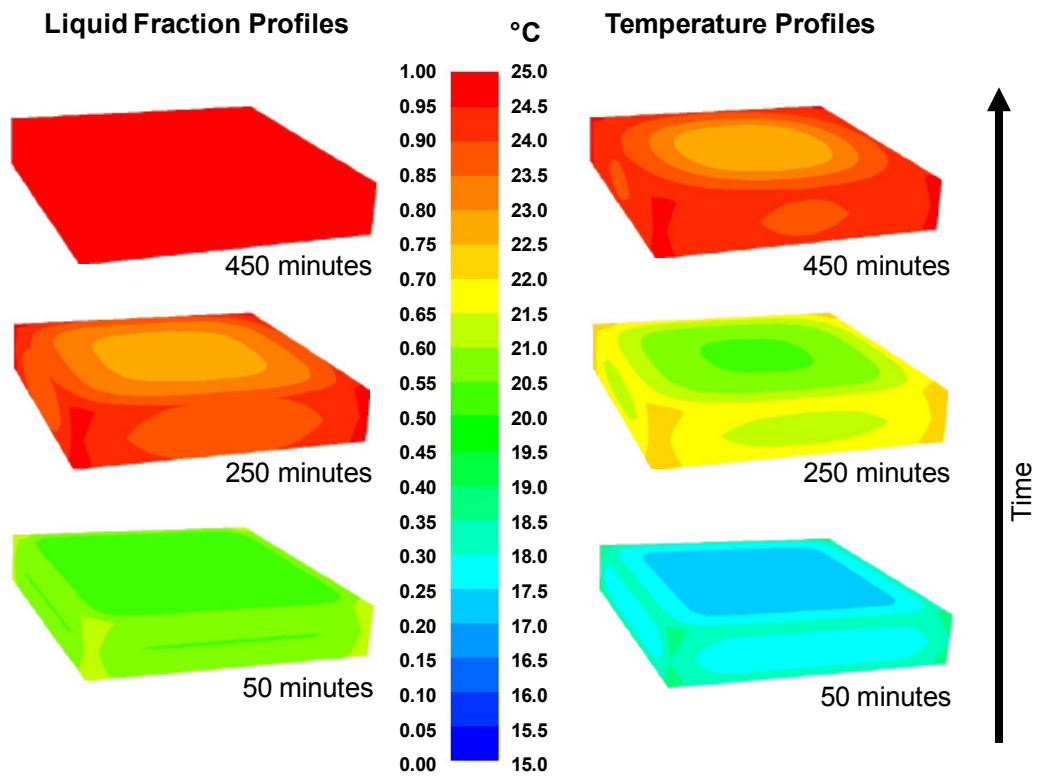
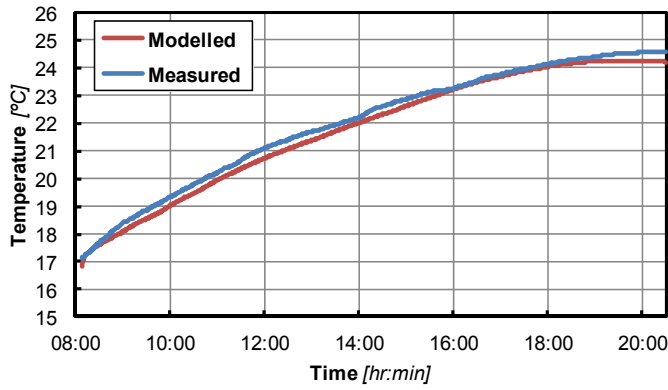


Figure 5.7 Contours of temperature. The A22,Al,EC module at three stages of heating. The progression of heat from the corners and edges towards the centre can clearly be seen. At 450 minutes the module is entirely melted. The air temperature at this is 25.17°C. Apart from a variation in minute number, the pattern of liquid fraction and temperature profiles is very similar for the other modules, so they are not presented here.

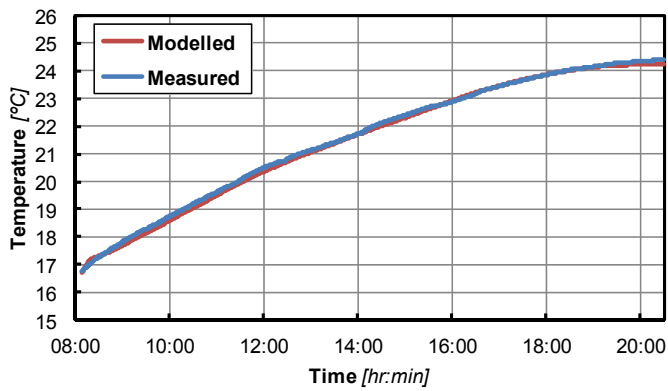
Validation curves for thermocouples A, B, C and D (see Figure 5.1 or Figure 5.6) are presented here. In most cases good validation of the models has been obtained, with some notable deviations. Figure 5.8 shows the modelled and measured temperature

profile of thermocouples in the A26,Al,EC module. A very close correlation may be observed. It is significant that the module's temperature range is almost entirely between the melt onset and melt end temperatures of the A26 PCM. The curve therefore indicates a simultaneous gain in sensible and latent heat. This contrasts with the curve in Figure 5.9, for the A22,Al,EC module, in which thermocouples B, C and D display good correspondence until the material reaches T_{liquidus} . Here the temperature immediately rises more rapidly and deviates a maximum 1.0°C from the measured values. This is because the model assumes a simple step function for the variation in heat flow to/from each element, rather than a smooth curve, as indicated in Figure 5.5. The limitation of the FLUENT solidification/melting solver is the transition between wholly sensible and partially latent heating/cooling processes.

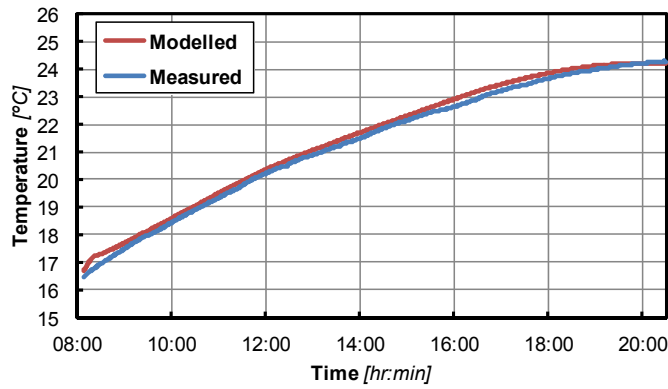
Figure 5.8 Model validation for A26,Al,EC. Thermocouples A, B, C and D. A convective heat transfer coefficient of $9 \text{ W/m}^2\text{K}$ was applied in the model for every 50 minute sub-period.



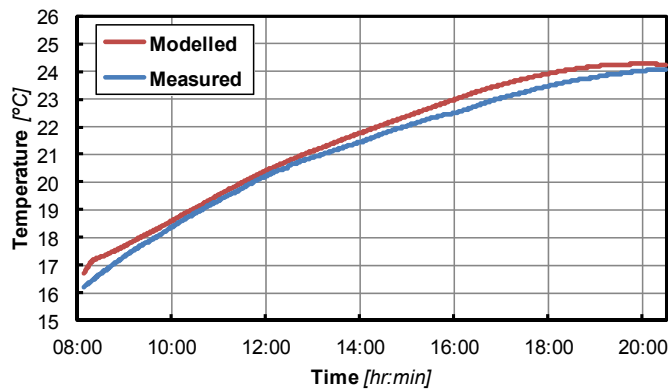
(A)



(B)

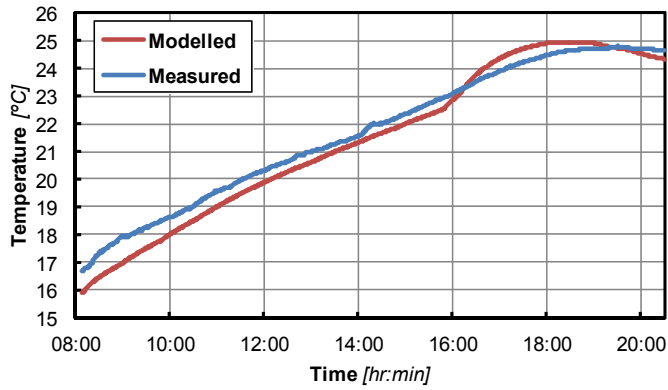


(C)

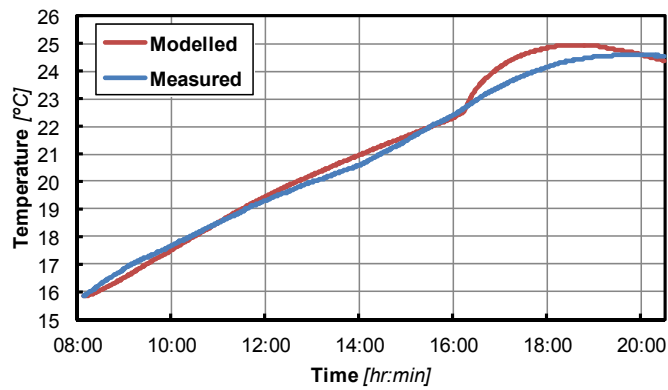


(D)

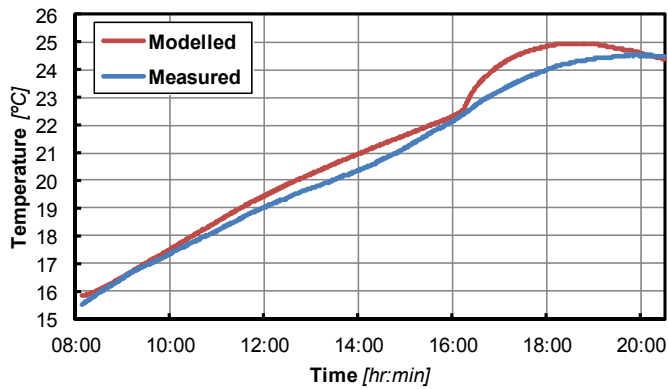
Figure 5.9 Model validation for A22,Al,EC. Thermocouples A, B, C and D. A convective heat transfer coefficient of $7 \text{ W/m}^2\text{K}$ was applied in the model for every 50 minute sub-period.



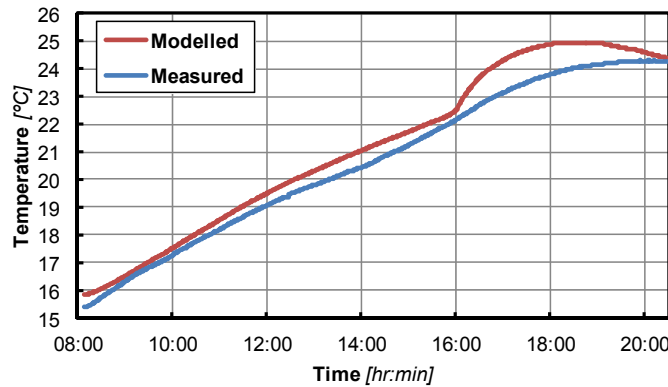
(A)



(B)



(C)



(D)

Figure 5.10 shows curves for the A22,Bl,EC module. Good correlation is observed and the same sharp rise as seen in Figure 5.9 is observed when the model reaches T_{liquidus} . The model curves then peak and fall at an earlier time and lower temperature than the actual module. This is most likely due to an additional localised radiant heat source acting upon the module, direct sunlight being a strong possibility as the module had a good view of the window.

Figure 5.11 shows good validation of the A22,Bl,IC model. Deviations are generally less extreme for the module cooled indoors because the air temperature variation is lower.

Figure 5.10 Model validation for A22,B1,EC. Thermocouples A, B, C and D. A convective heat transfer coefficient of $9 \text{ W/m}^2\text{K}$ was applied in the model for every 50 minute sub-period

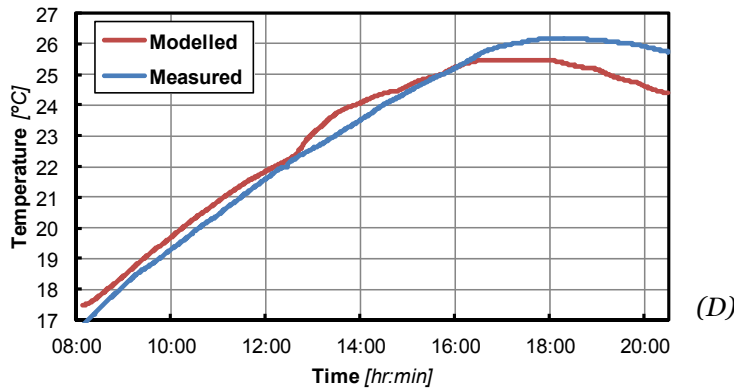
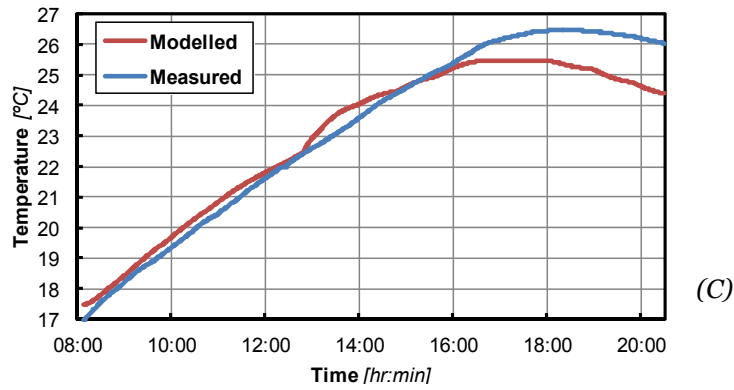
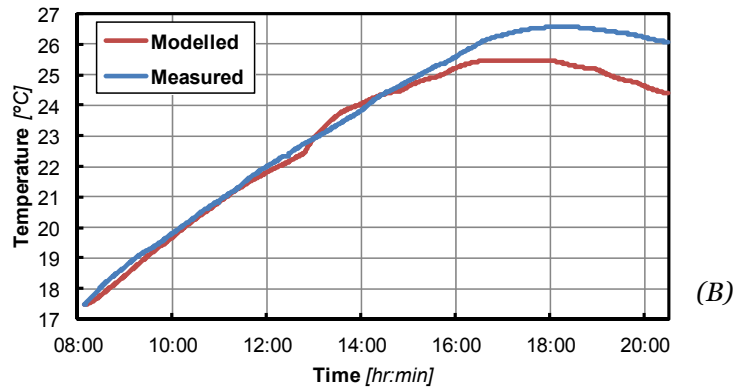
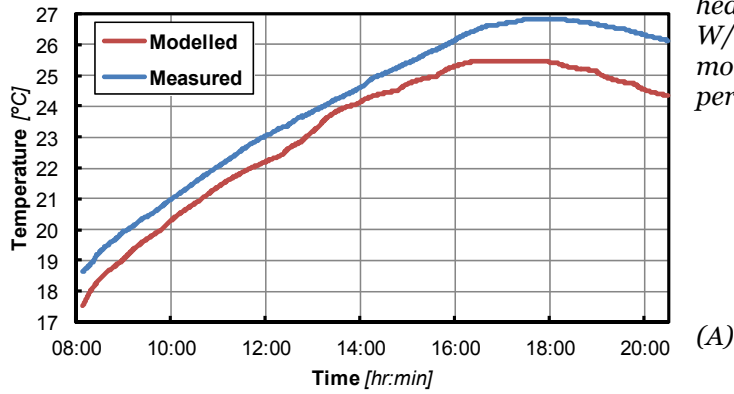
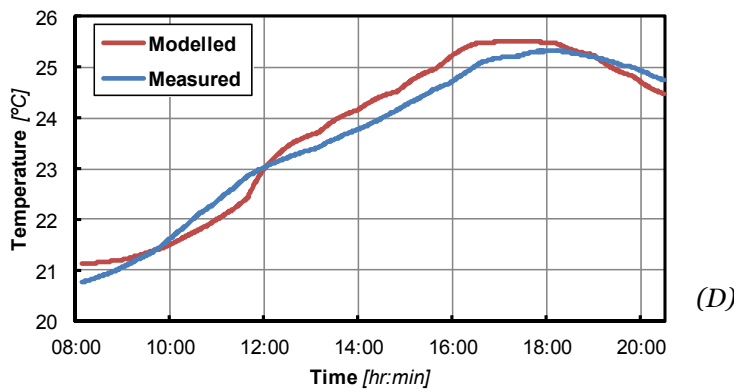
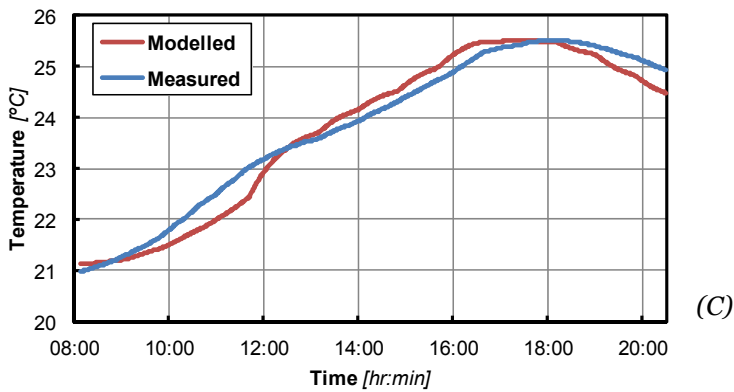
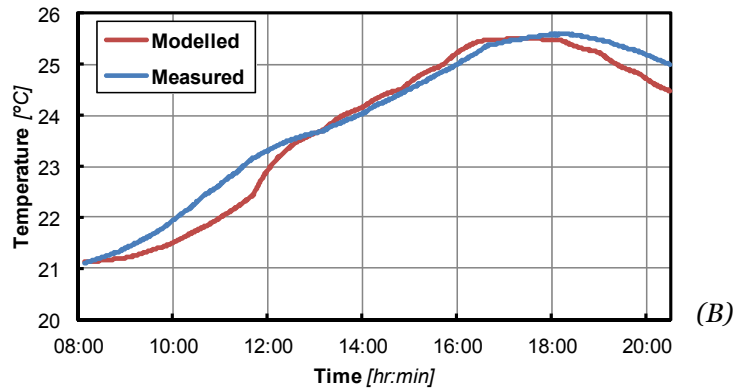
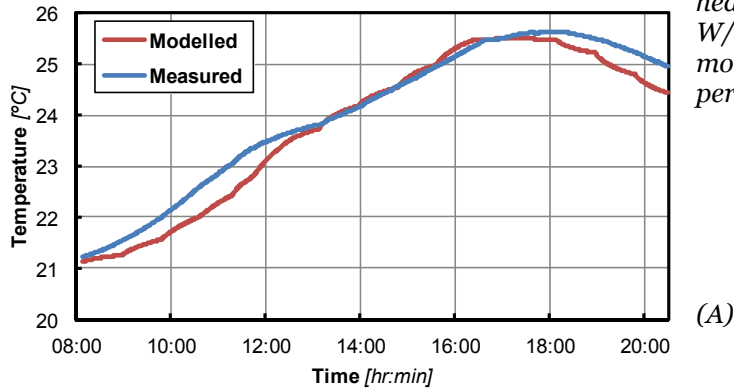


Figure 5.11 Model validation for A22,Bl,IC. Thermocouples A, B, C and D. A convective heat transfer coefficient of $7 \text{ W/m}^2\text{K}$ was applied in the model for every 50 minute sub-period.



5.2.2 Average Liquid Fraction and Surface Heat Transfer Rate Profiles

Profiles have been generated for a single charge period, from 8:08 am to 08:30 pm. The air and globe temperatures for this period are displayed in Figure 5.12.

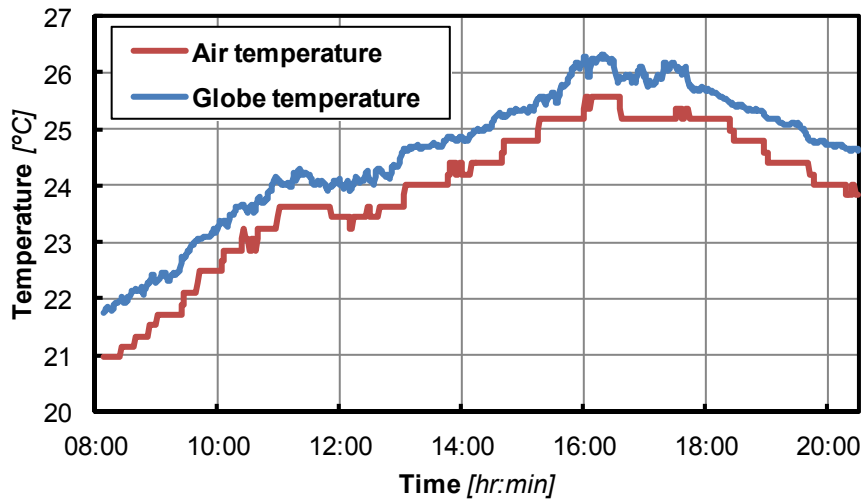


Figure 5.12 Internal air and globe temperatures. Period 8:08am to 20:30pm.

In general the results are best understood through comparison of two identical modules that differ in one respect - cooling location, surface material or PCM type. All modules were heated by the internal environment and so melted, at differing rates, over the course of the day.

Figure 5.13 shows the average liquid fraction profiles for the four panels. The A22,B1,IC module was already 88% melted at the start of the period, compared with 56% for the equivalent externally cooled module, A22,B1,EC.

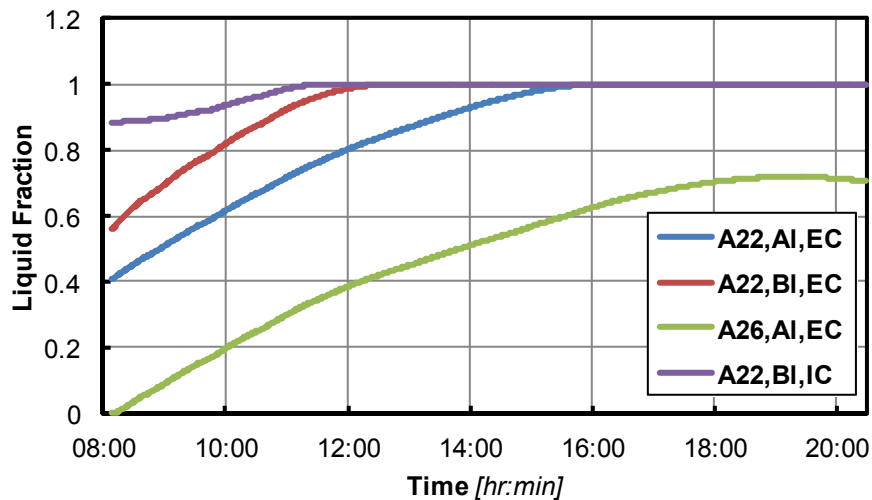


Figure 5.13 Average liquid fraction profiles of the four modules.

This indicates that the internally cooled module was unable to sufficiently reject heat during the previous night. Outside, a large amount of rain had fallen and temperatures had dropped to a minimum of 14.5°C , with maximum recorded wind speeds of 1.3 and 0.7 measured at 8:30 pm and 7:20 am, respectively. All this contributed to the higher heat rejection rate achieved by the externally cooled module. By contrast, no detectable air flow was measured around the internally cooled module and the temperature only dropped to a minimum of 19.8°C . This is because the room experiences a low ventilation rate at night, due to windows being closed for security reasons. In addition, significant heat gains resulted from eighteen computers, three printers and a refrigerator. At 11:42am the internally cooled module has completely melted and at 12:47pm so has the externally cooled module – i.e. the liquid fractions reach a value of one. After this, only sensible heating occurs.

The A22,Al,EC module was 41% melted at the start of the period; 15% lower than its black counterpart, A22,BI,EC. However, this difference is not due to the aluminium module achieving a higher heat transfer rate the previous night. It is due to the extremely rapid absorption of heat by the black module during the time that the modules were brought inside and set up for internal monitoring. This is supported by the high heat transfer rate seen in the black module at the beginning of the charge period (see Figure 5.14) and the fact that the black module had achieved a

lower temperature than the aluminium module at the end of the cooling period; 15.7°C and 17.6°C, respectively. The A22,Al,EC module became fully melted at 16:15 pm.

The partially molten state of the A22 modules at the start of the period is seen as a disadvantage of the material. At this time the surface temperatures (the warmest part of the modules) of the A22,Al,EC and A22,Bl,EC modules are 16.7°C and 18.6°C, respectively. The modules are significantly melted at temperatures below the thermal comfort zone (taken to be 20°C - 24°C). This behaviour can be explained with reference to Fig. 5.5 which shows the DSC results for the A22/LDPE composite. Here the substance is shown to start to melt at 11.22 °C (even lower in fact.) The portion that melts at temperatures below the thermal comfort zone either decreases the possibility of effective heat rejection at night (as in this case) or removes heat unnecessarily from the room. In both cases valuable storage capacity is not available for cooling. To minimize volume and weight of PCM, a material with a similar energy density and a transition zone more closely aligned to the thermal comfort zone, should be sought.

This problem applies similarly to A26 but here the excess capacity is found largely above the thermal comfort zone with the material becoming fully melted at 27.28°C. The A26,Al,EC module differed from its counterpart A22,Al,EC module (and the other modules) in that it was completely solid at the start of the discharge period due to its having a higher melt temperature. At the end of the period it is only 70% melted. The maximum room temperature was 25.56 °C, not high enough to fully melt the A26 despite being above the thermal comfort zone.

Figure 5.14 shows the surface heat transfer rates for the same charge period and modules.

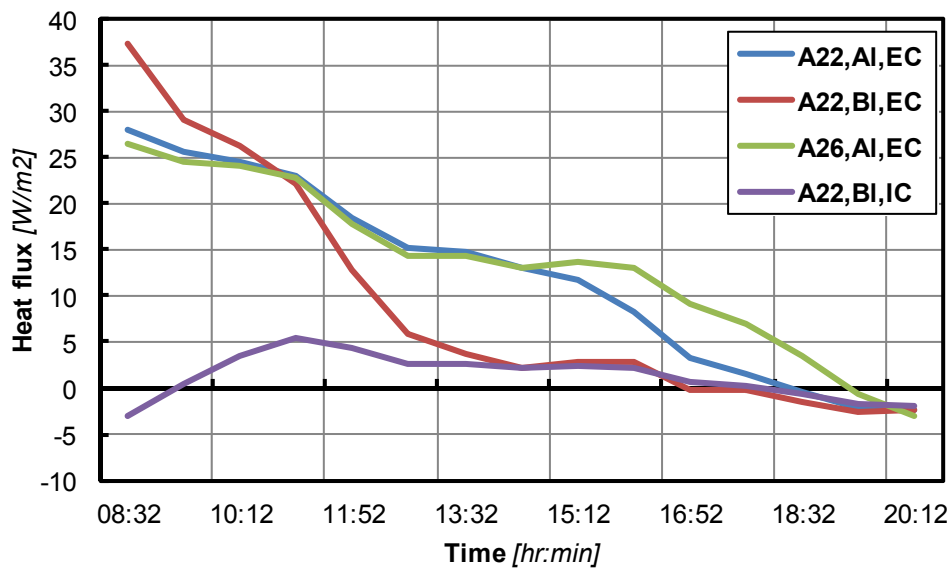


Figure 5.14 Surface heat flux profiles of the four modules. Positive values indicate heat flow into the module.

The general design conflict to be noted here is that as the temperature rises throughout the day, the cooling capacity of the modules fall. All start at a maximum and fall continuously due to increasing surface temperatures, apart from the A22,BI,IC module. At 8:32 this module is transferring heat at 3.25 W/m² rising to 12.22 W/m² at 10:12 due to increasing globe and air temperatures. This is only possible because it begins the period with such a small temperature difference with its environment. The higher heat fluxes achieved by the externally cooled modules are more desirable for a cooling system, with values of 37.33, 27.93 and 34.47 W/m² achieved initially for the A22,BI,EC, the A22,Al,EC and the A26,Al,EC modules, respectively. The A22,Al,EC exhausts its capacity so quickly that from 14:22 onwards it is transferring heat at the same rate as its internally cooled counterpart. This rapid heat transfer is why it completely melts so early. It should be noted, however, that a full scale installation would hold the internal temperature down and so produce a more level heat flux over time.

The A22,Al,EC module starts at a lower heat flux than its black counterpart, A22,BI,EC, but by 11:52 is transferring heat at higher rate because of its lower temperature. The higher heat flux is due to the black module's radiant interaction with the environment. The aluminium module has negligible radiant interaction.

Because the black module heats up quicker, its heat exchange rate falls quicker due to a lower temperature difference between the surface and the surroundings. In this instance the aluminium module appears to function more desirably as it maintains a higher heat flux for most of the period; particularly during times of peak temperature.

The A26 module maintains the most steady heat flux because of its negligible radiant interaction with the environment and the fact that it never exhausts its latent heat capacity. In towards the end of the day it is transferring heat faster than its A22 counterpart due to the A22,Al,EC exhausting all of its latent heat capacity, causing it to hasten towards thermal equilibrium with the room.

5.3 Conclusions

The modelling method proved effective with good validation obtained in most cases; however a limitation in the FLUENT solver was revealed when significant deviations were observed between model and reality when the model reaches an average liquid fraction of 1.

The generated average liquid fraction profiles and total surface heat transfer rates provide a clear basis for comparison of module performance and several conclusions were reached:

The A22 material was shown to melt at excessively low temperatures, causing much of its thermal storage capacity to either not be accessed, in cases when not all heat can be rejected at night, or exhausted unnecessarily by removing heat from the room at low temperatures. This problem exists in the opposite way for the A26 material because it cannot fully melt, even at temperatures above the comfort zone.

The A22,BI,EC module transfers heat and exhausts its latent storage capacity quicker than the equivalent aluminium-covered module, A22,Al,EC, which maintains a more steady heat transfer rate, showing radiant interaction to be a significant element in the heat transfer to the modules.

The A22,BI,IC transferred far less heat and became fully melted earlier than its externally cooled counterpart. This highlights an opportunity to greatly increase

heat rejection through the transport of PCM modules outside at night and highlights the need for effective ventilation, should the modules remain inside
All modules' surface heat fluxes declined significantly, reaching zero W/m² before the end of the charging period. This must be avoided in a full scale system to ensure cooling is achieved throughout the day.

These conclusions fed into the design and modelling of the NewMass system described in chapters 7 and 8.

References

- Bagheri, H.M., Bansal, P.K., Coad, W.J., Fulk, K.M., Hittle, D.C., Wells III, J.W. and Yuill, D.P. (2009) *2009 ASHRAE Handbook: Fundamentals*, SI edn, ASHRAE, Atlanta.
- Cengel, Y.A. (2003) *Heat Transfer: A Practical Approach*, 2nd edn, McGraw-Hill, New York.
- Cheechern, T. (2009) *The Application of the Shrinking Core Model to Phase Change Materials (Masters Dissertation)*, Brunel University, Uxbridge.
- DuPont (2010) *Energy Management*. Available:
http://energain.co.uk/Energain/en_GB/benefits/energy_management.html
[01/11/2011].
- Ilkzell (2010) *Ilkatherm Ceiling*. Available:
http://www.ilkzell.de/en_baudecke.php [21/02/2010].
- Phase Change Material Products Limited (2009) *PlusICE Phase Change Materials*. Available:
http://www.pcmproducts.net/files/plusice_range_2007_hydrates.pdf
[26/07/2010].

Phase Change Material Products Ltd (2010) *PlusICE Phase Change Material Passive Cooling Products*. Available:
http://www.pcmproducts.net/files/passive_cooling_catalogue-2010-1.pdf
[23/09/2010].

PRODUCT TESTING

A thermal test cell was designed and constructed to test PCM cooling systems in a controlled environment. The cell was ultimately used to test the NewMass prototype system but prior to this two product tests were conducted. The Energain panel (DuPont, 2007a) and the RACUS ceiling tile (Datum Phase Change, 2011) are both commercially available passive PCM products. Energain panels are probably the most commonly known PCM building product and have been available for several years. They were developed by DuPont, who have sought to promote the panel's capacity to be simply installed behind plasterboard on walls and ceilings without the need for extensive training or alteration of existing fit-out procedures.

They are supplied in 1 x 1.2 m, 5.26mm thick units and are similar to the A22 panels used in the Passive PCM Sails tests. Formed of a shape-stabilised paraffin/copolymer composite (60% paraffin, 40% copolymer, by weight) and covered with thin aluminium sheeting it is designed to be cut to size in order to fit any wall or ceiling (DuPont, 2007b). This ease of utility is a considerable benefit for the product however the RACUS ceiling tile, released within the last two years, may lay reasonable claim to being even easier to install. The 600 x 600 x 15 mm tiles are formed from 1 mm gauge mild steel and hang from a typical false ceiling grid for cooling of internal environments, typically offices. The shallow tray that is created by the shape of the tile is filled with a composite material composed of BASF micronal capsules and a patented binder. The capsules are around 5 µm across and contain paraffin that melts around 23 °C (Micronal also comes in varieties which melt at 21 and 26 °C) (BASF, 2011). The tiles are available in various concentrations of micronal.

Energain panels have been subjected to extensive testing including academic studies by Kuznik and Virgone (Kuznik and Virgone, 2009), for instance, in which

the decrement factor with Energain panels installed in a full scale test was 0.79, as compared to a control test. RACUS ceiling tiles have also been subjected to monitoring but results are only available through informal communication with Datum Phase Change. Independent academic studies are not known about. In fact the tests presented here were seen as an opportunity for Datum Phase Change to better understand and promote the product. Some details of the test cell and the results gained may be found on the RACUS website <http://www.datumphasechange.com> (Datum Phase Change, 2012).

The tests presented in this chapter may be of interest for several reasons. Firstly, they present independently acquired results of a hitherto unstudied PCM product, RACUS ceiling tiles. Secondly, conducting both product tests under the same conditions allows direct comparison between the products; this has not been seen before. RACUS tiles and Energain panels are both passive paraffin-based products, with similar phase transition zones, which may be easily installed but have crucial differences in terms of containment and where they may be located in a room. It is also worth noting the fact that two of the world's leading chemical giants, DuPont and BASF have invested in PCM technology with significantly different products emerging as a result; BASF producing what is essentially a base composite material, which is then procured by other companies for incorporation into other products, and DuPont producing a simple but targeted final product. This chapter presents tests that compare the two.

Results show that the Energain panels had the lowest peak temperature and would save the most energy. However, the RACUS tiles, which performed similarly to each other, had more effect per unit mass of PCM used. They also rejected their accumulated heat more effectively than the Energain panels due to their increased exposure to the passing cool air.

6.1 Test Cell

The test cell concept is as follows: One space to represent a building, containing a heating or cooling system, itself contained within a larger space that represents an external environment – see Figure 6.1.

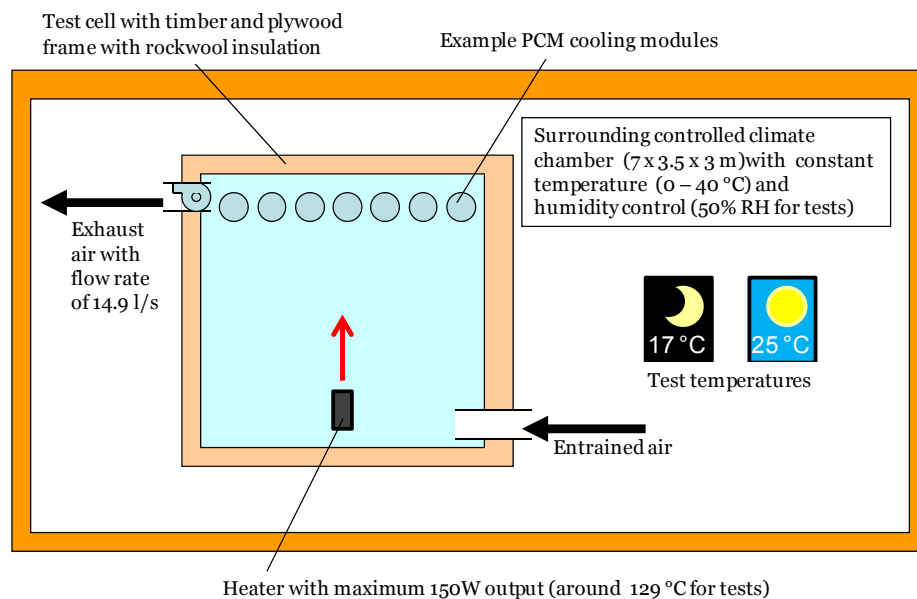


Figure 6.1 Conceptual schematic of the thermal test cell. Located inside the climate chamber at the Brunel University refrigeration laboratory.

It was designed to have the maximum internal volume possible, whilst being able to move in and out of the environmental chamber as required. Maximising the size of the test cell meant that real room conditions were as closely replicated as possible. The size of the cell affects the internal conditions in two important ways: The surface area to volume ratio of the space and the stratification of air in the space. In general, the smaller the volume, the larger the surface area to volume ratio. The larger the surface area the greater the heat loss or gain through the fabric and in the case of the Energain panel the more can be applied for the same volume to be cooled. Maximising the cell size brings its fabric heat transfer and surface area available for wall board application more closely to alignment with that of a real occupied space.

In the NewMass tests comprehensive test cell air monitoring was used to assess the stratification and convection cycle established. The air in a room will stratify if air flow rates are low enough but the effect will be less pronounced in smaller volumes. Any stratified fluid in a closed system will achieve thermal equilibrium, provided there is no internal heat source. This signifies a loss of stratification. In a stratified fluid the mode of heat transfer that drives it toward equilibrium is conduction. In a small volume, without much height, heat from the upper layers of warm fluid will be conducted through to the lower layers quicker

because it has less distance to travel. A greater height will mean a more prolonged stratification effect and this brings the cell closer to mimicking the effect on contained air in a real building.

Figure 6.2 displays images of the completed cell within the environmental chamber.



Figure 6.2 Images of the thermal test cell. The cell heater being checked whilst the externally located data loggers and thermocouples are labelled (left). The cell with its door open and laptop for data logging (right).

6.1.1 Construction and Dimensions

The cell was a timber frame construction, covered with plywood on the exterior, plasterboard on the interior and cavity wall insulation between. The insulation was Knauf Dritherm cavity slab 37 standard (slab) insulation; 100mm thick with a resistance of $2.25 \text{ m}^2\text{K/W}$. The cell had a window to allow a view of the interior when in operation and four industrial castors so it could be moved into position with relative ease. Figure 6.3 displays an axonometric representation of the cell with its main features and the wall build up.

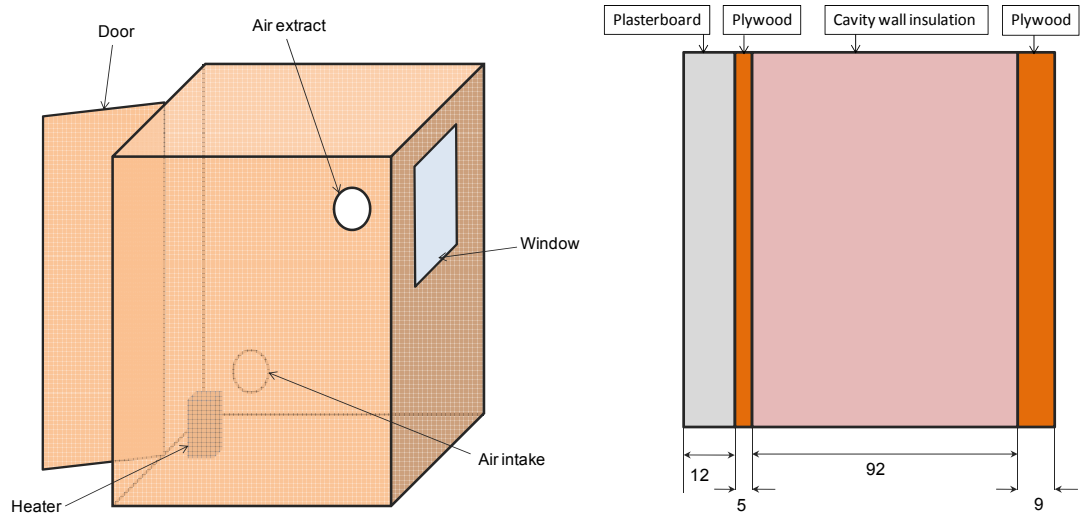


Figure 6.3 The test cell with heater, ventilation intake and extract, window and door (left). The wall build up; all dimensions in mm (right).

Figure 6.4 displays the dimensions and locations of all elements.

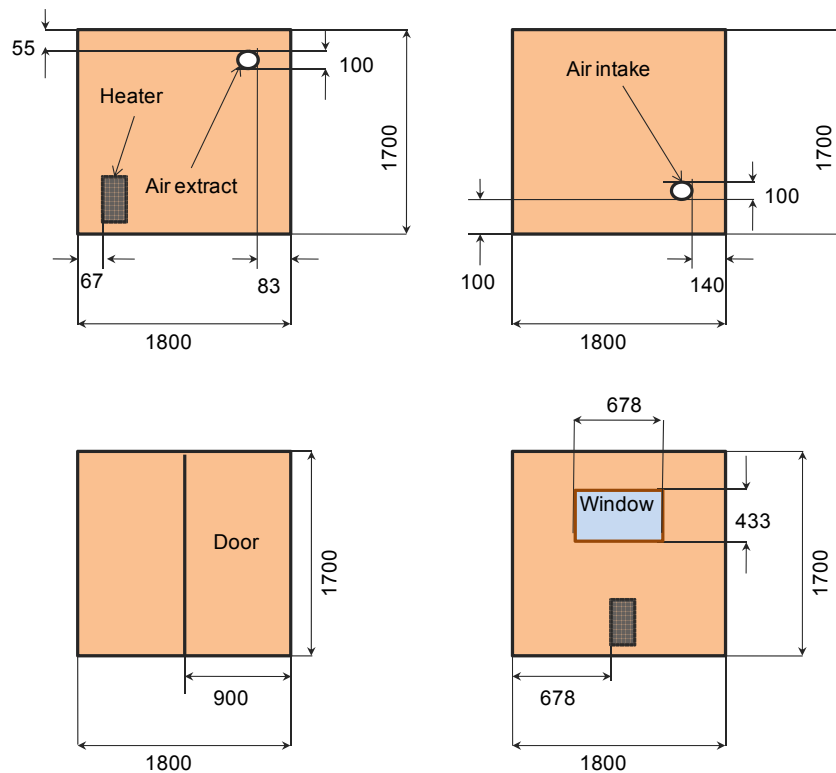


Figure 6.4 Test cell element locations and dimensions in mm.

6.1.2 Features

In its capacity as a representation of a building the test cell was fitted with a heat source and ventilation provision. CIBSE guide A provides benchmark values for heat gains in UK office buildings:

- Solar gains should be 60 – 90 W/m²
- Lighting gains should be 12 W/m²
- People (assuming 12/m² according to cibse guide a) are 6.7 W/m²
- Internal casual gains should be 15 – 25 W/m² (Arnold, 2006)

If it is assumed that solar and lighting gains do not occur concurrently a peak heat gain range of 200 – 298 W results. The building regulations 2006 L2A guide for commercial new-builds states that the average combined solar and internal gains should be not greater than 35 W/m² between 6:30 am and 16:30 pm on average (HM Government, 2006). For the test cell area this gives a value of 86W. A real building will experience a profile of heat gains rising and falling between minima to maxima. For the test cell it was decided that a constant heat gain would be applied, to mimic internal and solar gain, in order to simplify the experimental procedure. Therefore a heat source was needed that supplied at a rate part way between the average and peak values just quoted. The heater selected was an Omega CS060 150W enclosure heater. Its heating capacity varies with ambient temperature and this relationship is displayed in Figure 6.5. By knowing the test cell air temperature the exact heat output could be determined. This was important for detailed heat transfer analysis carried out in chapter 8. At a test cell air temperature of 25 °C the heater provides 129W of power.

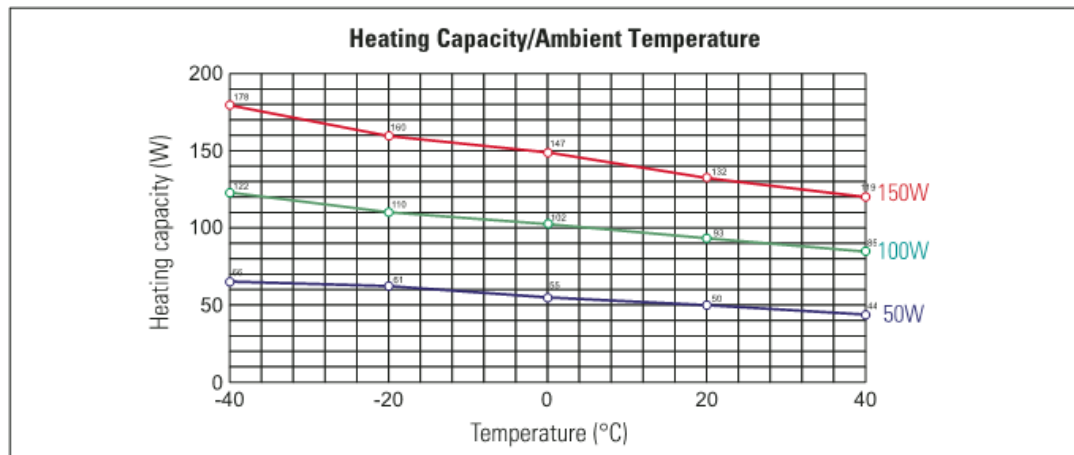


Figure 6.5 Variation in heating capacity of the test cell heater with ambient temperature (Omega, 2011). The red line refers to the model used.

This was judged to be a reasonable compromise between the average and peak values just quoted. (In fact the average of 86 W and 200 W is 143 W, suitably within the heaters range of output.)

The fan used in these tests was primarily present to pass air through the cell for discharge of the PCM's heat at night but because the test cell is supposed to function similarly to a building of that scale the ventilation rate achieved had to be within a realistic range. Building ventilation rates are dictated by the requirement to replace contaminated or polluted air with fresh air. In most buildings this is specified on the basis of carbon dioxide content since this is a gas which human beings produce and which becomes harmful in concentration. CIBSE guide A gives a high indoor air quality ventilation requirement of 20 l/s/person. Assuming an office with 12 m²/person the test cell's fresh air requirement would be 3.1 l/s (Arnold, 2006). However if at any time occupant concentration rose to a realistic level of 3 m²/person then a fresh air requirement of 16.3 l/s would result. The extract fan selected was an XIL 100T Xpelair fan, capable of a maximum extract flow rate of 14.9 l/s. This was able to draw air through the lower level entry duct, through the cell and then out at high level.



Figure 6.6 Test cell features. The heater Omega CS060 150W enclosure heater (left) and the XIL 100T Xpelair cell extract fan (right).

Both the heater and the fan were connected to mains power whenever their operation was required. Power cables were fed through a small conduit to allow either item to be engaged whilst the cell was sealed for testing. The ventilation outlet and inlet had caps to prevent undesired air flow during the charging tests. The heater was mounted on an aluminium bracket and heated the surrounding air by natural convection, drawing it in from beneath, across the internal heated plates and then out through the perforated grill at the top.

The cell was designed to allow comprehensive temperature monitoring of its contents. To this end 8 port Pico USB TC-08 thermocouple data loggers were fixed to the external facade and then to an externally located laptop. This allowed internally located type k thermocouples to be placed around the cell and for their wires to be fed through the aforementioned cable conduit and into the data loggers. The pico logging software allowed the laptop to log data from all 40 channels (5 loggers with 8 ports each), minute by minute, for as long as the particular test being run was required to last. The full extent of the logging potential was exploited in the NewMass testing; see chapter 8. The RACUS and Energain tests presented here provide a much smaller number of measurements.

6.2 Method

The product tests conducted in the test cell, as far as possible, followed the same procedure, under the same conditions, with the same parameters being monitored. The climate chamber allows a dry bulb air temperature to be set, adjusting heat or coolth input in response to a thermostat as necessary. For the tests presented here two temperature regimes were established in the climate chamber surrounding the test cell. During the daytime a constant temperature of 25 °C was applied and during the night a constant temperature of 17 °C was applied, each corresponding to average maximum and minimum UK summer temperatures.

Inside the test cell the heater was engaged on full power at the same time as the climate chamber temperature was switched from 17 to 25 °C, signifying the start of a daytime “charging” session. During charging the fan would be disengaged and the inlet and outlet ducts would be capped to prevent air flow. This was done at 9:00 am in the morning. At 5:00 pm in the afternoon a “discharging” session would begin when the climate chamber temperature would be switched back to 17 °C, the heater would be turned off and the fan would be engaged with the inlet and outlet duct caps removed.

This procedure was carried out for each of the product tests. The charging period would raise the temperature of the cell and some heat would be absorbed by the PCM units contained within. To observe the cooling effect that the PCM had on the room temperature profiles were compared to those obtained from a control test conducted under the same conditions without PCM units installed. When the discharging period occurred the PCM units were able to discharge their heat. A control test for this period was also carried out.

To monitor what was occurring in the test cell under these conditions thermocouples were located at 60 cm below the ceiling in the test cell and embedded within the PCM units. Temperatures were recorded at 1 minute intervals.

It is important to explicitly state the division of work and responsibilities during the design and conducting of these tests. The test cell design was orchestrated and largely carried out by me with assistance on the detailed fabric design and

construction from a timber frame builder and assistance with the selection and procurement of test cell features from Brunel Masters students.

I designed the test procedure in detail but the day to day running of the tests was conducted by Masters students, members of what is referred to in this thesis as the Brunel PCM research group.

The procurement and installation design of the PCM products was carried out by me in consultation with the suppliers DuPont and Datum Phase Change.

6.2.1 RACUS ceiling tiles

Two types of RACUS tile were tested: One filled with RACUS 73 formula and the other with RACUS 74 formula – see Figure 6.7.

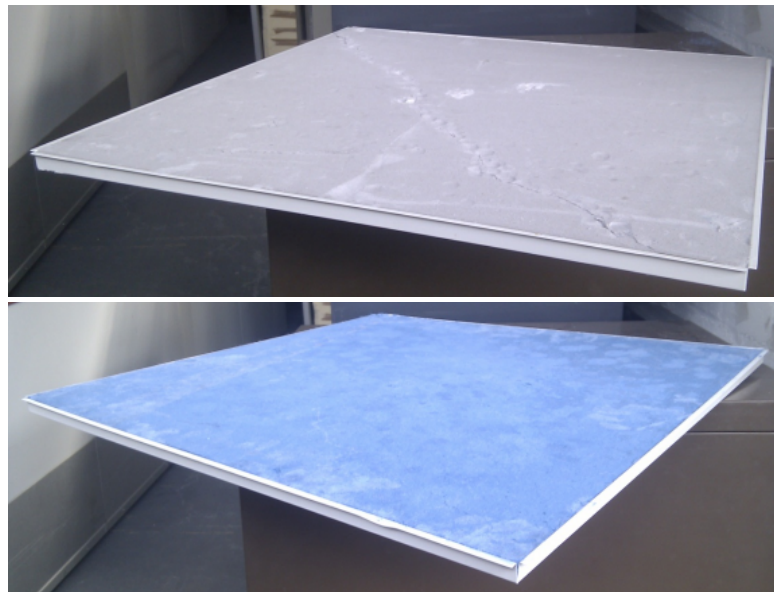


Figure 6.7 Tile with RACUS 73 (top) and tile with RACUS 74 (bottom) (Oyeleke, 2010).

RACUS 73 contains 50% micronal by mass and RACUS 74 contains 70% micronal by mass. James Oyeleke (Masters student) performed DSC analysis on samples of both compounds to determine the thermophysical properties detailed in Table 6.1 Thermophysical properties of micronal and RACUS formulations and earlier described in the literature review.

Table 6.1 Thermophysical properties of micronal and RACUS formulations (Oyeleke, 2010).

PCM formulation	Freeze onset temp (°C)	Melt onset temp (°C)	Melt peak temp (°C)	Freeze peak (°C)	Specific heat capacity (kJ/kg/K)
Micronal	21.85	23.23	24.67	20.44	1.85
RACUS 73	21.97	23.24	24.42	21.16	2.04
RACUS 74	21.86	23.23	24.89	20.81	1.72

The latent heats, micronal concentrations, densities and resultant latent heats per unit volume are displayed in Table 6.2.

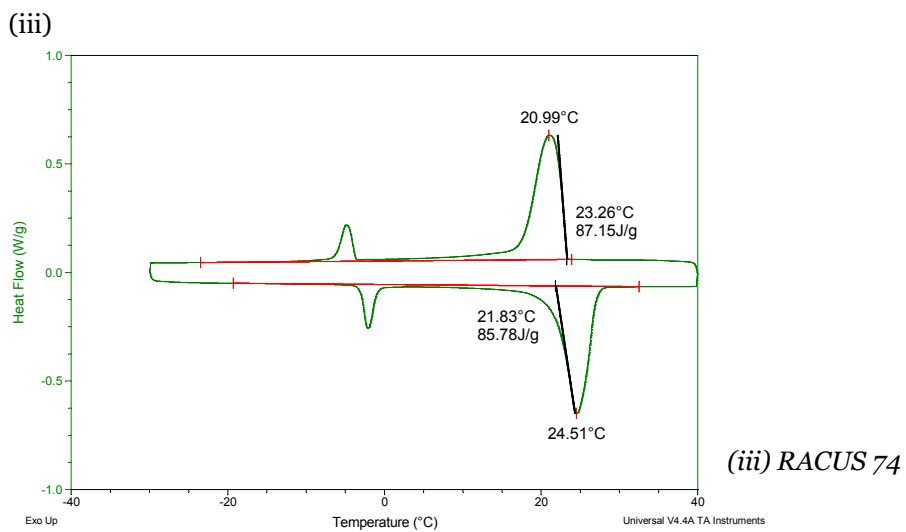
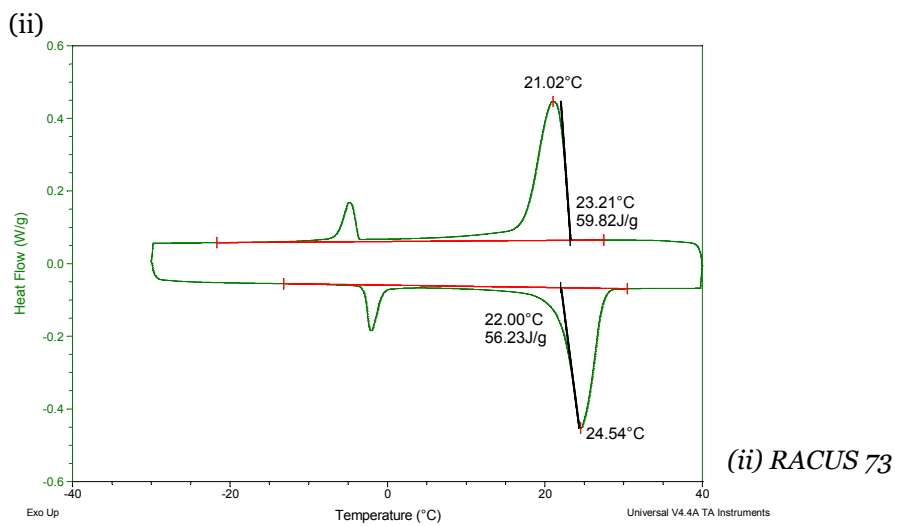
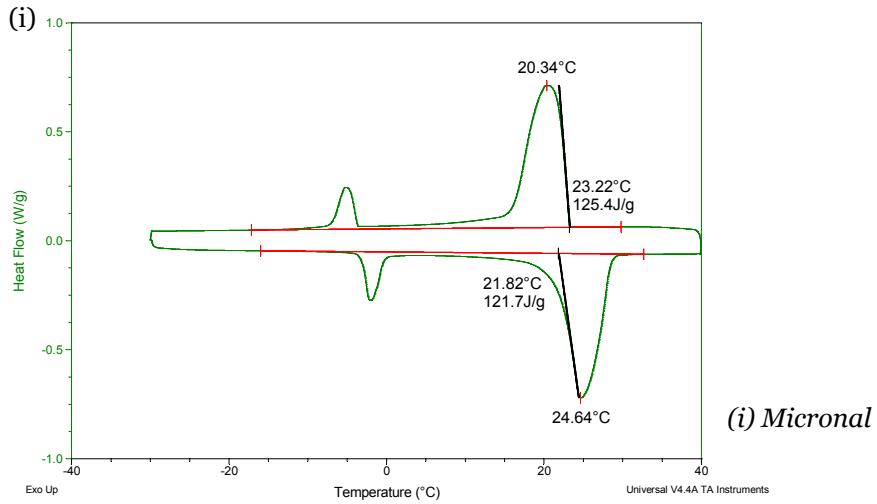
Table 6.2 Further properties of Micronal and RACUS. Latent heats (Oyeleke, 2010), concentrations by weight (Underwood, 2011), densities (Underwood, 2011) (BASF, 2011), and calculated latent heat per unit volume.

PCM formulation	Latent heat (kJ/kg)	Concentration Micronal by weight (%)	Density (kg/m ³)	Latent heat per unit volume (kJ/m ³)
Micronal	122.5	100	300	36750
RACUS 73	60.13	50	802	48220
RACUS 74	85.57	70	569	48690

It should be noted that despite the differences in micronal concentration the latent heat per unit volume is almost the same for the 73 and 74 formulations. The binder allows for a denser formulation and so increased binder content actually increased the content of the micronal as well.

The characteristic DSC curves for pure micronal, RACUS 73 and RACUS 74 are displayed in Figure 6.11.

Figure 6.8 DSC Curves for micronal, RACUS 73 and RACUS 74



The tiles were custom made to fit the test cell and arranged as shown in Figure 6.9. Upon production the supplier embedded 4 thermocouples within the central tile for each formulation to allow temperature monitoring – see same figure.

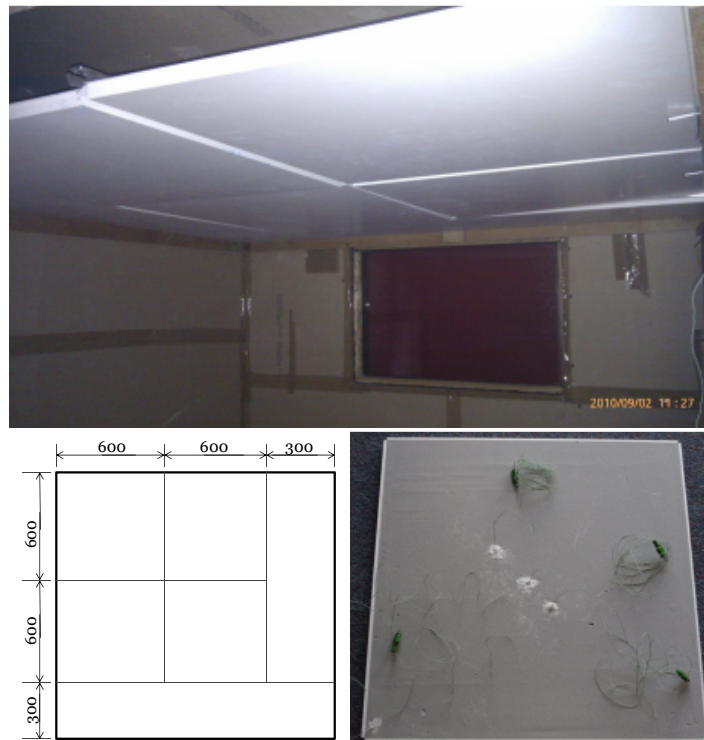


Figure 6.9 The RACUS test cell installation. Ceiling grid installation photo (Oyeleke, 2010) (top), ceiling grid layout in mm (bottom left) and RACUS tile with embedded thermocouples (right).

In total 26.66 kg and 18.92 kg of pure RACUS 73 and 74 were installed, respectively. This amounted to 13.33 kg and 13.24 kg of micronal in each respective case.

6.2.2 *Energain Panels*

Panels were obtained in sufficient quantity to cover all internal walls and the entire ceiling in the test cell. Adrien Capitani (university exchange student) installed the panels by removing the test cell's plasterboard, cutting the panels to size, screwing them into the timber structure and then replacing the plasterboard. The entire area

of the cell walls and ceiling (not the floor), minus the area occupied by the window and the ventilation inlet and outlet ducts, was covered with the panels; 12.77 m² in total. This equated to 60.46 kg in total. As stated earlier, Energain has a paraffin content of 60% which means that the total paraffin content of the installation was 36.27 kg.



Figure 6.10 Energain panels applied to the internal surfaces of the test cell.

To monitor the internal temperature of the panels thermocouples were inserted by pushing the tips into the soft composite material (in much the same way as thermocouples were inserted into the surface of the passive sail modules in chapter 5.)

Capitani performed DSC analysis on samples of the Energain panels and on the contained paraffin which was extracted by soaking slices of the panel in propan-2-ol, causing the contained wax to dissolve and separate from the copolymer.

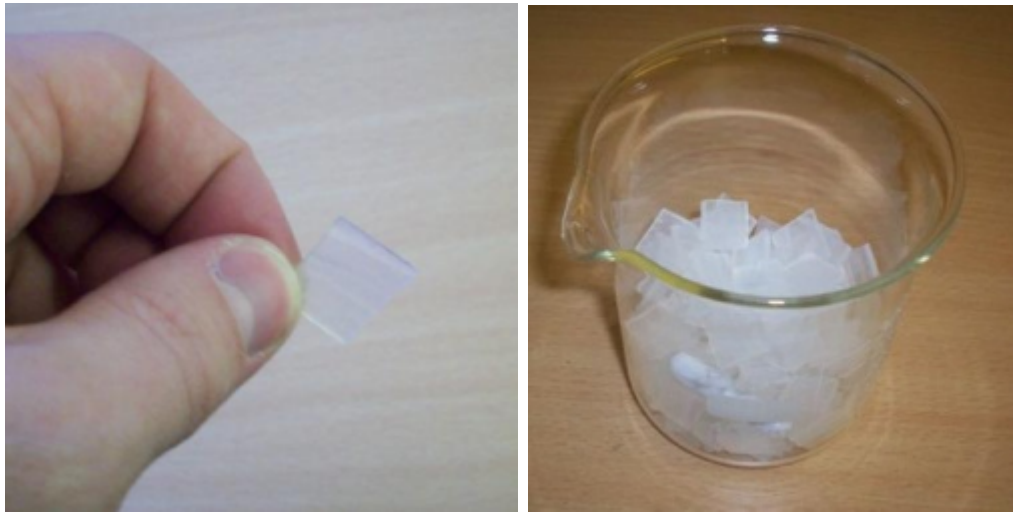


Figure 6.11 Paraffin extraction. A slice of the Energain panel (left) and slices in propan-2-ol for paraffin dissolution (right) (Capitani, 2011).

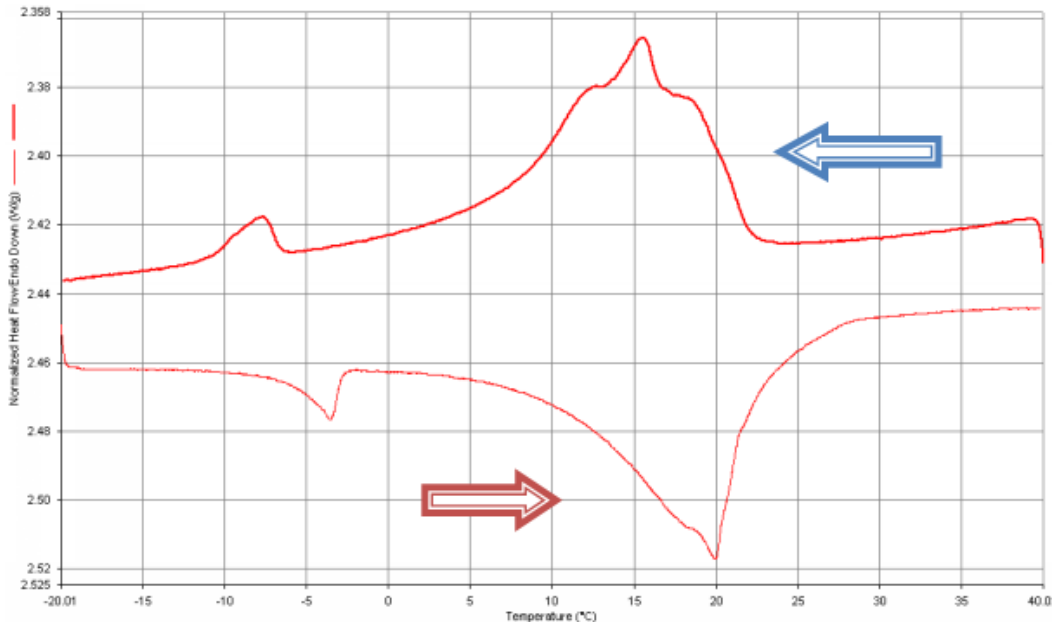
The thermophysical properties found are presented in Table 6.3 and Figure 6.12.

Table 6.3 Thermophysical properties of Energain panel and pure constituent paraffin (Capitani, 2011).

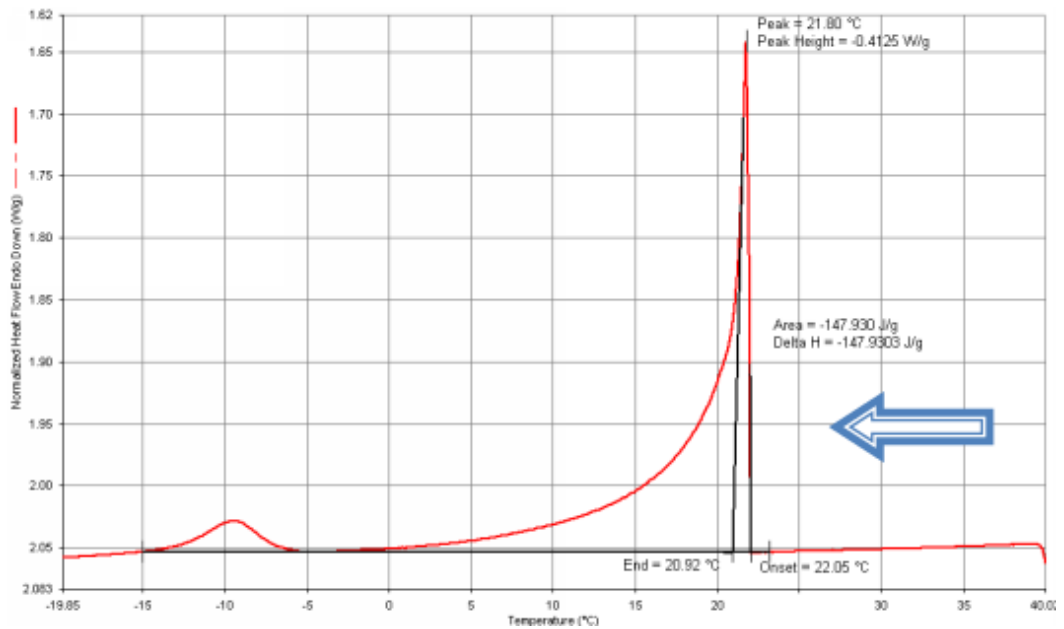
PCM	Latent heat (kJ/kg)	Melting onset temp (°C)	Melting peak temp (°C)	Freezing onset temp (°C)	Freezing peak temp (°C)
Energain panel	73	8.64	19.98	22.44	15.55
Energain pure	151.6	16.51	22.45	22.05	21.8

Figure 6.12 DSC curves for Energain panel and pure constituent paraffin.

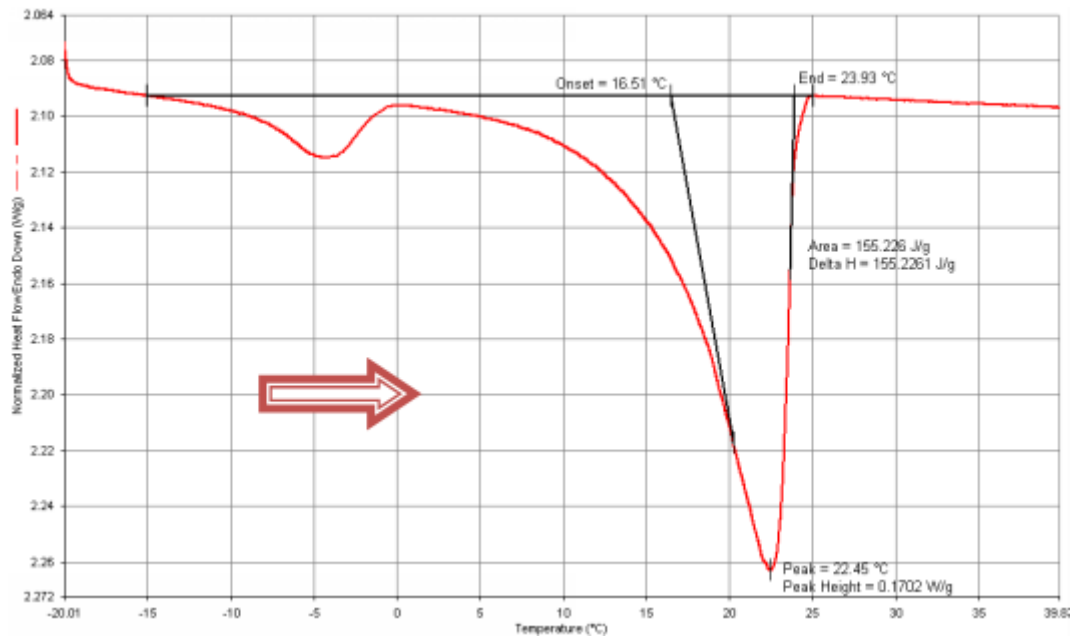
(i) Energain panel material.



(ii) Freeze curve of pure Energain paraffin.



(iii) Melt curve of pure Energain paraffin.



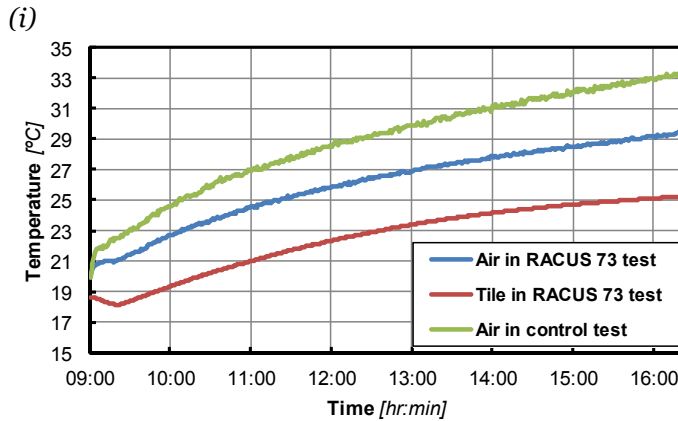
It is clear from Capitani's work that the combination of the paraffin with the copolymer has a significant effect on the melt and freezing peak temperatures with shifts of several °C in both cases.

The following section details the results found from the thermal test cell experiments.

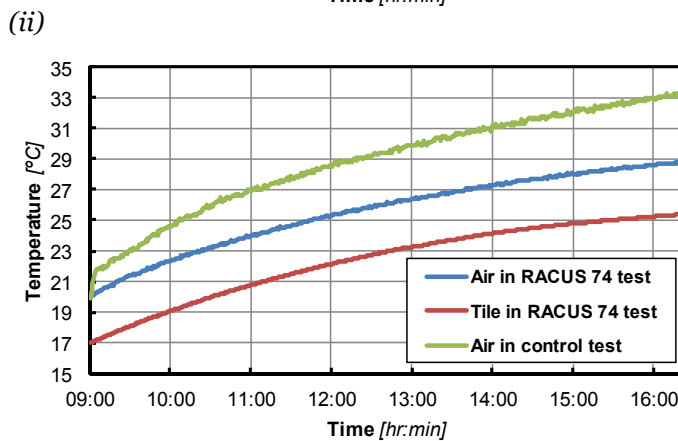
6.3 Results and discussion

Figure 6.13 displays the results of the charging test for all products. Each graph displays the temperature of the air at 60cm below the ceiling in the centre of the test cell for both the control and the product test. In the same graph the temperature of the PCM product installed is given.

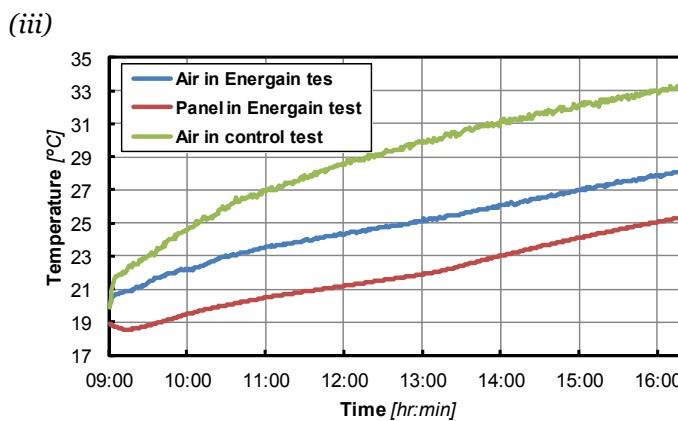
Figure 6.13 Charge periods. Product air, product PCM and control air temperatures.



(i) Temperature profiles for RACUS 73 tiles and control



(ii) Temperature profiles for RACUS 74 tiles and control



(iii) Temperature profiles for Energain panels and control

It is clear that at the outset that the air temperatures for the control and product are equal. However, in each case the control air temperature rises more rapidly than in PCM product cases. This demonstrates that all of the units have a significant effect cooling effect, reducing the peak temperature reached by several degrees. At the

same time the temperature of the PCM units may be seen to rise. This behaviour is similar to that observed in chapter 5; instead of reaching a phase change temperature and flattening off we see a continual rise in temperature as the contained PCM gradually changes phase.

Figure 6.14 displays all air temperature curves on the same graph for direct comparison between all products and control.

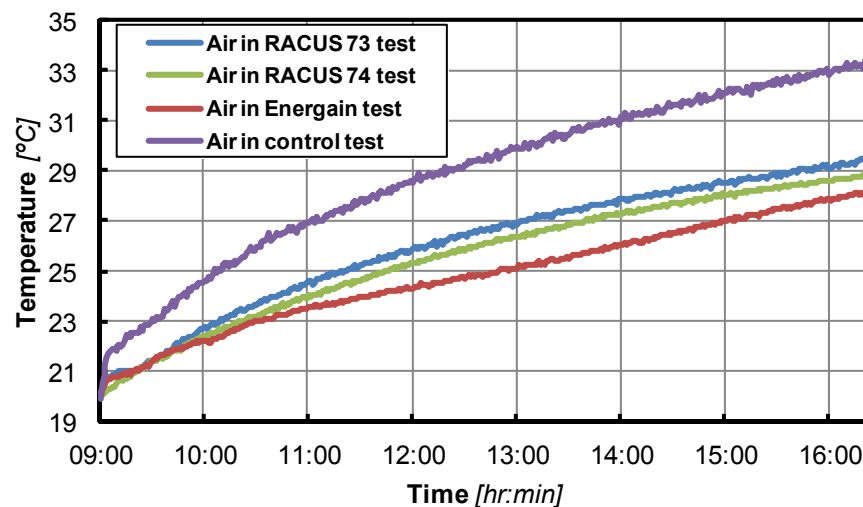


Figure 6.14 Combined charge results.

RACUS 73 performs worse than RACUS 74 in that the achieved temperature reduction is less. However, both formulations of RACUS perform very similarly with less than 1 °C difference between throughout the charge period. This is to be expected since the absolute micronal content is very similar for both. The Energain panels perform the best overall but it is important to note that the test cell coverage was far greater than that of RACUS which was only applied to the ceiling. This meant a greater surface area and quantity of PCM was available in the Energain case. The peak temperature results have been normalised according to floor area and mass of PCM to better understand this relationship. Cooling power has also been calculated by assuming that once the cell air temperature rises past a set point temperature of 25 °C the space should be actively cooled by a chiller operating with a COP of 3.5. The load that the chiller would meet is assumed to be equal to the output of the heater at 25 °C, which is 129W. The difference between the energy expended

in such a way between the control and a product test is then viewed as the energy saved by that product. Table 6.4 reveals all figures just discussed.

Table 6.4 Results for the product tests. Comparisons given on the basis of peak temperatures and energy savings and the same parameters normalised with respect to mass of PCM and floor area. CO₂ emissions are calculated assuming a 0.517 kgCO₂/kWh carbon factor.

	RACUS 73	RACUS 74	Energain	Control
Mass of PCM (kg)	13.33	13.24	36.28	0
Floor area (m)	2.45	2.45	2.45	2.45
Peak air temperature (°C)	29.5	28.8	28.1	33.3
Peak air temperature reduction (°C)	3.76	4.44	5.16	0
Peak air temperature reduction per unit mass (°C/kg)	0.28	0.34	0.14	0
Peak air temperature reduction per unit floor area (°C/m²)	1.53	1.81	2.11	0
Projected cooling energy required (Wh)	649	596	456	808
Projected cooling energy saved (Wh)	159	213	353	0
Percentage cooling energy saved (%)	19.7	26.3	43.6	0
Projected cooling energy saved per unit mass (Wh/kg)	11.9	16.1	9.7	0
Projected cooling energy saved per unit floor area (Wh/m²)	64.9	86.9	143.9	0
Projected carbon dioxide emissions (g)	95.9	88.0	67.3	119.4
Projected carbon dioxide savings (g)	23.5	31.4	52.1	0.0

As noted the Energain panels provide the greatest peak temperature reduction as well as the greatest energy and CO₂ savings. They also perform the best when compared on a per unit floor area basis but this would obviously be the case as the floor area is constant for all tests. In a real installation Energain panels would not be able to achieve the surface area coverage per unit volume air cooled, as seen in these tests. DuPont recommend an ideal correspondence of 1 m² of panel to 1 m³ of air that requires cooling. In the test cell this was greatly exceeded with a ratio of 2 m² surface

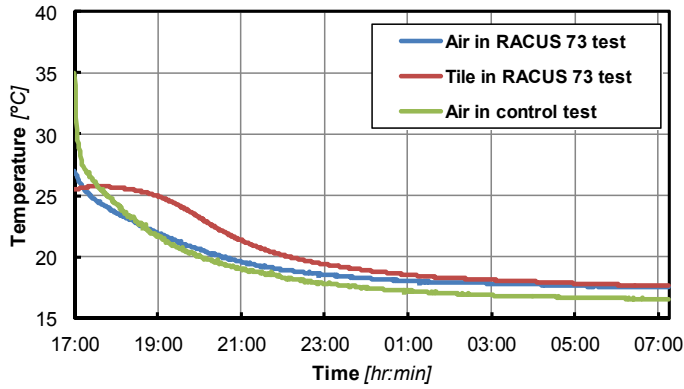
area of panels to 1 m³ of air contained. In a real space the volume of air will almost always exceed the surface area of walls and ceilings, due to the larger room size. This coupled with the restriction on installation locations, due to services, windows, furniture etc, means that in a real installation less positive results should be expected.

When the results are normalised with respect to the PCM contained the RACUS tiles are seen to perform better than the Energain panels. This is due to the far lower mass of PCM incorporated into the tiles. Of the two the RACUS 74 is seen to save more energy since the cell air rises above 25 °C around 20 minutes after the air in the RACUS 73 test.

Figure 6.15 displays the discharge process for all products. The control test air starts at a much higher temperature than the air in the product test cases. This is because the discharge results begin at the end of a charge period. Because it was not possible to start and stop all charge and discharge tests at exactly the same time, the data from the final minutes of some tests, including the control test, were removed so that what is seen is the comparison between data obtained under exactly the same conditions. The air in all product discharge tests starts at the same temperature. In a real situation the air in a room without PCM, at the beginning of a discharge period, would be at a higher temperature than the air in the same room with PCM. This is reflected in the control temperature displayed.

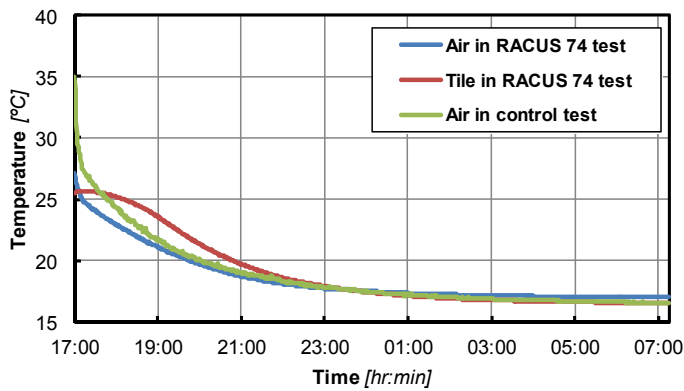
Figure 6.15 Discharge periods. Product air, product PCM and control air temperatures

(i)



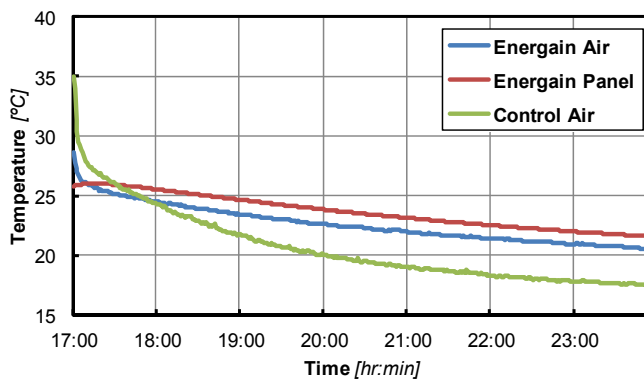
(i) Temperature profiles for RACUS 73 tiles and control

(ii)



(ii) Temperature profiles for RACUS 74 tiles and control

(iii)



(iii) Temperature profiles for Energain panels and control

It is important to note that the PCM is not at the same temperature for the start of the charge periods displayed. This is because during the previous night's discharge of heat the Energain panels were not able to reject all of their accumulated heat. This reveals superiority in the RACUS design. The RACUS formulation is in closer thermal contact with the circulated cool air because it is exposed on the top surface of the tile and only separated on the underneath by 1 mm of steel. Furthermore the circulated air is very effectively drawn over the tiles by the fan because it is situated in the ceiling void. Both of these factors promote heat transfer.

The Energain panels, on the other hand, are located behind 12 mm of plasterboard and air is not forced over its surface. The velocity of the air decreases as it enters the cell and increases again upon exit. The velocity across much of the plasterboard surfaces will be low.

This can be seen in the above figure where the Energain panels and cell air are able to effectively lose all their accumulated heat reaching the temperature of the control test cell air, whereas the Energain panels cool at a slower rate and do not reach the lowest temperature possible. This can also be seen in the combined Figure 6.16.

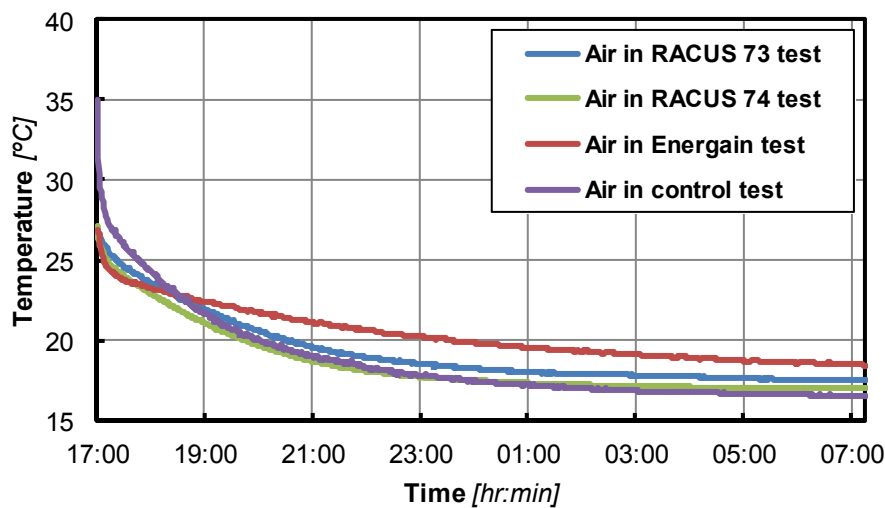


Figure 6.16 Combined discharge results.

6.4 Conclusions

It is first worth noting that the method devised for the constructed test cell proved successful, allowing the testing of the NewMass system to be undertaken with it.

Focussing on the products tested it is clear that the RACUS tiles in both formulations and the Energain panels had a significant effect on the test cell air temperature, reducing it by several °C as compared to the control test. The Energain panels performed the best in this respect but also contained the most PCM overall. When comparing peak temperature reductions on a per unit PCM mass basis we can clearly see that the RACUS 73 tiles have superior performance.

The RACUS tiles were also able to discharge their heat more effectively than the Energain panels since they are better exposed to the passing cool air. Furthermore they are easier to install and remove, requiring only the ceiling grid to be put in place.

The advantages of the RACUS design arise from the fact that the tiles are not integrated into the building fabric and are encased in a relatively conductive metal shell to promote heat transfer. These aspects of design lend support to the approach taken with the NewMass system which seeks further improvement to this type of application through the addition of an active cooling element. The design of this system is described in the following chapter.

References

Arnold, D. (2006) "Chapter 6: Internal heat gains" in *Environmental design: CIBSE Guide A*, ed. K. Butcher, 2nd edn, CIBSE, London, pp. 6-1-6-10.

BASF (2011) *Micronal PCM*. Available:

http://www.micronal.de/portal/load/fid443847/BASF_Micronal_PCM_Brochure%202009_English.pdf [01/10/2012].

Capitani, A. (2011) *Energy savings in buildings: Phase change materials*, Brunel University, Uxbridge.

Datum Phase Change (2012) *Brunel University Environmental Test Chamber*.

Available: <http://www.datumphasechange.com/index.php?brunel-university-environmental-test-chamber> [18/01/2012].

Datum Phase Change (2011) *Suspended ceiling tiles*. Available:

<http://www.datumphasechange.com/index.php?racus-honeycomb-ceiling-tile> [01/10/2011].

DuPont (2007a) *DuPont Energain*. Available:

http://www2.dupont.com/Energain/en_GB/ [29/04/2007].

DuPont (2007b) *DuPont Energain - Energy saving thermal mass systems: Installation Guidelines*, DuPont, Luxembourg.

HM Government (2006) *The Building Regulations 2000 - Conservation of fuel and power - Approved document L2A*, RIBA, London.

Kuznik, F. and Virgone, J. (2009) "Experimental assessment of a phase change material for wall building use", *Applied Energy*, vol. 86, no. 10, pp. 2038-2046.

Omega (2011) *Touch-safe heater: 50 - 150 W*. Available:

http://www.omega.com/Heaters/pdf/CSO60_Series.pdf [01/22/2012].

Oyeleke, A.J. (2010) *Controlled tests and monitoring of a semi-active PCM cooling system (Masters dissertation)*, Brunel University, Uxbridge.

Pico Technology (2011a) *Thermocouples*. Available:

<http://www.picotech.com/thermocouples.html> [22/01/2012].

Pico Technology (2011b) *USB TC-08 Thermocouple Data Logger*. Available:

<http://www.picotech.com/thermocouple.html> [22/01/2012].

Underwood, S. (2011) *Density of RACUS ceiling tile*, Datum Phase Change, London.

NEWMASS SYSTEM DESIGN

This chapter describes the design development of what became known as the NewMass system. There are three main sections. The first explains and defines the concept, drawing together all the conclusions from previous chapters and defining what makes the system worthwhile and unique. The second section describes the process of system element selection, from the envelope geometry to the material used to supplement the conductivity of the PCM. The third section describes the process undertaken to develop the detailed design, with precise specifications of all components.

7.1 Concept Design

The aim of this EngD was to develop new PCM systems that minimise the energy required to reliably cool buildings. In general it may be said that the more passive the system's operation the lower the energy it uses. However, we have also seen that passive systems have are limited in their capacity to cool by the available ceiling and wall surface area in a space. This is borne out through examples such as the previously noted predicted energy savings from DuPont Energain (DuPont, 2010) (35% due to its limited cooling and thermal capacity) and the evidence presented in chapter 6 that even though peak temperatures can be reduced they are still in excess of an acceptable threshold. Passive systems cannot be relied upon to cover the majority of the cooling load of a building, should it exceed these thresholds. An active system incorporating refrigeration is required in this common situation.

So the requirement for energy minimisation leads us towards passive systems and the requirement for reliable load coverage leads us towards active

systems. A system which can satisfy both of these aspects would therefore realise the aim of the project. With this combination of functions for improved performance the reader may be reminded of the definition given by Ashby of hybrid materials: a material formed from more than one material such that it possesses a set of characteristics not all found in the pure substances (Ashby, 2005). Here instead of a hybrid material we the need of a hybrid system.

A thermally activated PCM cooling system can satisfy these aims if operated in such a way that prioritises the passive aspect of the system whilst allowing refrigeration to provide supplementary cooling or heat rejection, as necessary. This type of system would conform to a combination of system types 1 and 5 from the matrix described in chapter 4. System type 1 passively cools the interior during the daytime and requires a heat transfer fluid to discharge the accumulated heat at night. System type 5 also passively cools the interior but passively releases the accumulated heat to circulated night air from natural ventilation. A system which employs natural ventilation to reject heat whenever possible will minimise energy consumption. A system that retains the ability to reject heat to a chilled water circuit when night air temperatures are too high, and that can engage that chilled water circuit during the daytime to meet any cooling load not met by the constituent PCM, will guarantee performance.

NewMass was developed to satisfy both these system aims. The principles that guided further design development were to maximise efficiency and minimise cost. It could be assumed that these principles always guide the practice of good engineering but it is argued that in the construction industry innovation is impeded by existing practice and the prevailing architectural norms. In the development of the NewMass system these considerations have not been ignored but the approach has been to focus primarily on the design of an efficient space cooling system, not accommodating existing construction practices. As discussed in the introduction and literature review thermal mass has long been used to restrict the temperature rise in a building but the mass also arguably had primarily structural, and often weather-protection, purpose. Modern day use of PCM has often sought to replace the thermal mass effect, which has been lost as buildings are constructed from increasingly lightweight materials, by producing units that integrate into the building fabric. It is argued that in the pursuit of more energy efficient buildings, the mediating function

of thermal mass could be more efficiently realised than by simply seeking to replace conventional thermal mass. The NewMass design is so-called as it seeks to realise the aim of best utilising thermal mass just described. Figure 7.1 shows the system concept.

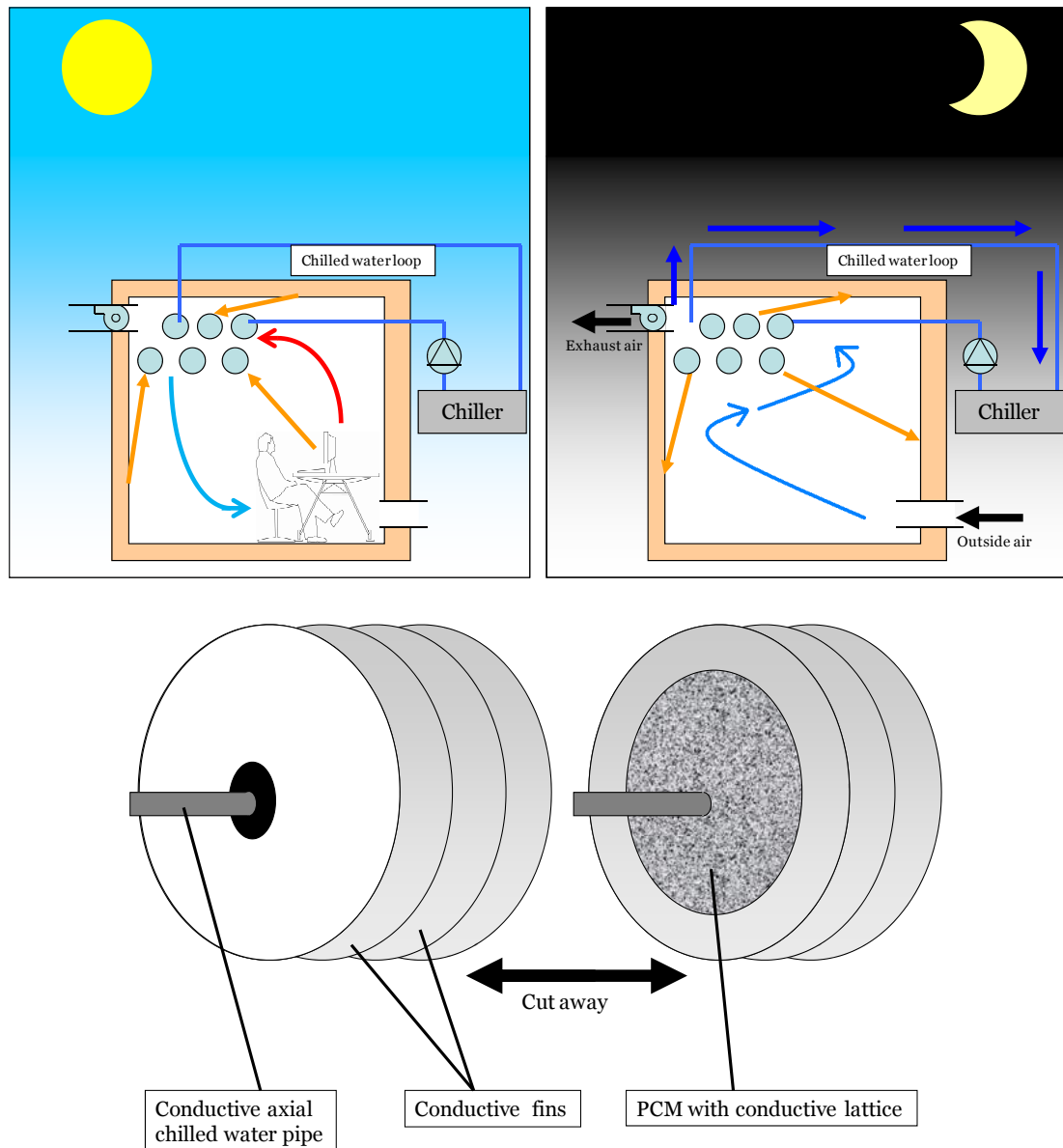


Figure 7.1 NewMass concept. System in charging mode during the day (top left), system in discharge mode (top right) and example of single unit (bottom).

As well as being a passive system with the option of active thermal discharge to chilled water circuit, the system contains several features which, in concert, constitute an entirely new design.

- **Non-integration into the building fabric:** The literature review showed that the capacity of passive elements integrated into the building fabric is limited because of limited surface area available. The concept of non-integration into the fabric was explored in the Passive PCM Sails design and the charging and discharging results from the product tests in chapter 6 suggest that non-integration can have significant benefits for performance.
- **Modular system with a cooling and thermal capacity that is decoupled from internal surface area:** Because of the non-integration just described the NewMass system has the potential to be decoupled from the internal surface of a room. By designing a system composed of modular units which can be arranged in a layered array, the system can be explicitly sized to accommodate the optimum proportion of cooling load instead of being coupled to the available wall and ceiling area.
- **Enhanced conduction through PCM to improve performance:** PCMs do not have an inherently high conductivity (for instance A22 has a conductivity of 0.18 W/m/K (Cheechern, 2009)). Increasing the conductivity maintains a higher cooling capacity for longer, can effectively increase thermal capacity and aids the discharge of accumulated heat. This will be explained in sub-section 7.2.6 on the conductive matrix.
- **Enhanced convective and radiative heat transfer at surface to maximise cooling capacity and heat discharge rate:** Increasing the rate of heat transfer through radiation and natural convection reduces the surface area required to cover the cooling load in a space. Fins are commonly used in other engineering fields where heat transfer via forced convection needs to happen at a high rate. Here that principle is applied in natural convection context in the occupied space. Maximising the emissivity and

absorptance of the unit also increases the radiant transfer rate. This was shown to work for the Passive PCM Sails in chapter 5.

- **Selection of PCM with sufficiently narrow phase transition zone in the appropriate temperature range:** PCMs intended to passively absorb heat from a space do that best when they operate within or just below the thermal comfort zone, as shown in the literature review. If too much heat is absorbed outside this range thermal capacity is wasted. This was seen in the Passive PCM Sails tests.
- **Control logic:** By establishing a control logic that prioritises the passive discharge of heat through natural ventilation, energy use is minimised. An active discharge to heat transfer fluid may be engaged only at such a time as it is necessary to fully discharge accumulated heat. Passive cooling throughout the day should also be prioritised, to save energy, until a set point temperature is reached whereupon high temperature cooling is enacted to maintain thermal comfort.

7.2 System Element Selection

The system was broken down into sub-components according to the hierarchy displayed in Figure 7.3.

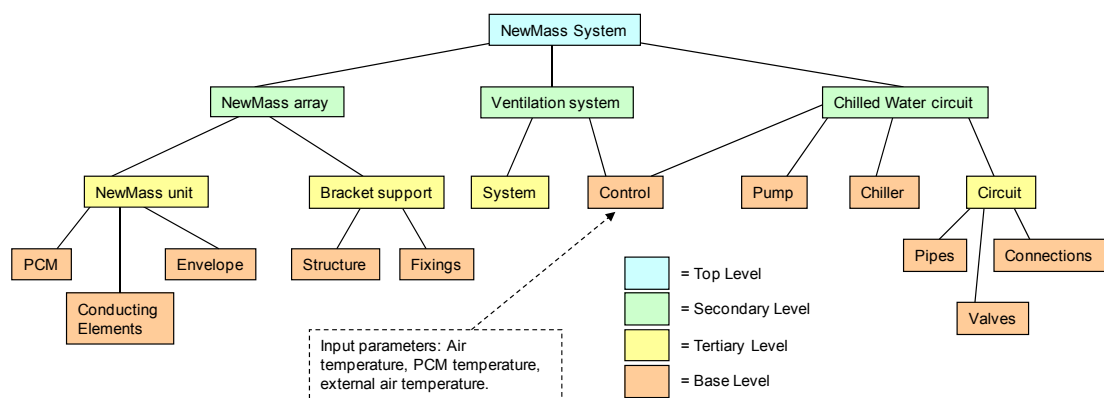


Figure 7.2 NewMass sub-system hierarchy.

Here the system is conceived of as being composed of sub-systems, themselves composed of further sub-systems. This hierarchy has not been detailed in full. For instance the chiller and pump, marked as base components here, are of course complex devices themselves with several component sub-system levels. In this case they are marked as base level components, being as they are, available off-the-shelf. For both a fully realised product and the prototype, each component and system must be specified. These selections are detailed below.

7.2.1 Unit Envelope Geometry

The decision was taken to use finned tubes as the NewMass unit envelope structure. There were three main reasons for this:

1. A horizontally orientated finned tube will allow warm air to pass between the fins, be cooled and then descend on a path unrestricted by any element of the structure. This allows it to function effectively as a cooling element in an occupied space.
2. Circular finned tubes are commonly manufactured for various applications, so the future supply of parts for any product is ensured.
3. The machining of end caps to effectively seal in the paraffin is relatively simple with circular ends.

The consideration of an unrestricted air flow path led to the rejection of flat plate variations. Based on utilising the RACUS panel design several potential flat plate geometries were considered; examples are displayed in Figure 7.3:

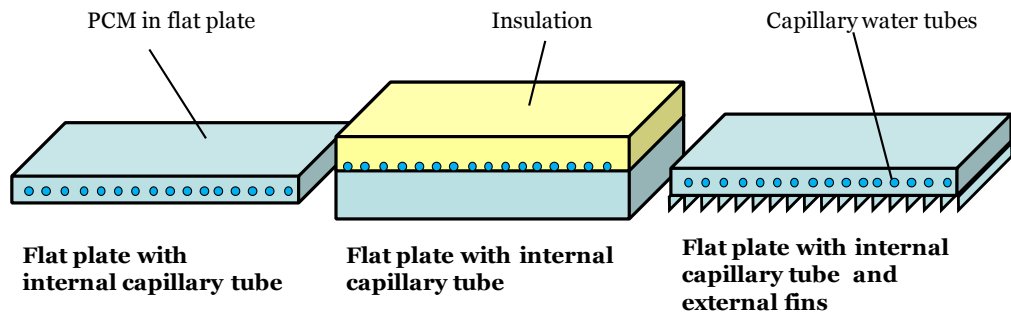


Figure 7.3 Three flat plate design variations. The central variation is essentially the same concept as the Ilkatherm panel (Ilkazell, 2010) described in the literature review but with a variation in the PCM type and containment thereof.

With flat plates the top surface, about half of the module's total surface area, is under-utilised because the heat transfer coefficient due to natural convection will be low for a cool horizontal surface located below a warmer fluid. In the case of the Ilkatherm-like variation presented above, the top surface is insulated so heat transfer is extremely restricted. Furthermore they are not as conducive to the layering. The RACUS panel for instance is designed to fit into a ceiling grid which essentially blocks the top surface from absorbing heat from the room.

Prisms allow units to be arranged in arrays several layers deep and their shape can allow for the free movement of air for a higher rate of heat transfer. Figure 7.4 displays cylinder and triangular finned prism options that can be layered.

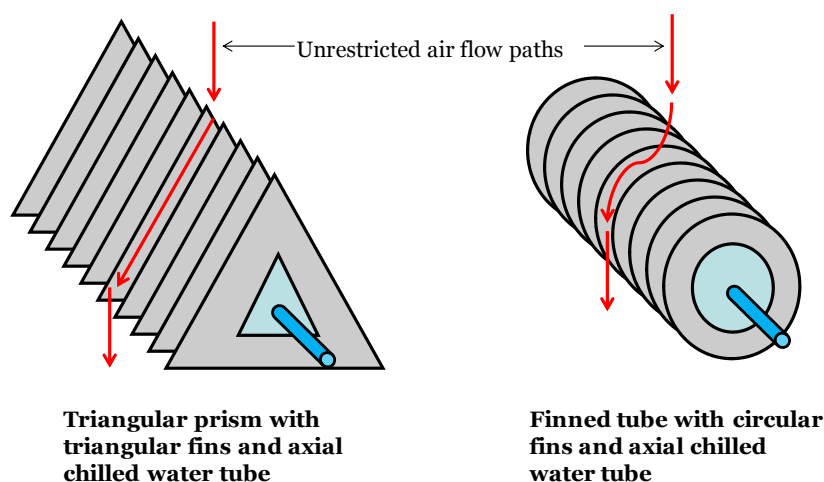


Figure 7.4 Finned prism options. Each unit here would allow air to flow freely between the unit's fins, cool and descend in the occupied space.

Axial fins were rejected because they would not encourage air to flow over the units and fall as it cooled. Instead, regions of stagnant air would be created where some of the fins met the base unit.

Of these options the finned tube was selected, as stated, for its availability and its being conducive to sealing with end caps.

7.2.2 Unit envelope material

The envelope material had to be rigid, strong, conductive and able to be shaped appropriately. A metal was therefore the appropriate choice, with steel, aluminium and copper being the main options.

Table 7.1 Comparative properties of metals. Conductivity at 25 °C (The Engineering Toolbox, 2011b) and density (The Engineering Toolbox, 2011a).

Material	Conductivity (W/m/K)	Density (kg/m³)
Stainless Steel	16	7850
Copper	401	8930
Aluminium	250	2712

Steel is less conductive and denser than copper and aluminium although it was considered as an option because discussions were had with a steel finned tube radiator manufacturer, Turnbull and Scott, about adapting the design to meet the requirements of the NewMass system.

Aluminium was finally selected as the envelope material due to its high conductivity compared to steel, and its lower cost, compared to copper. It is also less dense than steel, is sufficiently strong and stiff and can be anodised to increase absorptance and emissivity – see next section.

7.2.3 Unit envelope finish

The surface finish of the envelope was intended to have a high absorptance and emissivity to enhance radiative heat transfer. Although the majority of the cooling effect of the units is from convective heat transfer to the air, this cooling effect can be boosted by promoting the net absorption of radiation from any room surfaces, objects and occupants. Upon discharge the rate of heat transfer can be increased by promoting the net emission of radiation to any surfaces. These surfaces, the walls of the room for instance, can be cooled by circulated night air. This allows the units to discharge some radiation to the cooled surface. The higher the absorptance and emissivity in both these processes, the higher the rate of heat transfer.

Two types of finish were considered: Paint and anodisation. Of these, anodisation was selected due to the fact that the layer created at the surface of the aluminium is extremely thin compared to that of paint. A thicker paint finish would decrease the conductivity of the unit.

The anodising process increases the absorptance and emissivity of an aluminium surface. It also renders the surface hydrophilic which means it can be dyed to create coloured surfaces. A black anodised surface was chosen for each unit due to its high absorptance and emissivity, 0.88 for both (Natural frequency, 2012).



Figure 7.5 Anodised aluminium colour swatches.

Future designs could have different colours as desired.

7.2.4 *Finned tube manufacture*

Determining the source of the finned tubes was challenging. Initially, a compromise was sought between the optimal geometry for controlling the temperature in the test cell and what was available in terms of currently manufactured finned tubes. However this strategy ultimately failed because it is not possible to order a small number of aluminium finned tubes from any suppliers.

Finned tubes are available with several varieties of fin and a very large number of base tube and fin arrangement combinations. They are most commonly used in the petroleum industry where orders are typically a minimum of one ton in weight. It is not economically justified to operate the aluminium mills for less. After contacting a large number of finned tube manufacturers from across the globe it was established that aluminium tubes are commonly manufactured as standard to around 38 mm base tube diameter. In rare cases the maximum standard or custom aluminium base tube diameter was found to be 50.8 mm (2") (In fact this was disputed by several suppliers as being impossible.) Finned tubes are available in steel at larger sizes because instead of the helical winding process that is commonly used, fins must be welded. Aluminium welding is problematic since maintaining localised molten aluminium is difficult with the metal having such a high conductivity. Aircofin supply a tube of diameter of 50.8 mm with fins of up to 5/8" in height (Aircofin, 2010). However the number of fins per inch is higher than the optimum value (see section 7.3.1 below). This type of supply route was therefore abandoned in the knowledge that base tube diameters of 50.8 mm could be sourced for mass manufacture if required.

Having exhausted the route of standard manufacture a custom-built design was required. Several options were discussed with the metalwork technicians at Brunel. These were:

- Gluing flat rings to the outside of an aluminium base tube.
- Fixing flat rings to a base tube through thermal expansion of the base tube.
- Welding flat rings to an aluminium base tube.
- Cutting the fin spaces out of thick walled pipe.

Cutting the fin spaces was considered the best option as high quality results were most practically realisable by using a CNC machine in a standard operation. It also gave best thermal contact between the fin and the base tube.

7.2.5 Phase Change Material

The first consideration in PCM selection is the melt/solidification temperature, or more specifically, the phase transition zone. The literature indicates that a certain temperature range is desirable. For free cooling applications Butala and Stritih (Butala and Stritih, 2009) define a temperature range of 19 – 24 °C for PCM melting points because the air temperature should be between 3 and 5 °C higher to ensure sufficient heat transfer. This is corroborated by work by Arkar and Medved (Arkar and Medved, 2007) in which a ventilation system was filled with spheres of RT20 after it was numerically found that PCMs that melt in the range 20 to 22 °C are most suitable for free cooling applications. The NewMass system is primarily a passive application but in passive applications we see a similar temperature range being selected in the products of RACUS, Energain, Micronal etc.

The reason for this is not only the desired temperature difference between air and PCM in thermal charging mode. The PCM must be able to reject its heat to the night air whenever possible. This process favours a higher solidification temperature. The melting range is actually a compromise between the requirement for a low phase change temperature to promote thermal charging and a high phase change temperature to promote discharging. The upper limit of the air temperature in a space will vary with the thermal comfort factors noted in chapter 1 as well as building type and ventilation strategy. CIBSE guide A states that standard office environments should have an air temperature maximum of 24 °C where comfort cooling is applied (Arnold, 2006). For office with natural ventilation a mean temperature of 25 ±2 °C or an absolute maximum of 27 °C could be applied, according to CIBSE Guide B (Barnard and Jaunzens, 2005). A phase change temperature around 20 °C was concluded to be appropriate. A range of PCMs were therefore considered; these are listed in Table 7.2.

Table 7.2 Commerically available PCMs. All considered for integration into the NewMass system. Thermal capacity is a term defined here as the total latent and sensible heat storage capacity of a material over a defined temperature range. This is sometimes referred to by manufacturers as 'Heat storage'. 'n/s' means 'not supplied'.

Supplier	Composition	Name	Melt Temp °C	Freeze Temp °C	Density kg/m ³	Latent Heat kJ/kg	Specific Heat kJ/kg/K	Thermal capacity kJ/kg	Conductivity W/m/K	Flash point °C	
PCM Products	Salt hydrate (PCM Products, 2011a)	S19	19	n/s	1484	146	0.68	n/s	0.43	n/s	
		S21	21	n/s	1480	150	0.68	n/s	0.43	n/s	
		S23	23	n/s	1475	155	0.69	n/s	0.43	n/s	
	Paraffin	A22 (Cheechn, 2009)		19.79	18.71	785	169.33	2.12	n/s	0.18	n/s
		A22/LDPE (Cheechn, 2009)		19.31	18.51	852.7	73.41	2.3	n/s	0.26	n/s
		A23 (PCM Products, 2011b)	23	n/s	785	170	2.22	n/s	0.18	n/s	
	A24 (PCM Products, 2011b)	24	n/s	790	225	2.22	n/s	0.18	n/s		
Rubitherm	Paraffin	RT 21 (Rubitherm, 2011b)	21	n/s	840	n/s	n/s	134 (15 - 30 °C)	0.2	154	
	CaCl ₂ , urea + compound	SP22A17 (Rubitherm, 2012)	23	20	1490	150	n/s	150 (13 - 28 °C)	0.6	n/a	
BASF	Micronal powder (BASF, 2011)	DS 5008	23	n/s	250-350	100	n/s	135	n/s	n/s	
		DS 5029	21	n/s	250-350	90	n/s	125	n/s	n/s	
DATUM	Micronal Mg compound binder	RACUS 73 (Oyeleke, 2010)	24.42	21.16	833	58.27	2.047	n/s	n/s	n/s	
		RACUS 74 (Oyeleke, 2010)	24.89	20.81	833	83.85	1.72	n/s	n/s	n/s	

For the reasons below A22 paraffin was selected:

- **Correct melt temperature:** The A22 paraffin has been subject to DSC analysis in which its melt temperature was found to be in the region desired.
- **Appropriate energy density:** The DSC analysis also revealed a sufficiently high energy density. This should be contrasted with the energy densities of the A22/LDPE composite, the BASF Micronal powder and the RACUS formulations, all of which have a significantly lower energy density.
- **Non-corrosive to metals:** Paraffin is non-corrosive to metals and so can be combined with readily combined with metallic elements to maximise heat transfer rates.
- **Infinite cycle life:** Paraffin has an extremely high cycle life, as compared to hydrated salts which can separate over time and lose their thermophysical properties.
- **Narrow phase transition zone:** The A22 paraffin has latent heat capacity which is sufficiently focussed around the peak melt temperature. This can be contrasted with that found in the composite A22/LDPE material that was tested in the Passive PCM Sails design and found to waste valuable thermal capacity (see chapter 5). The comparison between the two materials is reproduced in Fig. 7.9.

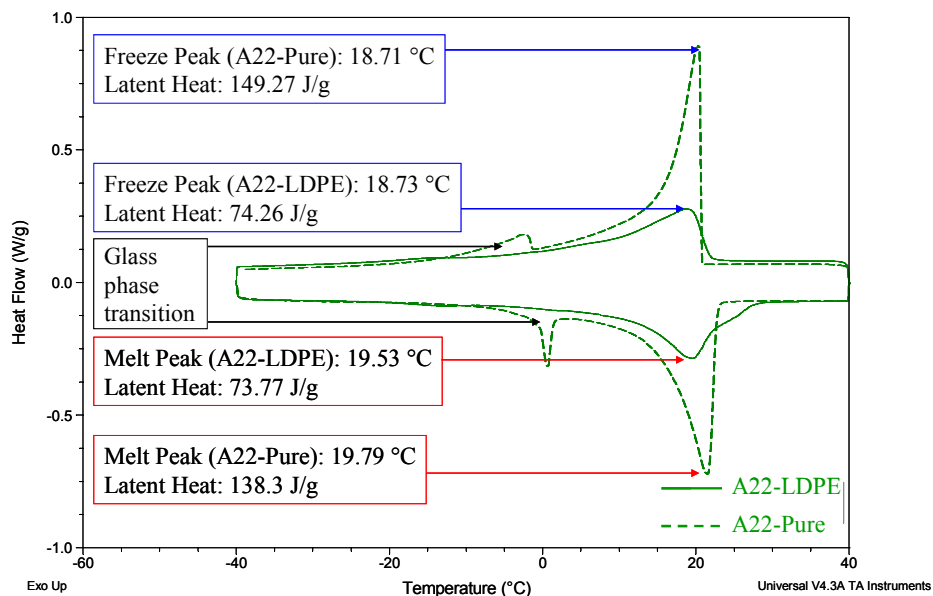


Figure 7.6 Combined pure A22 and A22/LDPE composite DSC curves.

It can be seen that the LDPE composite reduces the heights of the melting and solidification peaks, meaning that less useful cooling can be achieved with the same mass of material.

The great disadvantage to selecting paraffin is the flammability of the substance. There are three aspects to the way an object is viewed by a fire engineer: Its susceptibility to spreading flame, how much it adds to the combustible load and the risk of explosion.

The primary protection against a spread of flame is that the NewMass unit is a completely sealed metal container. It therefore cannot allow flames to spread. A significant risk is encountered when considering the combustible load, however. The paraffin will add significantly to the combustible load if it manages to escape from the container. The container was designed to withstand 6 bar internal pressure but if a fire has been burning for some time the paraffin in the tubes may have heated up, increasing the pressure. If 6 bar was exceeded then an explosion is a potential consequence. To mitigate against this risk each tube would be fitted with a pressure valve (two for additional safety) which would open above some predefined pressure threshold. This would allow paraffin vapour and potentially liquid to enter the space and this would add to the combustible load.

It is therefore concluded that the most significant fire issue for the system is the addition to combustible load. This aspect of the design would require further evaluation and testing before a product could be brought to market. The risk of fire is an ever present concern for building operators and occupants but the risks associated can be sufficiently mitigated through careful design.

A future design iteration that could provide an alternative to this approach could be to use hydrated salts as the PCM and protect the aluminium with a protective resin layer. This has been done by Rubitherm in their CSM panel which is formed of aluminium but has a resin layer to prevent corrosion internally (Rubitherm, 2011a). Unfortunately it was not possible to apply the coating technique to both the finned tube interior and the Raschig rings that formed the conductive matrix, using Rubitherm's current coating process. However, it is reasonable to assume that the process could be adapted to coat different geometries in the near future, in which case the paraffin in the units could be exchanged for salt with the

same melt temperature. If this were to happen attention would need to be paid to the potential separation that can occur in hydrated salts over time.

7.2.6 *Conductive matrix*

As explained in the literature review PCMs do not naturally have a high thermal conductivity. It is important to enhance this aspect of the material otherwise during a thermal charging process the PCM near to the surface of the module will absorb heat, change phase and rise in temperature before without sufficiently passing the heat to deeper layers. This results in a range of temperature and phases across the body of the PCM, with the centre remaining solid and at a lower temperature and the surface layers being melted and a higher temperature.

There are two reasons why this should be avoided: Firstly, if a portion of the PCM remains solid then it is not providing any useful function and its inclusion has been futile. Secondly, the surface temperature of the material partly determines the rate of heat transfer to the module, under convection and radiation. Increasing the conductivity of the material allows it to carry heat beyond the outer layers and prevent excessive heating, thus ultimately maintaining a higher rate of cooling. This is important for peak thermal load absorption, speed of latent heat discharge and effective supplemented cooling during daytime operation.

The desired outcome is to create a module which has very little temperature variation and therefore very little phase variation across the entire module. This can be done in several ways, some of which have been discussed in the literature review. The selected PCM, pure A22 paraffin has a conductivity of 0.18 W/m/K (PCM Products, 2011b) typical of paraffins. For the NewMass modules, four types of conductivity enhancement were considered:

- Internal fins
- Graphite fibres
- Random packings
- Metal foams

The employment of fins was rejected because although the overall conductivity of the unit would be enhanced heat would still be distributed non-uniformly. Instead of a single cool central core the fins would create multiple cores which would still be subject to the same problem. Figure 7.10 displays illustrative temperature profiles of a tube with PCM filling the annular space with and without axial fins.

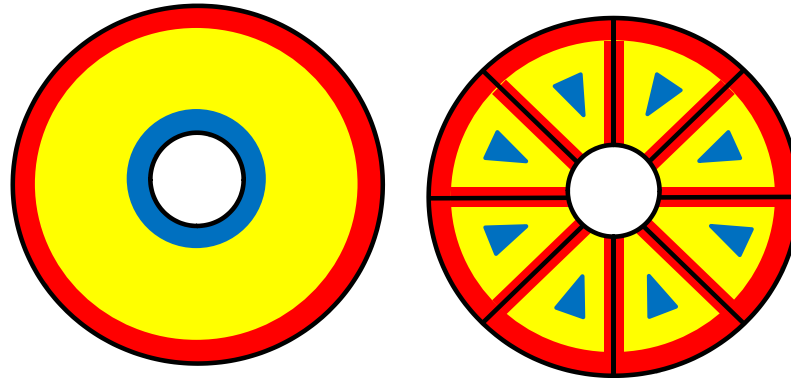


Figure 7.7 Annular space with (right) and without fins (left). High temperature melted PCM (red), medium temperature (yellow), low temperature (blue). Axial chilled water pipe (white).

Studies in the literature, for example Agyenim (Agyenim, Eames and Smyth, 2011), indicate non-uniform temperature distribution in tubes of the same design. It should furthermore be noted that such fins should make contact with the central chilled water pipe and the outer tube. This presents a significant fabrication challenge since welding to the internal tube is possible but it is not known how to insert the smaller finned tube into the larger tube and create good thermal contact between the fin tips and the outer tube.

A potential solution to both of these issues is to address the problem at a smaller scale. Graphite fibres and metal foams create conductive networks on a scale of 100s of μm to a few mms. A 'cold core' in this situation would be negligibly small. Effectively a composite material with partial thermal storage capacity of the paraffin and partial conductivity of the foam or fibres is created.

A PCM graphite composite is commercially available that is composed of paraffin with 10% graphite. The manufacturers claim that it has an in-plane conductivity of 25 W/m/K and a perpendicular-to-plane conductivity of 8 W/mK (SGL Carbon Group, 2011). It was not possible to obtain a sample of this substance

for testing. The main properties that were desired were the ability to flow and produce a uniform material throughout the annular space of the NewMass unit. Uniformity was important to maximise the thermal utility of the volume created. Any material that occupied the tube had to enter the annular space from one end of the tube, with the axial chilled water pipe in place. It was not clear what sort of molten properties could be established in the graphite PCM composite so this solution was rejected. It is worth noting that this remains a potential future design iteration if the practical issues of unit construction can be overcome.

Metal foams are used in a wide range of applications from shock absorption to mass transfer and distillation. The use of metal foam can also increase the conductivity of the material in a similar way to the graphite but on a larger scale. Metal foams are available in various metals, for example titanium, zinc and aluminium. There is a general distinction between open and closed pore structures. Open-pore structures allow other material to flow between and occupy the space created by the metal foam structure. This is essential for the creation of a PCM/metal foam composite material. An aluminium open pore foam is available from a company known as ERG (ERG, 2011a) and has relative density of 10%. This means that solid aluminium occupies just 10% of the volume it fills; the rest is void space that is filled by the PCM. By combining the foam with the A22 paraffin a compound substance would be formed with an energy density of 116753 kJ/m³. The effective conductivity of the substance is calculated with Eq. 7.1 (ERG, 2011b).

$$k_{\text{effective}} = 0.33 k_{\text{Al}} \rho_{\text{relative}} + k_{\text{A22}} \quad (7.1)$$

This equation is a modified version of that provided by ERG which assumes that the foam is surrounded by air and so a value indicating the effective conductivity of air in flux is replaced with the conductivity of A22 paraffin. Assuming a conductivity of 250 W/mK for the aluminium and 0.18 W/mK for the A22, this yields a value of 8.45 W/mK.

The metal foam was rejected for two reasons: Cost and manufacture. In fact these two issues are bound up together. The cost of metal foam was quoted at around 1 \$/inch³ (~ £0.64/16.39 cm) (ERG, 2010). This has implications for the future integration of foam should it be desired. However, costs were increased to an unfeasible level when a detailed manufacturing cost for all units was established.

ERG advised that the handling of metal foams requires experience due to the relative fragility of the substance which makes it extremely difficult to cut to size without breaking. In order for NewMass units to be fabricated such that good thermal contact was established between the foam, the axial chilled water pipe and the finned tube envelope, a very precise thermal contraction and expansion process would have to be undertaken to integrate all components. Essentially, the axial pipe and the foam elements would be slightly oversized and then cooled to low temperature using liquid nitrogen such that when the three components were brought together, they could slide into place and natural thermal expansion would yield the contact required.

This process would have greatly increased the cost. The quoted cost was \$1550 (~ £997) for the assembly of each tube alone (materials and shipping were excluded) (ERG, 2010). The decision was made not to attempt the manufacture at Brunel since the process of manufacture was too experimental and the risks were too high. The high price of the foam did appear to preclude immediate mass manufacture anyway.

The final solution was found in random packings. These are small high surface elements employed in the petroleum industry primarily for distillation and mass transfer. They will fill a container by forming a random structure created by their mutual support and that of the container walls.

Random packings include the Lessing rings shown in the literature review. If made from thermally conductive material they can be used to transfer heat rather than mass. Examples include the Pall and Cascade rings. The advantage of using a random packing is that it forms its own shape and can be easily poured into the annular space. There the random structure created naturally makes contact the chilled water pipe and the finned tube envelope. The structure is self-supporting and allows the liquid paraffin to be poured through the voids created. No space is unoccupied.

The packing selected was the Raschig ring; cylinders of metal (in this case aluminium) which have an equal diameter and length (Raschig Jaeger Technologies, 2010a). The reasons for their selection are as follows:

- High thermal conductivity of aluminium.
- Pourable material that instantly forms a lattice structure that is in thermal contact with any containing surfaces; in the case of NewMass these surfaces are the inside of the finned tube and the outside of the chilled water pipe.
- Sufficient stiffness for the lattice structure formed to be self supporting and uniform across the tube. (For a short time aluminium swarf, ribbons of aluminium created in milling processes, was considered to form the conductive lattice but its lack of stiffness meant it would compress under its own weight.)
- Large void volume. The quoted relative density for a packing formed of Raschig rings with these dimensions is 11%. This means the remaining 89% would be filled with paraffin.
- Precedence: The review conducted by Agyenim et al. (Agyenim *et al.*, 2010), discussed in the literature review, indicated that the addition of Lessing rings, similar random packings with an aluminium spine through each cylinder, had the greatest effect in terms of conductivity enhancement. The study conducted by Velraj et al. (Velraj *et al.*, 1999) showed that an effective conductivity of 2 W/mK was achieved for a 20% reduction in PCM volume.



Figure 7.8 Raschig rings. Barrel of Raschig rings (left) and individual rings (right).

The rings chosen were 6 mm units with a gauge of 0.5mm. This minimised the maximum void volume, thus improving uniformity.

It is not normally possible to accurately predict the effective thermal conductivity of hybrid materials since it is partly determined by the geometry of the structure. Most correlations will have been derived through experiment. In the case

of the metal foam the experimentally derived equation yielded a much higher value than that seen in the lessing ring experiment by Velraj et al. (Velraj *et al.*, 1999). This indicates that the metal foam equation cannot be applied directly to random packings. If it is applied to the Raschig rings with their *measured* voidage of 83.5% (obtained after filling the tubes in the final fabrication process) then an effective conductivity of 13.8 W/mK results. This is certainly too high. A figure much closer to the 2W/mK measured by Velraj et al is expected for the Raschig ring/A22 hybrid material.

7.3 Detailed Prototype Design

7.3.1 Envelope dimensions

The final dimensions for the finned tube envelope were arrived at through a process broadly divided into two stages:

- 1) Ideal dimensions calculated from empirically derived equations relating the finned tube dimensions to the test cell cooling required.
- 2) Determination of the closest possible dimensions to the ideal case that could be fabricated. Then re-applying the aforementioned equations to determine if the delivered heat transfer rate and thermal capacity produced is sufficient.

This section outlines these procedures.

In order to generate ideal dimensions for the NewMass unit envelope the system had to be sized according to cooling load, which determines the desired heat transfer rate at the envelope surface, and the total daily cooling demand, which determines the thermal capacity required by the system.

In other words the NewMass unit number and geometry may be determined by the load profile of the hottest day of the year. For the prototype, the system was sized according to the test cell conditions so the maximum load here was chosen to be the test cell heater's maximum output of 150W and the maximum permissible internal temperature was taken to be 26°C. Under these conditions it was assumed

that the heat flux across the envelope would be negligible since the external temperature in the climate chamber would be 25 °C.

It was decided that the units should be sized in the same way that an active system would be sized for a load-levelling scenario. This was because the system would have the ability to engage during the day to provide additional cooling and in this way could be said to function similarly to a load-levelling system. Indeed, a full scale system could be sized similarly to reduce capital costs.

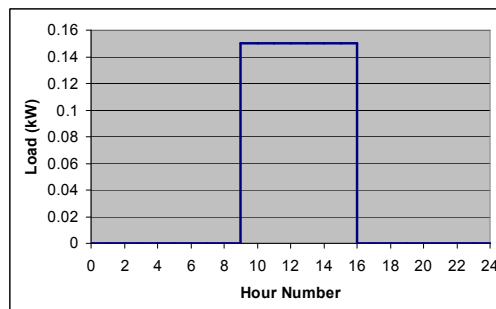


Figure 7.9 Profile applied for load-levelling.

The load-levelling load profile was averaged over the entire 24 hour period to give 43.75W. This value, multiplied by the number of hours when the load is zero, 17, provided the total energy to be stored: 743.75 kWh.

The *thermal capacity* of the PCM, that is to say the total amount of heat it can store over a range of temperature, was calculated using the following equation:

$$TC_{PCM} = \Delta T \times C_{p,PCM} + L_{fus} \quad (7.2)$$

For the Raschig ring aluminium the equivalent was found with Eq. 7.3, assuming the same cooling temperature range (the range of temperature over which the units can be said to usefully function.)

$$TC_{Al} = \Delta T \times C_{p,Al} \quad (7.3)$$

The energy density of the hybrid A22/Raschig ring material was calculated using the following equation:

$$ED = TC_{PCM} \times \rho_{PCM} \times \frac{V_{PCM}}{V_{hyb}} + TC_{Al} \times \rho_{Al} \times \frac{V_{Al}}{V_{comp}} \quad (7.4)$$

The predicted energy densities of the hybrid and the pure PCM are presented here:

Table 7.3 Properties of composite.

Energy density (ED) of compound (kJ/m ³)	Energy density of pure PCM (kJ/m ³)
116753.04	127034.6

The volume of compound material was then calculated using the following equation:

$$V_{comp} = \frac{U_{max}}{ED} \quad (7.5)$$

This is 22.9l. The base tube surface area was then calculated by finding the ‘effective heat transfer coefficient’ for that surface. The heat transfer coefficient as it applies to all surfaces including fins is determined by a number of dimensions detailed in Figure 7.10.

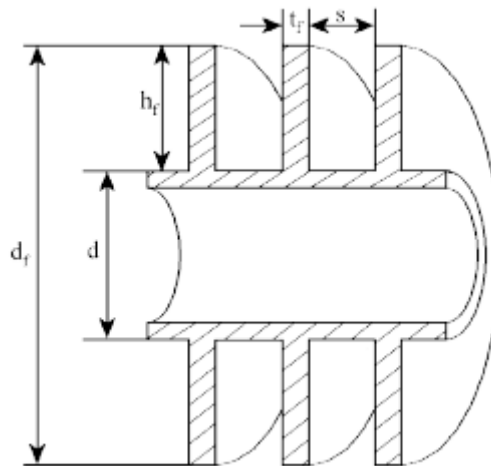


Figure 7.10 Finned tube with circular fin geometry (Mon and Gross, 2004).

All of these parameters will influence the rate of heat transfer across the base tube and an optimum arrangement was sought.

The literature contains very few empirically derived equations which relate all parameters of a horizontally orientated finned tube to a heat transfer coefficient for the case of natural convection. Examples for forced convection are more common, Mon and Gross (Mon and Gross, 2004) providing a good example in which the arrangement of finned tube banks, staggered or in-line is also evaluated for optimisation. In this work empirically correlated equations provided by Tsubouchi and Masuda (1970) were used to derive convective heat transfer coefficients for various finned geometries. In each case the derived value referred to the heat transfer coefficient through any part of the finned tube surface. To size the system, however, a heat transfer coefficient that refers only to heat passing through the base tube surface was required. Therefore, a value, referred to here as the effective heat transfer coefficient, was derived from the convective and radiative heat transfer coefficients that act on all surfaces by normalising with respect to the base tube area.

The effective heat transfer coefficient is defined in Eq. 7.6.

$$h_{eff} = h_{c,eff} + h_{r,eff} \quad (7.6)$$

where

$$h_{c,eff} = h_c \times \frac{A_{Tot} \eta_{fin}}{A_{Tube}} \quad (7.7) \quad \text{and} \quad h_{r,eff} = h_r \times \frac{F_{w,p} A_{Tot} \eta_{fin}}{A_{Tube}} \quad (7.8)$$

Here h_c is evaluated according to Tsubouchi and Masuda's (1970) empirically correlated equations (although Kreith and Bohn's (2001) particular presentation of the equations was used for calculation and description here.) As will be seen, no account is taken of the finiteness of the fins' conductivity, therefore a fin efficiency of 90% was assumed (Cengel, 2003). The characteristic length in these equations is taken to be the fin spacing, S , so the Nusselt number is defined as

$$Nu_s = \frac{h_c S}{k} \quad (7.9)$$

and the Rayleigh number is

$$Ra_s = \frac{g\beta(T_\infty - T_w)S^4}{\nu\alpha D} \quad (7.10)$$

The equations were derived through experiments on heated tubes. Because cooled tubes are being designed here, the temperature difference has been negated, with respect to the original equation.

One equation is given to evaluate heat transfer from the fin tips:

$$Nu_s = (0.44 + 0.12\xi)Ra_s^{0.29} \quad (7.11)$$

Two more are given for the lateral fin and tube surfaces in the case of short and long fins, $1 < \xi < 1.67$ and $1.67 < \xi < \infty$, respectively, where $\xi = D/d$. These are:

$$Nu_s = C_0 Ra_0^P \left\{ 1 - \exp \left[- \left(\frac{C_1}{Ra_0} \right)^{C_2} \right] \right\}^{C_3} \quad (7.12)$$

for short fins where

$$C_0 = -0.15 + (0.3/\xi) + 0.32\xi^{-16}$$

$$C_1 = -180 + (480/\xi) - 1.4\xi^8$$

$$C_2 = 0.04 + (0.9/\xi)$$

$$C_3 = 1.3(1 - \xi^{-1}) + 0.0017\xi^{12}$$

$$P = 0.25 + C_2 C_3$$

$$Ra_0 = Ra_s \xi$$

and for long fins,

$$Nu_s = \frac{Ra_s}{12\pi} \left\{ 2 - \exp \left[- \left(\frac{C}{Ra_s} \right)^{3/4} \right] - \exp \left[\beta \left(\frac{C}{Ra_s} \right)^{3/4} \right] \right\} \quad (7.13)$$

where

$$\beta = (0.17/\xi) + e^{-(4.8/\xi)} \quad \text{and} \quad C = \left\{ \frac{23.7 - 1.1 \left[1 + (152/\xi^2) \right]^{1/2}}{1 + \beta} \right\}^{4/3}$$

These equations apply in the Rayleigh limits, $2 < Ra_s < 104$. Because fins were expected to be tapered, heat transfer from the fin tips was disregarded.

In order to determine the optimal fin arrangement, heat transfer from the fins was evaluated for a large number of fin arrangements and base tube diameters, assuming a constant fin thickness of 1 mm, a T_w of 19.79 °C and a T_∞ of 26 °C. These temperatures are assumed to represent the limiting case when a maximum cooling load obtains in the thermal test cell. T_w is 19.79 °C as this is the peak melt temperature of the A22 paraffin and 26 °C is the maximum permissible temperature in the cell. The system must be sized to transfer heat at the maximum cooling load under these conditions. A peak cooling load value of 150 W was taken to ensure a slightly conservative sizing (the heater actually produces around 129 W at 25 °C.)

The fin arrangement which would produce the highest effective heat transfer coefficient was sought, as this will reduce the base tube diameter to a minimum. The fin arrangements evaluated were all combinations of a fin spacing range of 1 mm to 15 mm (with discrete steps of 1 mm) and a fin/tube diameter ratio range of 1 to 3 (with discrete steps of 0.2). All these fin arrangement combinations were evaluated for a base tube diameter range of 40 mm to 150 mm (with discrete steps of 2 mm).

The radiant heat transfer coefficient in Eq. 7.14 was estimated by applying the following equation:

$$h_r \approx 4\sigma\epsilon \left(\frac{T_b + T_{surr}}{2} \right)^3 \quad (\text{Biber, 2005}) \quad (7.14)$$

Here T_p was taken to be equal to the difference between the maximum permissible air temperature (26 °C) and the average difference between the air and globe temperature measured in the test cell during daytime operation, 24.66 °C.

The value of $F_{w,p} A_{Tot}$ was assumed to be close to but less than the product of a solid cylinder of diameter equal to that of the fins and a view factor of 1. Therefore

the value must be adjusted downwards by a factor. This factor was found by estimating a lower boundary value using Edwards and Chaddock's (Edwards and Chaddock, 1963) calculation of view factors for different finned tube geometries. It was found that for a representative case the mean of these lower and upper boundary values was ~ 20% below the upper boundary. Therefore for all cases the solid tube estimate, multiplied by a factor of 0.8, was used to conservatively estimate the value of $F_{w,p}A_{Tot}$.

The required surface area can then be calculated from the following equation:

$$A_b = \frac{\dot{Q}}{h_{c,eff}(T_\infty - T_w) + h_{r,eff}(T_p - T_w)} \quad (7.15)$$

With the volume and surface area known the geometry of the units can be calculated using the following simple geometry:

$$L_b = \left(\frac{A_b^2}{4\pi V_b} \right) \quad (7.16) \quad \text{and} \quad d = \frac{A_b}{\pi L_b} \quad (7.17)$$

Several variations in tube dimensions resulted that were suitable for the application. The dimensions selected are shown in Table 7.4.

Table 7.4 Selected fin tube dimensions.

Tube number	Tube length, L_b (mm)	Base tube diameter, d (mm)	Fin diameter, D (mm)	Fin spacing, S (mm)
5	1000	80	160	10

These dimensions represent what was ideally desired in finned tube geometry and fin arrangement. However, through the extensive investigations into finned tube manufacturers described in section 7.2.4 it became apparent that these ideal

dimensions were not attainable and finned tube manufacturers were not able to supply in such small quantities. Therefore alternative approaches were explored as described and the final design was selected to be the largest diameter finned tube possible that could be produced on a CNC machine; 50.8 mm ID base tube and 76.2 mm OD fins. The fin spacing was maintained but the thickness was doubled to 2mm to ensure integrity during machining. Tsubouchi and Masuda's equations were then reapplied to the final agreed design to determine the critical heat transfer rate. This was found to be 76.4 W for 6 units.

The chosen design fabrication was outsourced to a local prototype manufacturing firm. The following figures display the design.

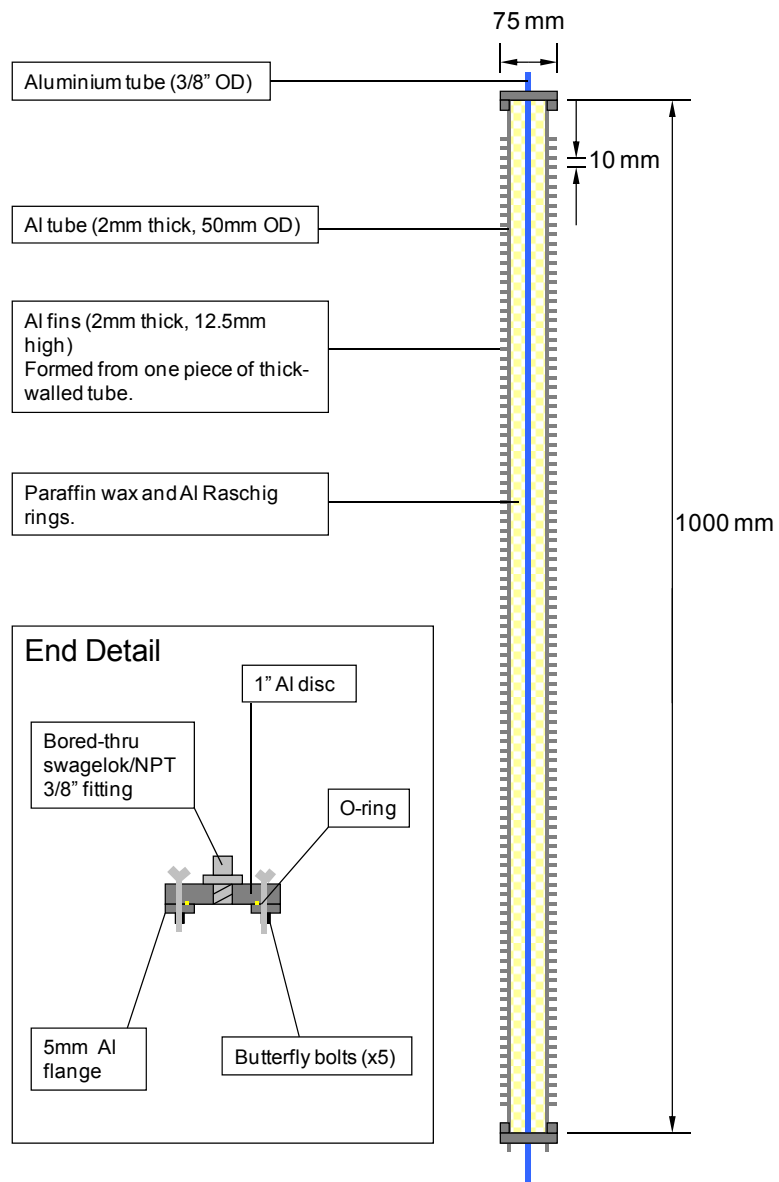


Figure 7.11 Final tube design concept.

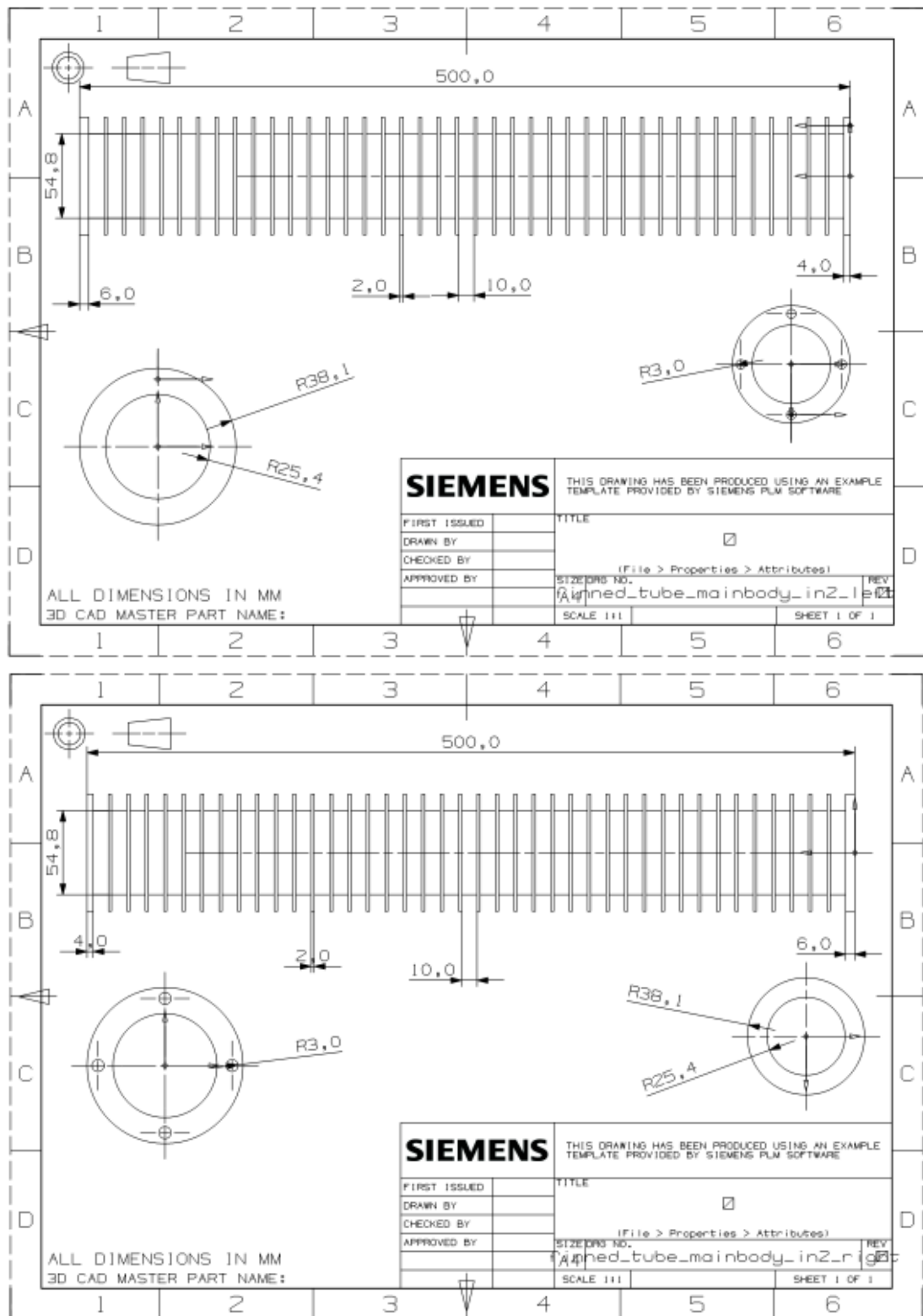


Figure 7.12 Finned tube engineering drawings. Left hand (top), right hand (bottom) (Couch, 2011).

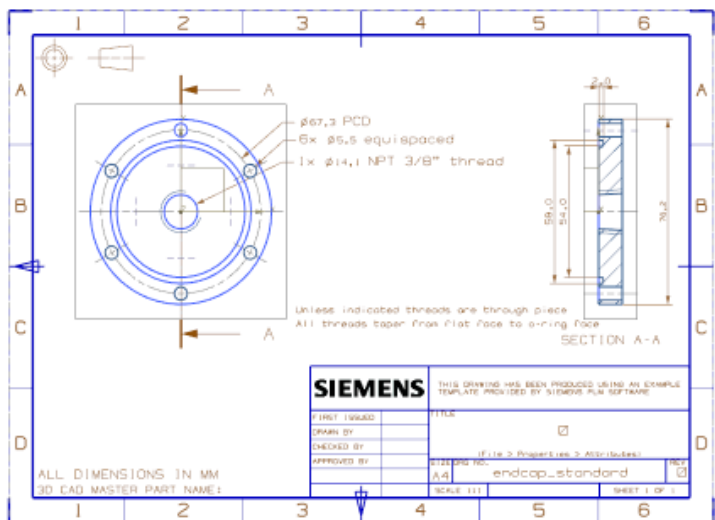
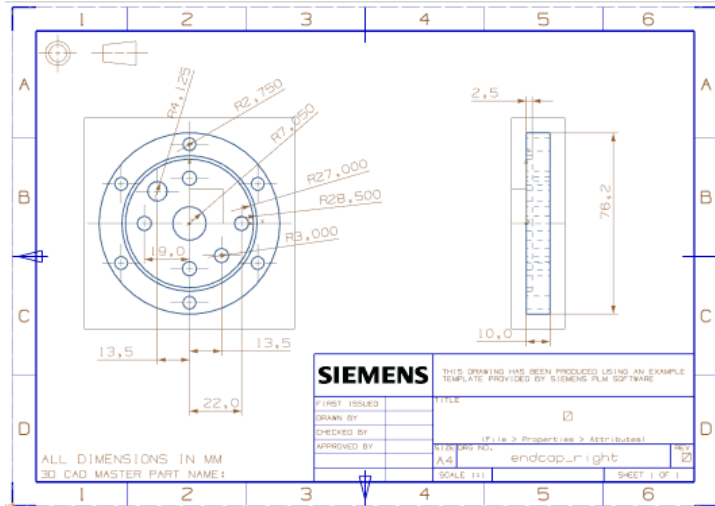
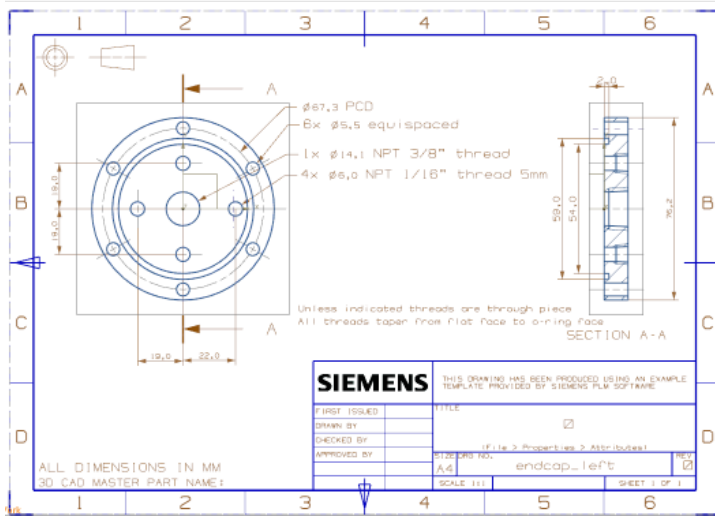


Figure 7.13 Cap engineering drawings. Left monitored tube cap (top), right monitored tube cap (middle) standard cap (bottom) (Couch, 2011).

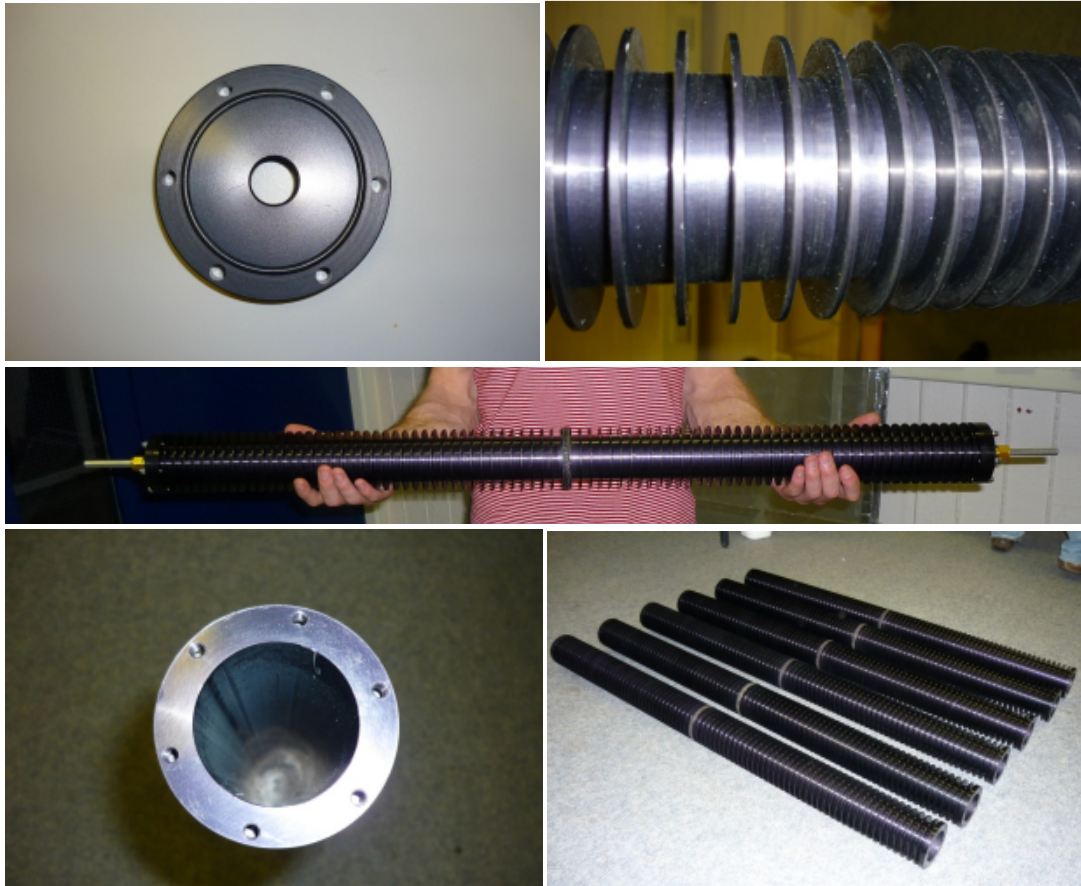


Figure 7.14 Finned tube and cap images.

7.3.2 Filling units

The filled tube contains an air pocket which expands and contracts as the PCM respectively contracts, when freezing and expands, when melting. The air pocket prevents a high pressure differential across the envelope of the tube which could result in a leakage of material or damage to the tube itself.

The air pocket's size was calculated by first asserting the following relationship:

$$V_{A(LPCM)} = V_S - V_{LPCM} \quad (7.18)$$

It was decided that the volume of the air pocket should double upon freezing so that the pressure difference across the envelope would be at 1/2 bar maximum, thus ensuring that the envelope would not be breached or distorted and that the transition zone of the A22 would not be altered. This is stated algebraically in Eq. 7.19.

$$V_{A(LPCM)} = 1/2 V_{A(SPCM)} \quad (7.19)$$

The equivalent of Eq. 7.19 for air in a tube with solid A22 is given in Eq. 7.20

$$V_{A(SPCM)} = V_S - V_{(SPCM)} \quad (7.20)$$

The thermal expansion coefficient was then required in order to relate the liquid A22 volume with the solid A22 volume. This was derived by measuring the volume of a known mass of A22 at 15 °C (largely solid) and then heating that sample in a warm water bath until it reached 25 °C (liquid) and then measuring the volume again. The results are presented in Table 7.5.

Table 7.5 Thermal expansion results for A22 paraffin.

Sample temperature (°C)	Sample state	Sample Mass (kg)	Sample Volume (m ³)	Sample Density (kg/m ³)
15	Largely solid	0.038498	0.000048	802.04
25	Liquid	0.038498	0.000050	769.96

Eq. 7.21 defines the thermal expansion coefficient.

$$\alpha_V = \frac{1}{V} \left(\frac{\partial V}{\partial T} \right)_P \quad (7.21)$$

This yields a value of 0.4 K⁻¹. The working temperature range of the units was to be between 12 and 25 °C so as to allow for the substance to complete melt over a charge cycle and continue to absorb heat in the liquid phase. Therefore using Eq. 7.22 the relationship in Eq. 7.22 can be derived.

$$V_{LPCM} = 1.05 V_{SPCM} \quad (7.22)$$

With the volume of air and A22 explicitly related for the conditions of solid and liquid PCM and given that the volume of air was set to double upon A22 freezing, Eq.s 7.18 and 7.22 could be combined to give the following relationship:

$$0.95 V_S = V_{LPCM} \quad (7.24)$$

This states that 5% of the space in the unit between the Raschig rings should be air and 95% should be A22 when liquid. The volume of the space between and around the Raschig rings was calculated using Eq.s 7.25 and 7.26.

$$S = 1 - \frac{V_R}{V_{AV}} \quad (7.25)$$

$$V_S = S V_{AV} \quad (7.26)$$

The solid volume of aluminium in the Raschig rings was calculated by filling a finned tube, containing the axial water pipe, with Raschig rings, weighing them (869.231 g) and applying Eq. 7.27 with an aluminium density of 2712 kg/m³.

$$V_R = m_R \rho_{Al} \quad (7.27)$$

The volume of air and Raschig rings was then calculated using 7.28

$$V_{A+R(LPCM)} = \frac{V_{A(LPCM)}}{S} \quad (7.28)$$

Simple geometry led from there to the depth of 4.5cm. The Raschig rings were poured and once they had reached up to 4.5cm below the top of the finned tube the liquid A22 was poured in until it reached the same height. This was the only way of ensuring that the right amount of paraffin was added. Once the correct level was reached the remaining space was filled with Raschig rings of a known weight and the unit was sealed with the end cap.

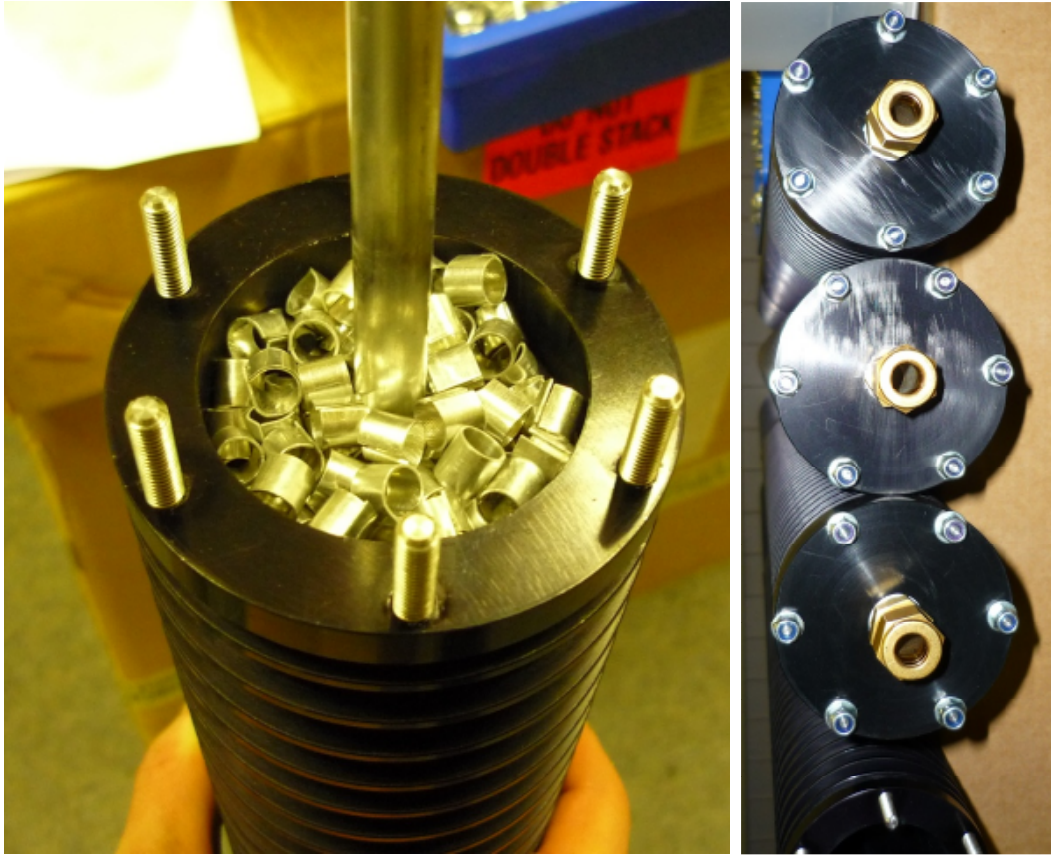


Figure 7.15 Tube with Raschig rings and sealed units.

7.3.3 Chilled water circuit

The chilled water circuit design consists of the NewMass unit array, chiller pump, control valve and all the interconnecting tubes. A flow meter was also included for monitoring.

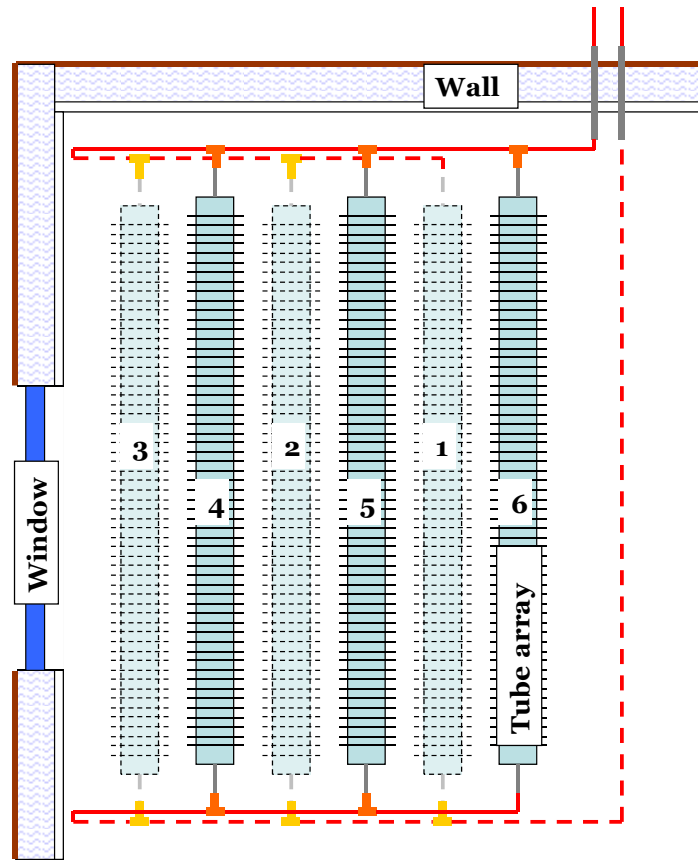


Figure 7.16 Finned tube array.

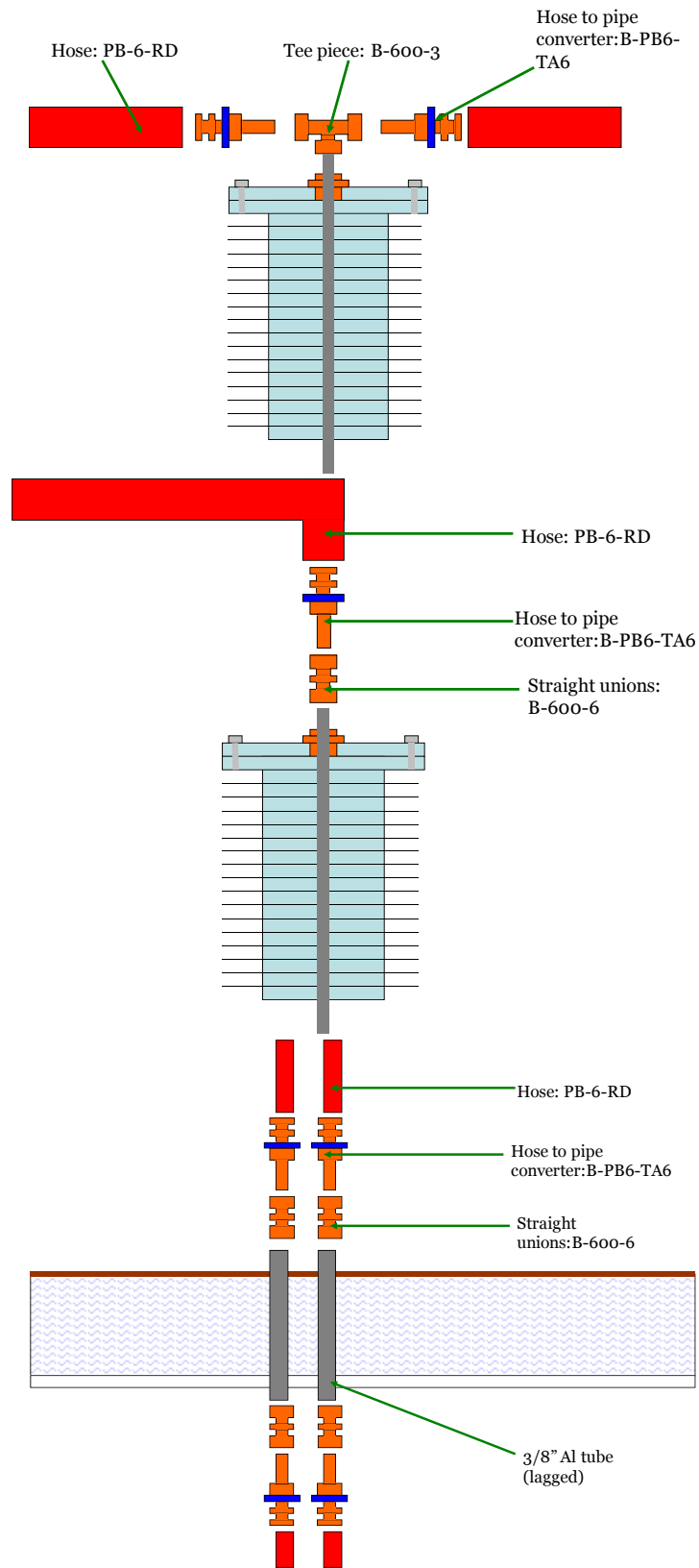


Figure 7.17 Chilled water circuit connections.

References

- Agyenim, F., Hewitt, N., Eames, P. and Smyth, M. (2010) "A review of materials, heat transfer and phase change problem formulation for latent heat thermal energy storage systems (LHTESS)", *Renewable and Sustainable Energy Reviews*, vol. 14, pp. 615-628.
- Agyenim, F., Eames, P. and Smyth, M. (2011) "Experimental study on the melting and solidification behaviour of a medium temperature phase change storage material (Erythritol) system augmented with fins to power a LiBr/H₂O absorption cooling system", *Renewable Energy*, vol. 36, no. 1, pp. 108-117.
- Aircofin (2010) *Finned tube geometries*, Aircofin, Nieuwe Pekela.
- Arkar, C. and Medved, S. (2007) "Free cooling of a building using PCM heat storage integrated into the ventilation system", *Solar Energy*, vol. 81, pp. 1078-1087.
- Arnold, D. (2006) "Chapter 6: Internal heat gains" in *Environmental design: CIBSE Guide A*, ed. K. Butcher, 2nd edn, CIBSE, London, pp. 6-1-6-10.
- Ashby, M.F. (2005) "Hybrids to fill holes in material property space", *Philosophical magazine*, vol. 85, no. 26, pp. 3235-3257.
- Barnard, N. and Jaunzens, D. (2005) "Section 2: Ventilation and air conditioning" in *Heating, ventilating, air conditioning and refrigeration: CIBSE Guide B*, ed. K. Butcher, CIBSE, London, pp. 2-1-2-142.
- BASF (2011) *Micronal PCM*. Available:
http://www.micronal.de/portal/load/fid443847/BASF_Micronal_PCM_Brochure%202009_English.pdf [01/02/2012].
- Biber, C. (2005) *A Radiative "Heat Transfer Coefficient"*. Available at:
<http://www.coolingzone.com/library.php?read=495> [23/092010].
- Butala, V. and Stritih, U. (2009) "Experimental investigation of PCM cold storage", *Energy and Buildings*, vol. 41, no. 3, pp. 354-359.

- Cengel, Y.A. (2003) *Heat Transfer: A Practical Approach*, 2nd edn, McGraw-Hill, New York.
- Cheechern, T. (2009) *The Application of the Shrinking Core Model to Phase Change Materials (Masters Dissertation)*, Brunel University, Uxbridge.
- Couch, W. (2010) *Development and testing of a novel PCM comfort cooling system (Masters dissertation)*, Brunel University, Uxbridge.
- DuPont (2010) *Energy Management*. Available:
http://energain.co.uk/Energain/en_GB/benefits/energy_management.html
[11/01/2011].
- Edwards, J.A. and Chaddock, J.B. (1963) "An Experimental Investigation of the Radiation and Free-Convection Heat Transfer From a Cylindrical Disk Extended Surface", *Transactions of ASHRAE*, vol. 69, pp. 313-322.
- ERG (2011a) *ERG Aerospace Corporation*. Available:
<http://www.ergaerospace.com/index.html> [22/01/2012].
- ERG (2011b) *Thermal Conductivity*. Available:
<http://www.ergaerospace.com/Thermal-transfer.html> [01/22/2012].
- ERG (2010) *Cost of finned tube with metal foam manufacture*, ERG, Oakland.
- Halliday, D., Resnick, R. and Krane, K.S. (1992) *Physics*, 4th edn, John Wiley & Sons, Inc., Chichester.
- Ilkazell (2010) *Ilkatherm Ceiling*. Available:
http://www.ilkazell.de/en_baudecke.php [21/02/2010].
- Kreith, F. and Bohn, M.S. (2001) *Principles of Heat Transfer*, 5th edn, Brokes/Cole, Pacific Grove.

Mon, M.S. and Gross, U. (2004) "Numerical study of fin-spacing effects in annular-finned tube heat exchangers", *International Journal of heat and Mass Transfer*, vol. 47, pp. 1953-1964.

Myslewski, R. (2011) *Boffins triple battery life with metal foam*. Available: http://www.theregister.co.uk/2011/06/29/aluminum_celmet/ [02/01/2012].

Natural frequency (2012) *Absorptance and Emittance*. Available: http://wiki.naturalfrequency.com/wiki/Absorptance_and_Emittance [10/05/2011].

Oyeleke, A.J. (2010) *Controlled tests and monitoring of a semi-active PCM cooling system (Masters dissertation)*, Brunel University, Uxbridge.

PCM Products (2011a) *PlusICE PCM (Hydrated Salt) (S) range*. Available: http://www.pcmproducts.net/files/s_range.pdf [21/01/2012].

PCM Products (2011b) *PlusICE PCM (Organic) (A) range*. Available: http://www.pcmproducts.net/files/a_range.pdf [21/01/2012].

Raschig Jaeger Technologies (2010a) *Raschig ring, metal*. Available: <http://www.raschig.de/Raschig-Ring-Metal> [02/01/2011].

Raschig Jaeger Technologies (2010b) *Ring division*. Available: <http://www.raschig.de/Random-Packing-Metal> [02/02/2011].

Rubitherm (2012) *Rubitherm SP22A17*. Available: <http://www.rubitherm.de/english/index.htm> [22/01/2012].

Rubitherm (2011a) *CSM module*. Available at: <http://www.rubitherm.de/english/index.htm> [01/02/2012].

Rubitherm (2011b) *Rubitherm RT 21*. Available at: <http://www.rubitherm.de/english/index.htm> [22/01/2012].

SGL Carbon Group (2011) *Ecophit: the graphite construction material for air conditioning in buildings*. Available at:
http://www.sglgroup.com/export/sites/sglcarbon/_common/downloads/products/product-groups/eg/construction-materials-ecophit/ECOPHIT_Uebersicht_e.pdf [02/01/2012].

The Engineering Toolbox (2011a) *Metals and alloys - densities*. Available:
http://www.engineeringtoolbox.com/metal-alloys-densities-d_50.html
[03/11/2011].

The Engineering Toolbox (2011b) *Thermal conductivity of some common materials and gases*. Available at: http://www.engineeringtoolbox.com/thermal-conductivity-d_429.html [03/11/2011].

Tsubouchi, T. and Masuda, H. (1970) "Natural Convection Heat Transfer from Horizontal Cylinders with Circular Fins", *Proceedings from the 6th International Heat Transfer Conference*. Paris, pp. NC 1.10.

Turnbull and Scott (2012). Available at: http://www.turnbull-scott.co.uk/commercial_heating_systems/finned_tube_radiators/
[05/06/2011].

Velraj, R., Seeniraj, R.V., Hafer, B. and Faber, C.S., K. (1999) "Heat Transfer Enhancement in a Latent Heat Storage System", *Solar Energy*, vol. 65, no. 3, pp. 171-180.

Chapter 8

NEWMASS SYSTEM TESTING

This chapter describes the assembly of the NewMass system, the methods employed in its testing, the results of those tests, the modelling of the system on a building level and the conclusions reached. There were two overarching aims:

- To assess the system's performance
- To establish energy savings

The system was installed in the test cell described in chapter 6 and performance was assessed through comprehensive monitoring of the cell air temperature. Various operation parameters and system characteristics were also derived from test measurements to inform the energy savings model and analysis. These were:

- Convective heat transfer coefficient of NewMass units.
- Effective conductivity of NewMass units.
- Correspondence between NewMass units enthalpy and temperature.

Energy savings were calculated via a heat balance model, employing the Eulerian method (a variation on that applied by Kuznik et al. (2009)), that found the difference between the predicted energy use for two cooling systems serving a typical UK office, the NewMass system and a conventional central cooling system serving fan coil units.

Several major conclusions were reached:

Firstly, that the system operates successfully in passive and supplementary cooling modes, suppressing air temperature rise and completely stabilising air

temperature at 24.5 °C, respectively. A heat transfer coefficient at the NewMass unit surface of 24.1 W/m²K at the start of the passive period eventually dropped to 0.4 W/m²K at the end. The period with supplementary cooling period saw a near constant heat transfer coefficient of 5.44 W/m²K achieved. A beneficial convection current was well-established, as shown by air temperature monitoring at several locations and a steady-state CFD model of the chamber produced by a member of the PCM research group.

Secondly, that discharge of heat to the chilled water circuit was very effective with unit temperatures dropping from that of a fully charged state to around 15 °C in around 3 hours with a flow temperature of 10 °C. The discharge of heat to air was less effective however, with a low heat transfer coefficient, 1 W/m²K, from non-ideal air flow across rather than between fins.

Thirdly, the energy savings model predicted 34% annual savings with the system, as compared to a cooling system operating with the same chiller and serving zones with fan coil units.

Due to the fact that multiple outcomes were sought at each stage during this process a summary of each specific aim, method, result and conclusion is presented in the table below. It may be useful to refer back to this table for guidance whilst reading the rest of this chapter.

Table 8.1 Summary table of the NewMass system experiment and modelling.

	Objective	Method	Results	Conclusion
1.	Observe the system's effect on air temperature in passive cooling mode.	Identical conditions to the control tests established with internal temperature monitoring for comparison.	Passive cooling significantly reduced room air temperature rise which exceeded 25 °C just after midday.	The system suppresses room air temperature rise, thus reducing cooling energy required and requires supplementary cooling at tested load and unit number.

2.	Observe the system's effect on air temperature in supplemented passive cooling mode.	Identical conditions to the control tests established with internal temperature monitoring for comparison. Chilled water delivered at 13.0 °C and 2 l/min	Supplemented passive cooling controlled the temperature well with a steady temperature of 24.5 °C achieved on activation of the chilled water system.	The system controls the room temperature extremely effectively at a relatively high flow temperature. Potentially low energy and high reliability.
3.	Obtain the thermal capacity and Temperature- 'unit enthalpy' functions for the NewMass units.	Results of the A22 DSC analysis combined with actual unit mass measurements to plot temperature vs unit enthalpy curves. Polynomials fitted to each section of the melting and freezing curves.	Polynomials with high R ² values in excess of 0.9999 obtained.	This method of obtaining temperature-enthalpy curves is simple, effective and accurate.
4.	Reveal the rate and depth of discharge in passive discharge mode.	Internal thermocouples inserted into one tube. Temperature – 'unit enthalpy' curve derived from DSC and NewMass unit thermal capacity to allow corresponding 'unit enthalpies' to be read from corresponding unit temperatures. Air extracted at 14.9 l/s with an inlet temperature of 17 °C.	Unit temperatures only fell by 3 °C during the 7 hours and 22 minutes of heat discharge.	Low rate of discharge from units due to a low heat transfer coefficient of 1.0 W/m ² /K and a low temperature difference between the NewMass units and the surrounding air. Low heat transfer coefficient most likely due to flow of air across rather than between fins.

5.	Reveal the rate and depth of discharge in active discharge mode.	As above in terms of internal thermocouples and a temperature-‘unit enthalpy’ curve. Chilled water delivered at 10 °C and 3 l/min	Extremely rapid discharge of heat resulting in a unit temperature of 14.9 °C after 3 hours and 13.6 °C after 16 hours of discharge.	Chilled water system extremely good at discharging heat. Lower limit of discharge temperature reached due to fabric gains at lower temperatures.
6.	Determine whether the predicted convection cycle was effectively established in the room.	Position columns of thermocouples in the cell above the heater, in the centre of the room and intersecting the NewMass units. Verify air flow pattern with CFD model of cell. (CFD work conducted by William Couch, Masters student.)	Evidence of a convection current is clear with the centre of the room and intersecting the NewMass units showing conventional stratification while air above the heater shows the inverse.	The NewMass units function well, reducing the temperature of the air around them causing it to sink and cool the room.
7.	Establish whether the Raschig rings had the desired effect of greatly reducing the temperature variation across an individual NewMass unit.	Internal thermocouples inserted into one tube. Calculation of thermal conductivity according to equation governing radial heat transfer in a cylinder	In all charging and discharging modes the temperature of the units varies very little within a single unit. A conductivity of 3.4 W/m/K was found with temperature and heat transfer data from active discharge.	The Raschig ring/A22 hybrid transfers heat very effectively. The surface temperature is kept to a minimum in charging and a maximum in discharging, thus promoting heat transfer.

8.	Assess the relative performance of the system in passive cooling mode through comparison of room temperature control to the Energain panel and RACUS tile.	Identical conditions to the tests conducted on the other 2 products established with internal temperature monitoring for comparison.	NewMass suppresses the air temperature rise similarly to the Energain panels and RACUS tiles. A noticeable increase in temperature profile gradient occurs at around 14:30.	The system performs as well as the other products for the majority of the day. The steepening in temperature profile indicates exhaustion of thermal capacity.
9.	Assess the relative performance of the system in supplemented passive cooling mode through comparison of room temperature control to Energain and RACUS.	Identical conditions to the tests conducted on the other 2 products established with internal temperature monitoring for comparison.	NewMass air temperature follows the same profile as in the unsupplemented passive cooling case but a significant difference is observed after the chilled water system is engaged.	The comparison to the other products tested shows that with supplementary cooling the NewMass system performs far better than the other products in terms of temperature control.
10.	Obtain combined convective and radiative heat transfer coefficient profile for passive cooling mode.	Enthalpy variation in each unit used as measure of heat flux through the finned tube envelope.	The heat transfer coefficient was shown to decrease over the period from 24.1 to 0.4 W/m ² K.	The heat transfer coefficient is partly determined by the rate of flow of air across the tubes. This decreases as the units warm and the convection cycle speed is reduced.
11.	Obtain combined convective and radiative surface heat transfer coefficients for supplementary passive cooling mode.	The steady state conditions and no fabric gains/losses meant that all heat from the heater was absorbed by the NewMass units. Thus a heat transfer coefficient could be easily calculated.	A near constant 5.44 W/m ² K was obtained and confirmed by an equal heat transfer rate to the chilled water.	The heat transfer coefficient is slightly higher than that predicted due to the movement of air creating a forced convection condition.

12.	Use the obtained heat transfer coefficients and thermal capacity of the system to model the system and establish energy savings that could be expected of the system over a year in a typical UK office building	A model based on an annual cooling load for a typical UK office used an air-NewMass energy balance, along with obtained heat transfer coefficients and discharging controls to predict the energy savings over a year.	34% savings were predicted for a UK office.	The system has potential to dramatically reduce the energy consumed in cooling buildings.
------------	--	--	---	---

As well as results to satisfy the objectives detailed above, supplementary data was gathered to further inform the system analysis. This includes data such as the room temperature during active discharge mode. These results are presented alongside the main results to aid system understanding.

8.1 Calculations and modelling

This section describes the derivation of the NewMass unit temperature-enthalpy curves, the calculation of the heat transfer coefficients during different modes of operation and the structure of the energy savings model.

8.1.1 Temperature-enthalpy curves

The relationship between the temperature of each unit and the thermal energy they contained at any one time was sought in order to satisfy two objectives. Firstly it allowed the tracking of the NewMass unit enthalpy through the temperature measurements recorded within and on one unit. This meant that the heat transfer

coefficient at each moment could be derived. Secondly, it allowed for the construction of the annual energy savings model described in the following section. The DSC curves obtained for A22, and presented in chapter 2, provide data on the temperature of a sample and the heat flowing in or out of that sample on a second by second basis. This is presented in Figure 8.1 for the example of melting.

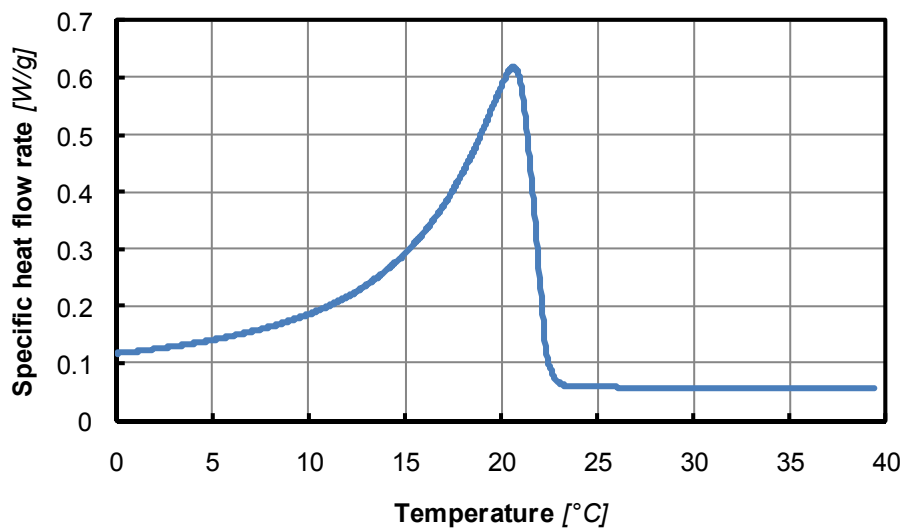


Figure 8.1 Specific heat flow vs. temperature for a DSC sample of A22 during melting at 2°C/min. All values below 0°C have been omitted since they are not required for the following analysis.

By cumulatively summing the heat flowing into the sample at each temperature we find a relationship between the thermal energy stored by the sample and the temperature of that sample.

$$H_T = h_{ref} + t \sum_{T_{ref}}^T \frac{\dot{Q}_T}{m_{A22,sample}} \quad (8.1)$$

Knowing the amount of PCM in the NewMass unit means we can extend this relationship to the heat that has flowed into the PCM in a unit, given its temperature. Furthermore by knowing the specific heat capacity and mass of aluminium we can extend this relationship to represent the entire NewMass unit – see Eq. 8.2 and Figure 8.2.

$$NM_T = m_{A22,NM} \left(h_{ref} + t \sum_{T_{ref}}^T \frac{\dot{Q}_T}{m_{sample}} \right)_{A22} + m_{Al,NM} C_{p,Al} (T - T_{ref}) \quad (8.2)$$

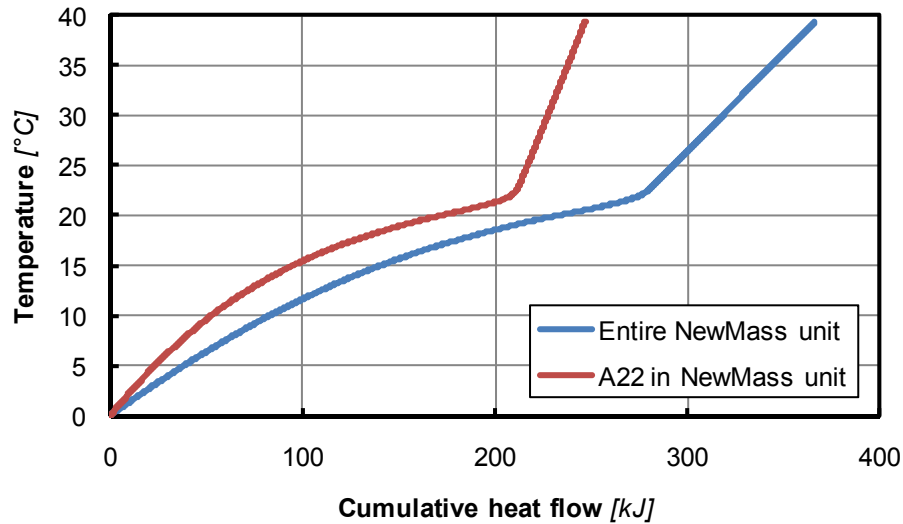
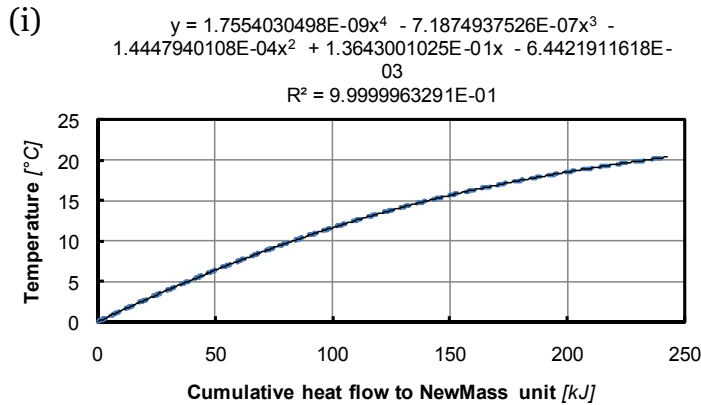


Figure 8.2 The cumulative heat flowing into and being stored by the NewMass unit, in terms of the A22 alone and the entire unit including all aluminium elements.

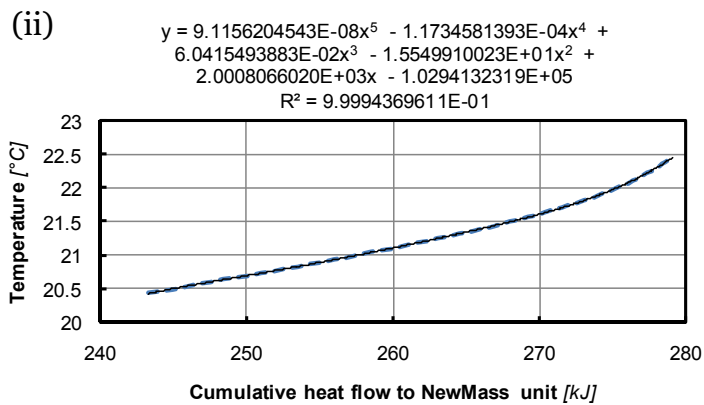
The blue curve shows how the NewMass unit will absorb heat at an ever decreasing rate until it reaches the point when all latent capacity has been absorbed and the rate of heat uptake becomes proportional to the temperature rise. The reason why the curve's gradient decreases during heating at lower temperatures is because the A22 absorbs ever-increasing amounts of heat as the temperature rises; as shown in Figure 8.1. The characteristic shape of the blue curve will be seen later in the chapter because, as should be expected, the temperature profile of the monitored unit is the same shape.

This curve can be seen to be formed of 3 sections: The gradually plateauing curve seen between 0 and 20.4 °C, the elbow, which only occurs between 20.4 and 22.46 °C, and the straight line between 22.46 and 40 °C. By splitting the curve into 3 sections we may accurately describe the relationship between unit temperature and its accumulated thermal energy as described by 3 polynomials. These are displayed in Figure 8.3.

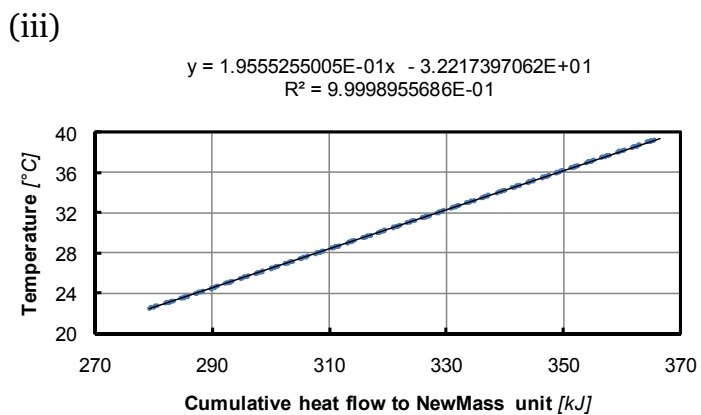
Figure 8.3 Polynomial curve fittings for the temperature-enthalpy melt curve of a NewMass unit. Dashed blue line: original curve. Black line: fitted function.



(i) 'Plateauing curve section'.



(ii) 'Elbow curve section'.



(iii) 'Straight line curve section'.

The polynomials may then be used to calculate the temperature of a NewMass unit given its enthalpy. Corresponding polynomials were derived to calculate the enthalpy of a unit with a given temperature. The equivalent curves were then also produced for cooling.

This method is seen as an improvement on the step function approach for representing the transition from sensible to latent cooling (and vice versa), as seen in the enthalpy porosity model employed in the Passive PCM Sails tests in chapter 5 and the research conducted by Ahmad et al. (Ahmad *et al.*, 2006). Here, the actual variation of enthalpy with temperature is much more closely approximated.

8.1.2 Heat transfer coefficient

From chapter 7, the heat transfer coefficient for a natural convection condition was predicted to be 2.31 W/m²K, as an average across the NewMass unit surface. The heat transfer coefficient was derived from experiment in two ways:

Firstly, it was calculated by deriving the internal energy rise of the units from their temperatures over successive time steps, using the Eq. 8.2. The rise in internal energy was equal to the heat transferred across the units' surface and by also recording the air temperature, Eq. 8.3 could be applied to find the heat transfer coefficient.

$$\dot{Q}_{NM_s} = hA_{NM} (T_{air} - T_{NM}) \quad (8.3)$$

This method allowed the heat transfer coefficient to be calculated over discrete time step periods of 1 minute, corresponding to periodic temperature recordings. The second method of derivation was to establish steady state conditions in the test cell by finding an equilibrium point at which the air in the test cell was close to the air temperature outside it and removing heat from the cell, through the chilled water circuit, at the same rate that it was being applied from the heater. With the system in equilibrium and no heat flux across the walls, since internal and external temps are equal, the heat flow in the cell passes from the heater to the air, from the air to the finned tubes and PCM and from there to the water flowing through the axial pipe. All heat flow rates are equal to the heater output so we therefore have an

opportunity to evaluate the heat flux and the heat transfer coefficient, for the finned tube surfaces and the axial water pipe, since we know the air temperature, PCM temperature and water temperature.

8.1.3 Effective thermal conductivity

Within the NewMass unit envelope, the A22/Raschig ring hybrid material is a cylinder and radial heat transfer is governed by Eq. 8.4.

$$\dot{Q}_{NM} = 2k_{effective}\pi L_{NM} \frac{T_1 - T_2}{\ln(r_2 / r_1)} \quad (8.4)$$

Here 1 and 2 refer to points and lesser and greater radii, respectively in the NewMass unit. The temperature at these points was measured with internal probe thermocouples that penetrated 15 cm into one of the units at either end, as described below. At each end two thermocouples are located in the same horizontal plane, one 7 mm from the axis and the other at the tube edge 25.4 mm from the axis. These thermocouples are labelled LH,L , LH,R , RH,L and RH,R in Table 8.5 and Figure 8.9 below. When the chilled water circuit was activated for night time active discharge the water temperature at the inlet and outlet were also monitored. As the flow rate of 3 l/min (divide by 6, the number of units) was known, the heat transferred to the water was calculated according to Eq. 8.5.

$$\dot{Q}_w = \dot{m}_w C_{P,w} (T_{out} - T_{in}) \quad (8.5)$$

The heat must be flowing into the chilled water at the same rate as it is being absorbed by the finned tube envelope if thermal equilibrium is established. Therefore Eq. 8.4 was able to be applied to allow the effective thermal conductivity of the hybrid material to be calculated.

8.1.4 Annual energy savings model

Energy savings are calculated using a purpose built heat balance model that represents a NewMass system installed in a UK office building.

To obtain a representative cooling load profile an IES model of an 8 storey, 3200 m² building with a simple cuboid geometry, 3.5 m storey heights and 40% glazing ratio was produced.

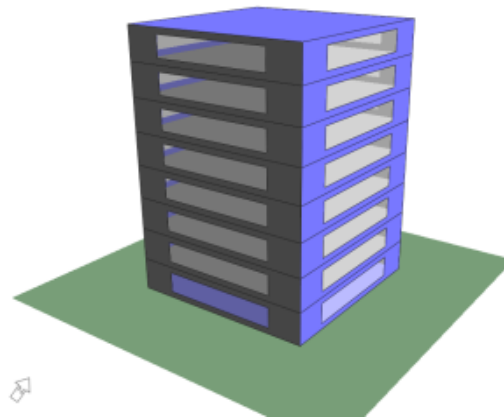


Figure 8.4 IES UK office model geometry.

The limiting values for fabric performance were selected from UK 2010 Building Regulations Part L2A:

Table 8.2 Fabric element specification (HM Government, 2010).

Element	U-value (W/m ² /K)
Roof	0.25
Wall	0.35
Floor	0.25
Windows	2.2 [g-value = 0.68]

Internal gains were established according to the ASHRAE 90.1-2007 standard profiles for lighting, equipment and people (ASHRAE, 2008). Maximum heat gain values were taken from CIBSE guide A:

Table 8.3 Heat gains (Arnold, 2006).

Heat source	Sensible heat gain (W/m ²)
People (at 12 m ² /person)	6.7 [Latent gain 5 W/m ²]
Lighting	12
Equipment	15

The model was run at hourly time steps for an entire year with London climate data. The hourly cooling plant load for the entire building was then selected from the results. This was then considered as the heat source in the following heat balance:

$$Q_{air_i} = Q_{air_{i-1}} + t(\dot{Q}_{hs} + \dot{Q}_{NM_s} + \dot{Q}_{NA})_i \quad (8.6)$$

Over 60 second time steps the heat balance establishes the amount of heat that flows into the room air. As well as heat sources the space is considered to have two heat sinks: the NewMass units and the night air. The change in air temperature is found by summing the heat gains, the heat gained/lost to the NewMass units and the heat lost through the influx of cool air at night. This is then multiplied by the heat capacity of the air.

$$T_{air_i} = T_{air_{i-1}} + \frac{Q_{air_i}}{C_{P,air} m_{air}} \quad (8.7)$$

The NewMass units are subject to their own heat balance which sees them exchanging heat with the air and the chilled water circuit when activated.

$$Q_{NM_i} = Q_{NM_{i-1}} - t(\dot{Q}_{NM_s} + \dot{Q}_w)_i \quad (8.8)$$

The model divides all 24 hour periods into daytime, 9:00am to 12:00am and night time, 12:00am to 9:00am. During the daytime the chilled water circuit is set to engage when the air temperature in the room exceeds 25 °C. Up until that point, or if 25 °C is not reached, the heat balance only evaluates the heat exchange between the heat gains the air and the NewMass tubes; operation is passive. The rate of heat exchange between air and NewMass unit is determined by Eq.8.9.

$$\dot{Q}_{NM} = N_{NM} h_{NM} A_{NM} (T_{NM} - T_{air}) \quad (8.9)$$

The heat transfer coefficient in this equation was that found in the NewMass tests. At each time step (duration 1 minute) it is the difference between the previous time step's air and NewMass temperatures that dictates the rate of heat flow in that time step. Air and NewMass temperatures are then rederived according to Eq. 8.7 and the temperature-enthalpy curve polynomials described above.

When the chilled water system is engaged it regulates the air temperature at a constant 24.5 C as found in the NewMass tests. At 12:00am the model sees the circulated external air as a negative load due to the difference between its temperature, obtained from the weather file, and the temperature of the internal air. This lowers the air temperature and allows the NewMass units to discharge their accumulated heat. If the units do not reach a sufficiently low temperature by 6:00am then the chilled water circuit is engaged at a flow rate of 0.5 l/min/unit to discharge any remaining heat.

The heat exchanged with the chilled water is evaluated by considering the temperature gain in the water to rise in proportion to the distance travelled. This means that the mean temperature of the water in the tube at any one time, T_{mean} , is equal to the average of the inlet and outlet temperatures, T_{in} and T_{out} , respectively. Assuming a mean temperature for the NewMass unit, $T_{NewMass}$, as well, the following two equations obtain for the rate of heat transfer between NewMass unit and flowing chilled water:

$$\dot{Q}_w = h_{Pipe} A_{Pipe} (T_{NM} - T_{mean}) \quad (8.10)$$

$$\dot{Q}_w = \dot{m}_w C_{p,w} (T_{out} - T_{in}) \quad (8.11)$$

Here A_{Pipe} is the wetted area of the aluminium chilled water pipe within the NewMass unit, 197.0 cm² (pipe internal diameter equal to 6.27 mm). The heat transfer coefficient was obtained from experiment, as described in section 8.3.2. Values for the inlet temperature and mass flow rate were demonstrated as being correct for desired temperature control through experiment as well. The temperature of NewMass units are found through the procedure just described.

Since we assume that T_{mean} equals the mean of the inlet and outlet temperature only two unknown parameters remain, the heat transfer rate and the outlet temperature. Being simultaneous equations these values may be easily derived. The required cooling power over any time step is then simply the product of the time step length and the heat transfer rate. Every time the system is forced to engage the chilled water system the energy required to deliver that coolth is calculated with reference to the equations describing the performance of a Trane CGAN 900 chiller, as described in the active system study in chapter 5. This provides input power data for any load and any external air temperature. The energy required to provide cooling from a conventional system is calculated with reference to the same equations but using the cooling plant load simply as it was obtained from the IES results. Pumping energy will vary in each case due to necessary service plans. It is accounted for here by taking a typical cooling capacity to pumping ratio for a fan coil system, in the conventional case, and a chilled beam system, in the NewMass case. These were obtained from the China Shipping House data. The ratios were multiplied by the maximum cooling load and applied for each minute of operation to approximate pumping energy input. The NewMass input energy is the subtracted from the conventional cooling system input energy, over the year, to obtain a value for total energy savings associated with the system.

8.2 System assembly and installation

8.2.1 Unit assembly

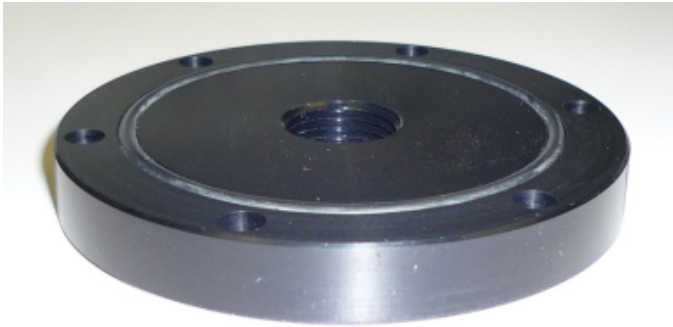
Assembly of the complete NewMass units was undertaken so that no leaks occurred and all elements could either be weighed or have their weights calculated.

For each tube assembly began with insertion of the O-ring into the groove in the end cap and then the fixing of the end cap onto the finned tube by screwing on nuts and washers to the exposed studs. The thread of the 3/8" Swagelok/NPT fitting was then wound with PTFE tape and screwed into the threaded central hole in the cap until tight. The 3/8" axial chilled water pipe was passed down the finned tube and out of

the Swagelok fitting so it protruded 60 mm, whereupon the Swagelok fitting was tightened to give good contact between the teflon ferrules and the chilled water pipe.

Figure 8.5 Stages in the NewMass unit sealing process

(i)



(i) End cap with O-ring inserted.

(ii)



(iii)



(ii) End cap screwed onto one finned tube end and the 3/8" Swagelok fitting screwed in with PTFE tape.

(iii) Chilled water pipe protruding 60 mm from the Swagelok fitting and tightened onto the aluminium pipe.

The precise mass of the paraffin added to each tube was found by subtracting the sum of the completed empty tube mass (tube itself, end caps, O-rings, chilled water pipe, Swagelok fittings, studs, nuts and washers) and the Raschig ring's mass from the mass of the completed filled tube. This was deemed to be a more accurate measure than pouring in a known mass of A22 since the liquid has a tendency to cling to any vessel's surface, meaning the poured volume is never the measured volume. The potential for any splashes and spillages could have further added to the inaccuracy.

Therefore, before filling with Raschig rings and A22, each tube was weighed. Both tube ends were completed (without tightening the second set of ferrules and nuts) in order for this to happen.

The loose end cap was then removed to allow the Raschig rings to be poured in. This was done in batches of known weights until the rings reached up to 4.5 cm from the top of the tube to give space for the air pocket described in chapter 7. The paraffin was then poured in until it reached the level of the Raschig rings. The remaining space was then filled with Raschig rings and the other end cap was fitted.

The tube was weighed again and the volume of PCM was calculated. This procedure was applied to 5 of the 6 NewMass units constructed. The resulting component mass for each tube is detailed in Table 8.4.

Table 8.4 *Masses of all NewMass units and their main constituents. All figures in kg.*

Tube	Total	Empty tube	Raschig rings	A22
1	4.585	2.485	0.869	1.230
2	4.540	2.467	0.877	1.196
3	4.565	2.480	0.888	1.197
4	4.575	2.490	0.871	1.214
5	4.575	2.495	0.889	1.191
6	4.740	2.495	0.960	1.256
Total	27.580	14.912	5.354	7.285

The difference in tube filling procedure for the 6th tube was due to internal thermocouples (detailed in section 8.3.1 on controls and monitoring) inserted to monitor the temperature of the unit through charging and discharging phases. In this case guide-holes for each thermocouple were formed from short lengths of malleable aluminium wire and fixed to the chilled water pipe with small jubilee clips – see Figure 8.6.

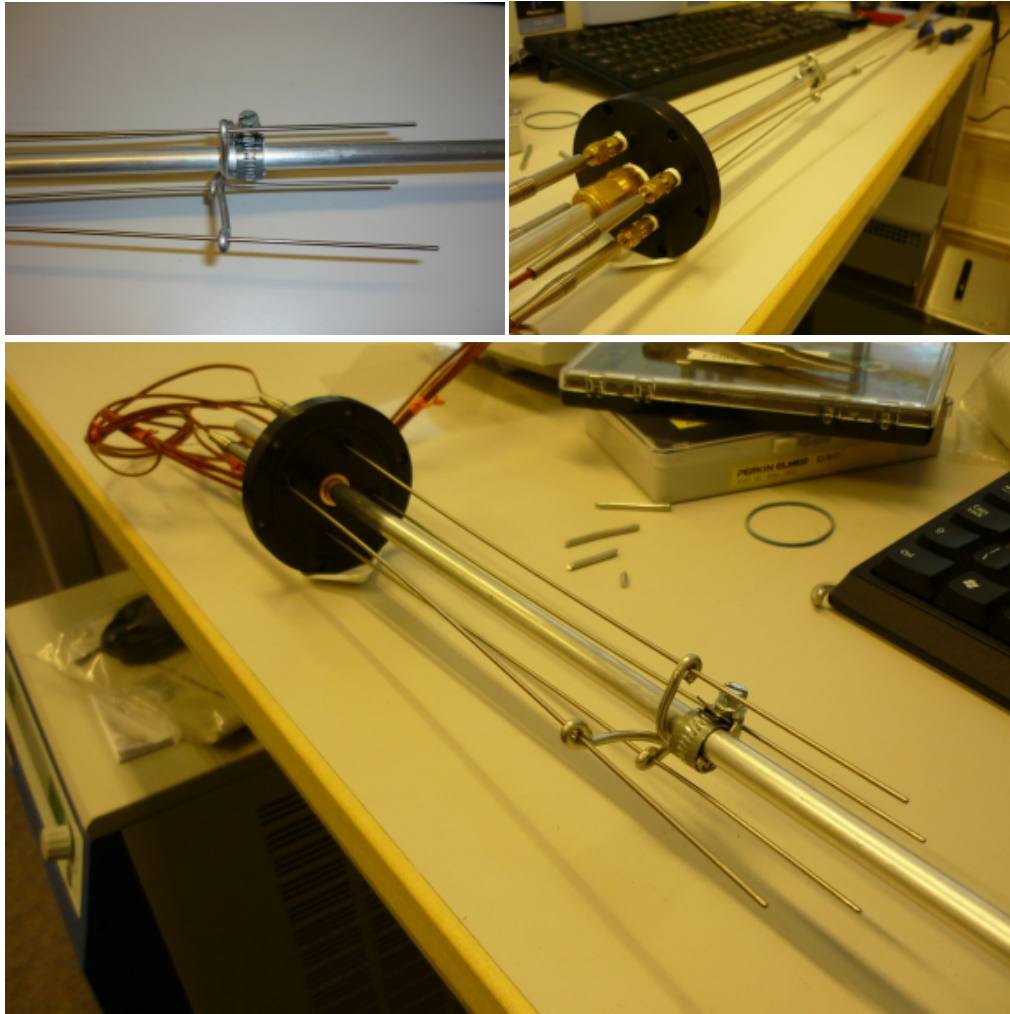


Figure 8.6 *The internal thermocouples and guide holes in unit 6.*

The exact location of the thermocouples in the end cap is displayed in Figure 8.7.

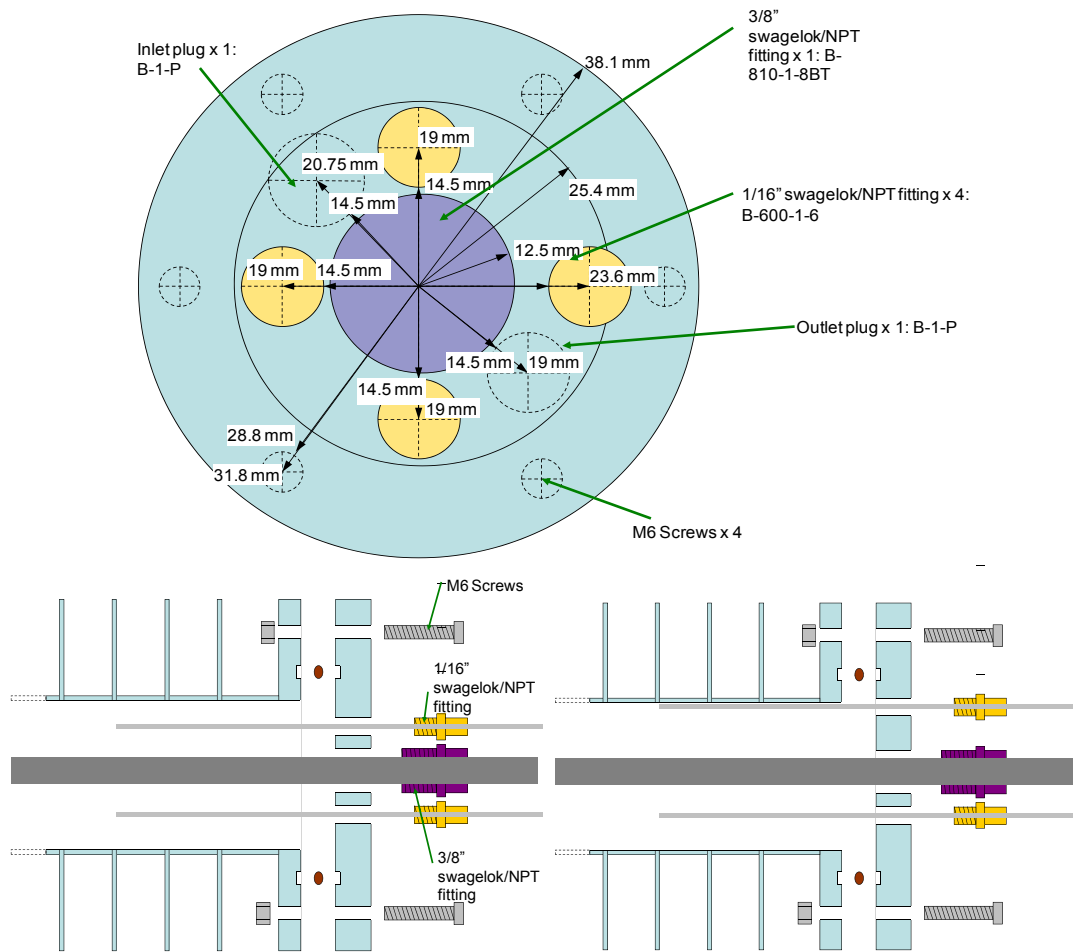


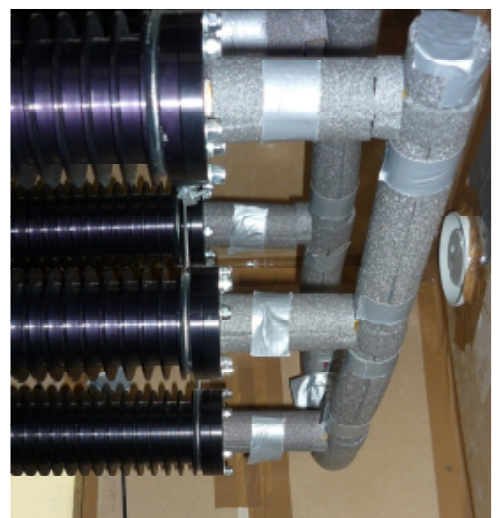
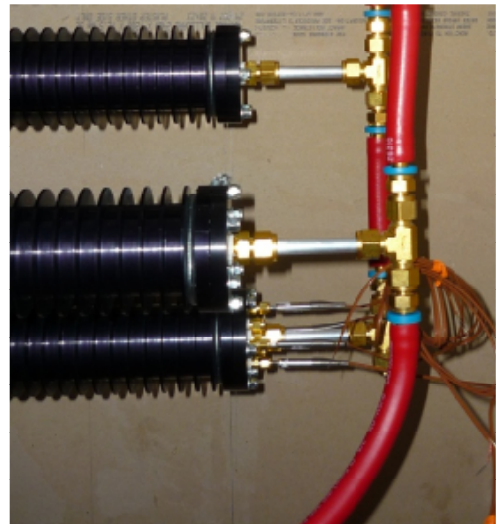
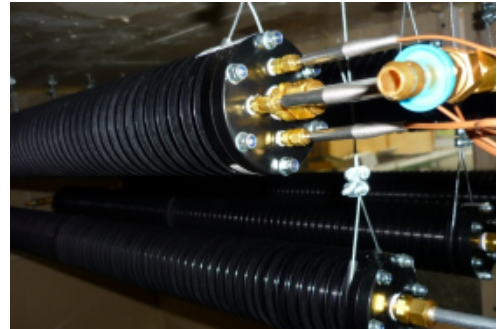
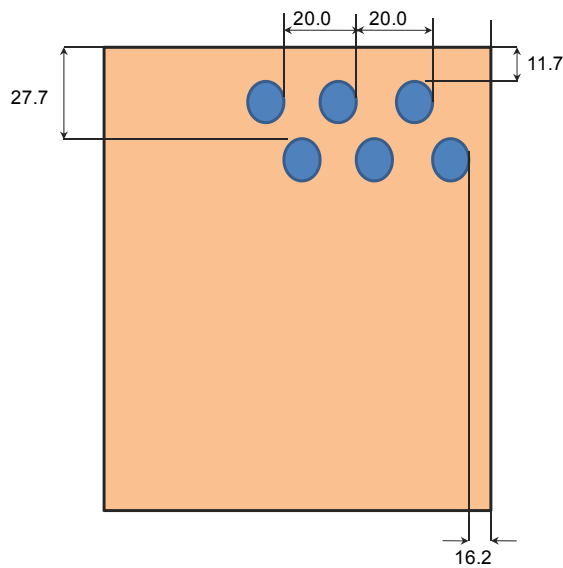
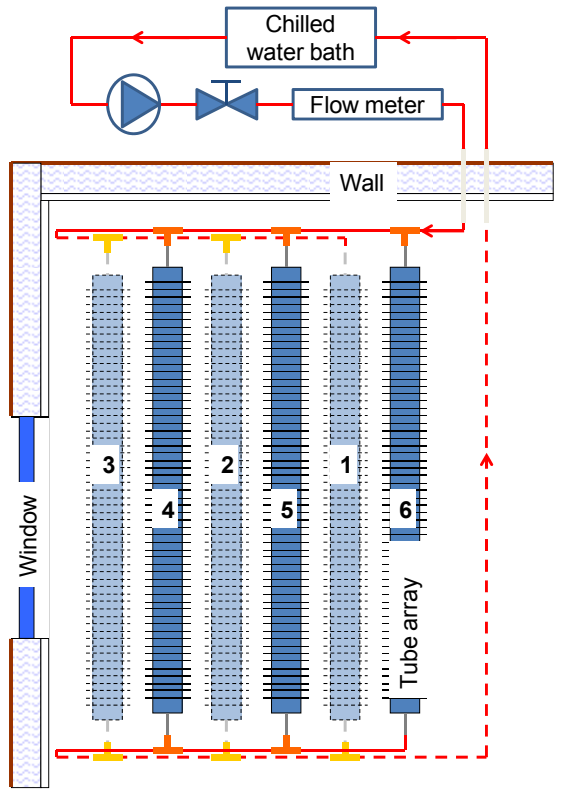
Figure 8.7 End cap with thermocouple design. Top image displays end caps design with ‘turning circles’ for all fittings. The bottom left image is a section view of the cap and the right is the plan view.

One end cap was fitted to the finned tube and chilled water pipe with the thermocouples in place. The tube was then filled with Raschig rings until they reached 15cm from the top. The remaining end cap was then lowered into position over the chilled water pipe and care was taken to ensure that the thermocouples found their guide holes. Before the cap was bolted on, the paraffin was poured in until it reached the equivalent height to 4.5 cm from the top. The cap was then bolted on and the remaining Raschig rings were inserted through purpose-cut holes in the cap. When the tube was full plugs were screwed into the holes, sealing the tube. It was then weighed. On to the end of each unit was attached a tee-piece. The tubes were now ready for installation.

8.2.2 Unit installation

The units were hung at 10 cm intervals in the cell using steel rope. Each unit was then connected to the adjacent unit in a reverse return arrangement – see Figure 8.8. This meant that the system was balanced with respect to water flow, meaning all tubes would receive the chilled water at the same rate. Inlet and outlet tubes were installed in the test cell walls and the units were connected, via these, to the chilled water system outside.

Figure 8.8 *NewMass system schematic, tube locations and images of the installation at stages of hanging, connection with hosing and insulation.*



8.2.3 Chilled water system

The chilled water system was comprised of a Cole-Parmer 6l polystat R6L chilled water bath, a Cole-Parmer 19 l/m pump (RZ-72010-25), a 3/8" Swagelok needle valve (B-1RS6), a Cole-Parmer 1.8 – 18 l/m inline flow meter flow meter (RZ32470-03) and the required connective hosing and connectors.

8.3 Main test method

Due to unavoidable maintenance work being carried out on Brunel's environmental chamber it was not possible to conduct tests on the NewMass system there. Instead an appropriate environment was found in the newly refurbished aeronautics laboratory. All system tests were conducted there, where external conditions were controlled to correspond with the tests that had been conducted in the climate chamber previously. This section describes those tests.

8.3.1 Controls and monitoring

System control may be split into three categories:

- External air temperature.
- Test cell heat gains ventilation.
- Chilled water system.

The external air temperature was controlled by three radiant heating sails that are centrally controlled by a Trend BMS system. Room heating adjustments were therefore requested from estates management, as and when required. Additional control of the external room temperature was achieved through the natural ventilation of excess heat, through high level windows, and the addition heat from a Dimplex RD 2009 H electric heater with a maximum output of 2000W.

Air temperature was monitored at 3 locations around the cell; see Table 8.5. For charging this was maintained at 25 °C (maximum divergence of ± 1 °C) and for passive discharging the air temperature was maintained at 17 °C (maximum divergence of ± 1 °C).

The test cell was heated and ventilated with the equipment detailed in chapter 6.

The monitoring of the system and test cell consisted mainly of thermocouples, the location of which are detailed in Table 8.5 and Figure 8.9. Most were the same type as described in chapter 6 with the exception of the eight thermocouples located inside unit 6. These were Omega type K 150 mm sheathed probe thermocouples. The hukesflux sensors described in chapter 6 were also employed to monitor the flow of heat across the test cell envelope.

Table 8.5 Thermocouple locations.

Region	Location	Code
Inside monitored unit	Right hand side (facing window), top	RH,T
	Right hand side (facing window), left (facing cap)	RH,L
	Right hand side (facing window), bottom	RH,B
	Right hand side(facing window),right(facing cap)	RH,R
	Left hand side (facing window), top	LH,T
	Left hand side (facing window), left (facing cap)	LH,L
	Left hand side (facing window), bottom	LH,B
	Left hand side (facing window), right (facing cap)	LH,R
Surface monitored unit	Central fin	FT6,F
	Central base tube	FT6
	Right hand (facing window) base tube	FT6,R
	Left hand (facing window) base tube	FT6,L
Unmonitored units	Unit 5 base tube	FT5
	Unit 4 base tube	FT4
	Unit 3 base tube	FT3
	Unit 2 base tube	FT2
	Unit 1 base tube	FT1
Water temperatures	Unit 6 inlet	FT6,WPR
	Unit 6 outlet	FT6,WPL
	Unit 6 outlet (internal)	LH,WO
	Water bath	WB
Internal air	Above heater (close)	ALL,H
	Above heater (medium)	AML,H
	Above heater (high)	AHL,H
	Room centre (low)	ALL,C
	Room centre (medium-low level)	AM-LL,C
	Room centre (medium)	AML, C
	Room centre (high)	AHL, C
	Below units (low)	ALL, FT
	Below units (medium)	AML, FT
	Below units (high)	AHL, FT
	Between unit levels	ABFT
Above units	AAFT	
External air	Window wall	EAWW
	Door Wall	EADW
	Logger wall	EALW
Radiant temperature	Globe thermometer	GT
Ventilation	Inlet	AI
	Outlet	AO

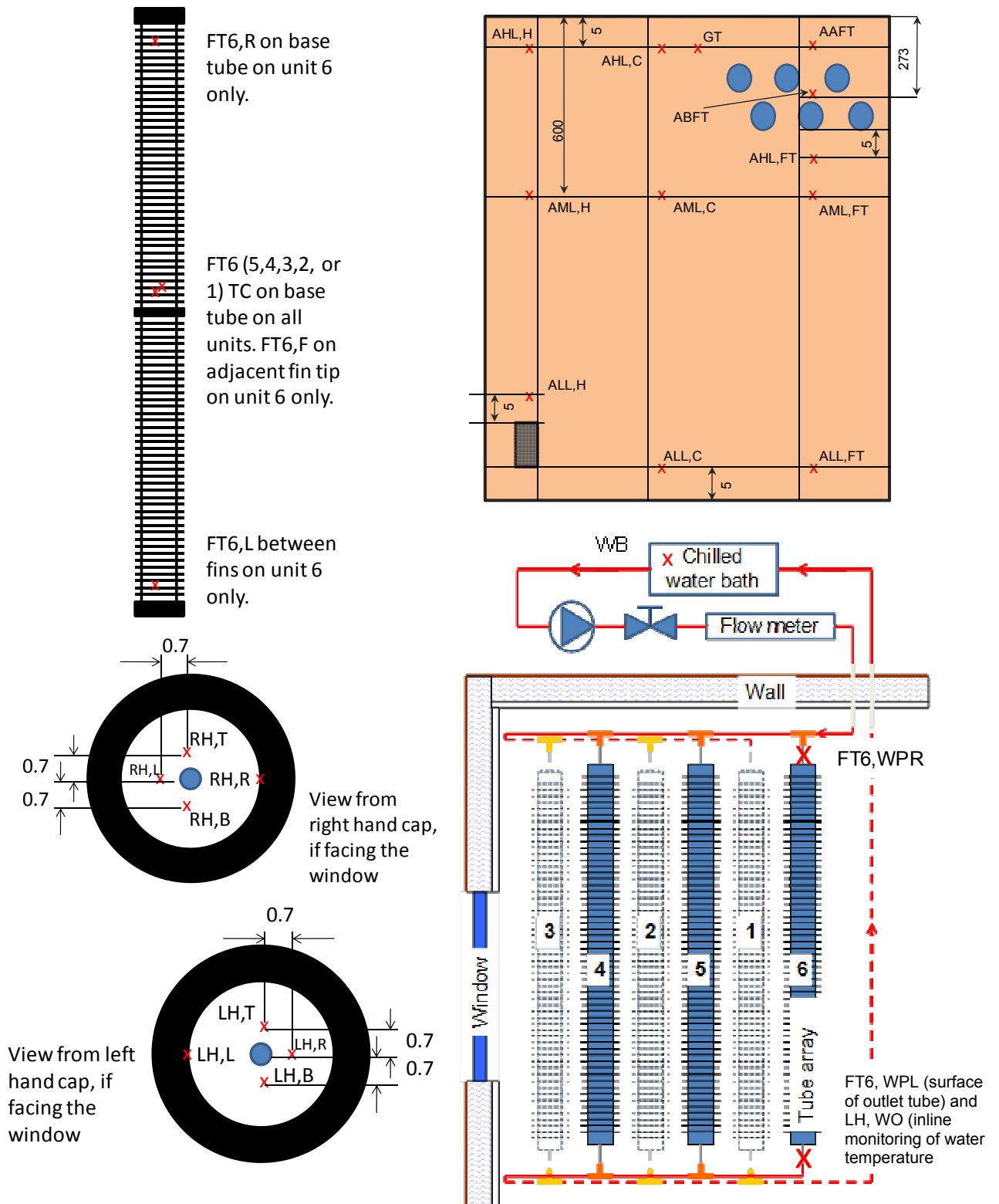


Figure 8.9 Thermocouple locations, each marked with a red x and labelled consistently with Table 8.5. Thermocouples inside unit 6 all penetrated 15cm into the tube.

The chilled water system temperature was controlled through adjustment of the set point in the chilled water bath. The flow rate was controlled with the needle valve.

With the system installed the flow rate range was obtained before full charge and discharge tests could commence. This was done by switching on the pump and chilled water bath and observing the flow rate with the control valve fully open. The range was found to be 0 – 3.1 l/min, as measured by the flow meter. Before the full charge and discharge tests commenced the pipe network, connecting the chilled water bath to the pump and the flow meter, was adjusted so as to reduce the pressure drop in the system and achieve a higher flow rate. The result was a range of 0 – 3.85 l/min.

The flow meter had been previously calibrated by timing the flow of water into a volumetric flask. The readings given by the flow meter were found to be correct as the following table shows:

Table 8.6 Results from flow meter calibration

Volume delivered (l)	Time taken (s)	Flow rate (l/min)	Flow meter reading (l/min)
1	12.6	4.8	4.8
1	30.0	2.0	2.0
0	-	0	0

8.3.2 Test Procedure

The tests performed consisted of a series of thermal charge and discharge operations designed to establish how the NewMass system performs and to derive the parameters required for the understanding and modelling of the system:

- Passive charging.
- Supplemented passive charging.
- Passive discharging.
- Active discharging.

Due to the fact that the location of the tests could not be controlled overnight all discharge tests were done during the day. This meant that combined, continuous charge and discharge cycles were not possible.

The first test performed was the passive charging test. In preparation the chilled water circuit was engaged at 3 l/min and 6 °C during the previous night. This ensured the PCM was appropriately discharged. Allowing the PCM to reach a low temperature through discharge to the air was not possible because the external space's temperature had to remain elevated so that charging conditions could be immediately enacted in the morning of the test.

The test was started by first ensuring the external temperature was at 25 °C. The chilled water bath and pump were then turned off, the heater was engaged at full power and data logging began. The ventilation intake and outlet were both capped the entire time. Data was then simply logged every minute while the external temperature was controlled to stay between 24 and 26 °C, until the end of the day.

In order to confirm the anticipated air flow and derive a heat transfer coefficient numerically, as opposed to Tsubouchi and Masuda's empirically derived method presented in chapter 7 (Tsubouchi and Masuda, 1970), an ANSYS FLUENT model of the test cell with NewMass units and heater was constructed by Masters student, Will Couch, according to my instructions (Couch, 2010). A steady state model room condition was modelled to capture the likely air movement and heat transfer over a discrete time period during the charging process. The period targeted was the critical time at which the contained paraffin has reached its melting peak; thus absorbing most heat per unit temperature rise but very close to latent capacity exhaustion. The model consisted of a cuboid geometry conforming to the test cells dimensions. The walls were assumed to be adiabatic since the internal temperature should equal the external temperature (i.e. both at 25 °C) if the system is performing correctly at the critical moment described; therefore no heat flux across the envelope. The fluid contained was assigned the thermophysical properties of air and a gravity condition was applied. The solver was then able to account for buoyancy driven flow. The heater was set to produce the maximum 150W of heat from its surface and the NewMass units' temperature was set to 20.6 °C, corresponding to the peak melt temperature of the paraffin; see Figure 8.1. The results for air velocity, temperature and convective heat transfer coefficient obtained are presented in section 8.4.1.

The assisted passive charge test followed exactly the same procedure as the passive charging test until the temperature in the centre of the cell reached 25 °C. At that moment the chilled water system was engaged, providing 13 °C water at 2 l/min. In a full scale installation the system would be engaged automatically by thermostat. The aim here was to control the temperature in the room before it exceeded a thermally comfortable level.

The temperature and flow rate of the system provided heat extraction equal to the heat gain in the cell to establish thermal comfort conditions. Both the temperature and flow rate of the water determine the rate of discharge from the NewMass units, as shown in Eq. 8.11. To maintain a constant temperature within the test cell the water flowing through the NewMass units had to remove the same amount of heat as that being added by the heater, 129 W. With 6 units in total each unit had to remove 21.5 W. For laminar flow in a cylinder, a commonly accepted Nusselt number of 3.66 may be used to derive the heat transfer coefficient from Eq.8.12

$$Nu = \frac{h_{pipe} D_{pipe}}{k_w} \quad (8.12)$$

A value of 338 W/m²/K was obtained and by assuming a predicted NewMass unit temperature of 16.7 °C (3 °C higher than the average temperature found when discharging at 10 °C) Eq.s 8.10 and 8.11 were used to try combinations of inlet temperature and flow rate that were located within the operational range of the chilled water bath and pump and would achieve the required rate of heat removal and.

In order to control the temperature for passive discharge the PCM units were heated rapidly by circulating 30 °C water and switching on the heater. Once the PCM reached 28 °C and the external air temperature had settled to 17 °C the heater and water system were switched off, the ventilation duct caps were removed, the fan was engaged at full power and data was logged throughout the period.

In a full scale installation active discharge would be enabled when the passive discharge process is insufficient to cool the PCM. The external temperatures are

therefore high and so in this case the surrounding temperature is not reduced to 17 °C. Because the external air temperature did not have to be controlled for this test it was conducted overnight. Initial conditions were those found at the end of a typical passive charge period. The test began with the heater being turned off and the chilled water system being engaged at 10 °C and 3 l/min. Ventilation duct caps were in place.

8.4 Results

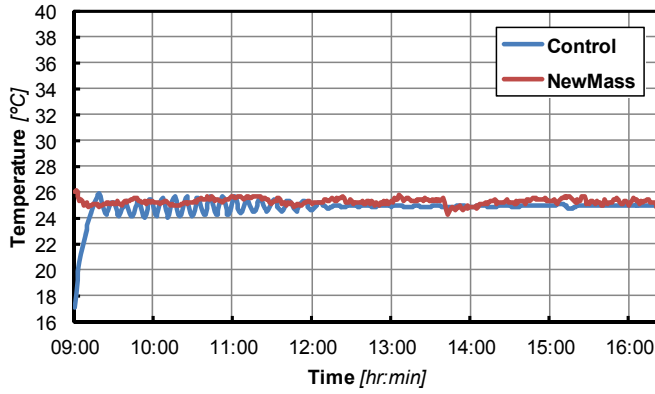
Results are divided into sections corresponding to the operation modes described in the previous section with a dedicated energy savings section at the end. In the passive charging, supplemented passive charging and passive discharging cases comparison to the corresponding control test is made to indicate system performance. This is then explained in terms of the various system parameters monitored and comparisons are made to the previous product tests. A corresponding control test is not required in the active discharge case since an equivalent active discharge without PCM is not possible. Therefore results of the active discharge are discussed mainly in terms of the system's ability to reduce the temperature of the PCM sufficiently.

8.4.1 Passive charging

Figure 8.10 shows comparisons between air in the test cell, with and without the NewMass system installed, for two heights. The globe thermometer temperature in both cases is also shown. In order to justify the comparison the profiles of the mean external temperatures in both cases is shown in the first graph presented.

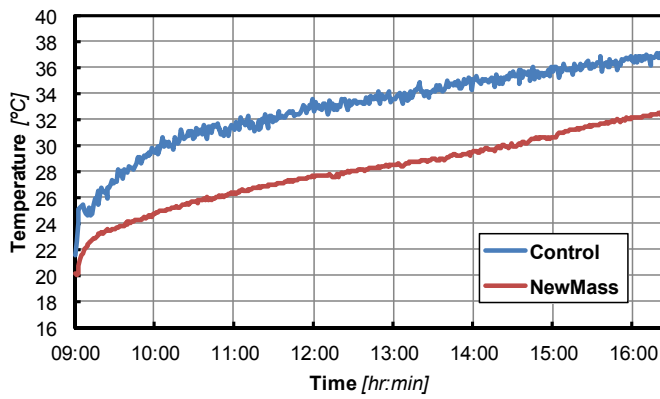
Figure 8.10 NewMass and control comparison for passive charge period.

(i)



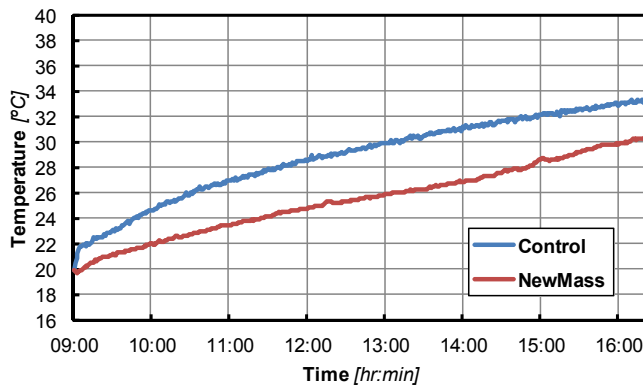
(i) Mean external temperature profiles.

(ii)



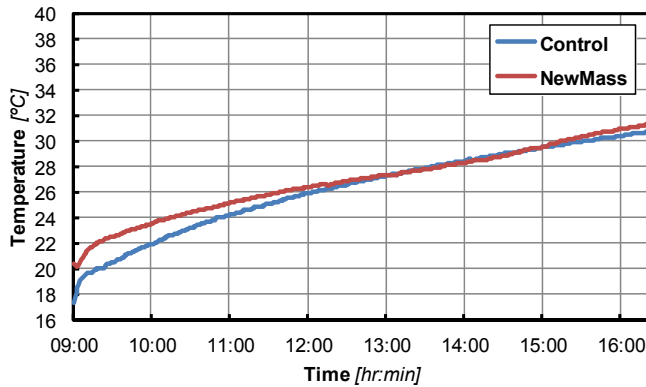
(ii) Internal air at high level temperature profiles (AHL,C in Figure 8.9 and Table 8.5).

(iii)



(iii) Internal air at medium level temperature profiles (AML,C in Figure 8.9 and Table 8.5).

(iv)



(iv) Internal globe temperature profiles (GT in Figure 8.9 and Table 8.5).

Graph (i) shows that both temperatures are extremely close and the range of 24 – 26 °C is kept well within for the entire period after initial stabilisation. Internal air temperature profiles may therefore be legitimately compared. The difference evident at the beginning of the period is due to the control test being conducted in the climate chamber which allowed the temperature to be quickly adjusted from the previous discharge (night time) phase, with external temperature of 17 °C, to 25 °C. This only took 15 minutes. The same operation was not possible when testing the NewMass system but the difference is considered negligible.

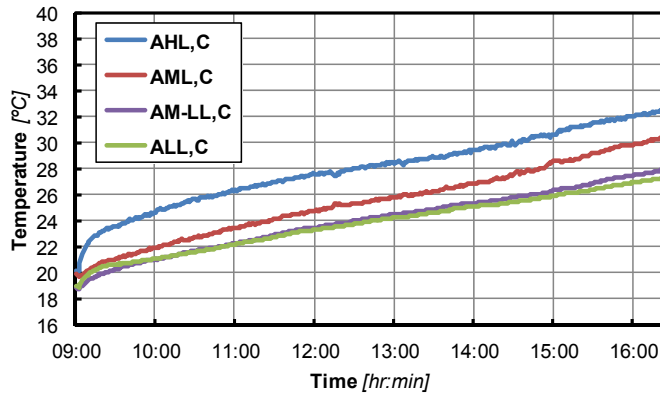
At both heights of internal air temperature we can see that despite the same initial temperature the control test temperatures rises much more rapidly. The temperature at medium level in the NewMass case is taken to represent the occupied level and we can observe that it clearly exceeds the maximum permissible temperature of 27 °C before the end of the day. This indicates that the system needs more capacity to passively meet a full load over a whole day with the heat gain applied.

Graph (iv) shows the comparison of globe thermometer reading which starts off at different temperatures but displays a clear coalescence over the period. What we are seeing here is the temperature of the walls of the cell which is the same for both cases since the PCM is not incorporated within them. The influence of the tubes themselves on the globe temperature is shown to be negligible as the radiation-emitting surface area is low.

We now turn to comparisons between air temperatures at different heights in the room, displayed in Figure 8.11.

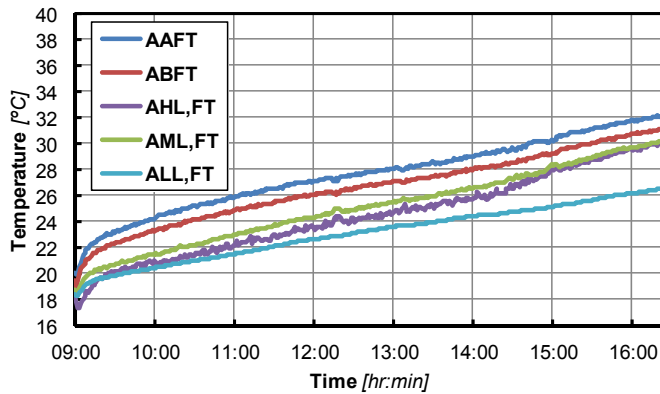
Figure 8.11 Temperatures at different heights for three columns of air in the test cell with the NewMass system during a charge period.

(i)



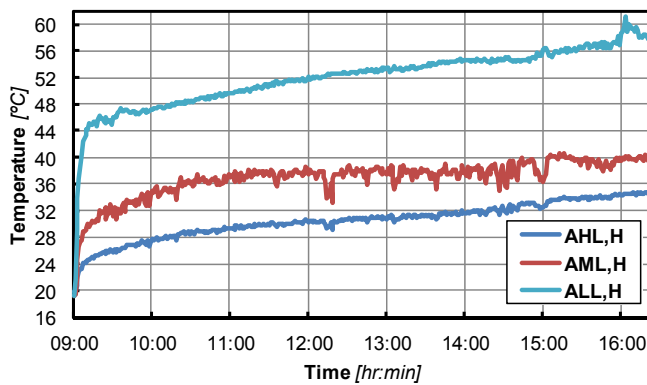
(i) Temperature profiles for temperatures in a vertical column in the centre of the room (see Figure 8.9 and Table 8.5).

(ii)



(ii) Temperature profiles for temperatures in a vertical column intersecting the NewMass units (Figure 8.9 and Table 8.5).

(iii)



(iii) Temperature profiles for temperatures in a vertical column above the heater (see Figure 8.9 and Table 8.5).

In graph (i) stratification is evident as the higher the air, the warmer it is, at any given moment. Stratification is also apparent in the vertical column of air intersecting the finned tubes. The trend is only bucked by the air at medium and high level, below the tubes. Clearly the air that has been cooled by the tubes and so sinks below them is cooler than the surrounding air, including the air below it which has been mixed with the warmer surrounding air.

The air above the heater shows the reverse effect for the obvious reason that it is generating heat at a low level which then rises and mixes with cooler air. The presence of a convection cycle is indicated by the stratification pattern in the room. The warmed air rises above the heater and plumes across the ceiling where it meets the finned tubes. These cool the air causing it to sink. This analysis is well supported by Couch's CFD model of the cell. Figure 8.12 shows the temperature distribution and velocity of the test cell air as per conditions described.

We can see the same convection cycle pattern in both images. Warm air rising from the heater moves at up to 0.437 m/s. After meeting the NewMass units velocity appears to increase again and streams of around 0.13 m/s are formed below each module. The staggered positioning of the modules also is shown to work well, with upper level tube air streams able to fall between the gaps in the lower level tubes.

Figure 8.13 shows the temperatures at various points in and on the surface of the NewMass units.

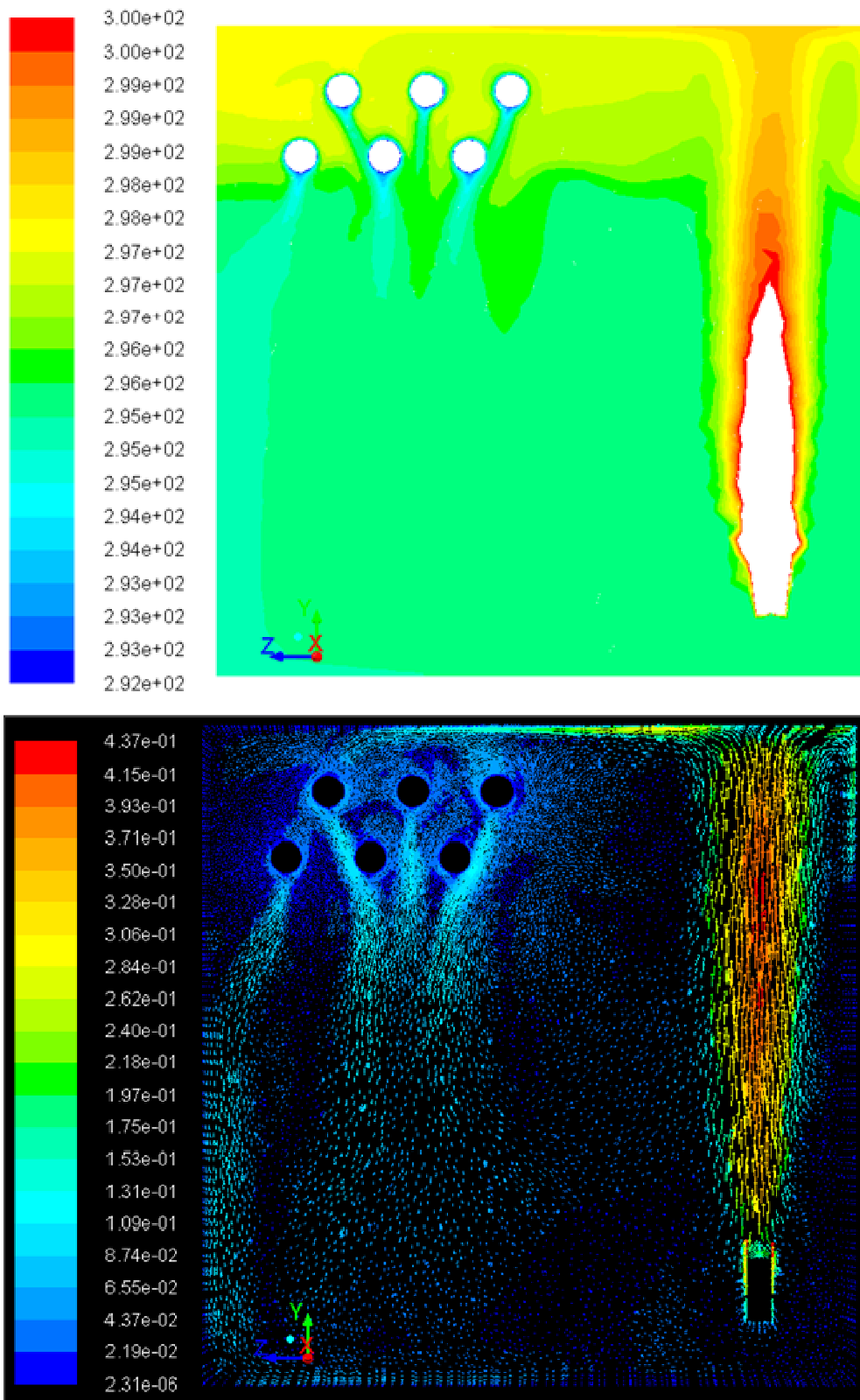
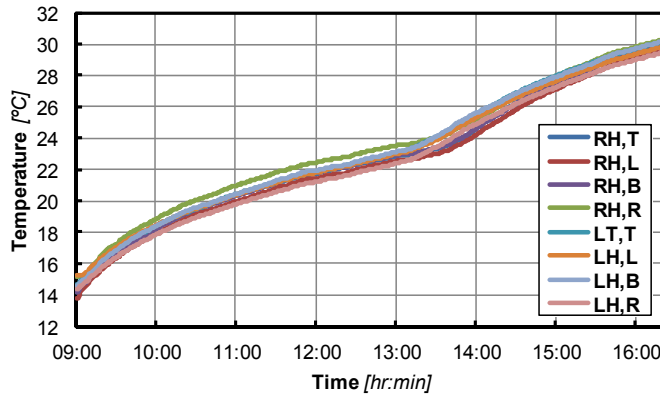


Figure 8.12 CFD model results (Couch, 2011). Air temperature contours in K (top) and air velocity vectors in m/s.

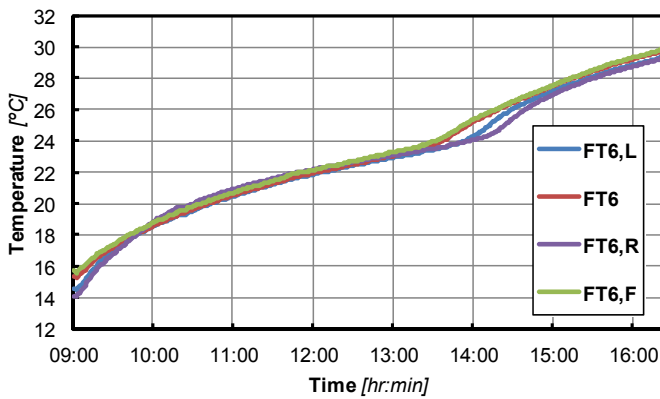
Figure 8.13 Temperature profiles for locations within and on the surface of the units.

(i)



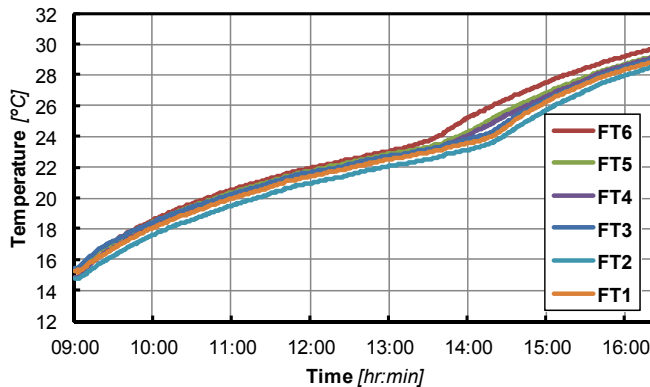
(i) Internal unit temperature profiles for locations in unit 6 (see Figure 8.9 and Table 8.5).

(ii)



(ii) Surface temperature profiles for unit 6 (see Figure 8.9 and Table 8.5).

(iii)



(iii) Surface temperature profiles for all units (see Figure 8.9 and Table 8.5).

It is the purpose of the system to limit the rate of increase in air temperature in the cell. The PCM during this period can be seen to fully melt as it takes in heat from the air in graph (i). The rise in PCM temperature is seen throughout the day but a sudden increase in the rate of temperature rise is observed at 14:25 when the substance becomes fully melted and its latent capacity is exhausted. The proximity of all internal temperatures indicates that the Raschig rings are performing their role of distributing heat evenly, very well.

Graph (ii) displays the difference between different locations on the surface of tube 6. We can observe a greater temperature difference between horizontal locations than between the base tube and a neighbouring fin. This shows fin efficiency to be high. The ends of the tube take longer to absorb heat due to the thick end caps. This appears to restrict the flow of heat.

A very similar pattern is evident on the surfaces of all the finned tubes. The PCM contained is largely dictating what temperature the surface of the aluminium reaches. With all three graphs we can observe a very similar shape to that predicted by Figure 8.2.

Figure 8.14 displays the heat transfer coefficient profile for the period.

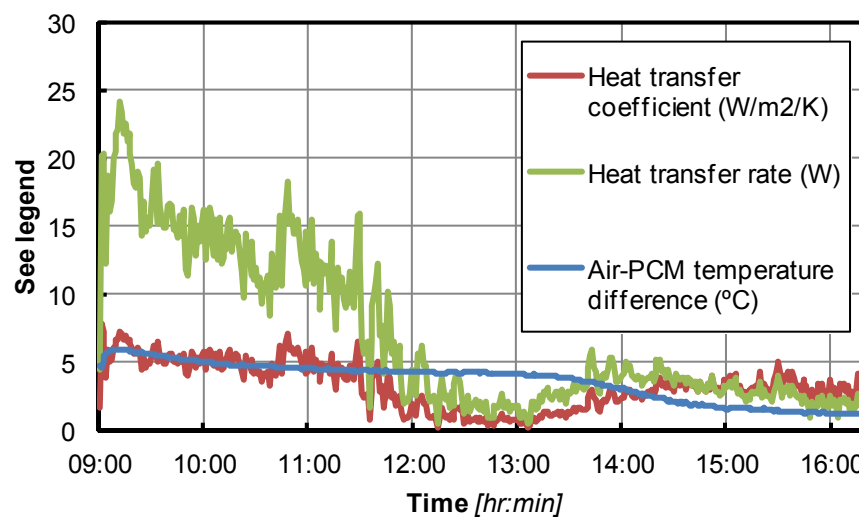


Figure 8.14 The heat transfer coefficient profile for the period along with the heat transfer rate and the difference between the PCM and the air temperature.

The heat transfer coefficient was predicted to be a constant 2.31 W/m²/K for the case of natural convection alone (see chapter 7). This is rightly shown to be a conservative

estimate. The natural convection cycle, which manifests as a result of the heated air rising from the heater and the cooled air falling from the NewMass units, is an air flow which itself drives the heat exchange and increases the rate of heat transfer. The CFD model of the test cell revealed a slightly higher heat transfer coefficient. This is presented in Table 8.7 Values for heat transfer coefficient from empirically derived equation, CFD modelling and experiment., along with the prediction from Tsubouchi and Masuda's empirically derived equation and the average of the values found through experiment.

Table 8.7 Values for heat transfer coefficient from empirically derived equation, CFD modelling and experiment.

Source of value	Heat transfer coefficient W/m ² K
Prediction from empirically derived equation (see chapter 7, (Tsubouchi and Masuda, 1970))	2.31
Prediction from CFD model (Couch, 2011)	3
Mean experimentally determined value	3.28

It is clear that the experimentally derived value is the highest. In the test the heat transfer rate and the heat transfer coefficient all rose simultaneously but the heat transfer coefficient did not rise in *direct* response to the increasing air-PCM temperature difference, though. Instead the temperature difference becomes a driving force in the convection cycle, the tubes cooling the air, causing it to sink and drawing more air over the NewMass units. It is this which causes a rise in the coefficient. The heat transfer rate, pushed to a maximum of 24.1 W/m² by the rising temperature difference and induced air flow then begins to fall as a result of the slowing of the air flow. The air flow slows due to the reduction in relative temperature, and therefore buoyancy, of the air column rising from the heater and the surrounding air. During this time the difference between the air and PCM temperatures is almost constant, decreasing slightly, at around 5 °C. This temperature difference decreases more rapidly once the latent capacity of the PCM is exhausted.

In a full scale installation the rise and fall of the heat transfer coefficient will vary greatly with the movement of air in the space. The units should be placed in

locations below the soffit which do not have significant heat sources below them, as in the cell, to allow a convection cycle to form. The rate of air flow in this cycle will depend on the temperature and heat transfer rate of the heat source, as well as the number of NewMass units installed.

The heat flux through the ceiling of the cell is presented in Figure 8.15.

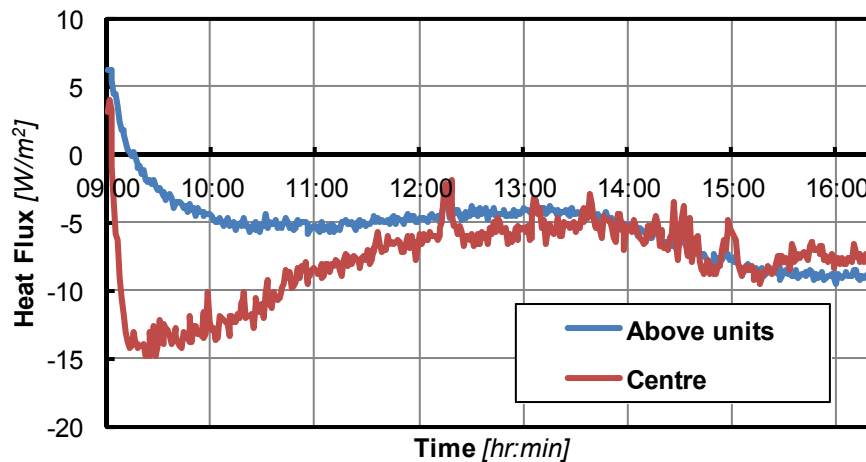


Figure 8.15 The heat flux through the cell ceiling for two locations: Above the NewMass units and in the centre of the room.

The values are all negative apart from the beginning of the period because of the layer of hot air located just below the ceiling.

Now we examine the performance compared to the other systems tested. Figure 8.16 compares the air temperature profiles at medium level for all installations tested:

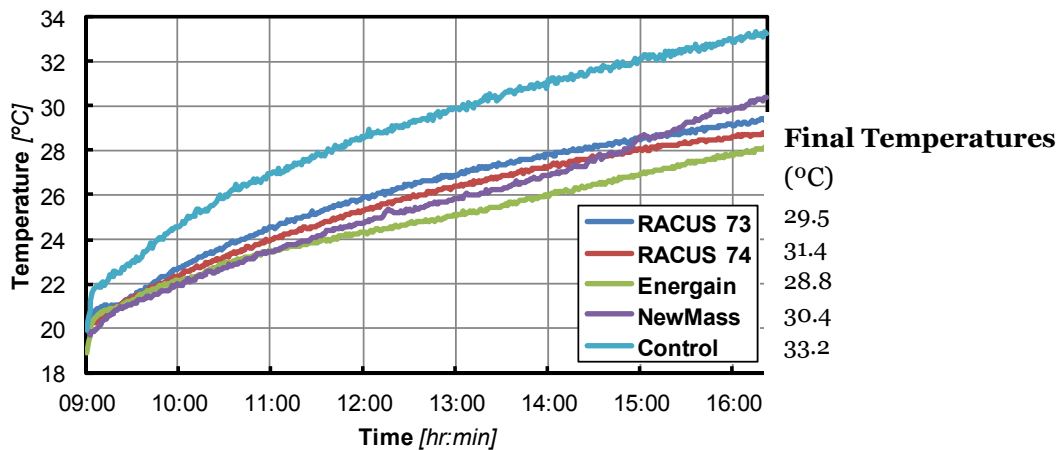


Figure 8.16 Medium level air temperature profiles of all four installations and the control test at AML,C (see Figure 8.9 and Table 8.5).

All installations are shown to provide temperature moderation when compared to the control test. Energain performed the best, narrowly better than the RACUS 74 installation. The NewMass system performs well, displaying a profile very close to the RACUS and Energain installations, until just before 15:00. Here we can see the air temperature beginning to rise more rapidly than the Energain and RACUS installations. This is due to the units exhausting their latent heat capacity leading to a more rapid temperature rise which in turn leads to a decreased cooling effect on the room air. A lag is clearly evident in this process. Figure 8.13 (iii) shows all units exhausting their latent heat capacity at around 14:00.

It is important note that the clear increase in rate of temperature rise in the NewMass case does indicate well that it appropriately ceases to function at unacceptably high room temperatures when its latent heat is exhausted. This is a positive design aspect that results from the relatively narrow phase transition zone.

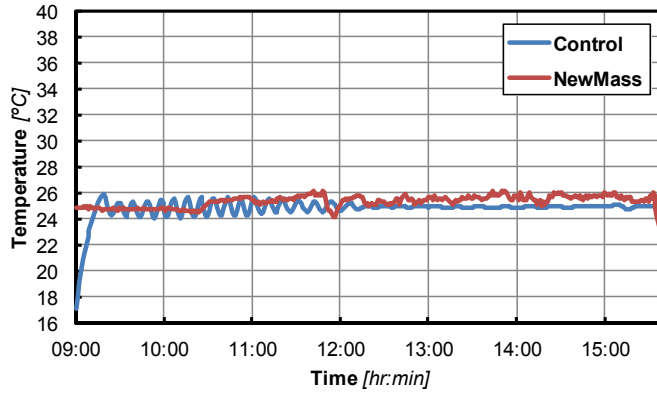
Generally lower room temperatures could be achieved passively by installing more tubes or increasing the volume and mass of A22 in each tube. However by engaging the active cooling element of the system, performance is assured with the current installation. This is described in the following section.

8.4.2 Supplemented passive charging

Figure 8.17 shows the equivalent of Figure 8.10 for the supplemented passive charging case – i.e. comparisons between the NewMass system and the control for external temperature profiles, air temperature at high and medium level profiles and the globe temperature profiles. The external temperature profiles are shown to be extremely close in the same way as for the straight passive test. What is clear when we examine the air temperature profiles is that a greater temperature difference between the control and NewMass tests is achieved in this instance. Focusing on graph (iii) the point at which the air temperature in the NewMass case rises above 25 °C is clear. At this time the chilled water system was engaged providing 13 °C water at 2 l/min to the system. This reduces the air temperature to an almost perfectly constant average of 24.5 °C. This clearly demonstrates part of the value of the chilled water system to control room temperatures when the system's capacity has either been exhausted or a cooling set point is reached in the room.

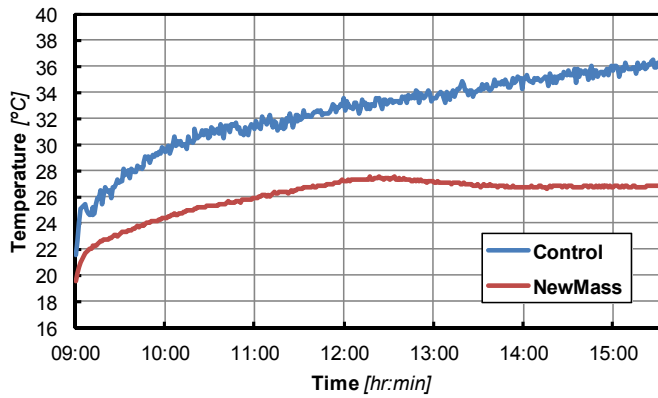
Figure 8.17 NewMass and control comparison for supplemented passive charge period.

(i)



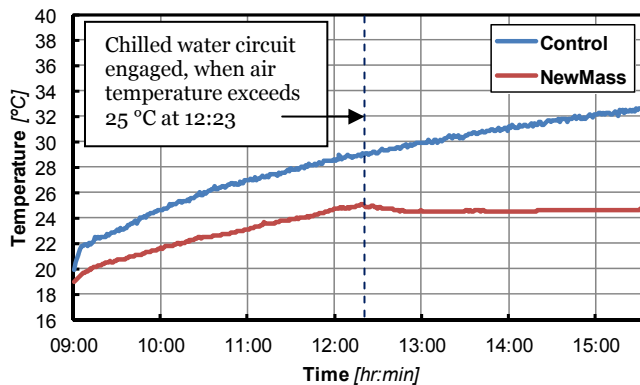
(i) Mean external temperature profiles.

(ii)



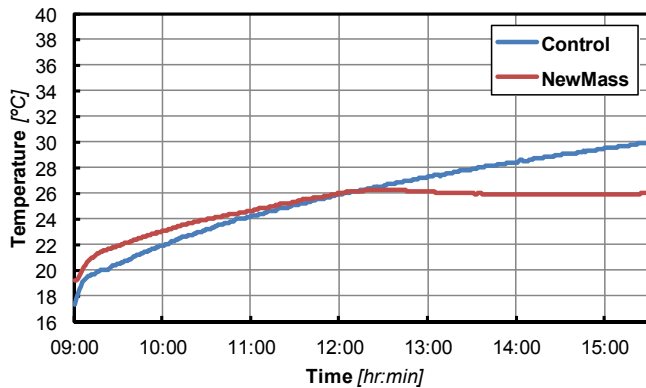
(ii) Internal air at high level temperature profiles (AHL,C in Figure 8.9 and Table 8.5).

(iii)



(iii) Internal air at medium level temperature profiles (AML,C in Figure 8.9 and Table 8.5).

(iv)



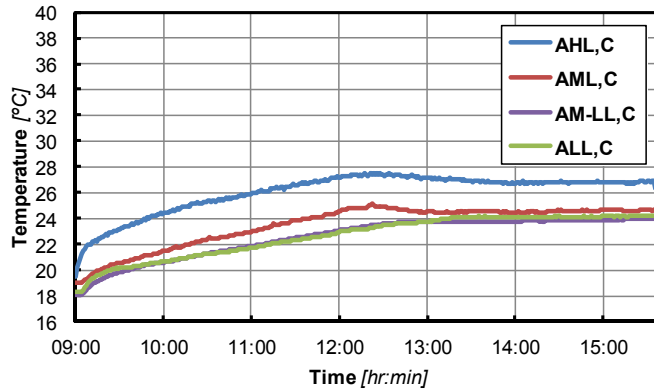
(iv) Internal globe temperature profiles (GT in Figure 8.9 and Table 8.5).

The air stratification graphs for this example are presented in Figure 8.18. In graph (i) (air column in the centre of the cell) we see what is expected. The temperature profiles rise as in the purely passive case but when the air at medium level reaches 25 °C and the chilled water system is engaged the air at high and medium level reduce and stabilise. Obviously the performance is now much improved. It is interesting to note that the air at medium-low and low levels are less clearly affected and in fact continue to rise in temperature but only slightly.

The pattern of stratification is maintained and this is also the case for the column of air intersecting the NewMass units. The same pattern of stratification is seen and the effect of engaging the chilled water system is clear. Again it is worth noting that the air at low level is clearly less affected by the chilled water system's effects. This suggests that a layer of warmer air persists just above floor level across the cell. The column of heater air experiences a reduction in temperature at medium and high levels but not just above the heater where the heating element clearly dominates.

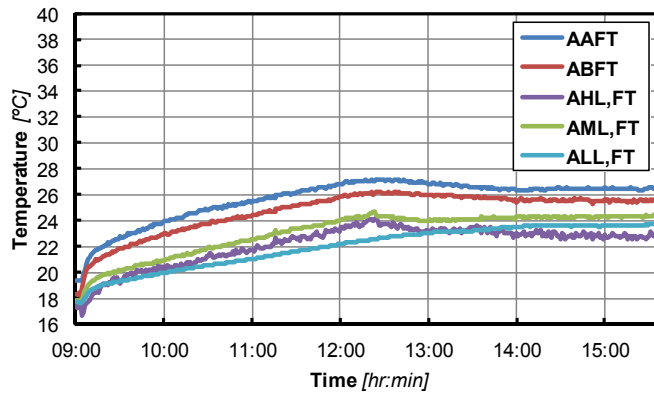
Figure 8.18 Temperatures at different heights for three columns of air in the test cell with the NewMass system during a supplemented cooling charge period.

(i)



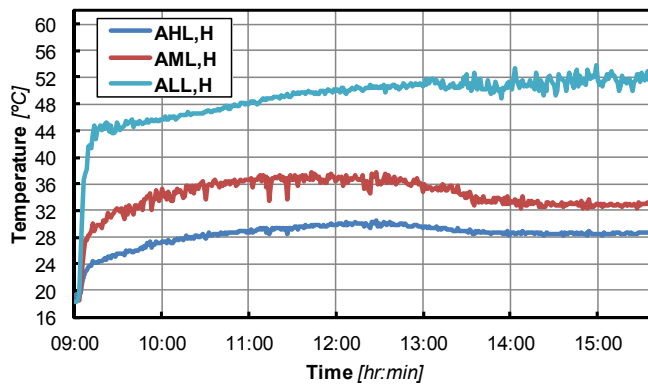
(i) Temperature profiles for temperatures in a vertical column in the centre of the room (see Figure 8.9 and Table 8.5).

(ii)



(ii) Temperature profiles for temperatures in a vertical column intersecting the NewMass units (Figure 8.9 and Table 8.5).

(iii)



(iii) Temperature profiles for temperatures in a vertical column above the heater (see Figure 8.9 and Table 8.5).

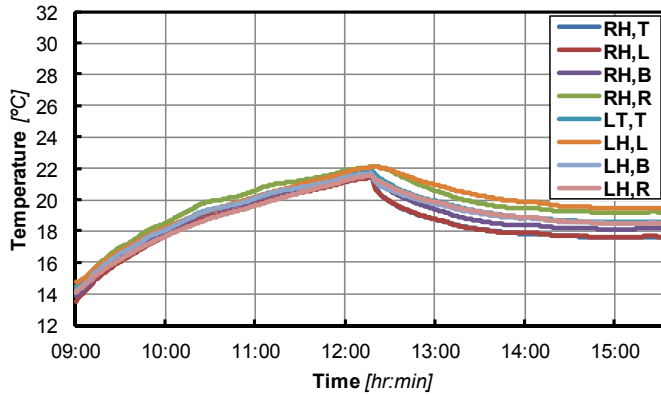
The equivalent of Figure 8.13 for the supplemented passive charge period is presented in Figure 8.19 . In all graphs the transition from passive to active operation is extremely clear with a sudden fall in temperature seen when the chilled water system was engaged. All temperature curves level off to an equilibrium before the end of the period.

After the chilled water system is engaged we see a spreading out of temperatures. This is because the chilled water removes heat at a much higher rate than it was picked up in the passive charge period. A clear temperature differential is evident across the tube body. The internal temperatures show a general trend of increasing temperature from right to left, consistent with the right hand side being the entry point for the chilled water.

Focusing on graph (ii) we can see that the ends of tubes are cooler due to conduction around the aluminium envelope from the cap connected to the axial water pipe. The fin tip is at the highest temperature being in most contact with the air and furthest from the chilled water flow.

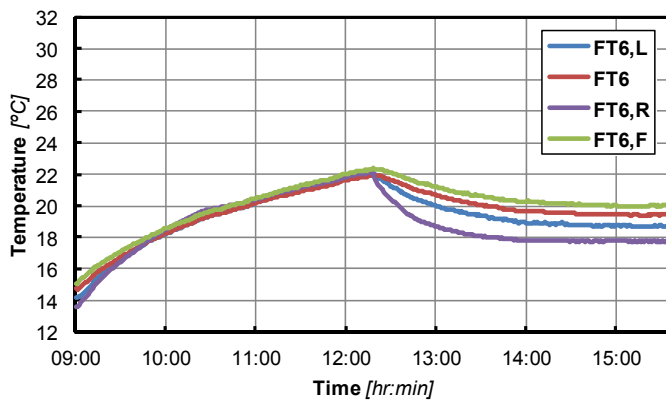
Figure 8.19 Temperature profiles for locations within and on the surface of the units during a supplemented cooling period.

(i)



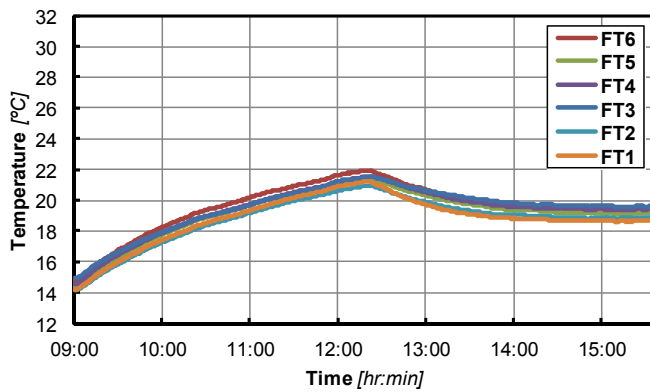
(i) Internal unit temperature profiles for locations in unit 6 (see Figure 8.9 and Table 8.5).

(ii)



(ii) Surface temperature profiles for unit 6 (see Figure 8.9 and Table 8.5).

(iii)



(iii) Surface temperature profiles for all units (see Figure 8.9 and Table 8.5).

The heat transfer coefficient profile is extremely similar to that of the purely passive charging period until the chilled water system is engaged. This should be expected since all conditions were the same up to that point; see Figure 8.20.

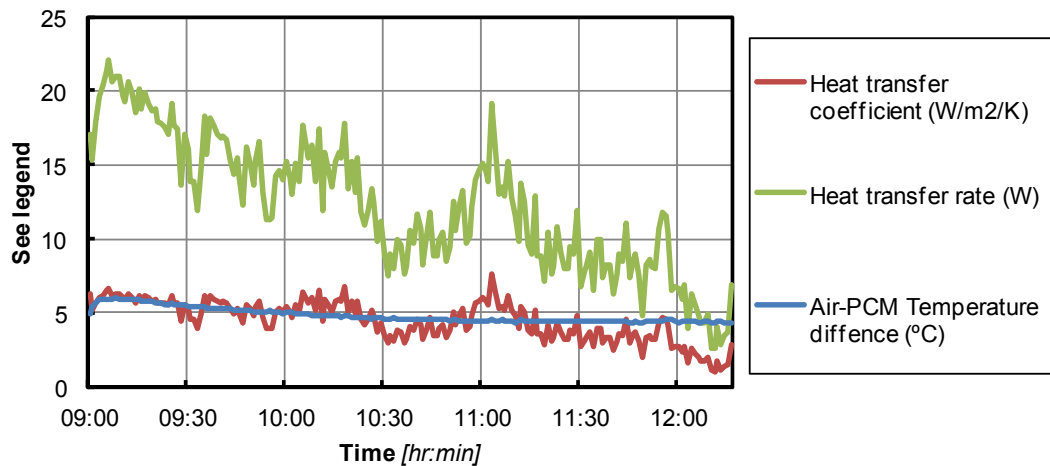


Figure 8.20 Heat transfer coefficient profile for NewMass passive charge period. Heat transfer rate and the difference between the PCM and the air temperature, included.

When the chilled water system was engaged the NewMass units continued to gain heat from the room air but began losing it to the chilled water. Once the system had reached equilibrium the rate of heat transfer was equal at the finned tube surface and the chilled water tube surface. This is because the NewMass units were cooling the air at exactly the same rate as the heater was heating it – hence the constant temperature. The heat flux across the walls at this point was assumed to be negligible since the external air temperature and internal air temperature were within 1 °C of each other. Indeed if we examine the heat flux in the centre of the ceiling during the period of thermal equilibrium we can see that it is around 0 W/m²; see Figure 8.21.

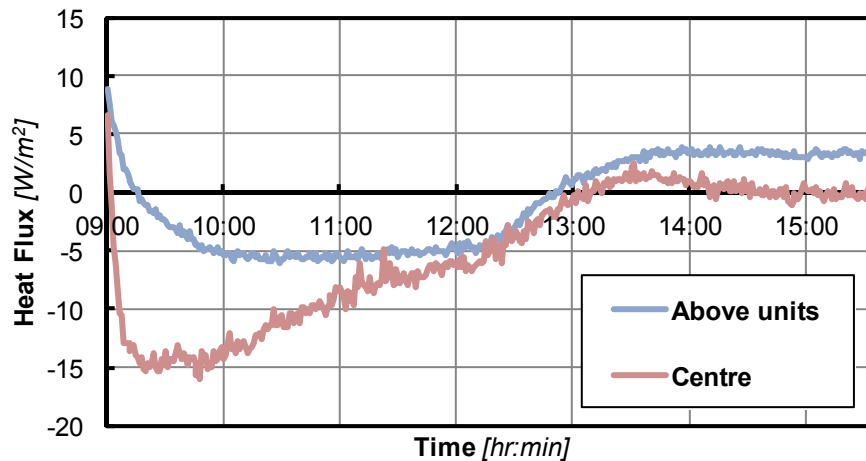


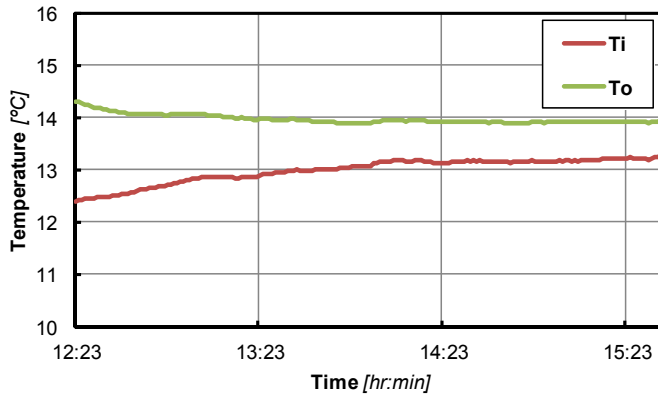
Figure 8.21 The heat flux through the cell ceiling for two locations: Above the NewMass units and in the centre of the room.

The chilled water system must have also been absorbing heat at the same rate in order to maintain the equilibrium. The heat transfer coefficient for the units in this was therefore the heat supplied by the heater divided by the total surface area and the air-PCM temperature difference at that time. This was found to be $5.44 \text{ W/m}^2\text{K}$.

The heat absorbed by the chilled water confirms the magnitude of heat flowing through the combined system. Figure 8.22 shows the inlet and outlet water temperatures for unit 6 along with the heat transferred to the water. The heater was giving out 128.75 W of heat when the system was in equilibrium. This means that each NewMass unit and by extension each axial water pipe should be absorbing one sixth of this amount; 21.46 W . The water flowing through the axial pipe in unit 6 actually absorbs on average 25.22 W ; a slight increase that should be expected since, out of all the units, unit 6 absorbs the most heat being positioned in the warmest and most prominent location.

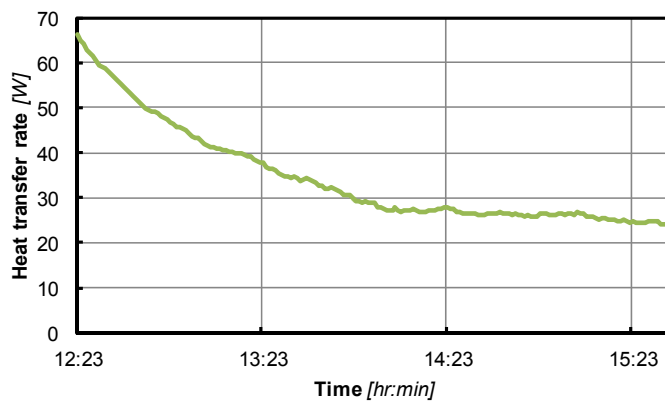
Figure 8.22 Inlet and outlet temperatures as well as heat exchange for the water flowing through unit 6.

(i)



(i) Inlet and outlet temperatures for the water flowing through unit 6.

(ii)



(ii) Heat transfer rate to the water flowing through the axial pipe in unit 6.

The comparison to the other products tested shows that with supplementary cooling the NewMass system performs far better than the other products, with the obvious cost of energy input.

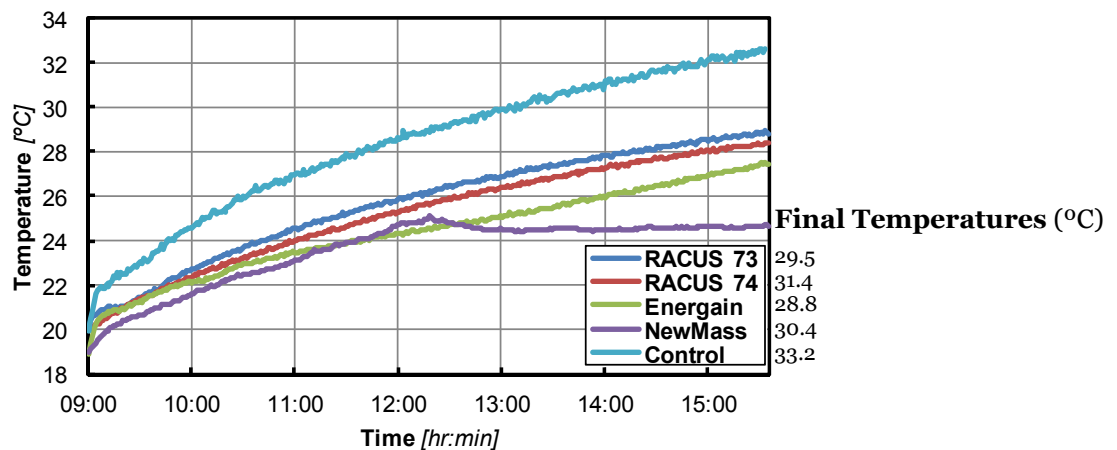


Figure 8.23 Medium level air temperature profiles of all four installations and the control test at AML,C (see Figure 8.9 and Table 8.5).

This additional coolth may be produced more efficiently than a fan coil system which would be used to supplement the cooling of the other products. This is because the a flow temperature of 13 °C would be produced at a higher COP than the typical 6 °C flow water used in fan coil systems. Alternatively, a lower flow temperature could be mixed with return water to achieve a higher inlet temperature, as with the chilled ceilings in China Shipping House, however this would bring less efficiency benefits.

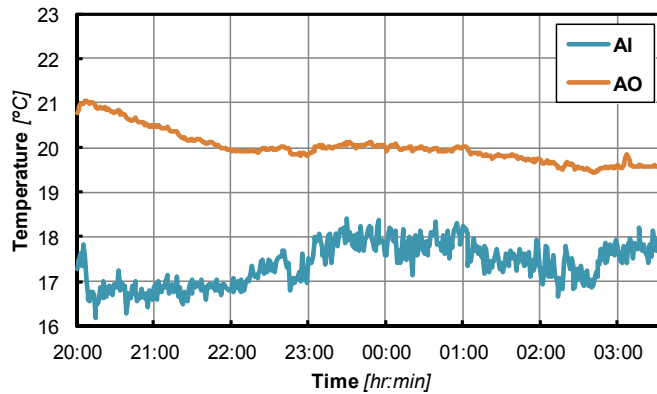
8.4.3 Passive discharge

The results from the passive discharge test are given here. Figure 8.24 displays the air temperature throughout the cell, as well as the ventilation inlet and outlet temperatures. The ventilation inlet air temperature stayed mostly within the 16 to 18 °C band over the period, occasionally rising slightly above 18 °C. The outlet air temperature can be seen falling in an uneven way which corresponds to the fluctuations in inlet temperature.

We can see that each column of air decreases in temperature whilst remaining stratified (with the heater turned off this air is now stratified in a predictable way.) In each case there appears to be a levelling of the slope at around 11:00pm. This is due to the stabilising presence of the NewMass units as they discharge their heat.

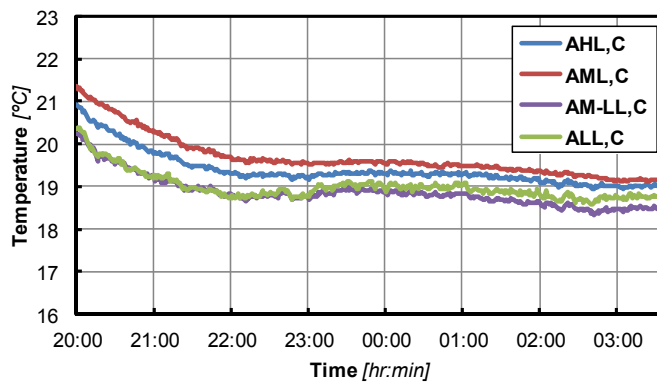
Figure 8.24 Temperatures at different heights for three columns of air in the test cell with the NewMass system, plus ventilation air, during a passive discharge period.

(i)



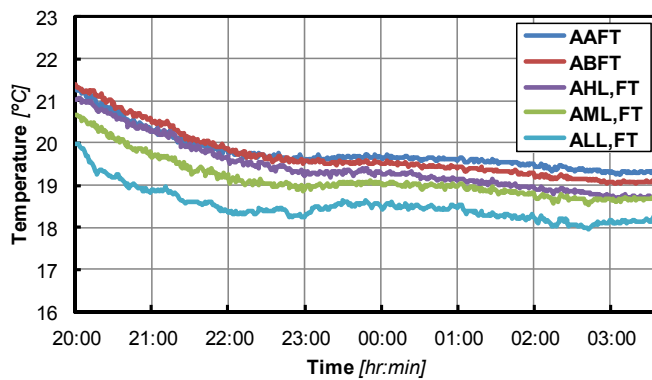
(i) Ventilation inlet and outlet air temperatures (see Figure 8.9 and Table 8.5).

(ii)



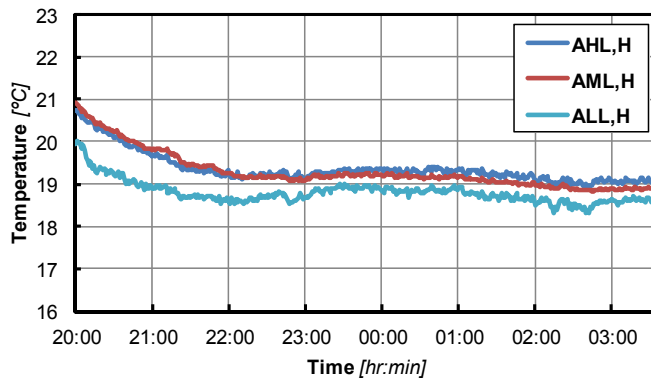
(ii) Temperature profiles for temperatures in a vertical column in the centre of the room (Figure 8.9 and Table 8.5).

(iii)



(iii) Temperature profiles for temperatures in a vertical column intersecting the NewMass units (Figure 8.9 and Table 8.5).

(iv)



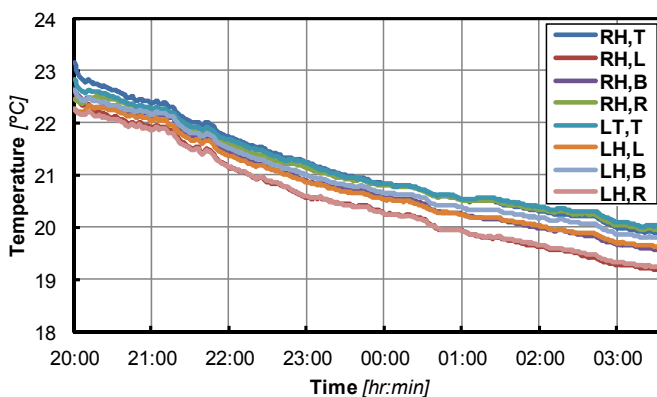
(iv) Temperature profiles for temperatures in a vertical column above the heater (see Figure 8.9 and Table 8.5).

Figure 8.25 displays the unit temperatures for this period. In all cases we can observe a fairly linear fall in temperature, though these are no doubt the start of curves which would eventually tend towards the inlet air temperature. Internal temperatures are similarly close within the unit 6 to the passive charging case. This is less evident in the graph because a smaller temperature range is covered during the discharge period. This trend is not entirely carried through to the tube surfaces because the tube ends clearly cool faster than the centre.

What is clear is that the tubes do not lose enough energy to perform at the same cooling capacity the following day. Clearly part of the reason for this is that the incoming air temperature is above the temperature of the units at the start of the charging period, around 14 °C. However, it is also because the heat transfer coefficient is relatively low.

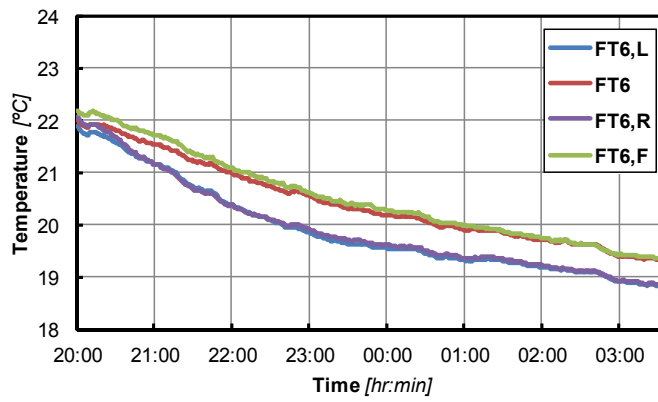
Figure 8.25 Temperature profiles for locations within and on the surface of the units.

(i)



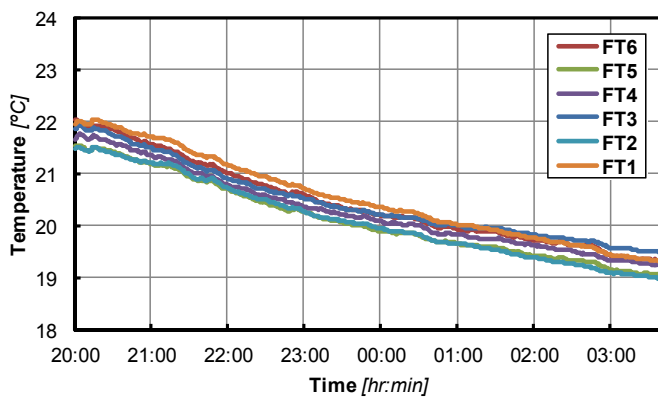
(i) Internal unit temperature profiles for locations in unit 6 (see Figure 8.9 and Table 8.5).

(ii)



(ii) Surface temperature profiles for unit 6 (Figure 8.9 and Table 8.5).

(iii)



(iii) Surface temperature profiles for all units (see Figure 8.9 and Table 8.5).

A higher coefficient was expected considering the fact that the air is being drawn over the tubes by the extract fan.

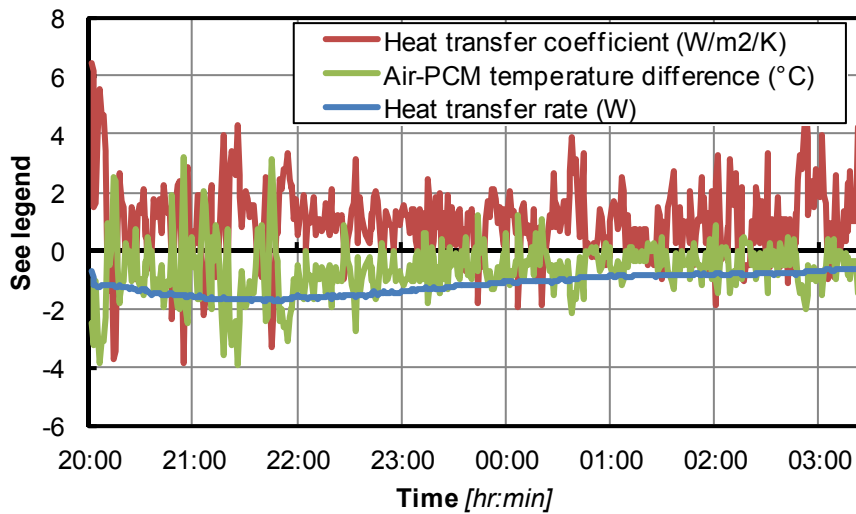


Figure 8.26 The heat transfer coefficient profile for the period along with the heat transfer rate and the difference between the PCM and the air temperature.

The problem is believed to be the orientation of the units with respect to air flow. Air was actually drawn across the fins rather than between them. In this instance the fins help to insulate the tubes by forming a barrier to the passing air. In a full scale installation this effect should be avoided. Tube orientation should allow forced or naturally convected air to pass between fins.

These results highlight the importance of an effective night cooling strategy. To establish the truth of this occurrence, further tests on the discharge rate of individual tubes with air flowing across the tubes in different directions is suggested. This situation could also be modelled in CFD.

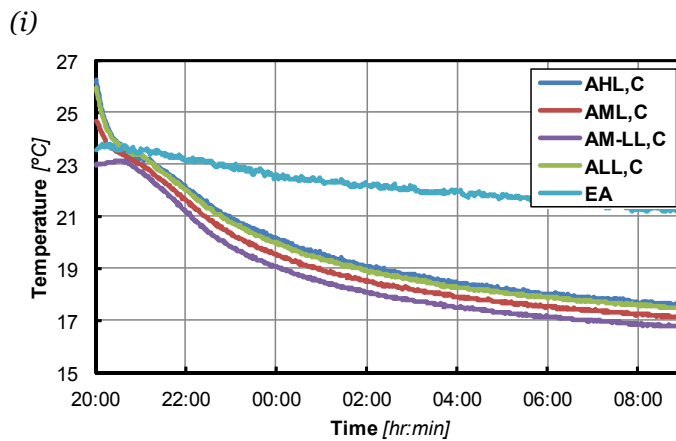
8.4.4 Active discharge

Figure 8.27 displays all internal air temperatures as well as the external air temperatures and the globe temperature (both in graph (i)).

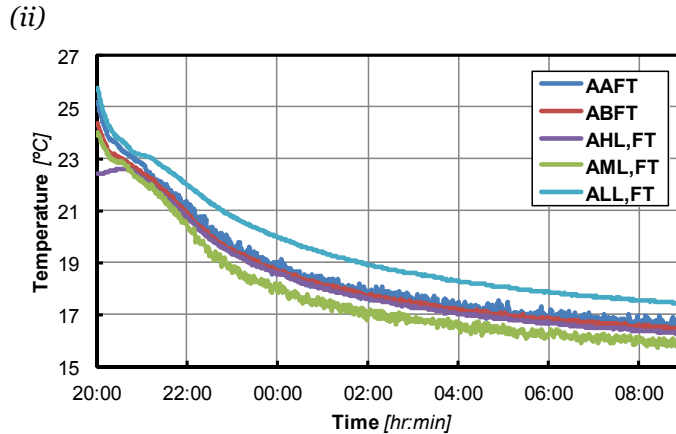
The external temperature steadily falls over the course of the night to a low of 21.05 °C. These temperatures would not be low enough to discharge the heat stored in the NewMass units. Active discharge is therefore justified. In the centre of the room the stratification seen in the daytime is for the most part preserved with the exception of the low level temperature which indicates that the air closest to the

floor is slightly warmer due to the floor. All temperatures descend as the tubes cool the air. This is an undesired result of the NewMass system design.

Figure 8.27 Temperatures at different heights for three columns of air in the test cell with the NewMass system during an active discharge period.

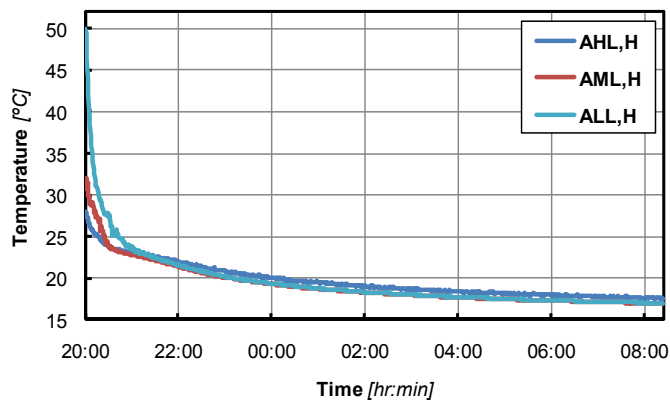


(i) Temperature profiles for temperatures in a vertical column in the centre of the room (see Figure 8.9 and Table 8.5).



(ii) Temperature profiles for temperatures in a vertical column intersecting the NewMass units (Figure 8.9 and Table 8.5).

(iii)



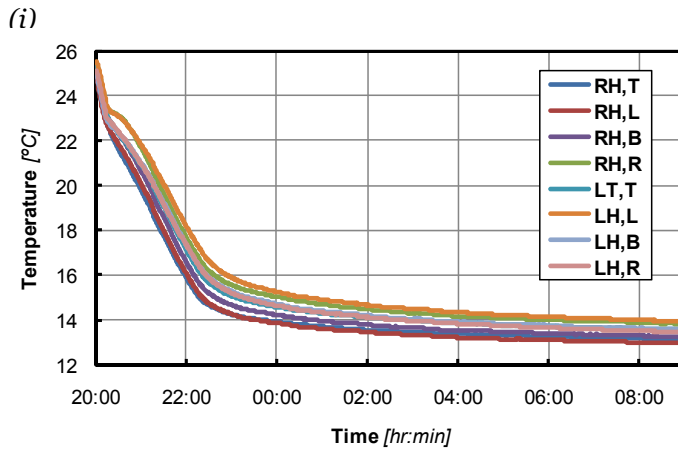
(iii) Temperature profiles for temperatures in a vertical column above the heater (see Figure 8.9 and Table 8.5).

Ideally the tubes would discharge their accumulated latent heat without cooling the air but this would require night time insulation, an idea explored in chapter 9.

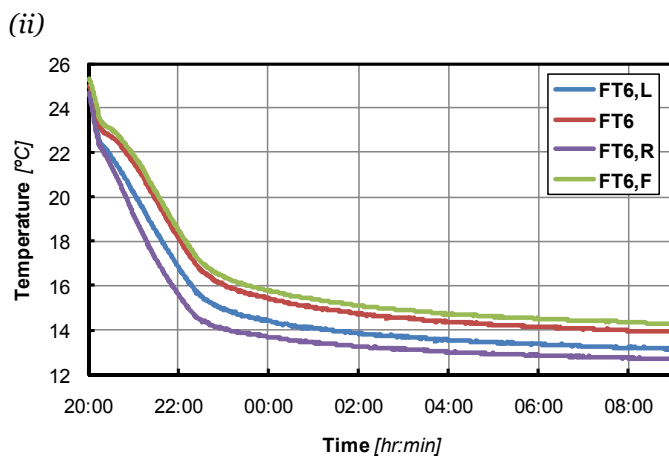
Looking at graph (ii) the air immediately surrounding the finned tubes is all cooled to a similar degree but the air at medium level below it is at a lower temperature. Interestingly this trend does not continue to the floor but as with the central column of air, the portion just above the floor is consistently at a slightly higher temperature.

The PCM was reduced in temperature to around 15 °C in about 3 hours – see Figure 8.28. At that point the gradient flattened out because the bath has reached its set point. The PCM approaches an average equilibrium temperature of 13.3 °C. The pattern of temperature distribution is of course very similar to that seen in the supplemented passive charge case.

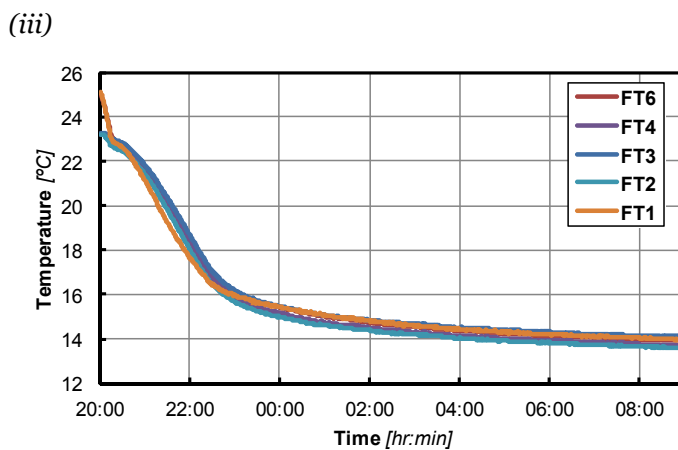
Figure 8.28 Temperature profiles for locations within and on the surface of the units during an active discharge period.



(i) Internal unit temperature profiles for locations in unit 6 (see Figure 8.9 and Table 8.5).



(ii) Surface temperature profiles for unit 6 (see Figure 8.9 and Table 8.5).

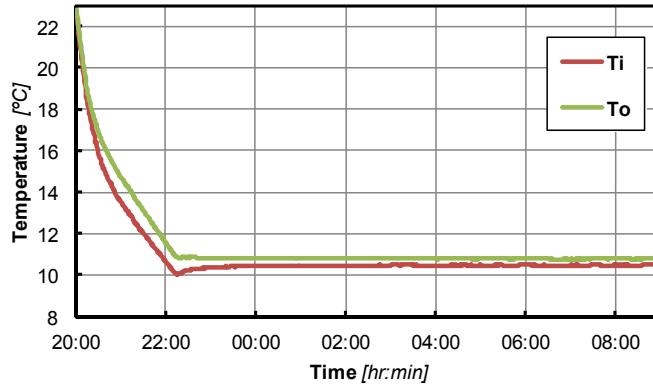


(iii) Surface temperature profiles for all units (see Figure 8.9 and Table 8.5).

The heat exchanged to one tube over that time is shown in Figure 8.29.

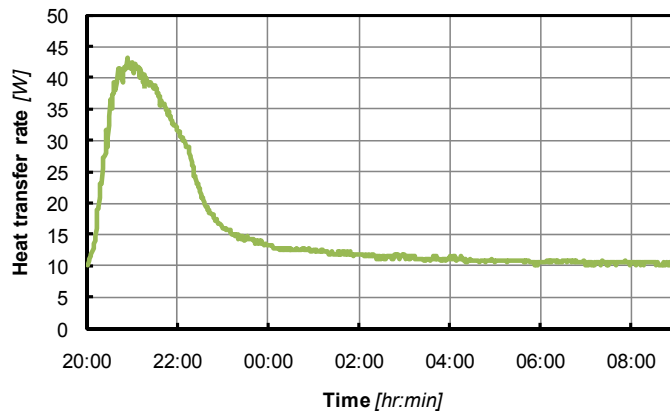
Figure 8.29 Inlet and outlet temperatures as well as heat exchange for the water flowing through unit 6 in active discharge.

(i)



(i) Inlet and outlet temperatures for the water flowing through unit 6.

(ii)



(ii) Heat transfer rate to the water flowing through the axial pipe in unit 6.

Here we observe a rise in heat transfer rate as the chilled water temperature reduces under through heat loss to the evaporator in the water bath. This raises the temperature difference between the NewMass unit and the water. A maximum is reached because the unit falls in temperature and the chilled water reaches the set point temperature. The heat transfer then tends towards a constant value of about 10W.

During this period, as described in section 8.1.3, the effective conductivity of the A22/Raschig ring composite was found to be 3.4 W/mK. As predicted, this is lower than the 8.45 W/mK calculated for metal foam and lower than the 25 W/m/K

(in-plane) and 8 W/m/K (perpendicular-to-plane) claimed for the graphite/paraffin composite from SGL Carbon Group (SGL Carbon Group, 2011). It is, however, significantly higher than the 2 W/mK found by Velraj et al. (Velraj *et al.*, 1999) and 18.9 times higher than the conductivity of the paraffin alone (0.18 W/mK). The Raschig things have been shown to be a simple and effective solution to conductivity enhancement.

8.4.5 Energy savings

The parameters derived from experiment were applied to the energy savings model as described in section 8.1.3. The IES model produced an annual cooling load that is displayed in Figure 8.30 along with the ambient temperature profile for that period.

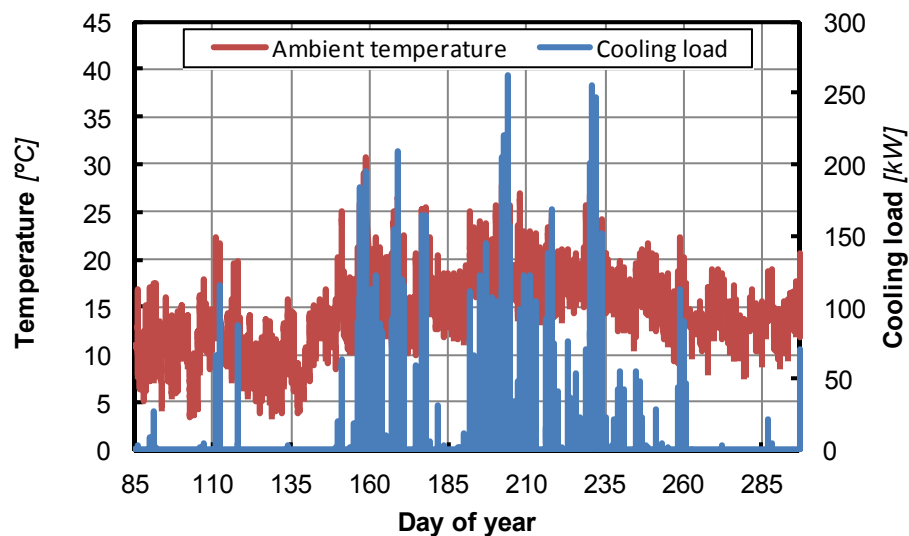


Figure 8.30 Ambient temperature profile and IES cooling load for the example London office.

Here we have the expected rise in temperature and correspondingly cooling load peaking in summer. When the cooling load was applied to the heat balance model a temperature profile of internal air and NewMass temperature was produced. A sample of this is displayed in Figure 8.31 for three days in July.

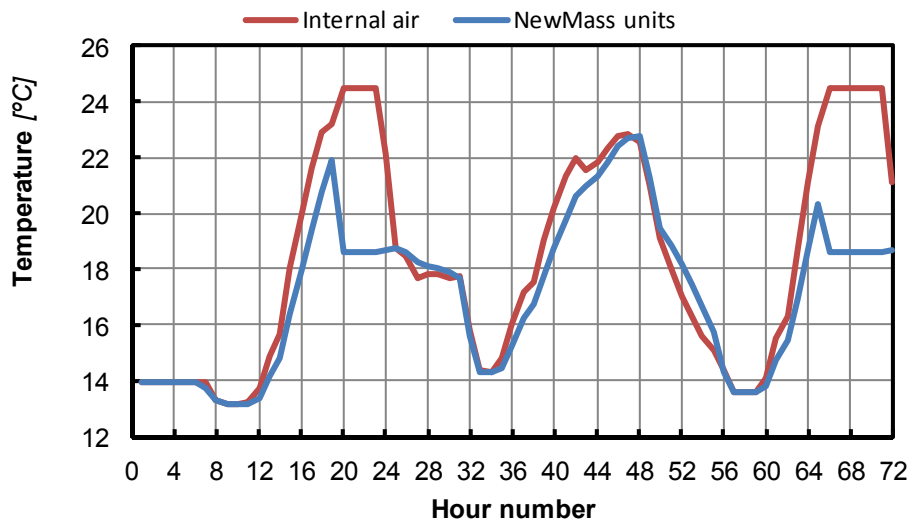


Figure 8.31 Internal air and NewMass unit temperature profiles for heat balance model. Monday 14th to Wednesday 16th July.

The model can be seen to function as designed with the internal temperature rising faster than the NewMass units on each day. Supplementary cooling through circulation of chilled water may be seen to be activated at 20:00 on Monday and 18:00 (hour number 66) on Wednesday. This results in a steady 24.5 °C temperature for the air and a sharp decrease in the NewMass unit temperature. At night on Monday and Tuesday the air temperature can be seen to drop below the NewMass unit temperature allowing it to discharge some of its accumulated heat passively. We can even observe the point at which the freezing of the paraffin begins on Tuesday night when it reaches 19.4 °C, the freezing onset for the A22 sample used in the NewMass units.

On Monday and Tuesday nights the active discharge function of the system is engaged to remove more heat from the units. On Monday the circulated night air failed to reduce the unit temperature by more than 2 °C so the amount of heat actively discharged is greater than that on Tuesday night where the night air is able to reduce the unit temperature by almost 8 °C. The active discharge leads to excessively cool air in the space throughout the morning and part of the afternoon. This is an undesirable effect of the system and may be solved in three ways which are discussed in the conclusion. It may also be observed that the majority of the cooling occurs in the late afternoon and evening. This may be explained by the

corresponding ambient temperature and cooling load profile presented in Figure 8.32.

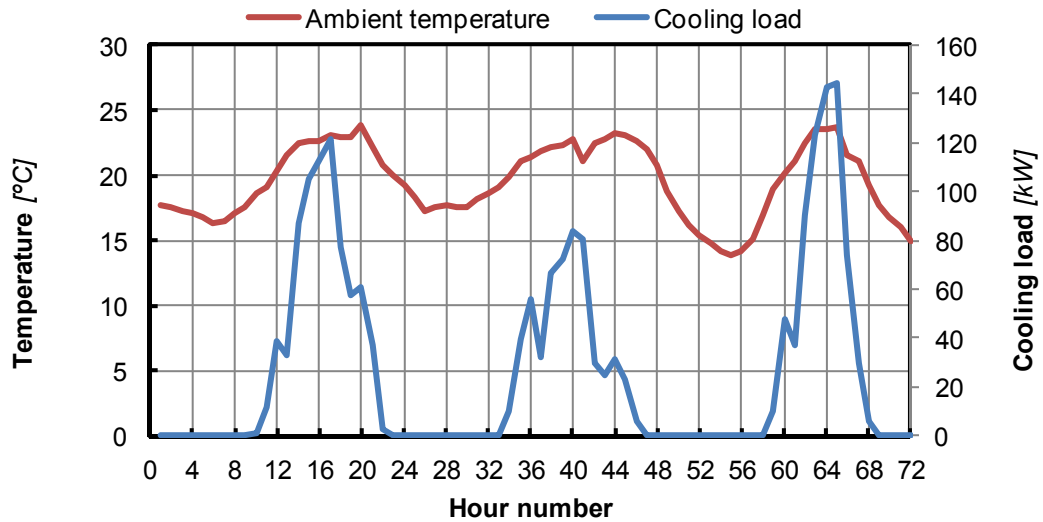


Figure 8.32 Cooling load and ambient temperature for Monday 14th to Wednesday 16th July.

The air temperature is seen to remain high until the late in the evening, even peaking at 20:00 on Monday. This causes the load profile to be shifted more towards the afternoon than might normally be expected.

The calculated energy saving for the entire year, as compared to a conventional cooling system with fan coil units, was found to be 34%. Table 8.8 shows the energy that would be expended by the two systems and the associated carbon emissions, assuming a carbon factor of 0.517 kgCO₂/kWh (Department for Communities and Local Government, 2010).

Table 8.8 Annual energy use of a conventional cooling system and NewMass.

System	Energy (kWh)	CO ₂ (kg)
Conventional cooling	13269	6860
NewMass	8842	4572
Difference	4427 (34%)	2289 (34%)

These savings are certainly a significant figure but it should be remembered that it only applies in this particular circumstance. Further improvements to the system can be made and these are discussed in the conclusion.

8.3 Conclusions

Several conclusions can be made from the results just discussed. Firstly, the system was clearly seen to suppress the room air temperature rise, thus reducing cooling energy. The NewMass units function well causing the surrounding air to sink and cool the room. However it did require supplementary cooling in this case, due to insufficient thermal capacity. The heat transfer coefficient is partly determined by the rate of flow of air across the tubes. This is thought to decrease as the units warm and the convection cycle speed is reduced.

The heat transfer coefficient is slightly higher than that predicted and this is thought to be due to the movement of air creating a forced convection condition.

In supplemented passive charging mode the system controls the room temperature extremely effectively at an efficiently produced chilled water temperature. The surface temperature was kept to a minimum in charging and a maximum in discharging, thus promoting heat transfer.

In passive discharge mode there was a low rate of discharge from units due to a low heat transfer coefficient of $1.0 \text{ W/m}^2/\text{K}$ and a low temperature difference between the NewMass units and the surrounding air. The low heat transfer coefficient is most likely due to flow of air across rather than between fins.

In contrast the chilled water system was extremely good at discharging heat. A lower limit of discharge temperature was reached due to fabric gains at lower temperatures.

The system performed as well as the other products for the majority of the day but the steepening in temperature profile indicates exhaustion of thermal capacity. In the supplementary cooling case the comparison to the other products tested showed the NewMass system to perform the best by far.

In general it may be concluded that the system performed well in terms of cooling delivered to the room. The energy savings model gave an indication as to what

savings might be expected in a full scale installation. A 34% saving, coupled with the effective system performance demonstrates that it is worth pursuing the further product development with a view to commercialisation.

As part of this process there are some specific avenues of research that should be explored. Firstly, the operation of the systems chilled water circuit could be further optimised as the relationship between chiller power and pumping energy for a full scale installation has not been determined. It may be the case that a higher flow rate and higher chiller flow temperature would achieve greater overall savings, although the difference is not expected to be large in comparison to current predicted savings.

Secondly, the system design should address the overcooling of the space in mornings after active discharge of heat has occurred the previous night. One solution to this is the addition of a retractable insulative cover that would shield the tubes from the space during discharge. Not only would this maintain more comfortable air temperatures but it would make the discharge process more efficient since heat gains during that period would be lower. The compact nature of the tube design lends itself to this approach. Referring back to the work conducted in chapter 4, this system would be a version of system type 2. In section 4.4.2 a conceptual design was presented in which an insulating curtain is drawn across fabric elements for discharge. In the case of the NewMass system, because of their location, the insulation could be applied with less disruption at the occupied level.

Thirdly, with a system design established and tested, a life cycle assessment would allow a broader environmental case to be made. In general, there is a lack of this type of research into phase change material products and near-future research work should be more targeted at this area.

The following chapter details the overall conclusions for the EngD.

References

- Ahmad, M., Bontemps, A., Sallee, H. and Quenard, D. (2006) "Thermal testing and numerical simulation of a prototype cell using light wallboards coupling vacuum isolation panels and phase change material", *Energy and Buildings*, vol. 38, pp. 673-681.
- Arnold, D. (2006) "Chapter 6: Internal heat gains" in *Environmental design: CIBSE Guide A*, ed. K. Butcher, 2nd edn, CIBSE, London, pp. 6-1-6-10.
- ASHRAE (2008) *90.1 User's Manual - ANSI/ASHRAE/IESNA Standard 90.1-2007*, ASHRAE, Atlanta.
- Couch, W. (2011) *Development and testing of a novel PCM comfort cooling system (Masters dissertation)*, Brunel University, Uxbridge.
- Department for Communities and Local Government (2010) *National Calculation Methodology (NCM) modelling guide*, Department for Communities and Local Government, London.
- HM Government (2010) *The Building Regulations 2000 - Conservation of fuel and power - Approved document L2A*, RIBA, London.
- Kuznik, F. and Virgone, J. (2009) "Experimental assessment of a phase change material for wall building use", *Applied Energy*, vol. 86, no. 10, pp. 2038-2046.
- SGL Carbon Group (2011) *Ecophit: the graphite construction material for air conditioning in buildings*. Available: http://www.sglgroup.com/export/sites/sglcarbon/common/downloads/products/product-groups/eg/construction-materials-ecophit/ECOPHIT_Uebersicht_e.pdf [02/01/2012].
- Tsubouchi, T. and Masuda, H. (1970) "Natural Convection Heat Transfer from Horizontal Cylinders with Circular Fins", *Proceedings from the 6th International Heat Transfer Conference* Paris, pp. NC 1.10.

Velraj, R., Seeniraj, R.V., Hafer, B. and Faber, C.S., K. (1999) "Heat Transfer Enhancement in a Latent Heat Storage System", *Solar Energy*, vol. 65, no. 3, pp. 171-180.

CONCLUSION

This EngD project began with the aim of developing new low energy PCM systems for cooling buildings. The ultimate result was the design and testing of a system known as NewMass. The system combines the low energy aspects of a passive system with the performance guarantees of an active system. Energy savings of 34% were predicted for a UK office. The concept design of the system, which was described in chapter 7, came about through the drawing together of conclusions from the literature review and a series of projects that were detailed in the intervening chapters.

The literature review revealed, in the case of active systems, that most incurred an energy cost to the cooling system they were incorporated into. However this is not always the case and the potential to save energy still appears possible. This perceived potential led to the study of an active cooling system with PCM tank in an occupied UK office. Here it was revealed that negative energy savings were being made, 687 kWh or 10.6% of the total cooling energy over a 6 day period. The main reason for this was that under-cooling in the PCM prevented it from rejecting accumulated heat and reduced the tanks' thermal utility; only 28% of capacity was utilised. DSC analysis revealed that the hydrated salt freezes at 5.53 °C, which is too low for significant refreezing. This finding, as well as stressing the need for appropriate PCM selection, lent further weight to the argument that energy saving benefits of active systems are at best marginal. This focussed the research on systems with some form of passive or free cooling element.

The literature review revealed an opportunity to develop new PCM cooling systems and improve on the energy use and performance of those currently in use. In the

cases of passive, free cooling and thermally activated systems, all were found to have the potential to save a significant amount of energy and to have their own advantages and disadvantages in terms of application.

Passive systems have been heavily researched and are available as a variety of products, including wall boards and ceiling tiles. Reductions in peak room air temperature of several degrees are commonly reported and significant energy savings (35% claimed by DuPont (2010)) may be achieved. Passive systems are, however limited in their *thermal* and *cooling capacity*. This is due to limited surface area for application and barriers to heat transfer created by light fittings, service conduits and furniture etc. Consequently spaces with passive applications will often require a conventional cooling system. An ability to reject heat on warm nights and the potential for high fan energy are further potential disadvantages.

Free cooling systems have become the subject of increasing research over the past few years and commercial products, such as Artica (2009), have emerged. Free cooling systems have the advantage of controlling the delivery of coolth to a space. Heat discharge at night is also targeted so less fan energy than for passive systems should be required. *Thermal capacity* of these systems will also be limited by the space and how easily it can accommodate the large ducts or facade-integrated units. Discharge of heat will also be limited by the night time temperatures achieved and so cannot be relied upon to cover high loads in hot periods.

Thermally activated systems are also becoming more common. These systems have the advantage of combining a fully passive charge period with the potential for active discharge of heat at night to a chilled water loop. This potential for passive charging and guaranteed performance is what inspired the development of the NewMass system design.

The literature review also found that the current methods of classification of PCM cooling systems are not clearly and consistently defined. An alternative taxonomy was developed in chapter 4 based on the thermal contact between the fundamental elements of all PCM cooling systems in charge and discharge modes. This equated to a mapping of the design space which allowed under-researched areas to be identified. This in turn led to novel system designs being developed.

It was found that systems with removable insulation have been underexploited. Six system types of this variety emerged and three of these were explored in the design

and testing of the Passive PCM Sails. These tests revealed that external discharging of the PCM units greatly increased thermal and cooling capacity. They also demonstrated that radiant heat transfer is significant, so passive designs should have surfaces with high absorptance and emissivity, and that a narrow phase transition zone is desirable in the PCM. These results informed the NewMass system design.

Chapter 6 detailed the construction of a thermal test cell and the testing of two well-known passive products: RACUS ceiling tiles and DuPont Energain panels. In that test the Energain panels were clearly shown to control the temperature better than the RACUS tiles. However, far more PCM, 36.28 kg as compared to the 13.33 and 13.24 kg of the RACUS 73 and 74 formulations, was required. It also covered far more area (all walls and ceiling) while the RACUS tiles only covered the ceiling area. When cooling and temperature reduction results were normalised with respect to the mass of PCM employed the RACUS tiles were shown to out-perform the Energain panels; 16.1 and 11.9 Wh/kg of cooling for the RACUS tiles, as compared to 9.7 Wh/kg for the Energain panels. This was seen to be largely due to the good thermal contact that the tiles were able to achieve with the air through non-integration into the building fabric. The Energain panels, however had to be installed behind plasterboard which also inhibited their ability to reject heat at night. This result lent further support to the concept of non-integration into the building fabric that fed through to the NewMass concept.

Chapter 7 drew together the many design lessons acquired in the preceding chapters and laid out the development of the NewMass system. This consisted of a development in the thermally activated systems and improves thermal and cooling capacity through the combination of a number of design elements that make the system unique. The concept design was broken into elements, each of which was investigated to find the most appropriate materials, geometries or components to perform their designated task. The final design consisted of a series of black anodised finned tubes, filled with Raschig rings and A22 paraffin, connected in an array and located within the space to be cooled. Cooling may be enabled passively or actively; likewise for discharging of heat. This flexibility in operation minimises energy consumption and ensures system performance. The enhanced heat transfer aspects of the design enhance its thermal and cooling capacity.

Chapter 8 detailed the final testing and modelling of the system. The system performed well, passively restricting the temperature rise in the cell similarly to the RACUS and Energain units. When the passive cooling was supplemented with 13 °C chilled water, the temperature was almost perfectly controlled with a final air temperature 24.6 °C achieved. Active discharge was found to work very effectively and during this test the effective conductivity of the A22/Raschig ring hybrid material, 3.4 W/mK, was derived from internal temperature probe data. This is 18.9 time higher than the conductivity of the paraffin alone for a reduction of just 16% in volume.

The tests did draw attention to some notable flaws with the system. Firstly, the passive discharge achieved a low heat transfer rate believed to be the result of air being drawn across rather than between the fins. This aspect requires careful consideration in future design development. Orientating the tubes so that they can take advantage of beneficial cross-flow will be essential.

Another disadvantage of the system is the overcooling of the occupied space when heat is discharged to the chilled water circuit. This reduces the discharge efficiency and thermal comfort. The proposed solution is to develop an insulative cover that will shield the units from the occupied space upon discharge.

Despite the disadvantages noted, the system performed well and the predicted savings are 34 % for a UK office, as determined by the dedicated energy balance model developed specifically for the NewMass system.

It is hoped that NewMass is seen as a logical design progression in the development of how thermal mass utilisation in buildings. Before the advent of refrigeration technology the utilisation of thermal mass, whether incidental or intended, was often the only way to maintain cool temperatures in buildings. The current use of electricity ultimately requires the extraction and burning of fossil fuels which contributes to the greenhouse effect and climate change. This work advocates the combination of traditional thermal mass concepts with modern refrigeration technology and the improved material properties afforded by phase change materials.

The NewMass design has generated interest from several companies and research institutions. At the time of writing Buro Happold was in talks about collaboration to develop the system into a commercially available product.

9.1 Publications

As a result of this research two conference papers and one journal paper have been published:

- ‘Tests of PCM ‘Sails’ for Low Energy Office Cooling.’ Presented at *The 11th UK National Heat Transfer Conference*, 6th – 8th September 2009, London
- ‘Development of passive and active PCM ‘sails’ for low energy cooling.’ Presented at the *Passive and Low Energy Cooling Conference (PALENC) 2010*, 29th September – 1st October 2010, Rhodes
- ‘Tests of Prototype PCM Sails for Office Cooling.’ Published in *Applied Thermal Engineering* (Volume 31, Issue 5, April 2011)

At the time of writing a further article was in peer-review for publication in *ICE Energy*: ‘Energy Performance of an Office Cooling System with PCM Tank’, based on the work described in chapter 3.

Also, at the time of writing a third journal paper concerning the development, testing and modelling of the NewMass system was being prepared for submission to the journal, *Building and Environment*.

9.2 Further work

This project has produced several opportunities for further work. Concerning the optimisation of the NewMass system there are several opportunities for optimisation and cost-cutting, both in production and operation:

- The operation of chiller and pump may be optimised to establish temperatures and flow rate that will minimise overall energy use.

- The prototype finned tube envelopes were designed to ensure successful operation in the controlled tests, however further detailed work could examine the potential to reduce the material required.
- The NewMass design as presented in this thesis was limited by availability of sufficiently large finned tubes and the fabrication capabilities in standard aluminium machining. However, if larger diameter tubes could be sourced then an investigation into the optimum tube diameter could be undertaken. Larger diameters mean fewer tubes, which could simplify installation, but less surface area and greater PCM thickness, which will reduce heat transfer rate.
- A related process may be undertaken for the Raschig rings to ascertain whether adjusting the size and voidage would have overall benefits in terms of material use and system performance.

Future design iterations for the NewMass system:

- Retractable insulation that would allow the units to retain the coolth they acquired at night until it was required during the daytime. This could take the form of individual covers that wrap each unit in insulation or one that covers several at a time. A retractable horizontal screen that isolates the entire zone in which the units are located is a simple solution but integration with lights and service ducts and conduits will complicate the problem. Research considering this aspect of design alone would be worthwhile.
- A hydrated salt version with an anti-corrosion resin coating on the Raschig rings and tube interior. This is likely to increase the thermal capacity of the system (within the same volume) due to the generally higher latent heat of hydrated salts. It would also, importantly, avoid the fire issues associated with a paraffin-based system. Furthermore the generally narrower phase transition temperature ranges of the salts would further confine the useful cooling performed by the NewMass system to a temperature range around the lower end of the thermal comfort zone; i.e. not exhausting system capacity at temperatures which do not indicate a need for cooling. A comparative study of active discharge rate and temperature would be very

interesting here, as the hydrated salt may better stabilise the unit temperature upon discharge.

- Griffiths and Eames tested a radiant ceiling panel which utilised PCM slurry. This was able to increase the specific thermal capacity of the fluid, as compared to water, which reduces pump power (Griffiths and Eames, 2007). If the water in the NewMass system was exchanged for slurry this could further reduce system energy. In general the hybridising of the system could yield significant performance and energy saving benefits. Referring back to chapter 4 hybridising is the combination of any of the 11 possible systems. The use of a PCM slurry essentially allows the movement of (some of) the PCM. This is an alternative to the movement of insulation.

It is hoped that the design space mapping work will inspire new design developments. Further work proposed is twofold:

- Firstly, a general research project into what type of newly proposed system would perform well in which buildings and which climates could be performed. This could take the form of a number of thermal models that could be run with different internal load patterns and different weather files to represent different building types and different climates, respectively.
- Secondly, particular system types could be chosen for development into fully realised systems. This EngD project seeks to cover some of the ground in the development of the Passive PCM Sails and NewMass systems but there are many more system types that could be explored; the ones involving removable insulation being particularly interesting.

Beyond the NewMass system itself, there are several opportunities to pursue in terms of research and development of PCM-related assessment and policy. Two examples are given here:

- There is generally a need to better understand the life cycle impact of PCMs and the systems into which they are incorporated. A calculation to predict the energy use and savings of the NewMass system was presented in chapter 8. However, this quantity only considers the energy expended through use. The production, transport and disposal of the system will require additional

not only require additional energy but will incur other environmental impacts as well. This is a complex matter with an extremely wide range of data sources, determining factors and interpretations. An extended research project aimed at understanding the wider environmental implications of employing PCMs in buildings is also recommended.

- As noted, the incorporation of PCMs into thermal models is not yet explicitly recognised in building regulations or certification schemes. Efforts should be made to standardise one or more recognised modelling procedures to improve the benefits to developers of employing PCMs to cool buildings.

References

Artica (2009) *Artica Technologies: Classic*. Available:

<http://www.articatechnologies.com/solutions.php> [03/01/2012].

DuPont (2010) *Energy Management*. Available:

http://energain.co.uk/Energain/en_GB/benefits/energy_management.html
[11/01/2011].

Griffiths, P.W. and Eames, P.C. (2007) "Performance of chilled ceiling panels using phase change material slurries as the heat transport medium", *Applied Thermal Engineering*, vol. 27, pp. 1756-1760.

Appendix

COMMERCIALY AVAILABLE PHASE CHANGE MATERIALS

Table A.1 Thermo-physical properties of some investigated fatty acids. (Kenisarin & Mahkamov, 2007)

PCM	Purity	Melting point (°C)	Heat of fusion (kJ/kg)	Sensible heat solid/liquid (kJ/kg °C)	Heat conductivity (W/mK)	Density solid/liquid (kg/m ³)
Capric acid		30.1	158			
		30.1	150–158	1.95/1.60–1.72	0.16 (s)	
	98 wt%	31.4	150.6			
Lauric acid	98 wt%	43.7	210.8			
		42.44	185.5			
	95 wt%	41–43	211.6	1.76 (25 °C)/2.27 (°C)	0.16 (s)	1007/862
		41.3	179			
		52.1–52.5	160–179	1.60–1.17 (l)	0.15–0.17 (s)	
	97 wt%	42.6	211.6	1.7/2.3		
	97 wt%	42.6	176.6			
		186±10	2.81±0.60/2.14±0.46			
Myristic acid		50.4–53.6	189			
		49.7–52.7	190–201	2.91/3.67	0.17 (s)	
		52.7	175.7			
	98 wt%	51.5	204.5	2.8 (35 °C)/2.42 (70 °C)		
		52.1	190			
	95 wt%	53.8	192.0	1.7/2.4		

PCM	Purity	Melting point (°C)	Heat of fusion (kJ/kg)	Sensible heat solid/liquid (kJ/kg °C)	Heat conductivity (W/mK)	Density solid/liquid (kg/m ³)
	95 wt%	53.0	181.0			
Pentadecane acid		52.5	158.6			
		57.8–61.8	201			
		63.28	202.9			
	99.3 wt%	64.0	208.2			
Palmitic acid	97 wt%	61.0	203.4	2.20 (40 °C)/2.48 (80 °C)		
		54.1	183			
	95 wt%	59.9	197.9	1.9/2.8		
	90 wt%	61.3	197.9			
		63.5	188.7			
		65.2–68.5	210			
		69.6	176.2			
	Com. grad	66	155			
Stearic acid		64.5	196			
	97 wt%	71.0	210.8			
	90 wt%	60–61	186.5	2.83 (40 °C)/2.38 (80 °C)		
	90 wt%	54.7	159.3			
Oleic acid	99.9 wt%	-5.3	75.5			
	90 wt%		45.3			

Table A.2 Thermo-physical properties of some investigated acid and alkyl ester PCMs. (Kenisarin & Mahkamov, 2007)

PCM	Type of composition	Melting point (°C)	Heat of fusion (kJ/kg)	Sensible heat solid/ liquid (kJ/kg °C)	Heat conductivity (W/mK)
Carpic acid (65.5 mol%)+lauric acid (35 mol.%)	Eutectic	18–19.5	140.8	1.97/2.24	0.143/0.139
Carpic acid (61.5 wt%)+lauric acid (38.5 wt%)	Eutectic	19.1	132		
Carpic acid+Lauric acid	Eutectic	18	120		
Carpic acid (73.5 wt%)+myristic acid (26.5 wt%)	Eutectic	21.4	152		
Carpic acid (75.2 wt%)+palmitic acid (24.8 wt%)	Eutectic	22.1	153		
Carpic acid (86.6 wt%)+stearic acid (13.4 wt%)	Eutectic	26.8	160		
Lauric acid (62.6 wt%)+myristic acid (37.4 wt%)	Eutectic	32.6	156		
Lauric acid (66.0 wt%)+myristic acid (34.0 wt%)	Eutectic	34.2	166.8		
Lauric acid (64.0 wt%)+palmitic acid (36.0 wt%)	Eutectic	32.8	165		
Lauric acid (69.0 wt%)+palmitic acid (31.0 wt%)	Eutectic	35.2	166.3		
Lauric acid (77.0 wt%)+palmitic acid (23.0 wt%)	Eutectic	33.0	150.6	1.77/2.41	
Lauric acid (80.0 wt%)+palmitic acid (20.0 wt%)	Eutectic	32.7	145		
Lauric acid (75.5 wt%)+stearic acid (24.5 wt%)	Eutectic	37.3	171		
Lauric acid+stearic acid	Eutectic	34	150		
Lauric acid (75.5 wt%)+stearic acid (24.5 wt%)	Eutectic	37	182.7	1.92/2.10	
Myristic acid (51 wt%)+Palmitic acid (49 wt%)	Eutectic	39.8	174		
Myristic acid (58 wt%)+palmitic acid (42 wt%)	Eutectic	42.6	169.7		
Myristic acid (65.7 wt%)+stearic acid (34.7 wt%)	Eutectic	44	181		
Myristic acid (64.0 wt%)+stearic acid (36.0 wt%)	Eutectic	44	182		
MA ₃ PA ₂ (myristic acid+palmitic acid)	Compound	47.3	173.8		
MA ₂ SA (myristic acid+stearic acid)	Compound	48.6	179.8		

PCM	Type of composition	Melting point (°C)	Heat of fusion (kJ/kg)	Sensible heat solid/ liquid (kJ/kg °C)	Heat conductivity (W/mK)
Palmitic acid (64.9 wt%)+stearic acid (35.1 wt%)	Eutectic	50.4	181		
Palmitic acid (64.2 wt%)+stearic acid (35.8 wt%)	Eutectic	52.3	181.7		
Palmitic acid+stearic acid	Eutectic	51	160		
Palmitic acid (50 wt%)+stearic acid (45.5 wt%)+other fatty acids (4.5 wt%)— <i>emersol 132</i>	Mixture	54–57	180		
PeASA (pentadecane acid+stearic acid)	Compound	50.6	173.0		
Stearic acid (65 wt%)+palmitic acid (27.5 wt%)+other fatty acids (5.5 wt%)— <i>emery 420</i>	Mixture	51–56	180		
PASA (palmitic acid+stearic acid)	Compound	57.2	179.6		
Stearic acid (83 wt%)+palmitic acid (11 wt%)+other fatty acids (6% wt%)— <i>emersol 150</i>	Mixture	60–66	206		
Stearic acid (95 wt%)+palmitic acid (5 wt%)— <i>emersol 153</i>	Mixture	65–68	209		
Butyl palmitate (49 wt%)+butyl stearate (48 wt%)+other (3 wt%)	Mixture	17	140		
Methyl palmitate (65–90 wt%)+methyl stearate (35–10 wt%)	Mixture	22–25.5	120		
Methyl stearate	Compound	29.0	169		
Methyl palmitate	Compound	38.0	180		
Ethyl stearate	Compound		134		
Ethyl palmitate	Compound	23.0	122		

Table A.3 Thermo-physical properties of some investigated eutectic paraffins. (Kenisarin & Mahkamov, 2007)

PCM	Transition temperature (°C)	Heat of transition (kJ/kg)	Melting point (°C)	Heat of fusion (kJ/kg)	Sensible heat solid/liquid (kJ/kg °C)	Density solid/liquid (kg/l)
Dodecane				135±8	5.11±0.56/2.19±0.19	
			-9.6	216	2.21 (80 °C)	
Tetradecane			5.9	258		0.77 (liq.)
			5.8	227	2.22 (liq.)	0.759 (20 °C)
Purity—99%			5.4	227.5		
Purity—99%			3.64	172.1		
Pentadecane	-2	64.12	9.9	193.9		0.765 (20 °C)
			9.9	207	2.22 (liq.)	
			9.9	206		
Hexadecane			18.1	236	2.22 (liq.)	0.770 (20 °C)
			17.9	211.5		
				225±15.2	2.25±0.25/2.20±0.11	
Industrial grade			13.2–13.9	201		
Heptadecane			20.8–21.7	171–172	2.57 (s)	
Octadecane			28	250.7		
			28.1	244	1.91/2.22	0.779 (20 °C)
Industrial grade			24.7–28.2	203		
Heneicosane	32.8	80.94	40	155.49		
			40.2	213		0.778 (20 °C)
Docosane			44	196.4		

PCM	Transition temperature (°C)	Heat of transition (kJ/kg)	Melting point (°C)	Heat of fusion (kJ/kg)	Sensible heat solid/liquid (kJ/kg °C)	Density solid/liquid (kg/l)
			44	252		
			54.6–57.7	216–237	3.89/2.94	

Table A.3 Thermo-physical properties of some investigated paraffins. (Kenisarin & Mahkamov, 2007)

Heat storage material	Transition temperature (°C)	Melting range (°C)	Heat of fusion including transition heat (kJ/kg)	Sensible heat solid/liquid (kJ/kg °C)	Heat conductivity (W/mK)	Density solid/liquid (kg/l)
Suntech P116 Paraffin wax		43–56	266	2.95/2.51	0.24/0.24	0.818/0.760
Unicere 55 Paraffin		52.5–53.7	182–189			
Paraffin 44		44	167			
Paraffin 53		53	200			
Paraffin 64		64	210			
Paraffin 56 (Russia)		56±2	72–86		0.75 (25 °C)	1.06
Paraffin 57 (Russia)		57±2	98		0.7	
Paraffin 63 (Russia)		63±2	60			
Paraffin natural wax 79 (Russia)		79±2	80		0.63	1.20
Paraffin natural wax 84 (Russia)		84±2	85		0.72	1.20
Paraffin natural wax 106 (Russia)		106±2	80		0.65	1.20
Paraffin wax 53		53	184	2.05		

Heat storage material	Transition temperature (°C)	Melting range (°C)	Heat of fusion including transition heat (kJ/kg)	Sensible heat solid/liquid (kJ/kg °C)	Heat conductivity (W/mK)	Density solid/liquid (kg/l)
(commercial grade)						
Paraffin 53	35.4	53	164	2.13 (30 °C)/2.62 (70 °C)	0.28 (30 °C)/0.19 (70 °C)	0.978 (30 °C)/0.795 (70 °C)
RT 60 Rubitherm paraffin		58–60	214	0.93	0.2	0.850/0.775

Table A.4 Thermo-physical properties of some investigated inorganic substance. (Zalba *et al.*, 2003/2)

Compound	Melting temperature (°C)	Heat of fusion (kJ/kg)	Thermal conductivity (W/m K)	Density (kg/m ³)
H ₂ O	0	333	0.612 (liquid, 20 °C)	998 (liquid, 20 °C)
		334	0.61 (30 °C)	996 (30 °C)
				917 (solid, 0 °C)
LiClO ₃ ·3H ₂ O	8.1	253	n.a.	1720
ZnCl ₂ ·3H ₂ O	10	n.a.	n.a.	n.a.
K ₂ HPO ₄ ·6H ₂ O	13	n.a.	n.a.	n.a.
NaOH · 3 $\frac{1}{2}$ H ₂ O	15	n.a.	n.a.	n.a.
	15.4			
Na ₂ CrO ₄ ·10H ₂ O	18	n.a.	n.a.	n.a.
KF · 4H ₂ O	18.5	231	n.a.	1447 (liquid, 20 °C)
				1455 (solid, 18 °C)
				1480

Compound	Melting temperature (°C)	Heat of fusion (kJ/kg)	Thermal conductivity (W/m K)	Density (kg/m ³)		
Mn(NO ₃) ₂ ·6H ₂ O	25.8	125.9	n.a.	1738 (liquid, 20 °C)		
				1728 (liquid, 40 °C)		
				1795 (solid, 5 °C)		
CaCl ₂ ·6H ₂ O	29	190.8	0.540 (liquid, 38.7 °C)	1562 (liquid, 32 °C)		
				29.2	171	1496 (liquid)
				29.6	174.4	1802 (solid, 24 °C)
				29.7	192	1710 (solid, 25 °C)
				30		1634
				29–39		1620
LiNO ₃ ·3H ₂ O	30	296	n.a.	n.a.		
Na ₂ SO ₄ ·10H ₂ O	32.4	254	0.544	1485 (solid)		
				32	251.1	1458
				31–32		
Na ₂ CO ₃ ·10H ₂ O	32–36	246.5	n.a.	1442		
				33	247	
CaBr ₂ ·6H ₂ O	34	115.5	n.a.	1956 (liquid, 35 °C) 2194 (solid, 24 °C)		
Na ₂ HPO ₄ ·12H ₂ O	35.5	265	n.a.	1522		
				36	280	
				35	281	
				35.2		
Zn(NO ₃) ₂ ·6H ₂ O	36	146.9	0.464 (liquid, 39.9 °C)	1828 (liquid, 36 °C)		
				36.4	147	1937 (solid, 24 °C)

Compound	Melting temperature (°C)	Heat of fusion (kJ/kg)	Thermal conductivity (W/m K)	Density (kg/m ³)
				2065 (solid, 14 °C)
KF · 2H ₂ O	41.4	n.a.	n.a.	n.a.
K(CH₃COO) · 1 $\frac{1}{2}$ H ₂ O	42	n.a.	n.a.	n.a.
K ₃ PO ₄ ·7H ₂ O	45	n.a.	n.a.	n.a.
Zn(NO ₃) ₂ ·4H ₂ O	45.5	n.a.	n.a.	n.a.
Ca(NO ₃) ₂ ·4H ₂ O	42.7	n.a.	n.a.	n.a.
	47			
Na ₂ HPO ₄ ·7H ₂ O	48	n.a.	n.a.	n.a.
Na ₂ S ₂ O ₃ ·5H ₂ O	48	201	n.a.	1600 (solid)
	48–49	209.3		1666
		187		
Zn(NO ₃) ₂ ·2H ₂ O	54	n.a.	n.a.	n.a.
NaOH·H ₂ O	58.0	n.a.	n.a.	n.a.
Na(CH ₃ COO) · 3H ₂ O	58	264	n.a.	1450
	58.4	226		
Cd(NO ₃) ₂ ·4H ₂ O	59.5	n.a.	n.a.	n.a.
Fe(NO ₃) ₂ ·6H ₂ O	60	n.a.	n.a.	n.a.
NaOH	64.3	227.6	n.a.	1690
Na ₂ B ₄ O ₇ ·10H ₂ O	68.1	n.a.	n.a.	n.a.
Na ₃ PO ₄ ·12H ₂ O	69	n.a.	n.a.	n.a.
Na ₂ P ₂ O ₇ ·10H ₂ O	70	184		n.a.

Compound	Melting temperature (°C)	Heat of fusion (kJ/kg)	Thermal conductivity (W/m K)	Density (kg/m ³)
Ba(OH) ₂ ·8H ₂ O	78	265.7	0.653 (liquid, 85.7 °C)	1937 (liquid, 84 °C)
		267	0.678 (liquid, 98.2 °C)	2070 (solid, 24 °C)
		280	1.255 (solid, 23 °C)	2180 (solid)
AlK(SO ₄) ₂ ·12H ₂ O	80	n.a.	n.a.	n.a.
Kal(SO ₄) ₂ ·12H ₂ O	85.8	n.a.	n.a.	n.a.
Al ₂ (SO ₄) ₃ ·18H ₂ O	88	n.a.	n.a.	n.a.
Al(NO ₃) ₃ ·8H ₂ O	89	n.a.	n.a.	n.a.
Mg(NO ₃) ₂ ·6H ₂ O	89	162.8	0.490 (liquid, 95 °C)	1550 (liquid, 94 °C)
		149.5	0.502 (liquid, 110 °C)	1636 (solid, 25 °C)
			0.611 (solid, 37 °C)	1640
			0.669 (solid, 55.6 °C)	
(NH ₄)Al(SO ₄) · 6H ₂ O	95	269	n.a.	n.a.
$\text{Na}_2\text{S} \cdot 5\frac{1}{2}\text{H}_2\text{O}$	97.5	n.a.	n.a.	n.a.
CaBr ₂ ·4H ₂ O	110	n.a.	n.a.	n.a.
Al ₂ (SO ₄) ₃ ·16H ₂ O	112	n.a.	n.a.	n.a.
MgCl ₂ ·6H ₂ O	117	168.6	0.570 (liquid, 120 °C)	1450 (liquid, 120 °C)
		165	0.598 (liquid, 140 °C)	1442 (liquid, 78 °C)
			0.694 (solid, 90 °C)	1569 (solid, 20 °C)
			0.704 (solid, 110 °C)	1570 (solid, 20 °C)
Mg(NO ₃) · 2H ₂ O	130	n.a.	n.a.	n.a.
NaNO ₃	307	172	0.5	2260
	308	174		2257

Compound	Melting temperature (°C)	Heat of fusion (kJ/kg)	Thermal conductivity (W/m K)	Density (kg/m ³)
		199		
KNO ₃	333	266	0.5	2.110
	336	116		
KOH	380	149.7	0.5	2.044
MgCl ₂	714	452	n.a.	2140
NaCl	800	492	5	2160
	802	466.7		
Na ₂ CO ₃	854	275.7	2	2.533
KF	857	452	n.a.	2370
K ₂ CO ₃	897	235.8	2	2.290

The number of companies that specialise in producing/supplying materials for application specifically as PCMs, i.e. making use of their latent heat capacity, is relatively small. Several of the most prominent are detailed below:

- **Doerken:** A German company that supplies two types of fabric-incorporated PCM panel; the Delta-Cool 24 and Delta-Cool 28. (Doerken) (Doerken)
- **PCM Products:** A British company that supplies a large number of PCM products and raw materials. (PCM Products, 2008)
- **Climator:** Swedish-based provider of PCM cooling and temperature regulation products. These include Cooldeck panels for space cooling. (climator, 2007)
- **DuPont:** A large international manufacturing and chemical engineering company that produces 'Energain' panels for fabric-incorporated PCM cooling. (DuPont, 2007)

- **BASF:** An international chemical engineering company that produces micro-encapsulated PCM particles for fabric incorporation. (BASF, 2006) (BASF, 2006)
- **Rubitherm:** A German company that supplies raw PCM in various forms (powder, granules etc.) and PCM products such as compact storage modules for use in active storage systems. (Rubitherm)
- **Cristopia:** A French company that supplies tank systems containing plastic balls filled with ice or any of a range of PCMs for active cool storage. (Cristopia Energy Systems, 2011)
- **Mitsubishi Chemical:** A Japanese chemical company that produces a vast range of chemicals for multiple applications including PCMs. (Mitsubishi Chemical, 2011)

References

BASF (2006) *Raw Materials Range*. Available: http://www.micronal.de/portal/basf/ien/dt.jsp?setCursor=1_290823 [12/12/2007].

climator (2007) *Climator - Moving Energy in Time*. Available: <http://www.climator.com/> [21/12/2007].

Cristopia Energy Systems (2011) *Products*. Available: <http://www.cristopia.com/cristopia/english/products/indproducts.html> [14/09/2011].

Doerken *Intelligent temperature management*. Available: <http://www.doerken.de/bvf-en/produkte/pcm/index.php> [04/01/2009].

DuPont (2007) 2007-last update, *DuPont Energain*. Available: http://www2.dupont.com/Energain/en_GB/ [29/04/2007].

Kenisarin, M. & Mahkamov, K. (2007) "Solar energy storage using phase change materials", *Renewable and Sustainable Energy Reviews*, vol. 11, no. 9, pp. 1913-1965.

Mitsubishi Chemical (2011) *Products and Services*. Available: <http://www.m-kagaku.co.jp/webapps/pss/SearchProducts> [14/09/2011].

PCM Products (2008) *PCM* [Homepage of Phase Change Materials Products Limited], [Online]. Available: <http://www.pcmproducts.net/> [04/01/2009].

Rubitherm *Innovative PCMs and Thermal Technology*. Available: <http://www.rubitherm.com/english/index.htm> [04/01/2008].

Zalba, B., Marín, J.M., Cabeza, L.F. & Mehling, H. (2003/2) "Review on thermal energy storage with phase change: materials, heat transfer analysis and applications", *Applied Thermal Engineering*, vol. 23, no. 3, pp. 251-283.